

https://dspace.org/

Prediction of spontaneous combustion in coal by use of thermogravimetry

Mthabela, Zamashinga Amanda

2016

http://hdl.handle.net/10539/22185

Mthabela, Zamashinga Amanda (2016) Prediction of spontaneous combustion in coal by use of thermogravimetry, University of Witwatersrand, Johannesburg, <http://wiredspace.wits.ac.za/handle/10539/22185>

Downloaded from a DSpace repository. https://dspace.org/



Prediction of spontaneous combustion in coal by use of thermogravimetry

MSc (50/50) Research Project

Zamashinga Amanda Mthabela (1078100)

Submitted to

School of Chemical and Metallurgical Engineering, Faculty of Engineering and the Built Environment, University of the Witwatersrand, Johannesburg, South Africa

15 February, 2016

Declaration

I declare that this research report is my own unaided work. It is being submitted in fulfillment of the degree of Master of Science in Engineering (Metallurgy and Materials) to the University of Witwatersrand, Johannesburg, South Africa. It has not been submitted before for any degree or examination to any other University.



Z.A Mthabela

Student Number: 1078100

Singed on the 15th day of FEBRUARY Year 2016

Abstract

The self-heating of coals is a complex problem which has been occurring for centuries. This problem has been fatal to coal miners, an economical challenge to coal mines and a health risk in a release of greenhouse gases to the public in general. Therefore, everyone is affected by the self-heating of coal, which leads to spontaneous combustion when the ignition temperature is reached.

There are many test methods that have been used to test spontaneous combustion in coal, but all have one common factor or disadvantage of requiring long periods of time before a conclusion can be deduced. This then creates a need for a rapid and reliable method to test the liability of coal to self-heat in the coal industry and thus the motivation for this project.

The thermogravimetry analysis (TGA) method was selected to test the liability of coal to self-heat due to its short analytical duration. The Smith-Glasser oxidation test was selected to validate the TGA results obtained. The main aim of this project is to investigate the reliability of the TGA method to predict the propensity of coal to self-heat.

29 samples from different regions of South Africa were used, prepared to 250 μm for all the analyses and self-heating tests. All samples were analysed for proximate, calorific value, sulphur and petrographic properties before the spontaneous combustion liability tests began.

The TGA method followed two tests: 1) the O_2 adsorption and 2) the ignition test. Five different heating rates (3, 5, 7, 10, and 20) °C/min were run in order to obtain five derivative slopes which would be used to obtain the TG_{spc} index. The oxygen adsorption test studies the mass increase at low temperature under exposure of air between the temperature ranges of 100 – 300°C.

The Smith-Glasser oxidation test method studies the reaction of coal with O_2 and calculates the O_2 absorbed per amount of coal tested. The Smith-Glasser test results collaborated with most of the other analytical results, and with the TGA results to a certain extent.

The TGA spontaneous combustion liability test requires additional analytical work to back up its results because the results do not appear as accurate as the Smith-Glasser oxidation test. It also requires repeatability tests to ensure the integrity of the results.

Dedication

I would like to dedicate this paper to my mother Irene Nombukiso Madiba, for all the hardship and sacrifices she made to ensure I get a better education. Her courage, resilience, and determination have been my guiding light in achieving everything I set my mind to.

Ngiyabonga Ma for being my role model, for teaching me the difference between right and wrong and how a lady should conduct oneself and instilling the belief that anything is possible as long as you set your mind to it! I saw you do it and I knew it could be done.

"We do not believe in ourselves until someone reveals that deep inside us something is valuable, worth listening to, worthy of our trust, sacred to our touch. Once we believe in ourselves we can risk curiosity, wonder, spontaneous delight or any experience that reveals the human spirit."

— E.E. Cummings

Acknowledgements

I would firstly like to acknowledge the University of Witwatersrand for granting the study fund for this degree. I would also like to acknowledge the Clean Coal Research Technology Group for funding the research work and equipment for this research.

I am especially grateful to my supervisor Dr. Nicola Wagner for shaping this research from the initial stages and guidance to its completion. I would like to thank Ms. Nthabiseng Maledi for contributing her time and expertise in this investigation. I express my sincerest gratitude to Dr. Samson Bada for his professional contribution towards this research.

I give a special and heartfelt thank you to my always loving and supportive husband (Thabani Mthabela), for always keeping me in line by helping me to never lose focus of my goal, by setting the bar academically. I would like to thank him for always ensuring my health is first priority and helping me when I am unable to help myself, I thank the good Lord for giving me you. Thank you my love, for loving and caring for me, I will love you always.

I would lastly like to thank my family and friends for all their love, support, and encouragement through this journey.

Ngiyabonga (Thank you).

Table of Contents

CHAPTER 1

1. INTRODUCTION 1

1.1 PROBLEM STATEMENT 1

1.2 AIM 2

1.3 RESEARCH OBJECTIVES 2

1.4 RESEARCH QUESTIONS 2

CHAPTER 2

2. LITERATURE REVIEW 3

2.1 COAL 3

2.1.1 COAL FORMATION 3

2.1.2 COAL DEMAND IN SOUTH AFRICA 4

2.1.3 THE ADVANTAGES AND DISADVANTAGES OF COAL USE 6

2.2 SPONTANEOUS COMBUSTION OF COAL 6

2.2.1 FACTORS LEADING TO SELF-HEATING OF COAL 7

2.2.2 PREVIOUS INCIDENTS OF SPONTANEOUS COMBUSTION 9

2.2.3 THE IMPACTS OF SPONTANEOUS COMBUSTION ON THE ENVIRONMENT 13

2.3 PREVIOUS WORK DONE TO INVESTIGATE SELF-HEATING COALS 14

2.3.1 STATIC ISOTHERMAL METHOD 14

2.3.2 ADIABATIC CALORIMETRY METHOD 15

2.3.3 CROSSING POINT INDEX (CPI) 16

2.3.4 WITS-EHAC LIABILITY INDEX 17

2.3.5 DIFFERENTIAL THERMAL ANALYSIS (DTA) 17

2.3.6 MATHEMATICAL MODEL 18

2.3.7 THERMOGRAVIMETRIC ANALYSIS (TGA) METHODS 19

2.3.8 2ND TGA METHOD 20

2.4 PREVENTION OF SELF-HEATING IN COAL 22

2.4.1 CONTROL MEASURES (COALTECH RESEARCH ASSOCIATION, 2011) 22

2.4.2 MONITORING OF SELF-HEATING IN COAL 24

2.5 CHAPTER SUMMARY 24

CHAPTER 3

3 METHODOLOGY 25

3.1 PROJECT PLAN 25

3.2 SAMPLE PREPARATION 26

3.2.1 SAMPLE ORIGIN 26

3.2.2 SAMPLE SPLITTING 26

3.2.3 SAMPLE CRUSHING 26

3.2.4 SAMPLE REDUCTION 27

3.2.5 SAMPLE MILLING 27

3.2.6 SAMPLE STORAGE 28

3.3 COAL ANALYSIS 28

3.3.1 PROXIMATE ANALYSIS 28

3.3.2 GROSS CALORIFIC VALUE (CV) ANALYSIS 29

3.3.3 TOTAL SULPHUR ANALYSIS 30

3.3.4 PETROGRAPHY 31

3.4 SELF-HEATING DETERMINATION 32
3.4.1 TEST 1 - TGA METHOD (AVILA, 2012) 32
3.4.2 TEST 2: STATIC ISOTHERMAL METHOD (SMITH-GLASSER, 2005) 35
3.5 QUALITY ASSURANCE 36
CHAPTER 4
4 RESULTS AND DISCUSSION 37
4.1 PROXIMATE ANALYSIS 37
4.2 CV AND SULPHUR ANALYSIS 39
4.3 PETROGRAPHIC ANALYSIS 41
4.4 SELF-HEATING TEST: TGA 42
4.4.1 IGNITION TEST 42
4.4.2 O_2 ADSORPTION 46
4.5 SMITH-GLASSER TEST 51
4.6 QUALITY ASSURANCE RESULTS AND DISCUSSION 54
4.7 %ERROR CALCULATION 58
4.8 COMPARISON OF RESULTS 61
CHAPTER 5
5 CONCLUSION 65
CHAPTER 6
6 RECOMMENDATION 67
CHAPTER 7
7 REFERENCE LIST 68
CHAPTER 8
8 APPENDICES 74
8.1 APPENDIX A 74
8.1.1 Proximate Analysis
8.2 APPENDIX B 88
8.2.1 TGA O_2 ADSORPTION 88
8.2.2 TGA IGNITION TEST 103
8.3 APPENDIX C 132
8.3.1 SMITH-GLASSER OXIDATION TEST 132
8.4 APPENDIX D 136
8.4.1 REPEATABILITY TESTS 136
8.5 APPENDIX E 138
8.5.1 PETROGRAPHY ANALYSIS 138
8.6 APPENDIX F 142
8.6.1 MINE DISASTERS 142
8.6.2 SPONTANEOUS COMBUSTION MINE DISASTERS 143
8.7 APPENDIX G 144
8.7.1 CHANGES IN COAL PROPERTIES 144

CHAPTER 1

1. INTRODUCTION

1.1 PROBLEM STATEMENT

Spontaneous combustion is a hazard that has been linked to the coal industry for years, if not centuries. Coal oxidation is a slow process that leads to the smouldering of coal, which with time, may result in self-heating and may eventually lead to spontaneous combustion when the temperature has reached its ignition point. This exothermic reaction occurs in the following manner according to Grapes (2010):

$C + O_2 \rightarrow CO_2 + Heat$.....Equation 1 (Grapes, 2010)

Spontaneous combustion can occur during the mining, transportation and storage of coal and through un-rehabilitated coal mines. Challenges presented by spontaneous combustion are: substantial loss of resources; causes of atmospheric air pollution; and possible loss of human life.

The oxidation reaction in coal, which results in self-heating, can be prevented from occurring through better management and handling of the coal. This can be achieved by knowing the quality of the coal as determined by proximate and petrographic analysis, for example. In addition, spontaneous combustion liability tests can be performed to determine a risk profile associated with the coal.

The Smith-Glasser Test is a well-established test (Sipilä et al. (2012) that is a commonly used method for approximating spontaneous combustion liability in coal. The duration of this test can, however, be very lengthy, ranging from 4 hours to a week(s). The problematic self-heating coals normally do not take long to react in the Smith-Glasser test, but other coal samples ranging between the high and low rank coals can take days to react. There is always a need for rapid test results which will not be time and cost consuming, and thermogravimetric analysis (TGA) is potentially the answer to this need.

Spontaneous combustion tests have previously been conducted on the TGA, using oxygen adsorption and ignition tests to approximate spontaneous combustion. Although these tests have been deemed successful by Luo and Wang (2011) and Avila (2012), none of the results have been studied on South African coal, or compared to the Smith-Glasser test.

1.2 AIM

This project aims to assess the accuracy of the TGA method as a tool to test the liability of coal to self-heat. This project is based on the method presented by Avila (2012) through an article titled, "Predicting self-oxidation of coals and coal/biomass blends using thermal and optical methods".

1.3 RESEARCH OBJECTIVES

The main objectives of this project is to validate the TGA test methods in determining the liability of coal to self-heat, by comparing a large number of samples analysed to the well-used Smith-Glasser oxidation method. This will be achieved by:

- Investigating the reliability of the previously tested spontaneous combustion method (Avila, 2012) using the TGA test method.
- Measuring the coal reactivity through the use of the peak temperature, sample mass increase and the thermogravimetry spontaneous combustion index (TG_{spc} Index).
- Analysing the same samples tested in the TGA using the Smith-Glasser oxidation test.
- Comparing the two spontaneous combustion liability methods.
- Characterising the coal samples.

1.4 RESEARCH QUESTIONS

- Can the TGA method be used to determine the liability of coal to self-heat?
- Is the TGA method more accurate when compared to other spontaneous combustion test methods?

CHAPTER 2

2. LITERATURE REVIEW

The literature review discussed in this report highlights that, in order to understand self-heating in coal, one has to have an appreciation for coal itself. This can be achieved by understanding all principles relating to coal, starting from the formation of coal; demands and uses of coal; advantages and disadvantages of using coal.

The phenomena known as spontaneous combustion or self-heating of coal is also covered in the literature review and includes the process of self-heating, factors leading to self-heating, previous incidents from spontaneous combustion, impacts of spontaneous combustion, and analytical techniques to determine self-heating in coal.

2.1 Coal

2.1.1 Coal formation

South Africa is situated in the Gondwana region located in the southern hemisphere where many plants accumulated in the Permian swamps, million years ago. The decaying plants, frequently mixed with mineral matter, experienced compression and compaction, and were exposed to high temperatures over time (the coalification process), World Coal Association (2005), as displayed in Figure 1.

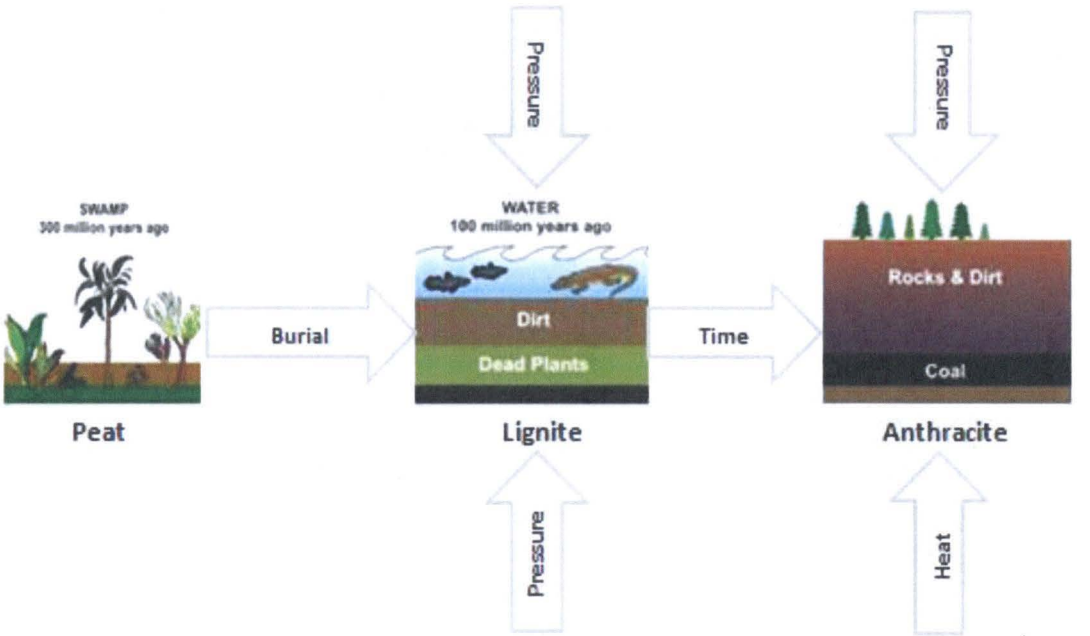


Figure 1: Coal Formation (EIA, 2013)

The coalification process is an important component in determining the coal's physical and chemical properties. Coalification stems from a combination of thermal effects and compaction, and coal rank increases with depth. Basically, the longer and deeper the coals

stays buried and exposed to appropriate conditions, the greater the transformations from peat ultimately into anthracite. Methane gas forms during the coalification process of higher rank coals, whilst the carbon dioxide and water form during the coalification process of lower rank coals (World Coal Association, 2005).

Higher rank coals have a higher carbon content, which means a higher heating value, which also mean lower hydrogen and oxygen content, compared to lower rank coals. Anthracites are types of high rank coals, typically rich in vitrinite and low in ash. The lower rank coals have the opposite properties, which are lower carbon content, lower heat value, higher nitrogen and oxygen content (these include some of the reasons why lower grade coal when not used quickly, may self-combust). The ranks of coals are structured as follows: peat, lignite, sub-bituminous, bituminous and anthracite, reflecting the increase in carbon content (Aziz, 2012), (Figure 2).



Figure 2: Coal Rank, (Aziz, 2012)

2.1.2 Coal Demand in South Africa

South Africa's (SA) energy is heavily dependent on coal as a source of energy (World Coal Association, 2005). The dependency on coal has increased through the years, as can be viewed from the source of energy in Figure 3. SA's coal production and consumption is amongst the top globally, with a production figure of 6.3 ton per capita in 2012, as illustrated in Figure 4. South Africa's coal consumption was rated 15th in the world (IEA, 2012) and this growth in the coal usage is directly proportional to the increase in polluting emissions.

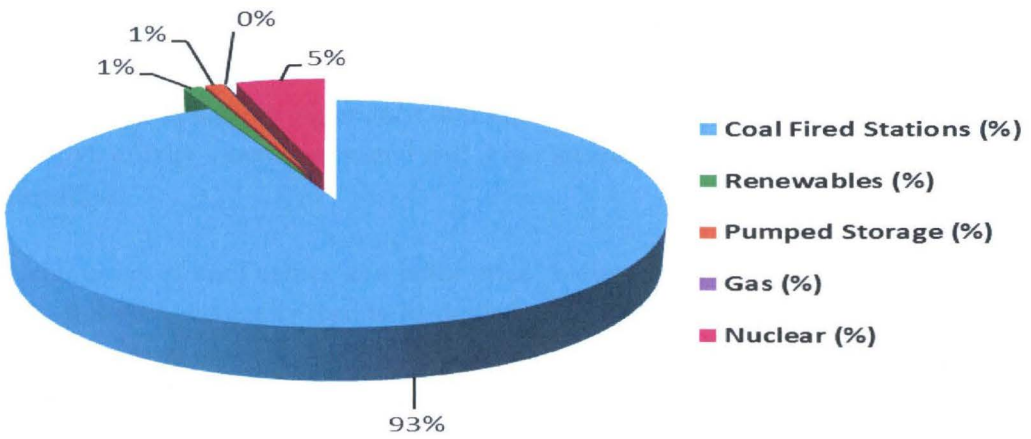


Figure 3: Eskom Resources of Energy (Eskom, 2012)

Coal is utilised in various processes such as power generation, transportation, and industrial processes which include metallurgical, cement and chemical processes. Coal is involved in our daily lives, because energy is vital to our existence; the other energy source alternatives only contribute 7% to power generation (Eskom, 2012).

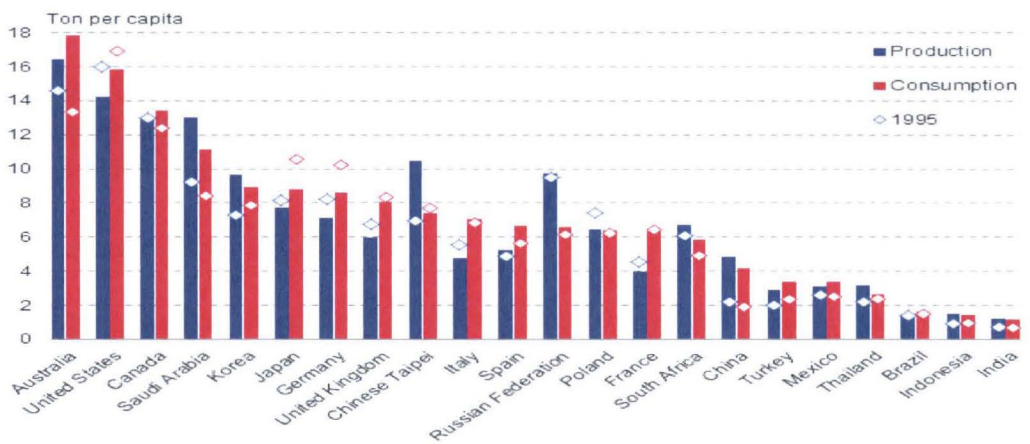


Figure 4: Global Coal production and consumption per capita (IEA, 2012)

Not only does coal provide a means towards cheap power, but it also creates coal mining jobs for the communities, which brings job security to many homes.

South Africa is one of the top coal exporting countries in the world and this causes high demand in the transportation of coal which requires high efficiency in order to increase the economy of the country (Transnet, 2014).

2.1.3 The Advantages and Disadvantages of Coal Use

The main advantage of using coal is that it is cheap because we have it in abundance; it is not a commodity that needs to be imported. Coal has been mined and exported for years; South Africa therefore has the experience and knowledge to handle it. Coal is easy to burn; it produces high energy when combusted and it has stable prices when compared with other fuel commodities.

However, the usage of coal comes at a hefty price. Large quantities of coal are used during combustion; this will eventually lead to its depletion. Combustion of coal is environmentally un-friendly as it produces unsafe by-products and gas emissions such as carbon dioxide (CO_2), sulphur dioxide (SO_2) and nitrogen dioxide (NO_2). Most mines are not rehabilitated after mine closure and that puts the lives of the communities at risks (Midwest Geological Sequestration Consortium, 2011) because spontaneous combustion can occur due to an exothermic reaction that slowly occurs through time. Coal mine fires are a common occurrence in the Witbank coalfield, as well as Kentucky coal mines.

The main shortcoming of coal combustion is the release of CO_2, which contributes to greenhouse gas accumulation. Large quantities of CO_2 are formed as a by-product of a number of industrial processes which include: fossil fuel combustion, ammonia synthesis, hydrogen production by a process of steam reforming and lastly fermentation (Midwest Geological Sequestration Consortium, 2011). The combustion of fuels which contain carbon such as: coal, petroleum distillates, methane and wood, results in the production of CO_2 (Midwest Geological Sequestration Consortium, 2011).

Low grade coal tends to spontaneously combust when not managed effectively in stockpiles, during transportation, and during production underground. The occurrence of spontaneous combustion is a costly and life threatening problem that wastes valuable resources.

2.2 Spontaneous combustion of coal

Spontaneous combustion of coal is a form of combustion that begins by self-heating caused by internal exothermic reactions in the coal particles (Coaltech Research Association, 2011). This is a slow process that takes time to occur, but can be very destructive once it gets going.

Carbonaceous matter can interact with oxygen in the air at ambient temperature to create a run-away temperature profile. The increase in temperature caused by the exothermic reactions creates conditions favouring spontaneous combustion. The reaction is normally slow under ambient temperature, but when heat increases and the temperature raised according to the Arrhenius law, the reaction rate increases exponentially:

$$v = c_r \cdot c_0 A \cdot e^{\frac{Ea}{RT}} \quad \text{..... Equation 2 (Coaltech Research Association, 2011)}$$

Where:
v = Reaction ($molg^{-1}s^{-1}$)
c_r = Combustible concentration (kg/m^3)
c_o = Oxygen concentration
A = Arrhenius Frequency Factor (s^{-1} or $s^{-1}C^{1-n}$)
Ea = Activation Energy (kJ/mole)
R = Universal gas constant = 8.314 $JmoleK^{-1}$
T = Temperature (K)

Exposure to air causes a continuous oxidation reaction of coal in coal dumps, un-rehabilitated closed coal mines, existing coal mines, coal shipments or coal stockpiles. The heat generated is normally trapped and increases, eventually leading to spontaneous combustion.

Three processes occur during the self-heating of coal according to Carras (1994):

- physical adsorption,
- chemical adsorption (which leads to the formation of carboxyl and other forms),
- oxidation (where O_2 and coal react to discharges gases such as CO, H_2O, and CO_2).

Horsfall (1985) goes further to explain the above mentioned three processes as follows:

Spontaneous combustion occurs in different stages, where:

- Oxidation occurs slowly as the rise in temperature builds up to about 50°C. Carbon monoxide (CO) can be detected at this stage.
- The oxidation picks up speed as the temperature continues to rise above 100°C and so does the CO.
- Water vapour and CO_2 start forming as the temperature gets to 138°C.
- The CO continues to rise as the temperature increases to 230°C and combustion can occur at this temperature.
- If the temperature is allowed to increase further on to above 350°C, coal ignition begins and the combustion will start at this point.

2.2.1 Factors Leading to Self-heating of coal

The trend of coal to self-heat is caused mainly by (Coaltech Research Association, 2011):

- Basic factors (Intrinsic) such as: the coal type (rank and petrographic elements), geological setting the conditions set by the environment and moisture content.
- Non-basic factors (Extrinsic): that is related to the mining of the coal, stockpile compaction, method of ventilation and climatic conditions.

As the reaction of these factors together under certain situations may result in self-heating it is therefore imperative for each factor to be understood for better management of coal, especially coal in stockpiles or under transportation.

According to literature review collected from Beamish and Arisoy (2008), Coaltech Research Association (2011), Falcon (1986), Fierro et al. (1999), Harris (1985), Horsfall (1985), Sengupta (1989), there are a number of factors leading to spontaneous combustion such as:

Rank of coal

The rank of coal is known as the degree of maturity or its coalification. This is the outcome of the depth and the intensity of heat experienced in the peat formation. Low rank coal tends to take up O_2 due to the high internal surface area which allows the C/O_2 contact. It is stated that low rank coals are more reactive than the high rank coals due to their high porous structure that allows them to absorb O_2 from its surroundings. The petrographic analysis will be highly important regarded in this aspect.

Moisture content

Coal has the ability to absorb water; therefore every coal has inherent moisture. The content of the water is dependent on the coal maturation. The amount of water in the coal directly affects the heating rate removal, when water vapour condenses, heat is liberated. Coal samples consisting of high inherent moisture content have a higher heating tendency. When dry coal comes into contact with humid air, the coal tends to spontaneously combust due to heats of wetting.

Pyrite content

The pyrite content is a mineral impurity in the coal that causes swelling when oxidised. The reaction between pyrite, moisture and oxygen is exothermic and may lead to the formation of hazardous chemicals such as sulphuric acid and iron sulphates.

Coal particle size

The coal particle size plays a crucial role in spontaneous combustion of coal. A smaller coal particle size has a larger surface area and generates more heat and has higher mass transfer coefficient. Since the oxidation of a coal begins at the surface, the large surface area generating from small particles is not ideal, because this increases the probability of a coal to self-heat.

Porosity

Porosity is the total surface area available and the voids which exist on the surface. This characteristic is very critical in spontaneous combustion, because the voids are a source of storage of moisture and gas which leads to self-heating.

Maceral composition

Oxidation attacks the non-aromatic part of the coal molecule; this more commonly occurs in low rank coals, in liptinite and vitrinite groups of bituminous coal.

Calorific value

The calorific value, also known as the energy value of coal, is the amount of potential energy that could be converted into heat. This means that a coal with a lower calorific value has a lower ability to convert the energy to heat.

Ventilation of coal

Combustion cannot occur without a supply of O_2. O_2 is provided by the numerous openings into old workings, and openings in the stockpile from the different sizes of the coal particles.

Heat transfer coefficient on the bulk surface

The heat transfer coefficient of coal has an inversely proportional relationship with the particle size. When the particle size decreases, it increases the specific surface area which leads to greater rates of reaction thus increasing the heat transfer coefficient of coal.

Coal storage facilities

The storage of low rank coal for a long period of time in an open space can lead to self-heating in the coal. Stockpiles are accessible more to heat and rain exposure than closed bunkers. Both heat and water content makes the coal more prone to self-heat.

Degree of compaction of the coal on a stockpile or dump

The degree of compaction of a stockpile is crucial in restricting the availability of air and effectively preventing self-heating of coal. The reduction of the pore volume between the coal particles will increase the degree of compaction.

2.2.2 Previous Incidents of Spontaneous combustion

The coal industry has had 511 fatalities in 43 incidents between the years 1886 to 2000 (Mine Accidents database, 2015), resulting from different causes such as explosions, rock fall, poison gas, fire, flooding, machinery and outbursts (Figure 5). A list with the information of the disasters can be viewed in Appendix F.

Coal dust is a powdered form of coal which is created during mining. Coal dust has a higher surface area per unit weight when compared to lumps of coal, and is more susceptible to spontaneously combust. The coal dust is explosive when suspended in air (NIOSH, 2012).

The most fatal incidents are closely associated with coal dust explosions. There are grey areas in some incidents in establishing the cause between coal dust and methane.

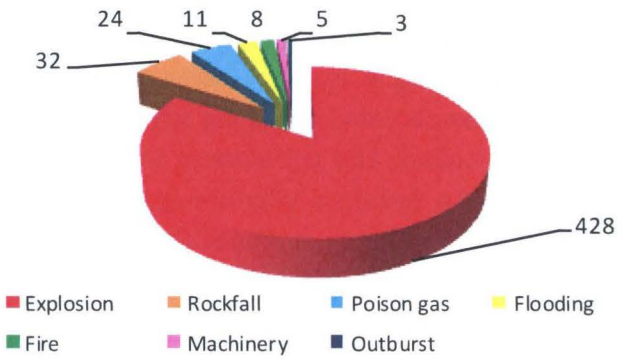


Figure 5: Coal Mine Fatalities Statistics from 1880 – 2000, Mine Accidents database (2015)

From the 428 fatalities occurring due to explosions, 227 (53%) of them resulted from spontaneous combustion (Figure 6). From the 26 explosion incidents, 5 incidents were due to spontaneous combustion arising from coal dust and in some cases a combination of coal dust and gas (Creighton, 2003); more information and pictures on some of the incidents can be viewed in Appendix F. There is little certainty in most reports of the actual causes of the explosion incidents between coal dust and gases, which leads to assumptions being used to conclude. Overall, these figures emphasize the dangers in coal mines due to spontaneous combustion in general.

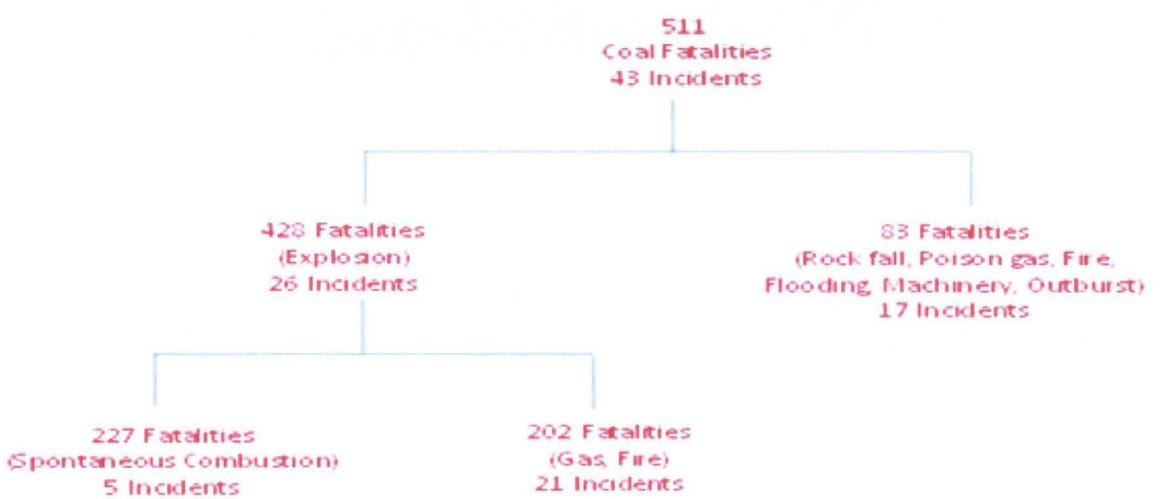


Figure 6: Breakdown of the fatalities, Mine Accidents database (2015)

Spontaneous combustion of coal has been an ongoing problem for decades in South Africa and globally. Countless incidents have occurred throughout the years making this a critical problem. A few cases will be discussed to add emphasizes the intensity of this phenomenon.

2.2.2.1 South African Incidents

Middleburg Colliery Incident

The Middleburg Colliery in South Africa based in the Mpumalanga region has been experiencing spontaneous combustion for over a period of 50 years. The first reported incident occurred in 1947 when the mine was being decommissioned. This occurrence was the end result of the pillar robbing process that was conducted in the 1930 and 1940s. Pillars consist of abundant coal and are normally removed when the mine boundary has been reached. The removal of the pillars causes the mining structure to cave in causing surface tension cracks which allows oxygen to seep through and leads to self-heating in the coal in the remaining pillars (Bell et al., 2001) (Figure 7).



Figure 7: Runaway tension fracture from the area of collapse, due to pillar failure (Bell et al, 2001)

New Vaal Colliery incident

The New Vaal Colliery situated in the Sasolburg Coalfield began mining low rank coal in 1985 and the first underground workings were mined in 1987. The first incidents of spontaneous combustion were reported in 1988. Old workings of unmined coal in the middle seam which were exposed caught fire and a cladding and dozing method was used to stop the fire rapidly within hours. Similar incidents were reported in 1989, and were always near the mouth of the old workings making it easier to extinguish. The fires had spread widely by February 1990, proving the inefficiency of this method; the mine opted to use sand to smother the fire. The sand could not effectively extinguish the fire, that by 1992 the fires became bigger and had consumed the whole length of the main pit, making it extremely dangerous to work on the pit. A decision was taken to buffer blast all areas of concern, by blasting all coal pillars thus sealing the entrance of the workings and preventing air from entering (Stenzel, 2002; Pone et al., 2007).

Kleinkopjie Colliery

The Kleinkopjie Colliery is a low ash metallurgical coal that has been experiencing spontaneous combustion for a lengthy period. The old workings are extensively flooded, from ground water outflow. The underground workings between the northern and southern parts of the operation, at the time, contained eleven million cubic metres of saline, neutral water. Dewatering occurred in time, ahead of mining, but three to four million cubic metres of water remained behind. The dewatering process allowed air to flow between the northern and southern sections, in order to dry the coal. The early dewatering of the area are suspected to have promoted the combustion by exposing the strata to oxygen Spontaneous combustion has been encountered in a localized area since October 1999. The shales above the Number 2 Seam roof are the most liable to spontaneous combustion; the Number 4 Upper and Lower Seams are also prone. It has been an ongoing problem that is currently being managed by cladding the cracks and openings with soil to prevent any admission of O_2 into the subsurface. Jeffrey (2002) gave another solution to this ongoing problem, by total extraction of the coal.

2.2.2.2 Global Incidents

Box Flat Mine, Swanbank (Australia)

The Box Flat Mine incident occurred in 1972 where 17 men lost their lives due to a fire caused by spontaneous combustion. The mine was sealed after the incident and no further inspection and investigation could be performed. A report was released after 99 days after the incident (Jones, 1983) and stated that the fire which occurred was directly initiated by spontaneous combustion.

Kianga Mine, Moura (Australia)

Another incident occurred in 1975 in the Kianga Mine which resulted in 12 fatalities. It found that the explosion was caused by a spontaneous combustion source which ignited flammable gas and which was propagated by coal dust (Loane, 1975). This incident was identical to the Box Flat Mine and was handled in the same manner. A report was issued 87 days after the incident, which stated that an explosion underground resulted from spontaneous combustion (Jones, 1983).

Westray Mine (Canada)

An incident occurred at the Westray Mine in Nova Scotia in 1992, which resulted in 26 fatalities. The coal dust was the hazard in this case; a previous enquiry had been made regarding this problem, but no effective action was taken (Jones, 1983).

Michael Colliery (Scotland)

This particular incident occurred in 1967 in a village of East Wemyss and resulted in 9 fatalities. No evidence could be obtained during the enquiry which led to the conclusion that the fire was initiated by spontaneous heating of coal from the roof of the Loader Mine (Stephenson, 1967). This fire led to the ignition of polyurethane foam that was used in the lining of the roadway (Jones, 1983).

Blair Athol Coal Mine, Australia

The Blair Athol Mine is well known for having difficulties with spontaneous combustion, Figure 8 displays one of the incidents that occurred (Mining Mayhem, 2009).

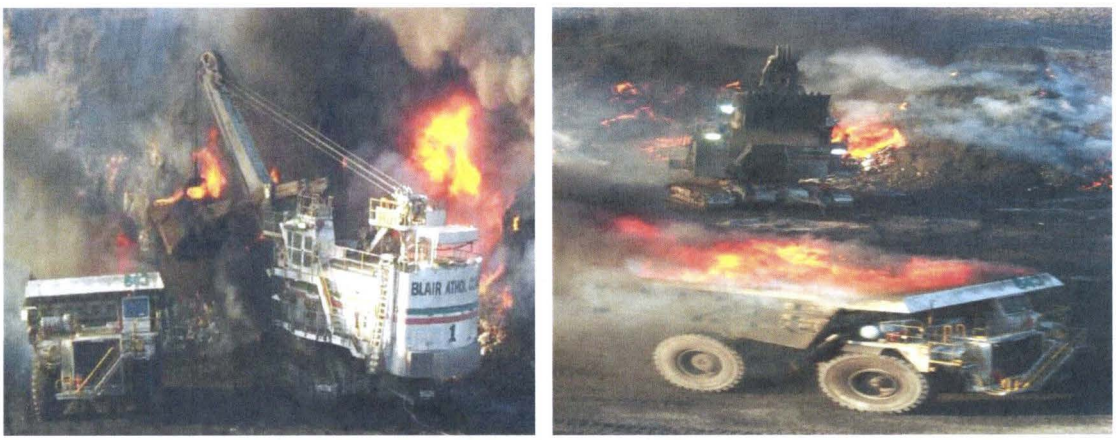


Figure 8: BHP's Blair Athol in Queensland (Mining Mayhem, 2009)

2.2.3 The impacts of Spontaneous Combustion on the environment

The impacts of spontaneous combustion are very severe when it comes to the following (Coaltech Research Association, 2011):

Safety:

- Hazards to mine workers or any person near the fire.
- Potential loss of life or injury.

The environment:

Toxic and flammable gases are released during the oxidation of coal and during spontaneous combustion and these always pose threats such as suffocation, poisoning, and explosions.

Explosive gases that are formed during the oxidation of coal:

- Hydrogen (H_2),
- Carbon Monoxide (CO) and
- Methane (CH_4).

Toxic emission that are released during spontaneous combustion:

- Carbon Monoxide (CO),
- Hydrogen Sulphide (H_2S),
- Sulphur Dioxide (SO_2) and
- Oxides of Nitrogen (NO_x)

Flammable gases that are present in small quantities and serve as indicators of possible threats:

- Ethane (C_2H_6),
- Acetylene (C_2H_2) and
- Ethylene (C_2H_4).

Financial Implications

- Loss of coal exports.
- Loss of equipment.
- Possible redeployment
- Compensation pay out to families that have lost their loved ones.
- Increased difficulty in the coal extraction and beneficiation.
- Decrease in coal quality.

2.3 Previous work done to investigate self-heating coals

There is a lot of evidence in the literature of the establishment of methods of investigating self-heating in coals. Different methods are briefly discussed below to help motivate the choice taken in selecting the TGA method as the method to determine spontaneous combustion liability in the current study.

2.3.1 Static Isothermal Method

The static isothermal method measures the reaction of coal with O_2 (Sevenster, 1961). Smith and Glasser (2005) also used this method and worked on the principle that when the coal adsorbs O_2, the oil in a beaker is displaced due to absorption; this becomes evident by the increase in the oil reading in the pipette. The Smith-Glasser oxidation test used the complete static isothermal apparatus (Figure 9), which consisted of a static isothermal reactor, turntable device, a balance and a computer program to monitor the tests. A blank sample was run with each sample to help compensate for any change in ambient temperature or pressure by taking the reading of the blank sample. The O_2 absorption is calculated as follows:

$$O_2\ absorption\ rate = \frac{\rho_{oil} \cdot V_{oil}}{(MW_{O_2}) \cdot (coal\ sample\ mass) \cdot (time\ period)}$$ ..... Equation 3 (Smith and Glasser, 2005)

Where:

ρ_{oil} = density of the oil (kg/m^3)

V_{oil} = volume of oil absorbed over the specified time period (m^3)

MW_{O2} = molecular weight of O_2 (g/mol)

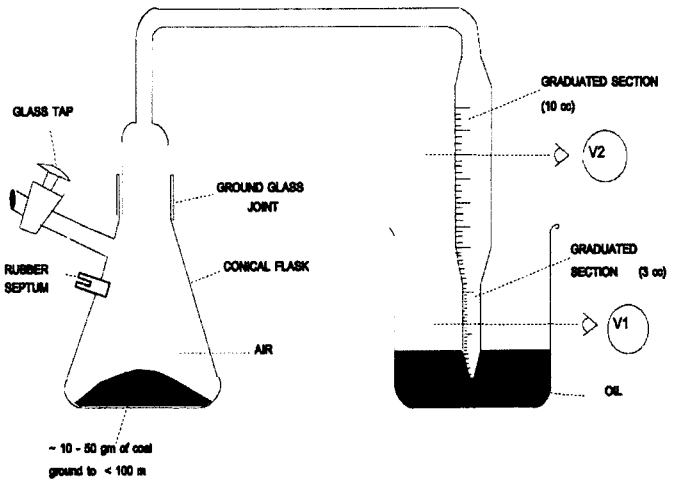


Figure 9: The Smith-Glasser Apparatus (Adamski, 2003)

This self-heating liability determining test is discussed further in Section 3.

There is no clear or specified time set for the duration of the static isothermal method. The duration depends on the coal rank, because lower rank coals tend to react quicker and can have test duration of 4 hours. Some coals take longer to react and can take days before a reaction can be observed. The duration of this method is a major disadvantage.

2.3.2 Adiabatic Calorimetry Method

Luo and Wang (2011) used the adiabatic calorimetry method, which consisted of an insulated reaction container holding a certain amount of coal sample ensuring minimal heat loss (Beamish. et al, 2000). The reaction container was placed in an adiabatic oven. After the sample was preheated and dried in the N_2 atmosphere, pure O_2 was passed through the sample. A thermometer was buried inside the coal sample, while another measures the oven temperature. Ideally, the oven temperature should be controlled to be equal to that of the coal sample to avoid heat exchange between the coal samples. Through such control, it was ensured that all the heat generated by the oxidation of the coal sample was used to sustain the reaction and to raise the temperature of the coal. The R70 self-heating rate index is a measure of spontaneous combustion propensity of coal and is defined as the average temperature increase per hour in the duration for the sample's temperature to increase from

40°C to 70°C temperature (Humphreys, 1981). The R70 test is an example of an adiabatic method (Luo and Wang, 2011).

R70 Method

Beamish and Arisoy (2008) described the R70 testing procedure as a process that uses a 150g sample of <212μm crushed coal that is dried at 110°C under N_2 for approximately 16 hours. While still under N_2, the coal is cooled to 40°C before it is transferred into an adiabatic oven. The coal temperature is then equilibrated to 40°C under the N_2 flow in the adiabatic oven. When equilibrium is reached, the O_2 is then introduced to the sample at a flow rate of 50mL/min.

A data logger records the temperature rise due to the self-heating of the coal. The time taken for the coal temperature to reach 70°C is used to calculate the average self-heating rate for the rise in temperature due to adiabatic oxidation. This is known as the R70 index, which is in units of °C/h. It is a good indicator of the intrinsic coal reactivity towards oxygen. In addition, the data from this test can be used to obtain kinetic parameters for the coal self-heating up to the trip temperature, which is set at 160°C. These kinetic parameters can be used as input to numerical models (Arisoy and Beamish, 2008).

The main disadvantage of this method is that according to R70 standard, 36 hours is required to deem the sample to have low propensity of spontaneous combustion when there is no apparent temperature rise (Luo and Wang, 2011). Therefore this means that 36 hours is required to ensure accuracy in the results and this makes it a lengthy method that requires sufficient time to complete (Figure 10).

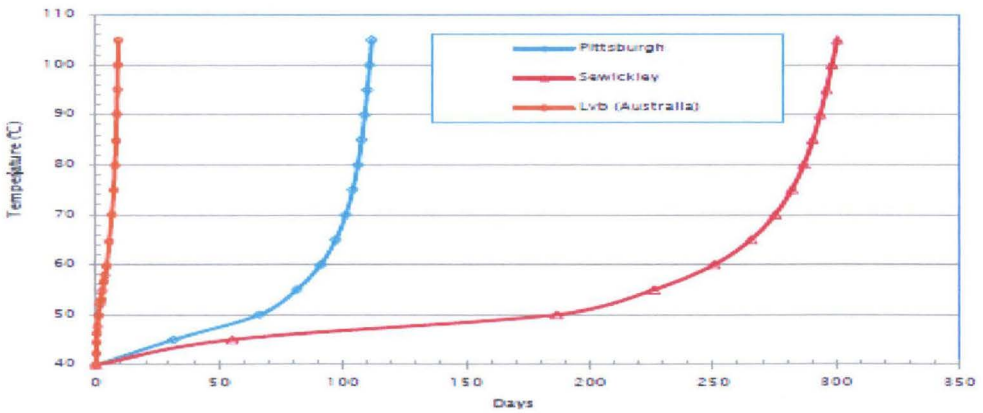


Figure 10: R70 Predicted self-heating curves of samples from the Pittsburg and Sewickley Coal seams illustrating the duration of R70 tests (Luo and Wang, 2012).

2.3.3 Crossing Point Index (CPI)

The main aim of the crossing point temperature (CPI) method is to attain the ignition temperature of the coal by obtaining the lowest temperature in which spontaneous

combustion is likely to occur. According to Sensogut and Cinar (2006), the coal is heated in a reaction tube inside a furnace at constant or temperature ramp of 2°C/h, with O_2 or dry air flowing through at a flow rate of 40mL/min, until the coal temperatures surpass the furnace temperature. The temperature at which the coal and the furnace temperatures match is known as the CPI (Feng et al., 1973). Ignition occurs at a temperature above the cross point temperature (de Korte, 2014).

A Cross Point Index was established by Feng et al. (1973) as follows:

$$CPI = \frac{\text{Average heating rate } 110°C - 200°C}{\text{Crossing point temperature}°C} * 100 \quad \text{..... Equation 4 (Feng et al., 1973)}$$

Coals that have a liability index below 5 are considered low risk to self-heat, those having liability index ranging from 5 – 10 are regarded as a medium risk, and those that have a liability index above 10 are classified as high risk to self-heating.

The disadvantage about this method according to de Korte (2014) is that the test variables need careful selection and all the variables, such as the furnace temperature, temperature ramp, flow rate, used in the test need to be specified.

2.3.4 Wits-Ehac liability Index

The Wits – Ehac Index is a method that uses a crossing-point temperature method and the slope of a differential temperature and time curve to indicate the propensity of coals to spontaneously combust (Uludag, 2007). This method uses the following formula:

$$\text{Wits - Ehac Index} = \frac{\text{slope of stageII}}{\text{crossing-point}}500 \quad \text{..... Equation 5 (Uludag, 2007)}$$

Coals which have a high Wits-Ehac Index have higher chances to spontaneously combust (Gouws and Wade, 1989). This method uses an oil bath, heater, and flow meter for air control, cell assemblies and a data capturing system. The samples are heated and the temperature difference between the coal and the inert reference material is measured and plotted against the temperature of the inert material. This test runs up to 200°C. This method was compared to the Smith-Glasser oxidation test and deemed successful by Uludag (2007). The Wits-Ehac Index values are between three and six, a higher value indicates a coal that is prone to self-heating. This test is not currently available.

2.3.5 Differential Thermal Analysis (DTA)

Several researchers such as Banerjee and Chakravarty (1967) and Gouws and Wade (1989) used the DTA to characterize the thermal changes in coal. Differential thermal analysis involves a method that heats a small coal sample and an inert reference sample at a constant heating rate. The temperature difference between the two samples is measured and used to

obtain the development of the occurring chemical and physical reactions (Avila, 2012; de Korte, 2014).

The coal sample temperature normally rises at a slow rate in the early stages due to inherent moisture, but gains momentum due to the exothermic reaction that occurs from oxidation and surpasses the reference sample temperature (Pattanakik et al., 2011). The differential time is then plotted against time or the temperature of the inert reference sample on a graph known as thermograms (Figure 11).

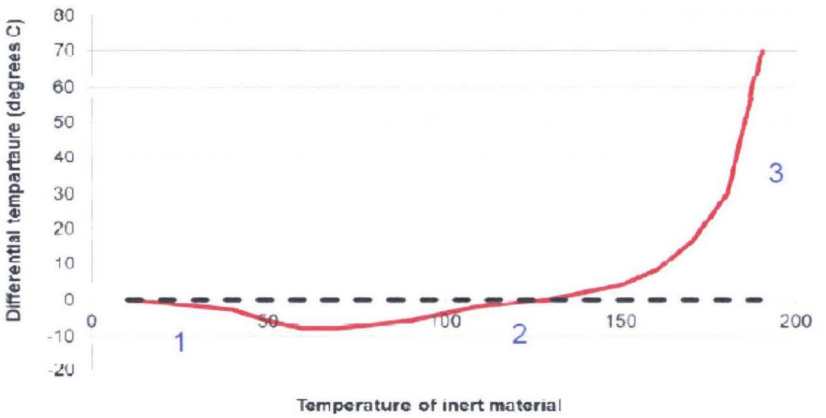


Figure 11: Differential thermograms (de Korte, 2014)

The disadvantages of using this method are that errors can occur if the differential thermocouple beads are not in the symmetrical centre of the cavities. Another form of errors occur if the sample shrinks from the wall of the cup, thus affecting the sample temperature overall (Pask and Warner, 1953). The DTA has limitations in terms of sensitivity, especially when the released heat is too small to detect, this leads to less accurate results when compared to the TGA (Klančnik et al., 2010). It is stated that the reaction or transition is only 20 -50% DTA and that there is uncertainty in heat of fusion (Barlow, 2013).

2.3.6 Mathematical Model

Previous work was conducted by Carras and Young (1994) where a mathematical basis for modelling self-heating in coal stockpiles was utilized. A heat generating mechanism and the heat-loss mechanism was quantified, then the heat overall balance could be obtained. This process not only describes the heat generation rate, but also the transportation of the heat generation rate through the stockpile and the causes on the surrounding environment. Carras and Young (1994) established three equations to describe heat, mass and momentum.

Heat Balance (Carras and Young, 1994)

$$(1 - \varepsilon)\, \nabla T \rho_s c_s (\partial T/\partial t) + \rho_a c_a U * \nabla_T - (1 - \varepsilon)\, \rho_s c_s K\ \nabla^2 T + G = 0 \quad \text{.....Equation 6}$$

Where:

∇T= temperature gradient (K/m)

ε = voidage
ρ = density (kg/m^3)
c = heat capacity of air and dry coal (J/kgK)
K = thermal diffusivity (W/m.K)
G = source term for heat
U = gas velocity (m/s)

This formula gives the rate at which the heat is accumulated or lost, transported and conducted through the coal matrix.

Mass Balance (for a gas e.g O_2 or H_20_g)

$\varepsilon(\partial B/\partial t) + \varepsilon U^* \nabla B - D_B \nabla^2 B + F = 0$ ..... Equation 7

Where:
B = concentration of the gas (mol/m^3)
t = time (s)
F = source/sink term
D_B = diffusion coefficient (m^2/s)

Momentum Balance
$U = (k/\varepsilon\mu)(-\nabla P + \rho g)$ .....Equation 8

Where:

∇P = pressure (Pa/m)

μ = dynamic viscosity (kg/m.s)
k = permeability of coal matrix (m^2/s)
g = acceleration due to gravity (m/s^2)

2.3.7 Thermogravimetric Analysis (TGA) Methods

TGA methods provide the following data: moisture loss, weight gain (which relates the O_2 adsorption) and weight loss (which relates the ignition point of the coal), which are crucial when testing coal's liability to self-heating.

A TA Instruments model Q-50 analyzer was used in the test by Luo and Wang (2011). A coal sample with a 50 mesh (297 μm) was run in the furnace under a specific temperature ramp and oxygen flowrate until a constant sample mass was measured. The test require about an hour to complete the run – a significant advantage over the R70 method (Luo and Wang, 2011). The thermogravimetric (T-G) curve is used to evaluate the propensity for self-heating, by viewing the weight gain during the low temperature oxidation (T_1) and the weight loss due to the occurrence of combustion (T_2). This method claims that a coal that is not likely to self-heat will not gain weight during this period; this is the complete opposite to

the observation made by Avila (2012). Previous TGA tests have not quantified the propensity of the coal to spontaneously combust directly and Wang et al., (2003) had stated that the reaction is too slight for detection by the instrument.

2.3.8 2nd TGA Method

According to Avila (2012), existing test methods for coal's propensity to self-heat focus on the primary parameters such as coal rank, temperature of coal deposits, heat evolution of stockpiles and the surrounding oxygen concentration, but ignore secondary parameters such as mass loss of coal, changes that occur in petrology, and the chemical composition as a result of weathering.

The TGA is still a secondary tool used to identify prone coals; it has the ability to provide the trend of the sample mass linked to changes in temperature. According to the literature reviewed from Sima-Ella (2005), Serageldin et al. (1984), Elder (1983), Kizgut et al. (2004), William (1986), the TGA has the ability to:

- give precise values for degradation temperatures of the coal during the oxidation process,
- quantify the adsorption and desorption of oxygen and quantify reactive or unreactive components of samples.
- assess coal reactivity,
- obtain kinetics parameters of fuels such as reaction order, activation energy and pre-exponential factors,
- calculate reactivity under different atmosphere conditions,
- quantify physical characteristics such as moisture, volatile, carbon and ash content.

Non-isothermal tests calculate the burning profiles of coal and char particles (Norton, 1993) and can be used to predict the operating conditions of industrial reactors. Most of these tests were designed to provide information about the oxidation reaction at high temperatures (Morgan et.al, 1986) (Cumming et al., 1982) and can reveal important information about the self-heating of coal (Serageldin et al., 1984). Marinov (1977) and Earnest (1988) have previously researched two potential non-isothermal tests:

First Test – the different stages of the weight loss can be spotted through a single heating ramp in air. There are several measurable parameters such as percentage of oxygen absorption, water desorption, starting combustion temperature, and peak and burnout temperatures that can be obtained from this test which depend on the applied specific heating rate.

Second Test - the effect of temperature on sample weight can be studied by using an integrated approach and calculating an index independent of the applied heating rate. This is done by performing parallel experiments at different heating rates, using a similar

experimental approach to calculate kinetics parameters by TGA (Wang, 2007). The derivative of the weight loss can also be associated with each heating rate to determine how coal reactivity is affected by changes in temperature. Coal samples could be classified in terms of its propensity to react with air, depending on the extent of the changes in temperature.

Successful attempts using thermogravimetry to estimate propensity of coals to spontaneous combustion have not been reported, and the potential uses of TGA to quantify coal oxidative behaviour represented a research opportunity to develop the method (Avila, 2012).

Avila (2012) used the TGA to predict the self-oxidation of coals, but used a different approach to Luo and Wang (2011), by using five different heating rates (Figure 12). During the early stages of heating, the derivative weight curve shows a linear segment that is approximated by a linear trend as illustrated in Figure 12. The linear stage of derivative weight loss begins after the moisture release occurring between 90°C - 120°C, and completes with an increase in the devolatisation rate that leads to the main combustion reaction occurring between 300°C - 350°C. The linear trend depends on the heating rate and this creates a relationship between the heating rate and mass loss for each sample.

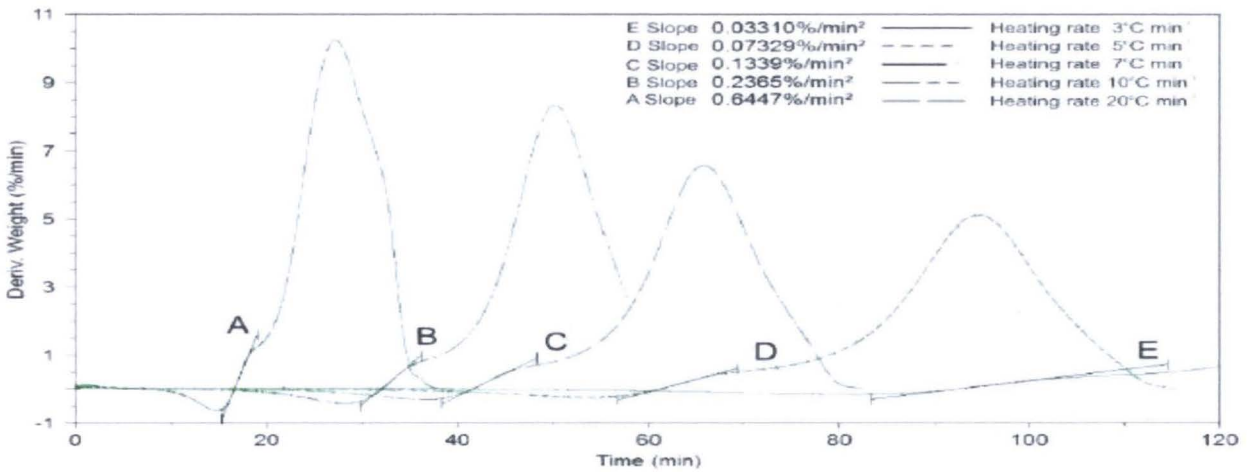


Figure 12: Derivative profiles used to obtain the TG_{spc} index (Avila, 2012)

The slope of the linear segment of the derivative curve is obtained from the different heating rates i.e. Slope A was obtained from the 20C/min heating rate. Avila (2012) used all the heating rate results to obtain the adsorption and ignition points. Five derivative weight curves are used to obtain the slopes of the linear segment, which give the TG_{spc} index (thermogravimetry spontaneous combustion index).

$$TG_{spc} = \frac{\Delta weight\ loss\ rate}{\Delta Temperature}\ (wt\ \%\ ^{\circ}C^{-1}\ min^{-1}) \quad \text{..... Equation 9 (Avila, 2012)}$$

This experiment views the results as: the higher the TG_{spc} index, the more reactive the coal, which will lead to self-heating. The adsorption results (Figure 13) show three characteristic weight loss curves.

- The curve that does not gain any mass is ruled by the desorption stage; this coal is very reactive and most likely to spontaneously combust.
- The curve that gains a little mass is in between desorption and adsorption, so this coal, under specific conditions, might self-heat.
- The last curve that has a huge mass increase is the least reactive coal and will not self-heat. This coal is ruled by the O_2 adsorption.

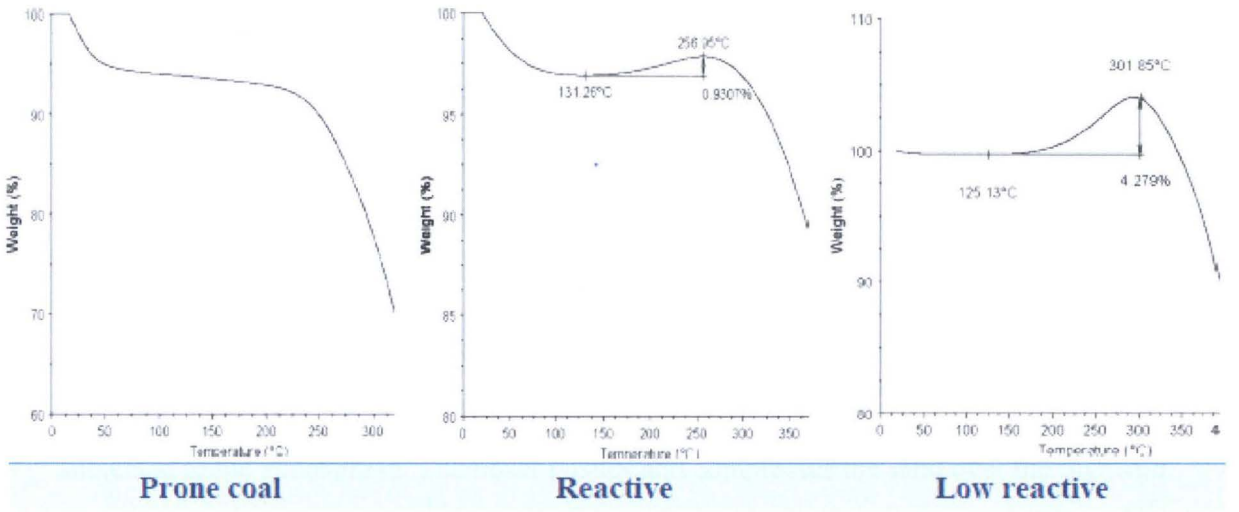


Figure 13: Oxygen adsorption curves illustrating the weight gain (Avila, 2012)

2.4 Prevention of Self-heating in coal

Spontaneous combustion mainly depends on oxidation, heat, time and availability, and therefore if all these three factors are managed effectively, then this problem would be prevented. The first step is to act swiftly when dealing with carbonaceous material by ensuring that, for example, stockpiles do not sit for long periods of time being incorrectly managed, and are well monitored. There is also a need to make sure that coal particles are placed strategically to allow ventilation within the stockpiles, (this can be achieved by storing the different coal particle sizes separately, or limiting the height of the stockpiles, or dissipating the coal materials which have fines) and avoid segregation. Fine coal stockpiles minimise most of the airflow thus decreasing the chances of spontaneous combustion occurring, than when mixed with bigger sized coal particles. Mines need to ensure that dumps are not left unmanaged and that the land is rehabilitated (Adamski, 2003; Yuan, 1991; de Korte, 2001).

2.4.1 Control Measures (Coaltech Research Association, 2011)

Effective control of spontaneous combustion can be achieved by using a combination of techniques. The control measures that can be applied in South African collieries can be listed in three groups:

- Reduction of oxygen
- Reduction of temperature
- Removal of fuel

2.4.1.1 Reduction of O_2 (Coaltech Research Association, 2011)

According to Schalekamp (2006), the control measures to reduce O_2 from the process can be implemented through the introduction of:

Sealing agents:

Sealing agents are not the most practical or economical solution to spontaneous combustion due to the large highwalls (estimation of 2km length x 60m height) that normally require sealing. This type of control uses a mixture of sealing agents such as calcium chloride (CaCl) and binder and filler agent such as bentonite.

Dozing over

Dozing is not the most effective method to control spontaneous combustion as ventilation still seeps through. This method places sand over the highwall in an attempt to close the old workings. This is normally performed immediately after the old workings have been subjected to the atmosphere. The dozer pushes and compresses the sand over the highwall.

Buffer blasting

Buffer blasting is a method used for sealing the old workings before mining commences, the old workings are blasted in a specific site without causing movement as an after effect of the blast. The blasted material collapses and is used to seal openings and limit air movement, thus helping to minimize the liability of spontaneous combustion. The pressure from the blast causes the contained material to forcefully move upward. Buffer blasting can also be used for other applications such as stabilizing the area above the old workings or improving stability of the highwall.

Cladding

Cladding is a method of sealing, which can be introduced in a form of soft material on top of a buffer zone. This method helps minimize the air flow coming into the buffer or inside the buffer. Lack of oxygen will not boost any occurrence of spontaneous combustion. This method however has disadvantages in terms of costs, it requires a lot of work such as loading additional material, levelling the material using a dozer, it is time consuming and all these factors adds to the cost expect.

2.4.1.2 Reduction of temperature (Coaltech Research Association, 2011)

The control measures used to reduce the temperature and thus controlling the reaction rate and spontaneous combustion are through the introduction of:

- Water cannons onto the high wall and in front of the dragline and during cooling, a mixture of water and Pyrocool is used to enhance the cooling effect (this is however an expensive and temporary solution).
- Nitrogen injection into old workings.
- Carbon dioxide injection into old workings, reduces burning rate by more than 20% by volume, replaces O_2, and cools down.

2.4.1.3 Removal of fuel (Coaltech Research Association, 2011)

The removal of the fuel can be done via:
• Excavation of hot or burning material.

2.4.2 Monitoring of Self-heating in coal (Coaltech Research Association, 2011)

The efficiency or success of these control measures is dependent on individual situations, such as mine layouts, the extent of the spontaneous combustion problems, and how the control measure are monitored. Guidelines were set by the Department of Energy in the USA to minimize the liability of spontaneous combustion, as summarized below:

- The heating rate increases with an increase in moisture content.
- Coals that have low calorific value are liable to self-heat.
- Coals that have high oxygen content are liable to self-heat.
- Sulphur plays a role in self-heating of coal.
- Smaller particles of coals are more liable to self-heat.
- Segregation in coal particle size poses a threat as larger particles of coal allows air to seep through and an exothermic reaction occurs when the small particle size coal oxidises.
- An increase in temperature doubles the reaction rate and raises the liability of coal to self-heat.

It is critical to know that a hot spot in freshly mined coal may not be visible for a month or two.

2.5 Chapter Summary

Coal is a high in demand commodity and South Africa is heavily dependent on it as a source of energy. Coal has disadvantages environmentally which creates concern and debates globally on its continuous usage, but also has advantages which are difficult to ignore. It is crucial to understand the quality of the coal in order to handle it efficiently. It is also important to know the intrinsic and extrinsic factors leading to self-heating of coal, in order to effectively manage the spontaneous combustion liability problem of coal. The TGA test as performed by Avila (2012) and the Smith-Glasser test as reported by Smith-Glasser (2005) will be used in this study

CHAPTER 3

3 METHODOLOGY

3.1 Project Plan

The flow diagram illustrates all the work that was performed in this project.

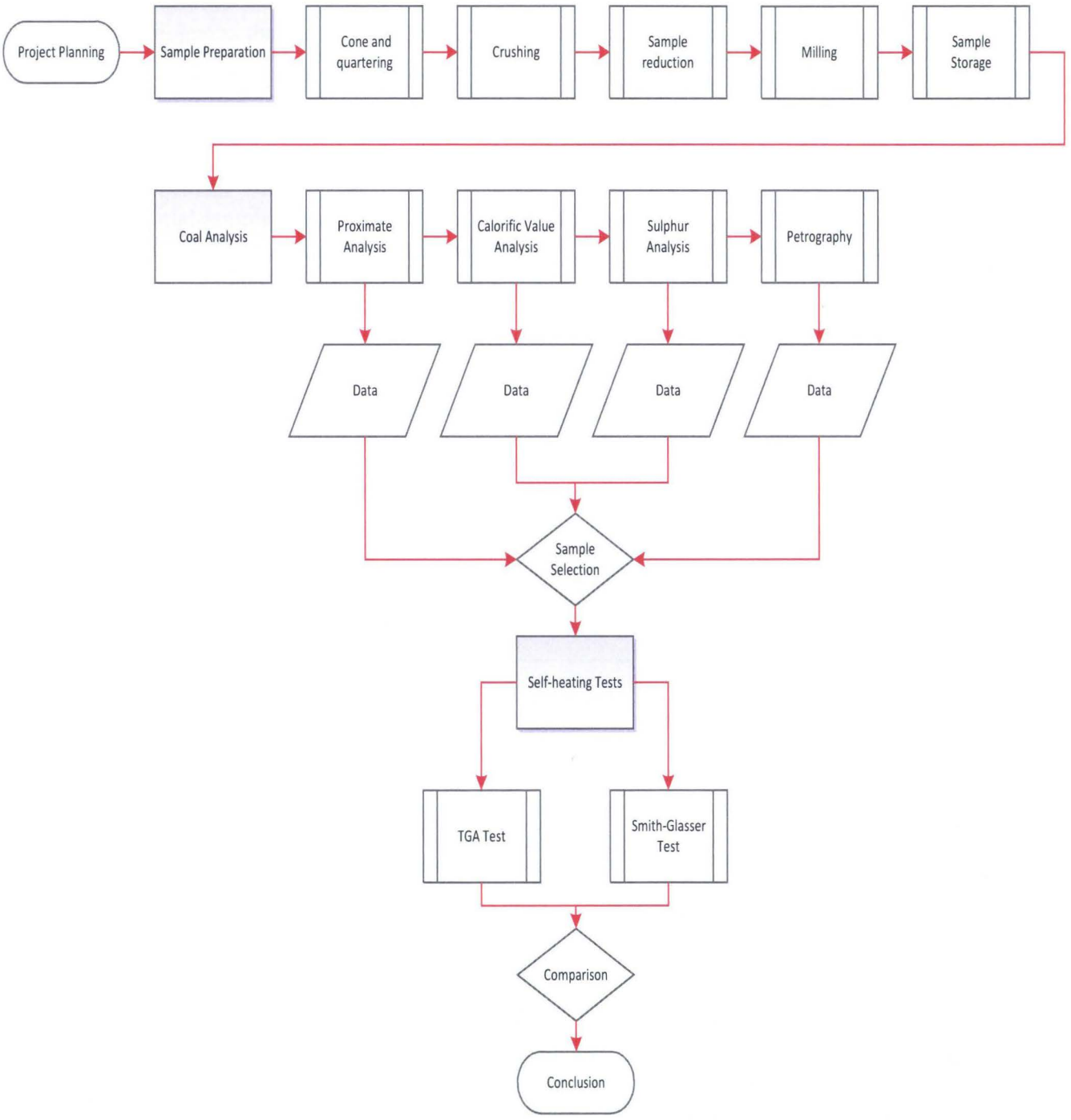


Figure 14: Flow diagram of project plan

3.2 Sample Preparation

3.2.1 Sample origin

A large number of samples were analysed, obtained from a variety of sources around South Africa. Some samples were known to be liable to self-heat, others less so. In total, 29 samples were scheduled to be assessed in this project. All samples were received in 2014. In most instances the sampling procedure is unknown, but this is not really of any consequence for the project as the focus is on the analytical techniques not the individual sample.

3.2.2 Sample Splitting

Large bags of coal were received and required to be reduced to representative samples before crushing sample; this helped avoid the lengthy labour of crushing and milling the entire initial sample. The cone and quartering method was utilized to split the coal samples. This method required a large work space and a large piece of plastic which acts as a working mat for the samples that will help eliminate any chance of sample contamination.

The entire sample is poured into a cone then flatted over the plastic cover. The sample was then divided into quarters and the two opposite quarters were retained for later use (if need be) and the other two quarters were built into a new cone (Figure 15). The cycle can be repeated four times or more depending on the size of the original coal sample.

For this project the cone and quartering procedure was repeated four times for each sample due to the large size of the initial coal samples and to ensure a proper representative coal sample was obtained.

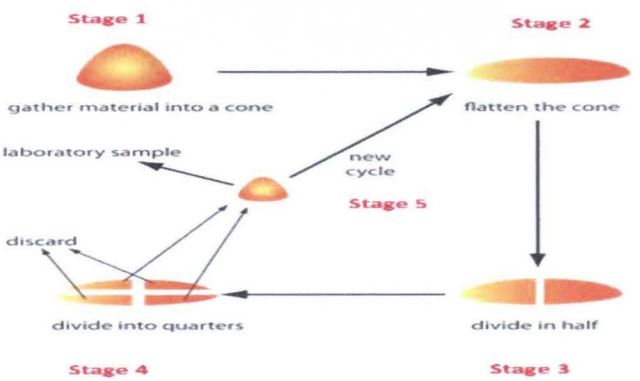


Figure 15: Cone and quartering - splitting method (Harvey, 2000)

3.2.3 Sample Crushing

All representative samples were crushed using a jaw crusher; to a particle size of ±4mm size range. Compressed air was used to blow any entrapped samples inside the jaw crusher and ensured the equipment was clean. A small portion of the sample about to be crushed was

crushed to further clean the jaw crusher ensuring that only the sample remained inside the machine. The representative sample was gradually poured inside the crusher until the entire sample was complete. The crushed sample was then transferred into a labelled plastic bag and sealed.

This procedure was repeated for all samples, especially the cleaning part to avoid contamination during this process.

3.2.4 Sample Reduction

The crushed samples were further reduced to a smaller quantity using an Endecott Riffle Divider (Figure 16). The Endecott riffle divider contains of the main splitting piece and three separating containers. Two containers were placed underneath the splitting piece and a sample was poured into the riffle divider and split into two receiving containers. One half of the sample was stored as a retained sample (for late use if necessary) and the other half was further split. Two containers were assembled underneath the splitting piece again and the 1st half was poured over the splitting piece and split again into two halves. This process was repeated three times; the 3rd half was transferred into a labelled plastic bag and stored for the next step.



Figure 16: Endecott Riffle Divider

3.2.5 Sample Milling

A RETSCH ZM 200 mill was used to mill all 29 samples to their required sizes for analysis. A 250μm screen was used in the mill to acquire the required particle size for the Smith-Glasser test, TGA, proximate analysis, CV and sulphur analysis. A 2mm screen was used to obtain the desired particle size for the petrographic analyses. The mill was cleaned after each run in order to avoid a build-up of sample accumulating inside the instrument, which can lead to a breakdown of the equipment. The milled samples were immediately placed into a labelled plastic container that had a seal on top. Complete insulation of the samples was critical for the spontaneous combustion tests.

3.2.6 Sample Storage

All the milled, sealed and labelled samples were immediately placed in the fridge to minimize oxidation.

3.3 Coal Analysis

3.3.1 Proximate Analysis

The proximate analysis provides information about the moisture content, volatile matter content, ash content, fixed-carbon content.

A Perkin Elmer (PE) TGA was utilized for the proximate analyses determination. The TGA has been explored as a swift, cost effective method for proximate analysis using one technique which is applicable to very small and representative samples, according to Beamish (1994) and Elder (1983). Extensive in-house studies have validated the use of the TGA for proximate determination.

A clean alumina crucible was placed inside the PE TGA stem using a tweezer and a PE TGA lid closed on top and the mass of the crucible was tarred and recorded. The crucible was then removed from the instrument using a tweezer and placed on a clean paper towel. An estimated weight of the sample was poured into the crucible, the crucible was placed back inside the instrument and the sample weight was read from the screen. A required mass of 11mg within ±0.2mg accuracy was required.

Once the correct mass was obtained the sample information was logged into the system. The following settings were logged into the TGA programme for the proximate analysis:

Temperature Program

- Start the run (this action occurs immediately)
- Switch the gas to nitrogen at a flow rate of 40ml/min (when segment starts)
- Hold the temperature for 3 minutes at 30°C.
- Heat from 30°C to 110°C at 30°C/min.
- Hold the temperature for 3 minutes at 110°C.
- Heat from 110°C to 700C at 30°C/min.
- Hold the temperature for 1 minute at 700°C.
- Switch the gas to oxygen at a flow rate of 40ml/min (this action occurs immediately)
- Heat from 700°C to 900°C at 30°C/min
- Hold the temperature for 1 minute at 900°C
- Switch the gas to nitrogen at a flow rate of 30ml/min
- Cool the temperature back to 30°C

The proximate analysis results are obtained from the mass/temperature graph, where different temperature ranges were used to calculate the moisture, volatile matter and fixed

carbon and all three results were subtracted from 100 to obtain the ash content. This was done in the following manner:

As Received Basis

Moisture (%): initial temperature ±30°C – 110°C

Volatile Matter (%): 110°C - 700°C

Fixed Carbon (%): 700°C – maximum temperature ±900°C

Ash content (%) = 100 – (Moisture + Volatile Matter + Fixed Carbon)

The Dry Basis results were calculated as follows (SGS Mining, 2013):

$$Volatile\ Matter\ (d.b) = \frac{100}{(100 - moisture\ content)} * volatile\ matter$$

..... Equation 10

$$\text{Ash content (d.b)} = \frac{100}{(100 - moisture\ content)} * ash\ content$$

..... Equation 11

$$Fixed\ Carbon\ (d.b) = 100 - (volatile\ matter\ (d.b) + ash\ content\ (d.b))$$

..... Equation 12

The dry basis results are used in the data analysis; the TGA graphs can be viewed in Appendix A.

3.3.2 Gross Calorific Value (CV) Analysis

The gross calorific value (CV) of coal is the heat produced by its complete combustion with O_2 per given mass of a fuel. This energy value of coal is the amount of potential energy in coal that can be converted into actual heating ability. The combustion process generates water vapour and certain techniques are used to recover the quantity of heat contained in the water vapour by condensation. The CV of coal can be expressed in two ways, also known as the methods of recovery: The higher CV (Gross Calorific Value) is where the water of combustion is completely condensed and the heat contained in the water vapour is recovered. The lower CV (Net Calorific Value) is when the products of combustion contain the water vapour and the heat contained in the water vapor is not recovered (Thomas, 2002).

This test was performed using the Drycal Modular bomb calorimeter. Calibration was required before any analysis could be performed to ensure the integrity of the instrument;

the calibration process uses a reference standard. A Benzoic Acid Calorific Value Standard in a form of a tablet weighing ±0.4g was used to calibrate the equipment.

One tablet was placed into a crucible and weighed; the mass was immediately logged into the instrument and the sample name was logged as CAL. The O-ring around the bomb cap was thoroughly sealed with a DC4 electrical insulating compound to ensure no air comes in or out of the bomb calorimeter once closed. A string of cotton was hooked onto the ignition wire then placed into the sample (it is critical for a connection to be present between the sample and the ignition wire or the sample will not ignite). The bomb cap was then slowly placed inside the bomb and locked in a clockwise direction. Oxygen gas was run up to 3.5 bars inside the bomb calorimeter. The latch was pushed to completely seal the bomb calorimeter. The bomb was then slowly placed inside the calorimeter; the experiment began immediately after the lid was closed. The calorific value results were obtained from the screen once the run was completed, recorded as MJ/kg.

3.3.3 Total Sulphur Analysis

Sulphur is present in coal is either organically bound combinations or associated with inorganic compounds such as pyrite (FeS_2), and especially in weathered coals as gypsum ($CaSO_4.2H_2O$), and as ferrous sulphate ($FeSO_4.7H_2O$). Significant amounts of other inorganic sulphates and sulphides such as barite ($BaSO_4$) and sphalerite (ZnS) may be present in trace concentrations in some coals. Sulphur is measured in three forms known as sulphate, pyritic and organic. The pyritic form can be partially removed physically prior to combustion, whilst the organic form cannot. The degree to which sulphur can be reduced in coal is primarily dependent on the form of sulphur contained in the coal therefore analytical methods for their accurate determination is crucial (Shimp, et al., 1977).

The total sulphur test is the most commonly test to obtain the sulphur content. The organic sulphur content is obtained from the difference between the total sulphur test and the two inorganic tests (pyritic and sulphate) (Paris, 1977). Total sulphur tests were performed in this project.

The total sulphur analysis was performed using a LECO SC632 instrument. This test requires a particle size of 250μm and a sample between 0.25g and 0.35g. Calibration was required before the instrument could be used especially if it is not operational daily.

The gas (O_2) valve was opened and the instrument was heated from the standby temperature of 650°C to 1350°C with temperature increments of 200°C. A system check is performed and the calibration process begins when the check test reflects that the instrument is ready for use. New crucibles are used to run the blank test; a mass of 1g is logged in and the crucible are analysed as Blank Samples. This test is repeated three times and the results are calculated. The calibration analysis was run after the blank samples. A LECO reference standard sample of 0.25g was weighed and logged into the instrument and run; this process was repeated 3 times and the calibration calculations were performed and saved. The reference standard was analysed again once, to check the calibration outcome. All 29

samples were analysed using the same calibration steps described above, the reference standard was analysed every three samples in order to continuously check the integrity of the instrument. The results reported as %Total sulphur were directly obtained from the LECO SC632 instrument, no calculations were required. The original results can be viewed in the discussion of results.

3.3.4 Petrography

Coal petrography analyses are an important characterization technique to determine a coal's rank (degree of coalification) and type (amount and category of macerals).

Petrography blocks were produced and polished using a Struers Polisher before they were analysed using the Leica DMP4500 reflected light microscope. The original results can be viewed in Appendix E.

3.3.4.1 Petrography Block Preparation

A coal sample of -2mm particle size was poured into a sample cup that has been coated with a thin layer of Vaseline. The coal sample was poured into the sample cup, half filling it. A Struers hardener was mixed with a Struers Epoxy resin in a cup at a ratio of 1:7 (g) and thoroughly mixed with a wooden spatula for a few seconds. The mixture was poured into the sample cup and the whole mixture was thoroughly mixed, ensuring that the Vaseline was not removed on the sides. The samples were stored for over 12 hours to allow them to set.

3.3.4.2 Petrography Block Polishing

The polishing procedure follows repetitive steps with a minor detail of changing the disc and settings required for each stage. The petrography blocks were removed from the cups by dipping the cup in a beaker filled with hot water for a few seconds. Once removed, the petrography block was labelled using an electrical scriber.

The Struers polisher has a maximum capacity of three petrography blocks per run. The blocks were polished using the MD-Fuga (with SIC 500 and SIC1000 grits), MD Firgo, MD Dac and MD Chem discs. Different lubricants were used for the different discs. The samples were rinsed after each run. All 29 samples were polished, rinsed and dried using compressed air. The procedure followed complies with SABS ISO7404 part 2.

3.3.4.3 Petrographic Analysis

Crucial data relevant to this project were the rank, vitrinite content and total reactivity of the coal samples. The petrography results were analysed and interpreted using the guidelines set by Falcon (1986) in Figure 17 to establish the coal's ability to self-heat. SABS ISO7404 part 3 and 5 were applied.

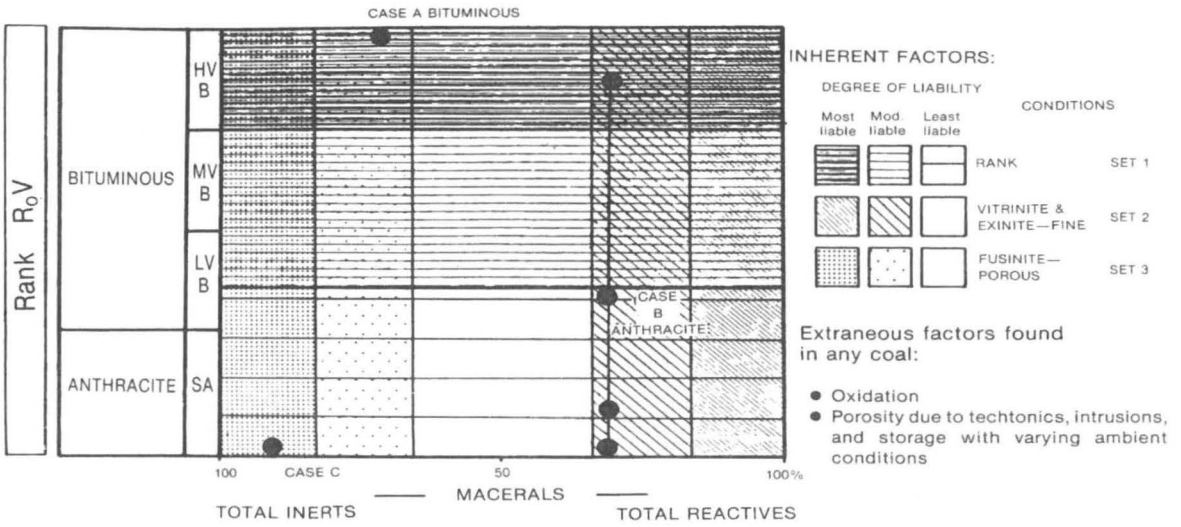


Figure 17: Liability of coals to spontaneously combustion as determined by inherent petrographic characteristics. Cases A, B and C are coals that have undergone rapid spontaneous combustion (Falcon, 1986)

3.4 Self-heating determination

Various spontaneous combustion liability tests have been practiced throughout the years by different researchers and all have a common disadvantage of having a long turnaround time for the analysis. The TGA method is the methodology chosen for this project, mainly due to its rapid analysis capability. In order to achieve the aim and objectives of this project, two test methods are required, namely the TGA adsorption and ignition test from Avila (2012) and the Static isothermal test from Smith-Glasser (2005).

3.4.1 Test 1 - TGA Method (Avila, 2012)

A TGA (TA SDT Q600), different to the one utilised in the proximate analysis, was used for the adsorption and ignition tests. The TGA program was set according to the required method (as stated on the following page), where the data storage was switched on and all the gases used in the test were selected with their flowrates. The instrument was equilibrated and the temperature ramps were started and the isothermal states were included at the required points of the run. The data was saved automatically after the experiment run was completed and can be retrieved from the TA Universal Analysis program.

A total number of 145 tests (29 samples * (3, 5, 7, 10, 20) °C/min temperature ramps) tests were performed in this project.

TGA Program

The following settings were set on the instrument:

- Data storage ON
- Select gas 1 (Nitrogen Baseline)
- Flowrate 70ml/min

- Equilibrate at 30°C
- Isothermal for 1.0 minute
- Select gas 2 (Air Tech)
- Flowrate 100ml/min
- Temperature Ramp of (3,5,7,10,20)°C/min to 400°C
- Data storage OFF

One test per sample was run in the TGA for both the O_2 adsorption (weight vs temperature) and ignition tests (derivative weight vs time curve). The results were obtained by changing the signal on the TG curve settings (Figure 18).

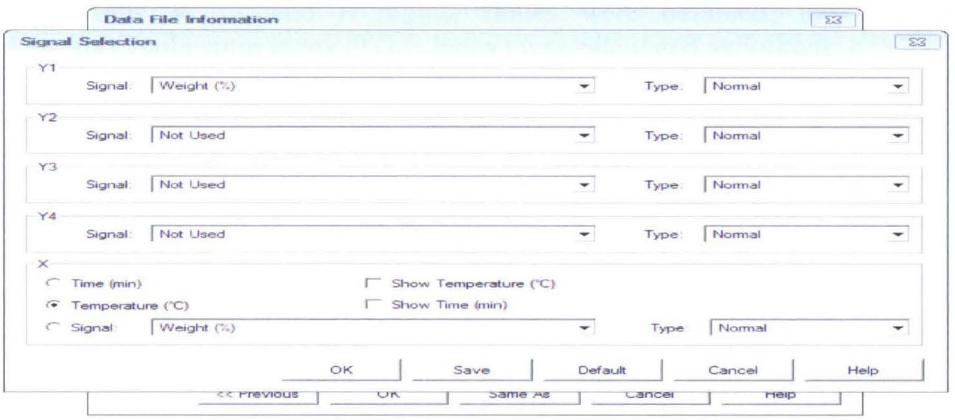


Figure 18: TGA Signal Selection

The ignition test studies the slopes of derivative weight curves between the range of 200°C – 350°C and the derivative weight of zero to sub-zero which is the oxidation area before the ignition point that begins at zero (Figure 19). The ignition point is circled on Figure 19.

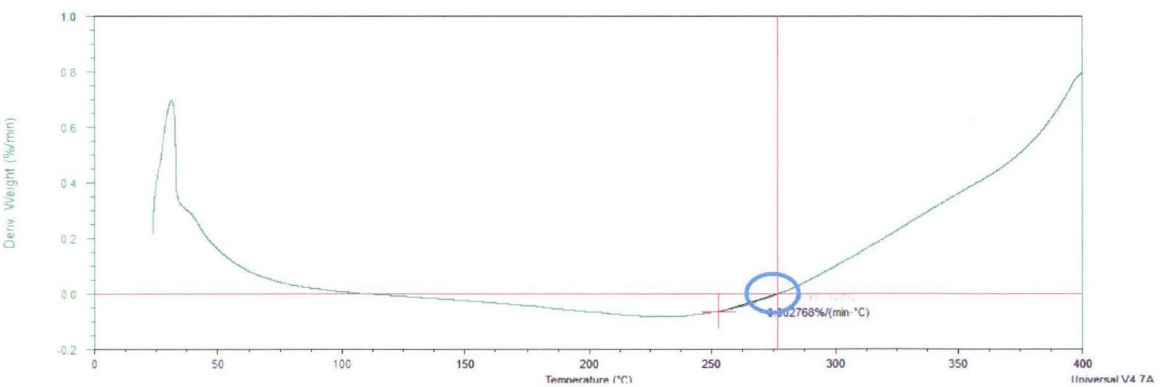


Figure 19: Derivative weight curve showing Ignition point

The ignition results give five derivative weight curves of the five heating ramps (3, 5,7,10 and 20) °C/min, which are used to obtain slopes of linear segment. The slopes of linear segment are plotted in a graph to obtain the R^2 (correlation coefficient) results that is known as the R^2_{graph}. A more detailed explanation is discussed in section 4.4.1.

The same five slopes of linear segment are used to obtain the calculated slopes of linear segments in the following equation:

$$\text{Slopes of linear segment}_{\text{calculated}} = \frac{\text{slope of linear segment}}{\text{temperature ramp}} \text{ (wt\% °C}^{-1}\text{ min}^{-1}\text{)} \ldots\text{Equation 13}$$

The calculated slopes of linear segments were then plotted in a graph to obtain the $R^2_{calculation}$. Equation 9 used by Avila (2012) was simplified to Equation 13 because the slopes were obtained directly from the derivative mass graphs which calculates the mass loss during the oxidation stage until the ignition point, this in the end means the same thing.

Once both the R^2_{graph} and $R^2_{calculation}$ values were obtained, the Thermogravimetry Spontaneous Combustion index (TG_{spc} Index) was calculated as follows:

$$TG_{spc}\text{ Index} = R^2_{(graph)} - R^2_{(calculation)} \text{ (wt\% °C}^{-1}\text{ min}^{-1}\text{)} \quad \ldots\ldots\ldots\ldots \text{ Equation 14 (Avila, 2012)}$$

The original results can be viewed in Appendix B. The TG_{spc} Index formulated by Avila (2012) is not based on previous work done or but on previous theories by. This is the reason why it became critical to validate the method against a well-established Smith-Glasser test.

The oxygen adsorption results give the mass increase of the sample, initial and peak temperature which helps determine the reactivity of the coal sample. The O_2 adsorption test looks at the relationship between the coal mass against the heating rate. The most critical points in the test are:

- the initial temperature - the initial point where the mass begins to gain weight, the initial temperature on Figure 20 has the value of 131.63°C.
- the peak temperature - where the sample reaches the highest mass increase, the peak temperature on Figure 20 has the value of 269.83°C.

These two points indicate the reactivity of the coal and the mass increase value. Further discussion of the O_2 adsorption test is covered in section 4.4.2.

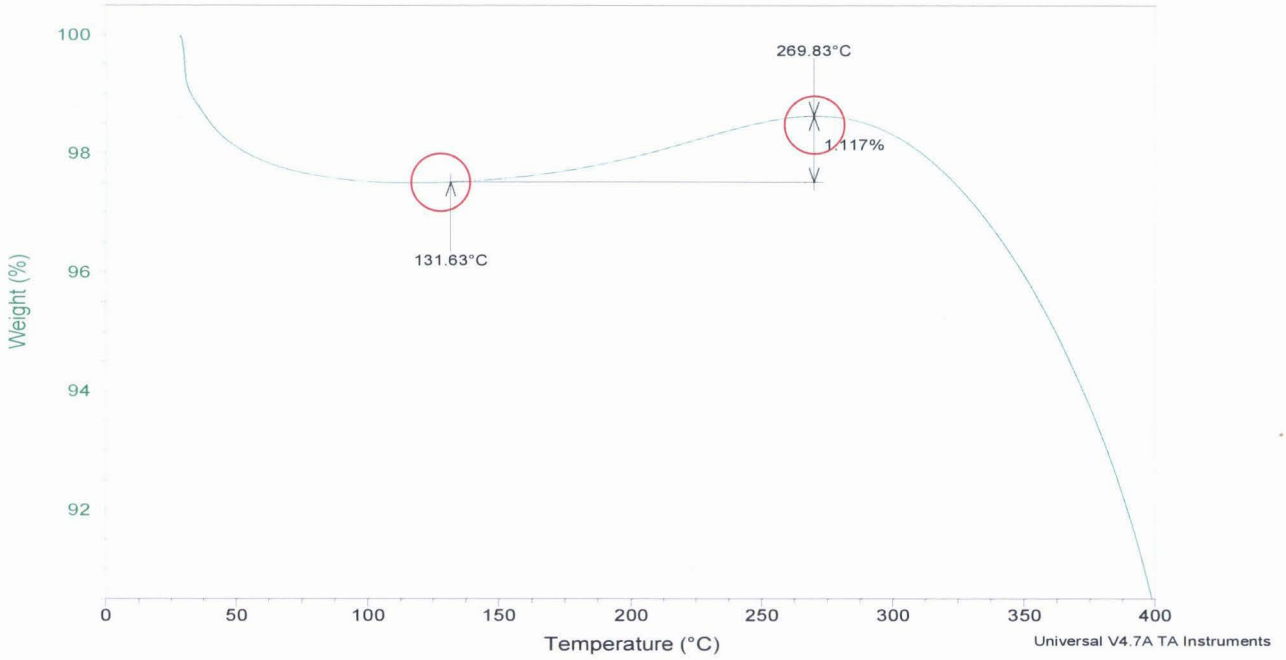


Figure 20: Adsorption Graph showing the Initial and Peak Temperature points

The test runs for the O_2 adsorption test were ramped to a temperature up to 400°C instead of the 500°C set by Avila (2012) because the peak temperature never passed 350°C. The peak temperature averages for all 29 samples were 275°C at 3°C /min temperature ramp, 286°C at 5°C/min, 292°C at 7°C /min, 300°C at 10°C /min and 314°C at 20 °C /min. The peak temperature averages proved that it was not necessary to run the tests up to 500°C. Running all 145 runs to 500°C would have been time consuming and unnecessary because both 400°C and 500°C runs would give the same peak temperature results. This means that the results would not be affected if the test temperature would accidently exceed 400°C.

3.4.2 Test 2: Static Isothermal Method (Smith-Glasser, 2005)

The Smith-Glasser oxidation test (Figure 21) also requires a well prepared sample that was prepared exactly as the samples used in the TGA test. Water was poured into the water bath and set to a temperature of 40°C. While the water heats up, the sample was weighed into the narrow neck flask and flashed with N_2 for a minute. The sample was immediately sealed with a stopper once the minute has elapsed. The narrow neck was then connected to a U-tube that is immersed in oil at one end. Vacuum grease was used to seal the connection of the narrow neck flask and U-tube end. Oxygen was flushed into the sample for a minute and the narrow neck flask sealed and placed inside the water bath set to 40°C. The joint connection was placed inside the water bath and held with clamps to ensure no movement during the test run. The timer was immediately started to record the duration of the test. Readings of the oil displacement are in ml of O_2 absorbed by a given mass of coal per unit of time. Only the selected samples were analysed due to the 48 hour duration of this test.



Figure(s) 21: Static Isothermal Method (spontaneous combustion liability test)

The amount of O_2 absorbed per kg of coal per minute, known as the O_2 absorption rate, was obtained using Equation 3.

The initial plan was to run a few selected samples through the Smith-Glasser test due to its long duration, but the first results did not correspond with the TGA results and the data from the analysis. All the samples were analysed in the end to give more quality assurance before a conclusion was made.

3.5 QUALITY ASSURANCE

Repeatability tests were performed for analysis that had no reference standards in place. The LECO sulphur tests were not repeated because the reference standard results were within specification, which emphasized the accuracy of the results.

All instruments were calibrated before analysis proceeded. The Drycal calorimeter used a Benzoic Acid calorific standard in a form of a tablet. The tablet was run through the same process for all analysis and the results were compared to the certified results.

TGA's were calibrated using the prescribed calibration methods, but no standards were run.

The petrographic analyses were undertaken by an accredited coal petrographer. All analyses were conducted in the Coal Lab School of Chemical and Metallurgical Engineering, University of Witwatersrand.

CHAPTER 4

4 RESULTS AND DISCUSSION

The results obtained from all the tests performed (proximate, CV, Total sulphur, petrographic properties and spontaneous combustion liability tests) are presented and discussed in this section.

4.1 Proximate Analysis

The proximate analyses were performed using the Perkin Elmer TGA, as presented in Table 1, and the graphs are presented in Appendix A.

Table 1: Proximate Analysis Results consisting of both as received basis and calculated dry basis

	Proximate Analysis						
	%As Received Basis				%Dry Basis		
Samples	Moisture	Volatile Matter	Fixed Carbon	Ash	Volatile Matter	Fixed Carbon	Ash
ZM1	3.06	30.05	57.30	9.59	31.00	59.11	9.89
ZM2	3.22	18.49	41.52	36.77	19.11	42.90	37.99
ZM3	2.01	21.56	44.81	31.62	22.00	45.73	32.27
ZM4	2.30	21.18	48.61	27.91	21.68	49.75	28.57
ZM5	2.60	26.92	60.04	10.44	27.63	61. 64	10.72
ZM6	1.87	21.97	54.83	21.33	22.39	55.87	21.73
ZM7	2.31	19.51	42.91	35.27	19.97	43.92	36.10
ZM8	3.39	22.54	59.78	14.30	23.33	61.87	14.80
ZM9	2.44	26.77	47.15	23.63	27.44	48.33	24.22
ZM10	2.20	20.41	45.15	32.23	20.87	46.17	32.96
ZM11	1.82	21.12	44.56	32.50	21.52	45.38	33.10
ZM12	4.24	32.70	52.25	10.81	34.15	54.56	11.29
ZM13	1.85	21.66	41.31	35.19	22.06	42.09	35.85
ZM14	2.32	14.67	22.49	60.51	15.02	23.03	61.95
ZM15	3.59	18.40	48.09	29.93	19.08	49.88	31.04
ZM16	2.43	18.01	35.77	43.79	18.46	36.66	44.88
ZM17	2.69	24.15	54.01	19.15	24.82	55.50	19.68
ZM18	1.71	20.47	42.66	35.15	20.83	43.40	35.77
ZM19	3.20	17.15	50.89	28.77	17.71	52.57	29.72
ZM20	1.73	16.82	41.74	39.71	17.12	42.48	40.41
ZM21	1.43	18.51	37.65	42.42	18.77	38.19	43.03
ZM22	1.00	14.78	19.74	64.48	14.93	19.94	65.13
ZM23	2.36	23.50	57.75	16.39	24.07	59.15	16.78
ZM24	1.86	16.67	30.15	51.32	16.99	30.72	52.29
ZM25	3.18	23.88	64.91	8.03	24.67	67.04	8.29
ZM26	4.82	25.20	55.10	14.88	26. 48	57.89	15.64
ZM27	1.19	21.23	29.56	48.02	21.48	29.92	48.60
ZM28	3.86	20.71	41.94	33.49	21.54	43.62	34.84
ZM29	0.27	16.04	35.83	47.86	16.08	35.93	47.99

Samples that have high inherent moisture have a higher heating tendency, as discussed in Section 2.2.1. Coal samples that have high ash content are in some cases liable to self-heat. The ash content in the coal is known to reduce the tendency of coal to self-heat, but some elements in the ash (iron, lime, soda compounds) might have accelerating effects, while other elements (silica and alumina) produce an impeding effect (Coaltech Research Association, 2011). This, therefore, means that the ash content is not a definitive indicator of liability of coal to self-heat. A high ash coal is usually designated as one having an ash content above 25% before washing and an ash content between (10 – 15)% after washing (Schernikau, 2010) and majority of the 29 coal samples have high ash content. The Coal Marketing International (2012) published the changes in coal properties as the coal changes rank and states that Bituminous coal has a volatile matter content ranging between 22 – 31% while (Schernikau, 2010) estimates 22 – 35% volatile matter. This means that majority of the analysed 29 coal samples are likely to self-heat when using these guidelines.

Majority of the literature does not give standard values to classify 'high or low' volatile matter, moisture or ash, therefore assumptions based on the results were utilised. The proximate analysis results illustrated that when the volatile matter value is above 24% (deemed high), the moisture value of that particular sample will be above 2% (deemed high) and the ash content above 10% (deemed high). From the 29 coal samples tested, only 8 coal samples (ZM1, 5, 9, 12, 17, 23, 25 and 26) had high moisture, volatile matter and ash all together at once.

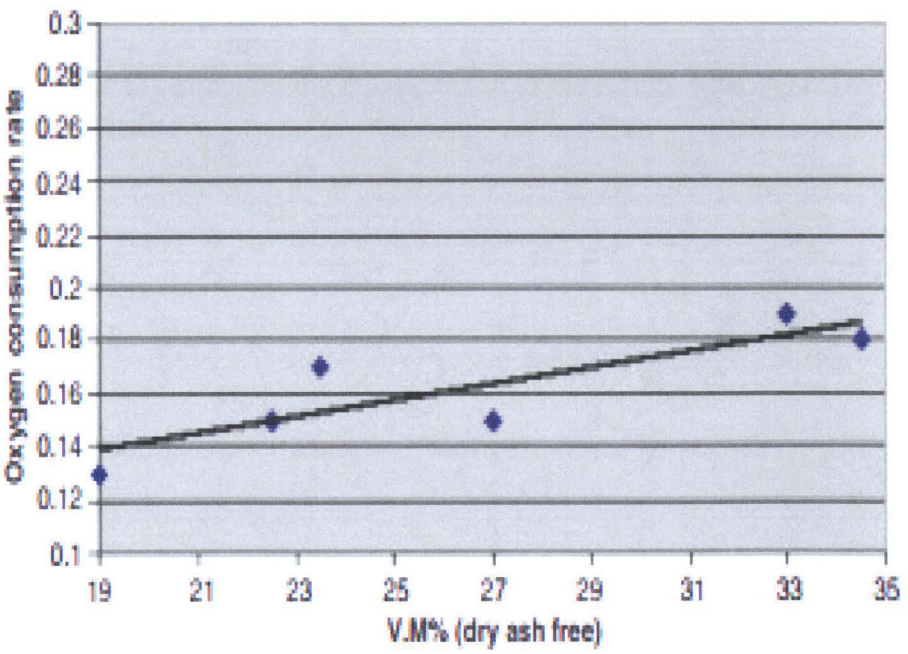


Figure 22: Rate of oxidation and volatile matter content (Uludag, 2007)

There is a direct proportional relationship in most cases between the inherent moisture, volatile matter and ash content, and from literature, all these factors may impact on spontaneous combustion liability. Theory states that the volatile matter is vital when dealing

with self-heating in coal. According to Uludag (2007), the rise in volatile matter increases the O_2 consumption (Figure 22), which increases the reaction rate, which will lead to self-heating of the coal. Thus, the 8 samples that are highlighted in Table 1 would be deemed highly reactive in terms of self-heating.

4.2 CV and Sulphur Analysis

Sulphur content is one of the indicators used to predict the liability of a coal to self-heat. Samples that have low sulphur content have low impurities and are not prone to self-heat, therefore sample ZM12 has a high potential to self-heat (Table 2); Sample ZM12 has the highest volatile content (Table 1) of all the samples and the highest sulphur content as well. In fact, all the samples that have high volatile content also have high sulphur content except for sample ZM25.

The classification of coal, according to Truś (2010), is that hard coal has a gross calorific value greater than 23.865 MJ/kg and a mean random reflectance of vitrinite of at least 0.6. Sub-Bituminous Coal has a gross calorific value of 17.435 – 23.865 MJ/kg and a mean random reflectance of vitrinite less than 0.6. Lignite/Brown Coal has a gross calorific value less than 17.435 MJ/kg and a mean random reflectance of vitrinite less than 0.6.

The 8 coal samples discussed in section 4.1 which had indicated a liability to self-heat having high volatile, high moisture and low ash are also having the same indication in the CV and sulphur results. All the 8 samples are having high CV and high sulphur, which was the expected outcome from the results.

Section 4.7 (Table 13) discusses the interpretation of the results with regards to self-heating liability in more detail.

Table 2: Calorific Value and Sulphur content results

Samples	CV (MJ/kg)	Sulphur (%)
ZM1	27.02	2.290
ZM2	16.19	1.110
ZM3	18.65	1.400
ZM4	19.62	1.160
ZM5	26.24	1.470
ZM6	22.25	1.810
ZM7	17.04	0.290
ZM8	25.22	0.891
ZM9	21.55	1.620
ZM10	17.72	0.915
ZM11	16.89	1.250
ZM12	25.97	2.660
ZM13	17.62	2.400
ZM14	6.47	0.229
ZM15	17.98	0.355
ZM16	12.85	0.862
ZM17	22.99	1.730
ZM18	16.51	1.450
ZM19	19.49	0.273
ZM20	15.01	0.446
ZM21	13.42	0.714
ZM22	5.85	0.804
ZM23	24.02	0.812
ZM24	17.75	0.862
ZM25	26.26	0.700
ZM26	23.06	1.620
ZM27	12.73	0.867
ZM28	16.26	0.600
ZM29	15.00	0.647

4.3 Petrographic Analysis

Table 3: Petrographic analysis results

Petrography					
Samples	Mean maximum reflectance of vitrinite % (calculated)	Total Reactive Macerals (vol%)	Vitrinite (vol%)	Liptinite Content (vol%)	Inertinite Content (vol%)
ZM1	0.74	66	54	5	35
ZM2	0.78	22	8	6	48
ZM3	0.69	40	29	6	39
ZM4	0.67	44	25	6	48
ZM5	0.66	59	40	6	47
ZM6	0.70	40	19	4	60
ZM7	0.72	33	16	3	51
ZM8	0.74	47	27	4	60
ZM9	0.69	62	48	8	24
ZM10	0.73	37	23	4	45
ZM11	0.69	27	12	3	53
ZM12	0.68	74	60	7	27
ZM13	0.70	44	33	4	35
ZM14	0.78	15	9	2	25
ZM15	0.85	31	14	4	52
ZM16	0.75	24	13	3	42
ZM17	0.67	57	41	7	40
ZM18	0.72	34	21	2	34
ZM19	0.76	35	13	2	63
ZM20	0.79	28	14	2	46
ZM21	0.75	34	20	4	37
ZM22	0.63	16	11	2	11
ZM23	0.68	53	40	4	45
ZM24	0.67	44	36	3	30
ZM25	1.20	29	19	4	77
ZM26	0.63	45	29	8	63
ZM27	0.65	68	47	17	36
ZM28	0.61	36	28	5	67
ZM29	0.99	60	55	2	43

According to Hackley et al., (2008), the mean maximum reflectance ranging between 0.54-0.95 % indicates the coal rank of high volatile bituminous. This seems to be the case with all the coal samples analysed (Table 3); all the samples have a mean maximum reflectance of above 0.6% and 18 coal samples have volatile matter content above 20%.

Sample ZM12 reports the highest total reactive macerals, which is another potential indication that this sample is liable to self-heating. The mean random reflectance of vitrinite is consistent through all the samples, all being Medium ranked bituminous coals, apart from sample ZM25; this sample falls into the High rank bituminous coal category, and may be therefore less likely to self-heat. Sample ZM27 is the only sample with liptinite content above 10%.

4.4 Self-heating Test: TGA

4.4.1 Ignition Test

Table 4 numerically displays the derivative slopes obtained at different temperature ramps from derivative curves (example in Figure 21), which are then combined and plotted into a graph (Figure 22) in order to obtain R^2_{graph} and $R^2_{calculated}$. All 5 derivative mass slopes (3°C, 5°C, 7°C, 10°C and 20C°) are required in order to calculate the TG_{spc} Index. The thermogravimetry spontaneous combustion index (TGspc Index) is calculated using R^2_{graph} and $R^2_{calculated}$.

Table 4: Five different temperature ramps (%/min) used to determine the derivative curve slopes

Samples	Temperature Ramps °C/min				
	3	5	7	10	20
ZM1	0.004256	0.009946	0.012670	0.019770	0.067020
ZM2	0.004042	0.009143	0.014810	0.021240	0.059220
ZM3	0.001132	0.005416	0.022280	0.046650	0.147000
ZM4	0.004433	0.008328	0.012830	0.027660	0.069850
ZM5	0.002533	0.005877	0.013290	0.041550	0.133100
ZM6	0.004769	0.008312	0.020580	0.027710	0.110800
ZM7	0.005342	0.008725	0.016010	0.028280	0.077100
ZM8	0.005904	0.011800	0.021400	0.037600	0.098200
ZM9	0.003166	0.005878	0.017500	0.033580	0.104800
ZM10	0.005967	0.009623	0.015940	0.029390	0.075190
ZM11	0.004516	0.008896	0.014740	0.028380	0.070180
ZM12	0.003189	0.005220	0.014920	0.033860	0.093750
ZM13	0.003838	0.007690	0.014270	0.029940	0.079450
ZM14	0.001223	0.003775	0.007051	0.008845	0.040490
ZM15	0.002916	0.006087	0.009402	0.018430	0.047170
ZM16	0.002308	0.006863	0.013530	0.019020	0.071270
ZM17	0.005108	0.011340	0.015600	0.036600	0.101400
ZM18	0.005639	0.009254	0.015540	0.029020	0.070580
ZM19	0.005540	0.012120	0.018820	0.028110	0.071510
ZM20	0.003350	0.006816	0.012770	0.021880	0.058170
ZM21	0.001690	0.005445	0.012110	0.02060	0.06096
ZM22	0.002765	0.005235	0.010110	0.021140	0.054450
ZM23	0.001919	0.010070	0.013800	0.027660	0.086270
ZM24	0.001505	0.006634	0.008190	0.020360	0.058970
ZM25	0.005122	0.015440	0.018420	0.042410	0.116300
ZM26	0.009476	0.019210	0.030540	0.049340	0.124600
ZM27	0.005265	0.011410	0.016160	0.024430	0.064050
ZM28	0.001780	0.006773	0.010500	0.029870	0.082560
ZM29	0.004742	0.008402	0.020130	0.027440	0.089890

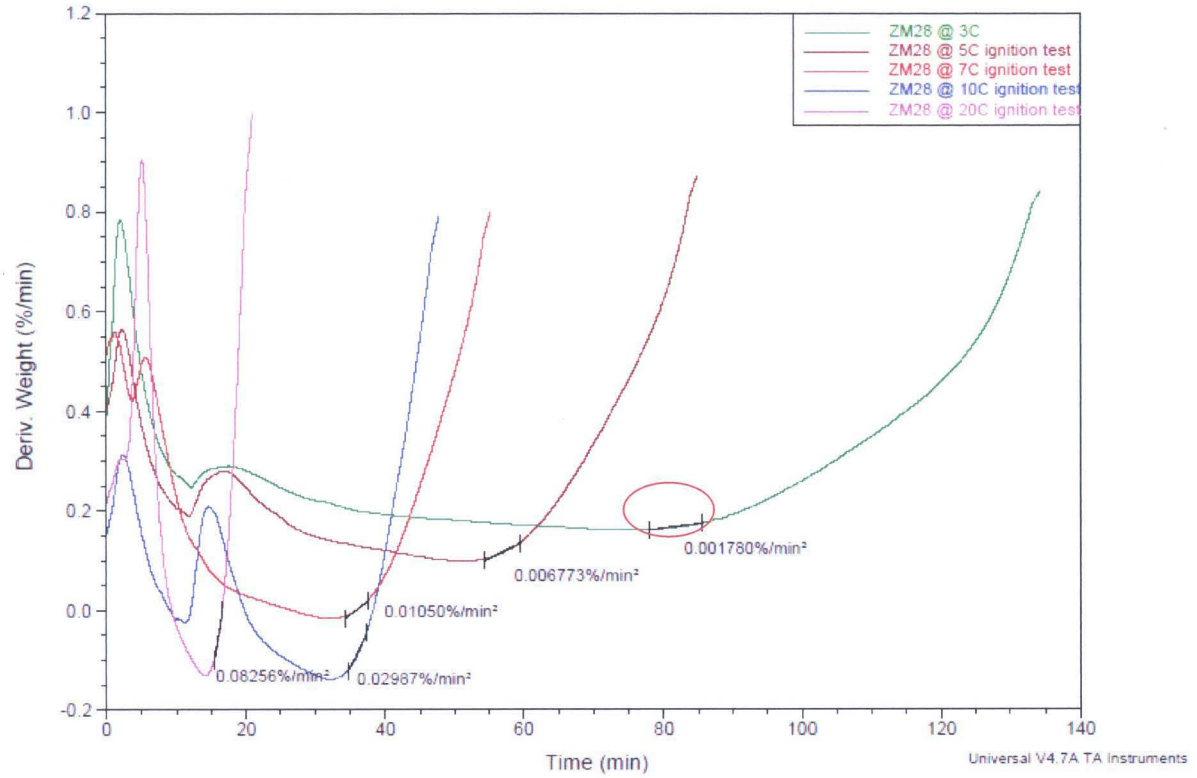


Figure 23: ZM28 Derivative weight curve at different temperature ramps (%/min)

Figure 23 illustrates that an increase in temperature ramp increases the reaction, and the reaction is quickest at 20°C/min.

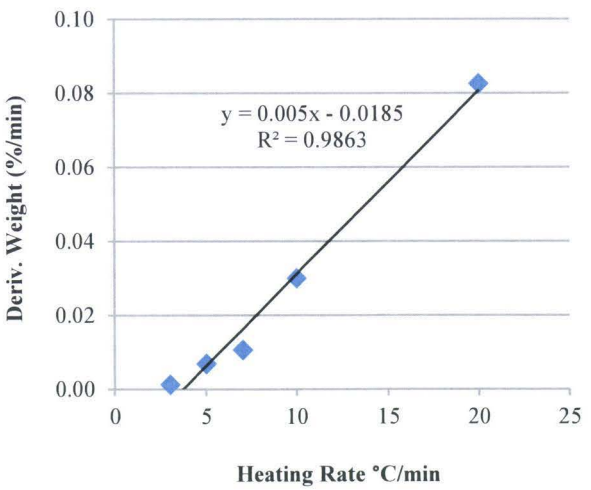


Figure 24: ZM 28 Slope of derivative weight curves (Linear segment) used to obtain used R^2 graph

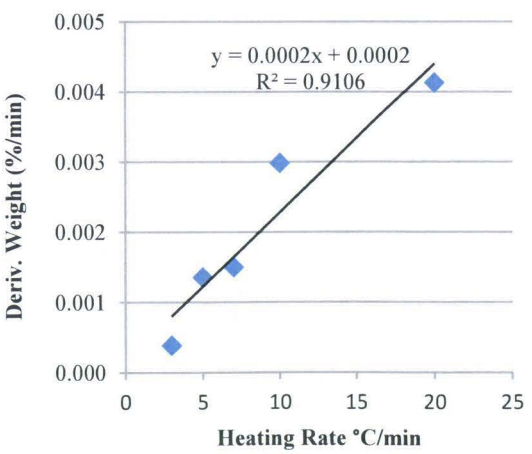


Figure 25: ZM 28 Calculated slope of derivative weight curves used to obtain $R^2_{calculated}$

The slopes of linear segment are obtained from the circled points in the graph in Figure 23; they are used to obtain the R^2_{graph} from the derivative weight curve. All five slopes of linear segment from the different heating ramps are then plotted into a graph (Figure 24) and used to obtain are R^2_{graph}. $R^2_{calculated}$ is obtained using Equation 13, using the slopes of linear segment from the graph, which divides the slopes of linear segment from Table 4 by the temperature ramps to obtain new (calculated) slopes of linear segment. The calculated slopes of linear segment are then plotted into a graph (Figure 25) to obtain $R^2_{calculated}$.

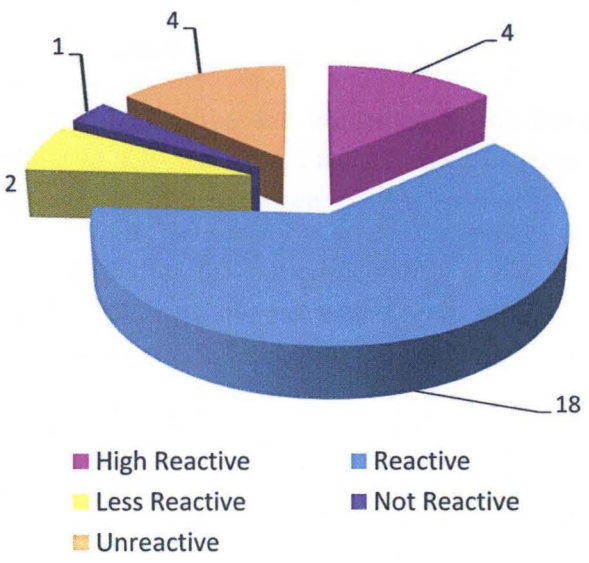
Table 5: TG_{spc} Index values for all coal samples

Samples	Graph	Calculated	TG_{spc} Index
	R 2	R 2	
ZM1	0.9682	0.9227	0.0455
ZM2	0.9893	0.9244	0.0649
ZM3	0.9868	0.9320	0.0548
ZM4	0.9890	0.9296	0.0594
ZM5	0.9754	0.9580	0.0174
ZM6	0.9626	0.9517	0.0109
ZM7	0.9883	0.9656	0.0227
ZM8	0.9932	0.9477	0.0455
ZM9	0.9838	0.9507	0.0331
ZM10	0.9901	0.9501	0.0400
ZM11	0.9934	0.9311	0.0623
ZM12	0.9868	0.9154	0.0714
ZM13	0.9898	0.9407	0.0491
ZM14	0.9520	0.9372	0.0148
ZM15	0.9916	0.9493	0.0423
ZM16	0.9708	0.9561	0.0147
ZM17	0.9834	0.9496	0.0338
ZM18	0.9926	0.9245	0.0681
ZM19	0.9947	0.9098	0.0849
ZM20	0.9928	0.9463	0.0465
ZM21	0.9904	0.9252	0.0652
ZM22	0.9908	0.9237	0.0671
ZM23	0.9834	0.9209	0.0625
ZM24	0.9835	0.9169	0.0666
ZM25	0.9847	0.9104	0.0743
ZM26	0.9947	0.9569	0.0378
ZM27	0.9912	0.9298	0.0614
ZM28	0.9863	0.9106	0.0757
ZM29	0.9786	0.9261	0.0525

As previously discussed in section 2.3.8, the derivative weight loss was linked with each heating rate to help determine how changes in temperature affect the coal reactivity. Coal samples were classified in terms of their propensity to react with air, on condition to the changes in temperature (Marinov, 1977; Earnest, 1988). The TG_{spc} index was formed based on this theory by Avila (2012).

Samples with a high TG_{spc} index are prone to self-heat if their O_2 adsorption mass increase values are low (Avila, 2012). The 8 highlighted samples (Table 5) showed correlation with the coal characterisation analysis (total reactive macerals, sulphur, volatile matter, gross calorific value) in the ignition test results. However, looking at the TG_{spc} index values only (Table 5) was not enough to predict the liability of the coal to self-heat; therefore one had to take into account all the information that could be derived from the TGA method, such as mass increase, peak temperature and coal reactivity (Marinov, 1977; Earnest, 1988).

The known high reactive coals samples were ran through the TGA by Avila (2012) and resulted amongst the highest TG_{spc} index values and the known low reactive coals resulted amongst the lowest TG_{spc} index values. The results correspond with the data relating to spontaneous coal fires caused by the coals. The results also agreed with other experimental tests carried out such as the crossing point temperature test and rank analysis. This correlation of results led to the outcome of the guidelines set by Avila (2012) in Table 6.



TG_{spc} Index		
High Reactive	:	0.070 >
Reactive	:	0.036 – 0.069
Less Reactive	:	0.030 – 0.035
Not Reactive	:	0.020 – 0.029
Unreactive	:	0.00 – 0.019

Figure 26: Coal Sample Reactivity using the TGspc Index as a guideline set by Avila (2012)

Table 6: Coal Reactivity Guidelines (Avila, 2012)

Figure 26 illustrates the reactivity of all the coal samples used in this project. The coal reactivity guidelines (Table 6) indicates that only 4 samples (ZM 5, 6, 14 and 16) from the total of 29 samples will not self-heat as they have a TGspc Index value between 0.000 – 0.019, which is deemed unreactive by the coal reactivity guidelines. However, not all these samples fully agree with the coal characteristic analysis (total reactive macerals, sulphur,

volatile matter, gross calorific value) prediction, as illustrated in Table 7. From theory one expects samples that have high total reactive macerals, high volatile matter, high sulphur, high ash and high moisture content to self-heat, and samples ZM5 and ZM6 TG_{spc} index results are not in agreement with these facts. Guidelines for all the self-heating determination tests performed and coal characteristics analysis are further discussed in section 4.7 (Table 13), gives values to 'high' and 'low' terms to the coal characteristics analysis.

Samples ZM14 and ZM16 coal characteristics data indicate that they are not likely to self-heat and the TG_{spc} index agrees fully with the data. The TGA method results indicate that the rest of the samples are liable to self-heat, but at different reaction rates.

Table 7: Agreement of guidelines with all the petrography and proximate analysis

Samples	Agreement with Analysis (Total Reactive Maceral, Moisture, VM, Ash, CV & Sulphur)	Total Reactive Macerals (%)	Moisture (%)	Volatile Matter [d.b] (%)	Ash [d.b] (%)	CV (MJ/kg)	Sulphur (%)
ZM5	Poor	59	2.6	27.6	10.7	26.24	1.47
ZM6	Poor	40	1.9	22.4	21.7	22.25	1.81
ZM14	Very Good	15	2.3	15.0	62.0	6.47	0.23
ZM16	Very Good	24	2.4	18.5	44.9	12.85	0.86

4.4.2 O_2 Adsorption

Avila (2012) stated that according to the theoretical reaction mechanism, highly reactive (liable to self-heat) coals are expected to show the highest weight gain, due to a potential 'affinity' to absorb oxygen.

However, after the experimentation Avila (2012) showed that, when a weight increase occurs following exposure to O_2, it was considered an endothermic stage in which O_2 molecules were adsorbed on the coal surface forming coal-oxygen complexes. However, at early stages (below 100°C) the adsorption reaction was masked by water desorption. According to the mechanism, the adsorption reaction was also restricted by the temperature range and the availability of reactive sites. The last stage was controlled by available free active sites, created by desorption of water molecules from the coal surface. This somehow explained the variances for the different coals samples during the TGA experiments, and the weight increase above 100°C.

When there was no weight increase, or little weight increase, it was regarded as desorption of water molecules. This was considered to be an exothermic reaction, which generates the majority of the heat responsible for the overall temperature rise in the coal sample. This reaction was also restricted by temperature range, depending on the stability of the complex solids formed. Coals prone to spontaneous combustion experienced a problem with water desorption when the coal-oxygen complexes headed the entire process. The stability of the solids complex was critical since the desorption reaction was fundamental. Less stable solid

complexes were desorbed at low temperatures, thus reacting exothermally with the oxygen gas to produce CO, H_2O and CO_2, which increased the temperature around the particles and finally increased the rate of the reaction (Wang, 2002). On the other hand, when the solids complexes formed were stable, the temperature range was wider and the peak temperatures were higher, producing a higher weight increase and a lower rate of reaction.

Samples that had a low mass increase tended to have a low initial and peak temperature (as previously explained in Figure 20), because the reaction rate occurred swiftly and there was no time for build-up; and these samples were liable to self-heat. Samples that had a high mass increase took a long time to react and this created the build-up hence the high peak temperature; these types of samples had a low reactivity and were less to self-heat. However, if these coals are not managed properly they may still self-heat over long periods of time and under unfavourable conditions.

As previously discussed, the TGA O_2 adsorption results are obtained from the O_2 adsorption graph, as illustrated in Figure 27. The initial and peak temperature can be read off and the mass increase is obtained from the circled area on the graph. All the raw data is included in Appendix B.

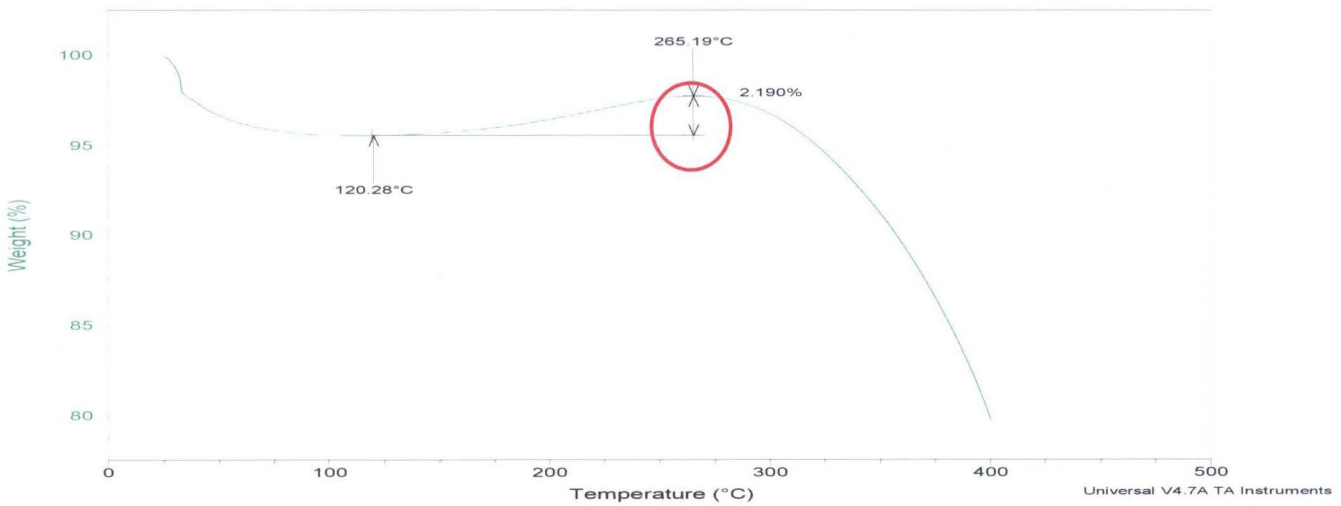


Figure 27: Sample ZM1 - O2 Adsorption graph illustrating the weight increase at 3°C/min

Table 8: O_2 Adsorption - weigh increase at different temperature ramps

	Total Weight Increase (%)				
	3°C/min	5°C/min	7°C/min	10°C/min	20°C/min
ZM1	2.190	1.849	1.672	1.501	1.116
ZM2	1.604	1.406	1.352	1.307	1.159
ZM3	1.896	1.640	1.606	1.565	1.350
ZM4	1.840	1.705	1.564	1.506	1.169
ZM5	2.551	2.469	2.266	2.123	1.770
ZM6	2.168	1.983	1.852	1.654	1.413
ZM7	1.844	1.708	1.625	1.572	1.340
ZM8	2.434	2.362	2.278	2.089	1.672
ZM9	2.033	1.955	1.835	1.640	1.307
ZM10	1.379	1.443	1.332	1.246	0.889
ZM11	1.417	1.265	1.208	0.994	0.836
ZM12	1.850	1.570	1.534	1.294	0.970
ZM13	1.336	1.295	1.224	1.094	0.831
ZM14	0.319	0.645	0.605	0.577	0.495
ZM15	1.490	1.444	1.384	1.341	1.124
ZM16	0.890	0.812	0.808	0.738	0.590
ZM17	1.691	1.636	1.413	1.388	1.064
ZM18	0.832	1.031	0.635	0.888	0.679
ZM19	1.585	1.470	1.324	1.232	0.986
ZM20	1.211	1.021	0.988	0.896	0.714
ZM21	0.945	1.001	0.953	0.868	0.666
ZM22	0.223	0.542	0.541	1.192	0.411
ZM23	1.496	1.501	1.239	1.228	0.904
ZM24	1.117	0.896	0.937	0.877	0.661
ZM25	1.934	1.672	1.570	1.378	0.987
ZM26	1.552	1.369	1.331	1.139	0.841
ZM27	0.700	0.611	0.536	0.474	0.354
ZM28	0.345	0.369	0.326	0.204	0.056
ZM29	1.531	1.325	1.358	1.243	0.883

The mass increase values (Table 8) indicate the reactivity of the coal; these results do not correspond with the TG_{spc} index. Samples ZM14 and ZM16 had low TG_{spc} indices, which is an indication of low liability to self-heat, but they have low mass increase values as well and this is opposite of what was expected. Literature states that a low mass increase means that the coal is highly reactive which should results in a high TG_{spc} index due to desorption of water molecules thus causing an exothermic reaction (Avila, 2012).

All Samples (ZM 14,16, 18, 21, 22, 27, and 28) which had a mass increase less than 1% (regarded as low) indicate a high liability in the coal to self-heat and the TG_{spc} index

correlated with these results, as all coal samples had high TG_{spc} index of above 0.06, except for sample ZM14 and ZM16 (Table 5). The two samples had low TG_{spc} indices of 0.0147 and 0.0146 and these values fall within the 'Unreactive' range according to the guidelines in Table 6.

The 8 samples, previously discussed, indicated liability to self-heat in the coal characterization results but had very high 'mass increase' results in the O2 adsorption test, which showed no correlation with the analytical data.

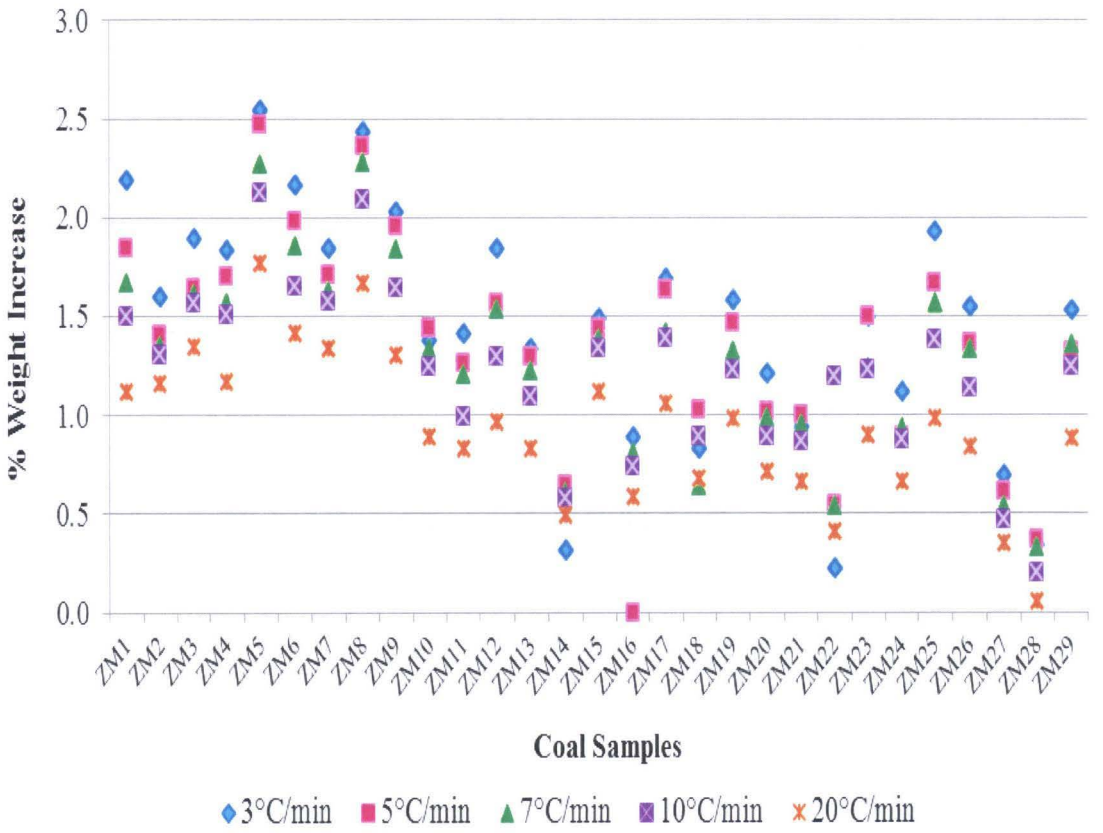


Figure 28: O_2 Adsorption - Weight Increase at different temperature ramps

The different temperature ramp rates produced different results pertaining to weight increase, with 3°C/min ramp rate consistently producing the highest values (Figure 28). The results correlate through all the temperature ramps (Figure 28), but the results in the 3°C/min temperature ramp are more sensitive giving the maximum adsorption rate.

Table 9: Sample Reactivity using initial and peak temperatures at different temperature ramps

	Initial and Peak Temperature at different Temperature Ramps (°C)									
	3°C/min		5°C/min		7°C/min		10°C/min		20°C/min	
	Initial Temp	Peak Temp	Initial Temp	Peak Temp	Initial Temp	Peak Temp	Initial Temp	Peak Temp	Initial Temp	Peak Temp
ZM1	120	265	136	274	145	277	158	287	161	298
ZM2	117	283	135	291	137	298	148	306	152	321
ZM3	126	272	138	280	140	289	148	295	150	312
ZM4	127	276	130	285	140	291	147	301	157	312
ZM5	118	267	116	281	122	286	134	294	152	306
ZM6	130	274	122	281	140	286	147	293	148	305
ZM7	117	278	123	290	132	296	131	305	150	320
ZM8	124	277	128	288	134	296	145	302	156	317
ZM9	134	268	141	279	150	286	155	294	164	305
ZM10	138	278	141	287	146	293	150	301	166	316
ZM11	129	280	141	289	141	296	154	302	167	320
ZM12	140	265	147	278	151	284	160	290	173	300
ZM13	132	271	141	283	151	290	158	296	174	309
ZM14	172	272	162	291	164	296	169	306	176	321
ZM15	124	281	140	290	149	298	158	309	164	322
ZM16	142	279	150	287	161	297	167	304	171	320
ZM17	148	275	149	284	156	293	160	303	173	315
ZM18	165	272	158	284	149	284	163	299	179	311
ZM19	136	284	142	293	151	301	156	309	175	322
ZM20	133	283	145	292	154	300	161	309	177	322
ZM21	149	276	149	289	154	295	157	303	166	316
ZM22	144	265	135	282	155	288	161	298	185	314
ZM23	143	275	143	284	155	289	166	300	183	310
ZM24	132	270	141	280	144	288	156	299	162	312
ZM25	144	275	147	285	154	292	169	299	175	313
ZM26	140	271	153	278	156	288	166	292	184	306
ZM27	148	271	160	276	166	287	183	293	198	306
ZM28	155	267	169	268	176	274	183	275	179	283
ZM29	149	320	164	334	167	341	165	347	192	363

The values provided in Table 9 are obtained from the O_2 adsorption graphs such as Figure 20 & 27. The coal reactivity is based on the initial and peak temperatures, TG_{spc} index and mass increase results. The assumption drawn from the results is that the higher the temperature difference (Peak – Initial) of a coal sample, the lower the mass increase and the lower the TG_{spc} index, then the less prone the coal sample is to self-heat (less coal reactivity). However, this assumption is not applicable to all the coal samples, because some coals begin to react at a later stage/ higher temperature.

The lowest peak temperature from all the 29 coal samples is 265°C and three samples ZM (1, 12 and 22) share this value. All three coal samples have high TG_{spc} indices (Table 5) of 0.0455 (reactive), 0.0714 (high reactive) and 0.0671 (high reactive). The mass increase of ZM12 and ZM22 were below 1% (low), while the mass increase of ZM1 was 2.19% (high). The two samples (ZM12 and ZM22) from the three were classified as having high coal reactivity, therefore liable to spontaneously combust. For samples such as ZM1 that did not fall within the guidelines fully, required the coal petrography and characterisation analysis to shed more light. Further guidelines including the coal and characterisation analysis are discussed in 4.7 Table 13.

Overall guidelines to help interpreting the results (Prone = liable to spontaneously combust) These guidelines can be used in conjunction to help predict the liability of a coal to self-heat, if all the data obtained from the spontaneous combustion liability tests corresponds with the descriptions below, then a prediction can be concluded.

	Prone	Not likely	
Mass increase:	low	high	
TGspc Index:	high	low	
Peak temp:	low	high	
Coal Reactivity	high	low	(construed from the three components)

4.5 Smith-Glasser Test

In the Smith-Glasser test, coal samples that are liable to self-heat exhibit the highest rise in the oil in the pipette, thus having a higher O_2 absorption rate. The results always give the same conclusion whether they are displayed as the O_2 absorption rate or as the rise in oil (Figures 29 and 30). In both graphs, ZM12 is more liable to self-heat than the rest of the samples.

The O_2 absorption rate decreased towards the end in Figure 29 due to the long duration of the test, unlike in Figure 30 where the oil height had increased showing coal reactivity. The O_2 absorption rate is time dependent and will reduce as the time increases. The results, however, between Figure 29 and 30 still give the same outcome because we are able to see that ZM12 is the most reactive and that ZM 26 is the least reactive.

The coal samples took longer to react in this particular experiment due to five tests being run simultaneously in the same water bath. Previous tests using the same sample reacted quicker when run alone in a smaller water bath. The O_2 absorption rate was higher in the previous tests due to a shorter duration because of the faster coal reactivity. The O_2 absorption rate is highly dependent on the duration; the longer the duration of the test the lower O_2 absorption rate as seen in the current tests. The temperature does not play a role in this experiment as the water bath was kept at a constant temperature of 40°C. Conversely, some coal samples take longer to react and require a longer duration (48 hours). Some samples began reacting

after 24 hours, thus proving that the longer the samples remains in the water bath gives it more chance to exhibit if it will self-heat.

Sample ZM 1, 26, 17, 12 were tested together and have the same times, hence they are displayed together in Figure 29. All the results can be viewed in Appendix C.

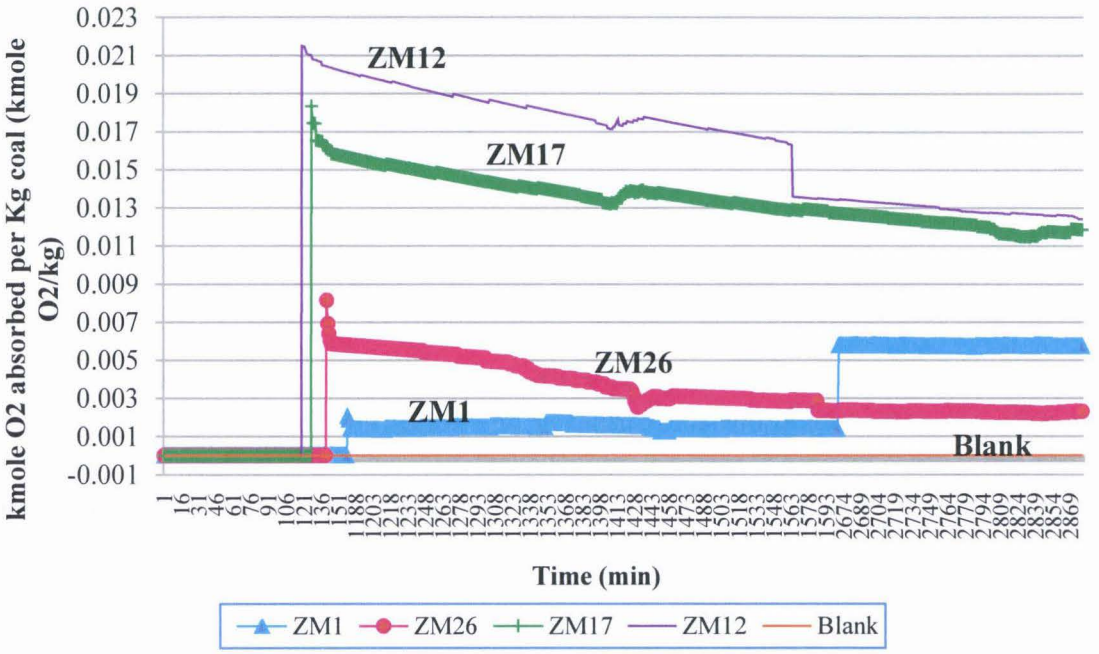


Figure 29: Smith-Glasser test – O2 absorption rate graph

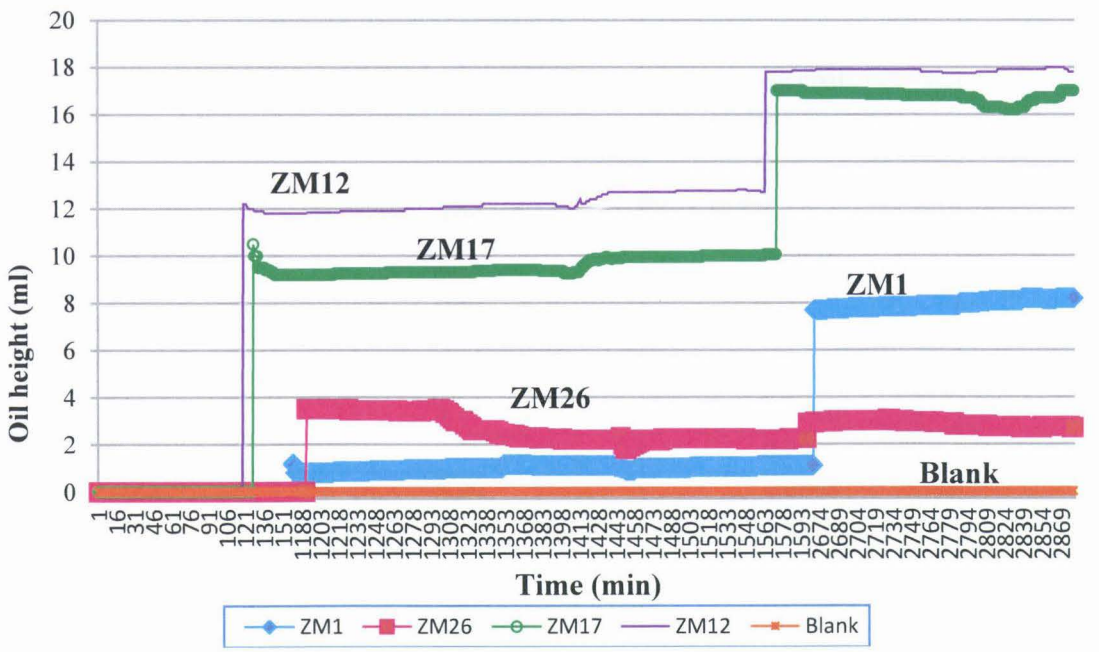


Figure 30: Smith-Glasser Oxidation Test – oil height

Table 10: Samples - ZM12, 17, 01, 26 Smith-Glasser results

Samples	Volatile Matter (%)	Reactive Macerals (%)	CV (KJ/kg)	Highest Rise in oil (ml)	kmole O_2 absorbed per Kg coal (kmole/min.kg)
ZM12	34.15	74.00	25.97	18	0.0215
ZM17	24.82	57.00	22.99	17	0.0183
ZM01	31.00	66.00	27.00	8.2	0.0058
ZM26	26.48	45.40	23.06	4.7	0.0081

Sample ZM12's proximate analysis, petrography results, CV results (Table 10) fully agree with the Smith-Glasser O_2 absorption results. The analysis proves that this sample will oxidize quicker than the three other samples. All the samples in Figures 29 and 30 will oxidize and react and are liable to self-heat, some will spontaneously combust quicker than others, but they will all spontaneously combust if not managed effectively.

Sample ZM17 has a lower volatile matter and CV compared to the other two samples (ZM 01 & 26), but has a higher absorption rate because it reacted quicker than the other two samples. The absorption rate is heavily dependent on the time the reaction occurred, ZM 17 reached its highest absorption rate at 19 hours and 10 minute at an oil reading of 10.5ml (whilst its highest oil height is 17ml, but this occurred at a later stage, which caused the absorption rate to drop). Hence, coal can react at different rates, and the reaction rate can slow down, but the overall O_2 adsorption can continue to increase.

Table 11: Oil height and O_2 Rate results for all samples

Samples	Highest Oil Reading (ml)	kmole O_2 absorbed per Kg coal (kmole/min.kg)
ZM1	8.20	0.0058
ZM2	0.00	0.0000
ZM3	4.90	0.0038
ZM4	3.20	0.0058
ZM5	1.10	0.0018
ZM6	0.20	0.0002
ZM7	0.70	0.0010
ZM8	2.25	0.0035
ZM9	5.90	0.0098
ZM10	0.50	0.0009
ZM11	0.40	0.0006
ZM12	18.00	0.0215
ZM13	7.60	0.0058
ZM14	1.85	0.0027
ZM15	1.00	0.0018
ZM16	3.70	0.0027

ZM17	17.00	0.0183
ZM18	0.70	0.0012
ZM19	3.00	0.0021
ZM20	0.70	0.0013
ZM21	11.50	0.0086
ZM22	0.00	0.0000
ZM23	16.70	0.0116
ZM24	7.80	0.0056
ZM25	8.85	0.0062
ZM26	4.70	0.0081
ZM27	0.00	0.0000
ZM28	1.80	0.0014
ZM29	0.75	0.0012

The oil reading gives the reactivity of coal's intensity to self-heat. Some coals have a lower oil reading, but may still be liable to self-heat as the very reactive coals because if they are left long enough under the right conditions they may well self-heat. The reaction time of the coal is key, because it dictates the outcome of the O_2 absorption rate as can be seen in sample ZM 5 and ZM18; where ZM 5 had a higher oil height but due to a longer reaction time had the same absorption rate as sample ZM18 which had a lower oil height and shorter reaction time.

The coal samples ZM (1, 5, 9, 12, 17, 25 and 26) in this test also indicated that the coal samples have the propensity to self-heat; this was in agreement with the petrography and proximate analysis data discussed already. Five other samples highlighted in blue are showing liability to self-heat in this test.

4.6 Quality Assurance Results and Discussion

It is always advisable to perform a repeatability test when performing test work to validate the quality of the work done.

The ignition tests were performed and both tests had excellent repeatability results, Figure 29 and 33 R^2_{graph} values have a difference of 0.0061 and Figure 32 and Figure 34 $R^2_{calculated}$ values have a difference of 0.0032. The repeatability was poor for the other two coal samples (ZM27&28) that were repeated, this could have been contributed by many instrument factors such unstable buoyancy forces, and turbulence effect arising from a gas flow (Czarnecki, 2000) that would not be evident while conducting the tests. This creates a need for further tests to be performed.

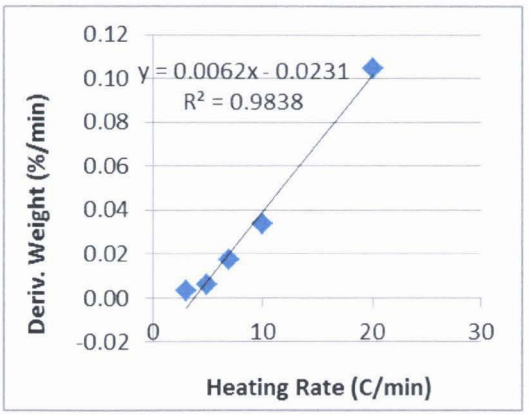


Figure 31: ZM9 Slope of derivative curves used to obtain R^2_{graph}

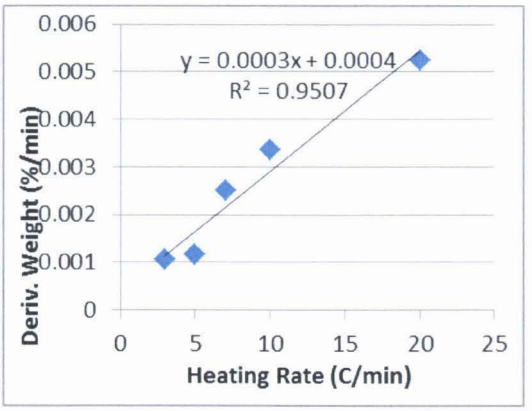


Figure 32: ZM9 Calculated Slope of derivative curves used $R^2_{calculated}$

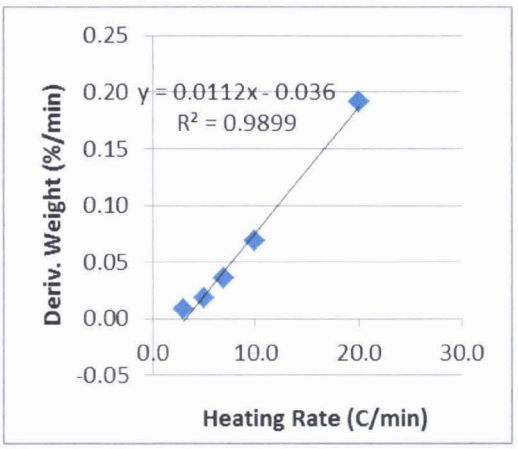


Figure 33: ZM9 Repeat R^2_{graph}

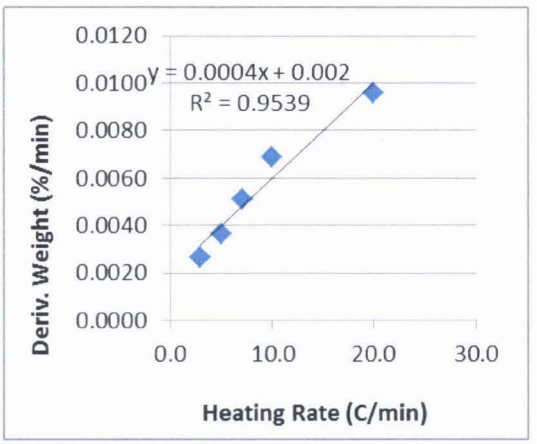


Figure 34: ZM9 Repeat $R^2_{calculated}$

Three samples were repeated, which means a total of 15 runs had to be redone in order to obtain the slopes of derivative curves; the repeatability results can be viewed in Table 12 and 13. The repeatability tests for the TGA method illustrated that there was a significant variation in the results, as can be expected from any test, when tests are repeated. ZM 28 and ZM 29 showed less repeatability when compared to ZM9 which had a lower TG_{spc} Index difference from the two tests run. Even though the repeatability results were not excellent, the results still gave the same meaning because for ZM27 both results according to Table 6 are highly reactive. For ZM28 the meaning slightly changed as the 1st test classified the coal as 'highly reactive' whilst the 2nd test classified it as just 'reactive' but in the end the same conclusion for the coal sample was made.

Table 12: TG_{spc} Index Repeatability

Samples	TG_{spc} Index		
	1st Test	2nd Test	Difference
ZM9	0.0331	0.0360	0.0029
ZM28	0.0757	0.0400	0.0357
ZM27	0.0614	0.0837	0.0223

In the O_2 adsorption test, there was also a slight difference in the O_2 adsorption mass increase results between the 1st and 2nd test, as shown in Figures 35 and 36. The initial and peak temperatures are very close between the two. There is a 0.192% mass increase difference between the two tests. The results still give the same meaning even with the slight difference.

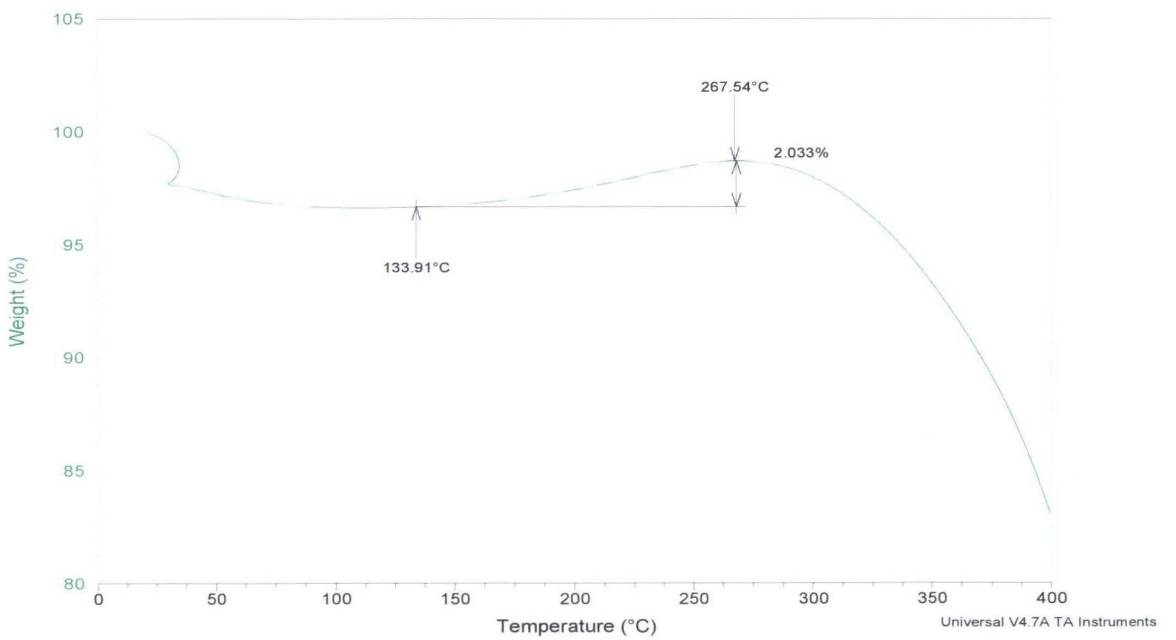


Figure 35: ZM9 O_2 Adsorption 1st test

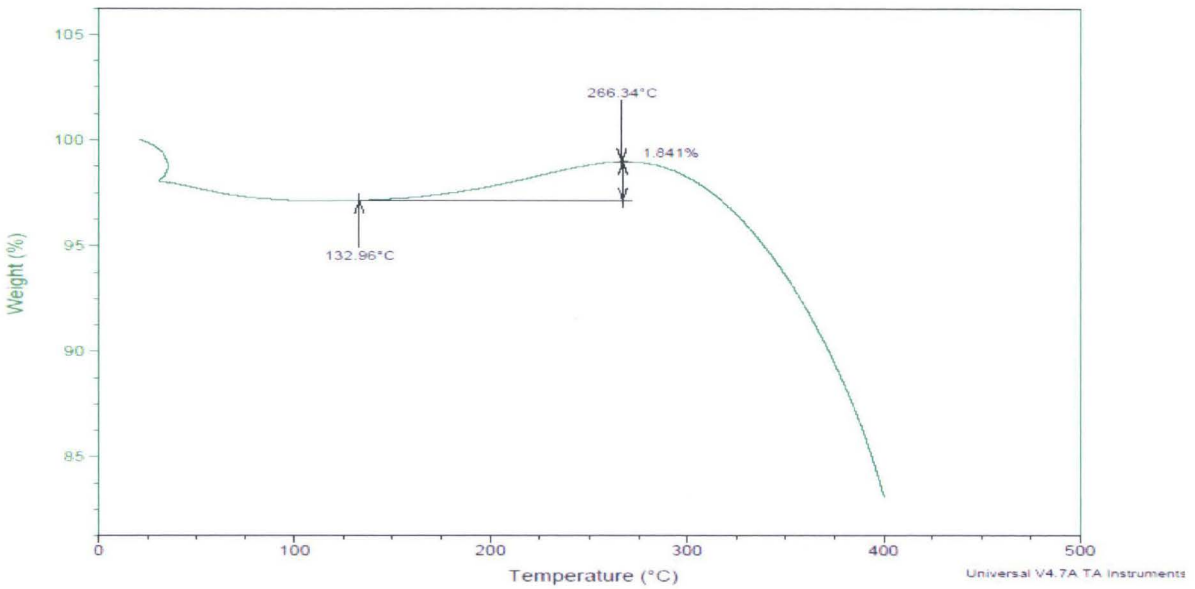


Figure 36: ZM9 O_2 Adsorption 2nd test

The mass increase results between the two O_2 adsorption tests (Figures 35 and 36) indicate the same reactivity of the coal, meaning the main objective of the repeatability tests has been achieved.

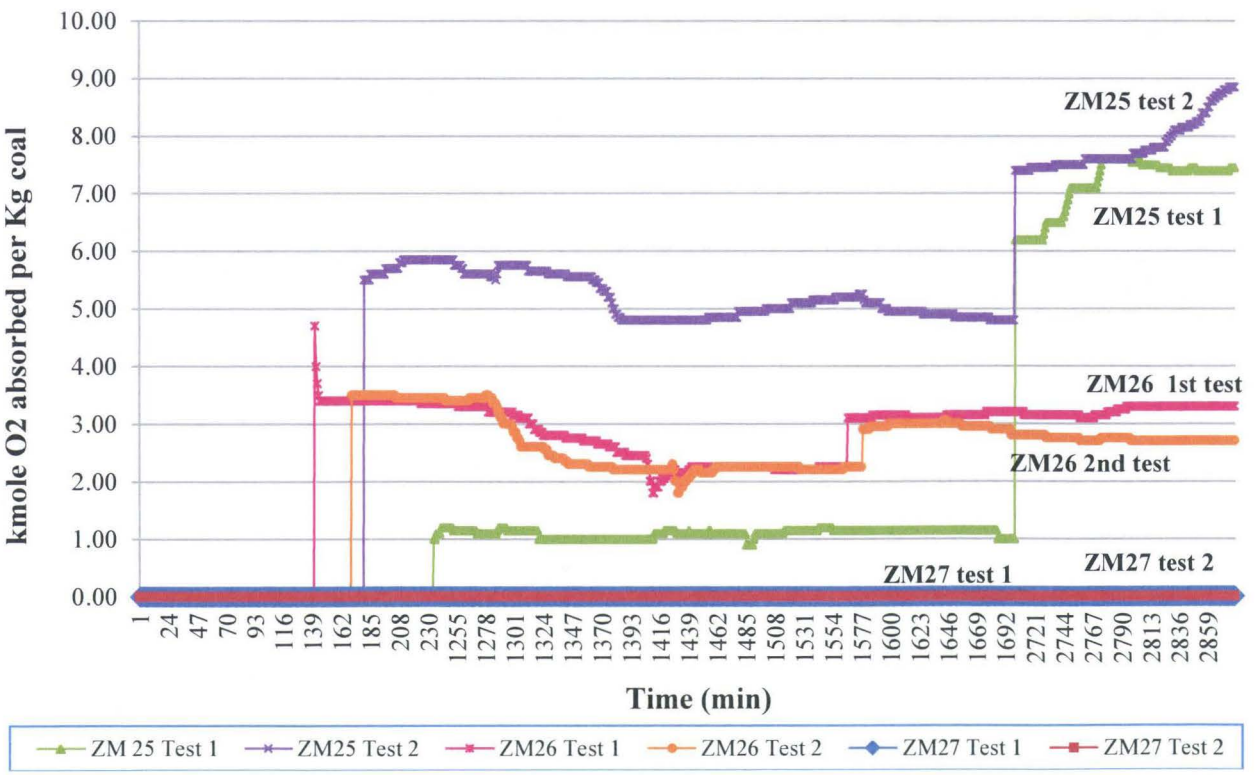


Figure 37: (ZM25, 26, &27) Smith Glasser test Repeatability Tests

There was a noticeable difference in the Smith-Glasser repeatability test's reaction times in all the tests, but the samples all gave the same conclusion after 48 hours (Figure 37).

4.7 %Error Calculation

Error (%) calculations are performed to help gauge the quality of the results, there is always errors in research and it is important to know the extent of errors in the results. The following formula in equation 15 was used to calculate the %error of the repeatability tests:

$$\%Error = \frac{\text{measured value} - \text{actual value}}{\text{actual value}} * 100 \quad \text{.....Equation15 (Shubert et al., 2013)}$$

The measured value was the difference from the two repeatability tests ([test 1 – test 2] or [test 2 – test1], depending on the bigger value since error needs to be positive), which is also known as the error. The actual value is the mean average a representation of all the samples. The % error was then calculated using equation 15, the actual value being the mean average. The results in Table 13 showed the concerning large standard deviation (STDEV) for samples 27 and 28 (due to the little number of repeatability tests run and large %error).

Table 13: Repeatability Samples %Error

Samples	1st Test	2nd Test	Mean	STDEV	Standard Error (SE)	Difference (Error)	% Error
ZM9	0.0331	0.0360	0.03455	0.002051	0.00145	0.0029	8.39
ZM27	0.0614	0.0837	0.07255	0.015768	0.01115	0.0223	30.74
ZM28	0.0757	0.0400	0.05785	0.025244	0.01785	0.0357	61.71

Standard Error (SE)

Calculations of the standard error (SE) were performed, which is the standard deviation of a sample mean that indicates by how much the sample mean can be expected to differ if other samples from the same population are used (Fraenkel et al., 2014). The following formula was used to calculate SE:

$$SE = \frac{s}{\sqrt{n}} \quad \text{..... Equation16 de Beer (2006)}$$

The standard errors results in Table 13 were also high, which gave an indication that the %error would also be high.

Confidence Limits (CL)

Confidence limits for the mean (Snedecor et al., 1989) are an interval estimate for the mean. Interval estimates are often wise to have because the estimate of the mean varies from

sample to sample. A confidence interval generates a lower and upper limit for the mean. The interval estimate was used to give an indication of how much uncertainty there was in the estimate of the true mean (value). The narrower the interval, the more precise the estimation would be.

Level of Confidence (LOC) are Confidence Limits (CL) expressed in terms of a confidence coefficient. Although the choice of confidence coefficient is random, in practice 90 %, 95 %, and 99 % intervals are often used, with 95 % being the most commonly used.

$$\text{CL:} \quad \mu = \chi \pm \frac{t0.05 * S}{\sqrt{n}} \quad \text{..... Equation17 de Beer (2006)}$$

Where:
μ = interval of the true value
t = t-values at 95% LOC
S = standard deviation
χ = mean value
n= number of samples

Confidence Interval (CI)

Confidence Interval is the range of values of the true value in the population that is expected to fall within, based on the study results (the set of all possible values). A range around μ was required and obtained as follows:

$$\text{CI:} \quad \chi - \frac{t0.05*S}{\sqrt{n}} < \mu < \chi \pm \frac{t0.05*S}{\sqrt{n}} \quad \text{..... Equation17 de Beer (2006)}$$

Relative Standard Deviation (RSD)

The precision test called the relative standard deviation (RSD) was added, which was used to give an indication of the precision of the results. A value of < 2% for the %RSD is usually considered an acceptable measure of good precision. This was not the case in the repeatability test results, as can be seen in Table 14. The RSD was calculated as follows:

$$\text{RSD} = \frac{S}{x} \quad \text{..... Equation18 de Beer (2006)}$$

Table 14: Relative Standard Deviation for all three repeatability samples

Samples	%RSD
ZM9	5.94
ZM27	21.73
ZM28	43.64

All the repeatability coal samples had a high RSD, which was not a good indication to the precision of the test. This was a very serious concern.

T-test

The *t*-test are used to compare a sample mean to an accepted value (a population mean), or to compare the means of two sample sets. The t-test consisted of three steps:

- Defining the null and alternate hypotheses,
- Calculating the t-statistic for the data,
- Comparing $t_{calculated}$ (t_{calc}) to the tabulated $t_{critical}$ (t_{crit}), for the appropriate significance level and degree of freedom. If $t_{calc} > t_{crit}$, we rejected the null hypothesis and accepted the alternate hypothesis. Otherwise, the null hypothesis was accepted.

$$t_{cal} = \frac{x - \mu 0}{S/\sqrt{n}} \quad \text{..... Equation19 de Beer (2006)}$$

When one deals with the hypotheses, one needs to establish whether the two sets of measurements are drawn from the same, or different populations. A hypothesis statement (*H*) is proposed:

Null Hypothesis H_0: $t_{calc} > t_{crit}$, rejected
Alternate Hypothesis H_a: $t_{calc} < t_{crit}$

The t_{crit} values were obtained from the t-distribution table (de Beer, 2006) and various statistical tables. The calculated t-value was compared to a critical t-value, which is a function of n, the number of analytical measurements made, as well as the degrees of freedom (DF)

$t_{crit} = t_{DF}$ (DF = n-1)

The null hypothesis were tested on all three LOC (80, 90, 95)%.

Table 15: ZM9 CI, t_{crit} and t_{cal} values for the t-test method at different confident levels

ZM9	LOC		80%	90%	95%
	tcrit		3.078	6.314	12.706
	CI	μ (+)	0.039	0.044	0.053
		μ (-)	0.030	0.025	0.016
	tcal		23.828		
	Reject if tcal>tcrit		tcal>tcritical	tcal>tcritical	tcal>tcritical

The results in Table 15; showed the confidence of interval to range between 0.016 – 0.053 for the 95% confidence level. This meant that the mean value for this sample (0.03455) was well within the confidence of interval range. The t_{cal} value, however, was bigger than t_{crit} and

therefore rejected by H_0, which meant the method could not be deemed accurate in all confidence levels.

Table 16: ZM27 CI, t_{crit} and t_{cal} values for the t-test method at different confident levels

ZM27	LOC		80%	90%	95%
	tcrit		3.078	6.314	12.706
	CI	μ (+)	0.107	0.143	0.214
		μ (-)	0.038	0.002	-0.069
	tcal		6.507		
	Reject if tcal>tcrit		tcal>tcritical	tcal>tcritical	tcal<tcritical

Table 16 and 17 showed that the mean average of the samples would also fall within the confidence of interval range; the negative values meant that the range would begin from zero. The H_0 rejected the t_{cal} value when calculated under the 80% and 90% LOC but was accepted by H_0 when calculated under the 95% LOC.

Table 17: ZM28 CI, t_{crit} and t_{cal} values for the t-test method at different confident levels

ZM28	LOC		80%	90%	95%
	tcrit		3.078	6.314	12.706
	CI	μ (+)	0.113	0.171	0.285
		μ (-)	0.003	-0.055	-0.169
	tcal		3.241		
	Reject if tcal>tcrit		tcal>tcritical	tcal<tcritical	tcal<tcritical

The t-test results further emphasized that the repeatability tests were not accurate and all the calculations (%error, standard error and RSD) conducted gave the same conclusion. A low amount of repeatability samples were run and this was a huge cause for the %error of the repeatability data to be poor. A rectification suggestion is given in the recommendations.

4.8 Comparison of Results

Both test methods (TGA and Smith-Glasser) were compared against the additional analytical analysis performed using the guidelines in Table 18 to establish the coal's reactivity and liability to self-heat. The summary of the comparison between the two test methods can be observed in Table 19. The coals are ranked from highly reactive (coals that are most liable to self-heat) to unreactive coals (coals that are most likely not liable to self-heating).

The results from the summary reveal that both tests do not correlate accurately with the analytical data. The spontaneous combustion liability tests results improve when one analyses the meaning behind the results; e.g. when a coal is 'reactive' according to the analytical results but yields a 'less reactive' result from the spontaneous combustion liability tests, then the overall conclusion on this coal is that it will eventually react (at different rates).

Table 18: Guidelines to help interpret the results regarding the reactivity of the coal

	Total Reactive Macerals	Sulphur (%)	Volatile Matter (%)	CV (MJ/kg)	Mass Increase (%)	Peak Temp (°C)	TGspc Index	Highest Oil Reading (ml)
High Reactivity	55>	2.0>	24>	23>	0 - 0.2	270<	0.070	7>
Reactive	35 - 54	1.5 - 1.9	20 - 23	17 - 22	0.2 - 0.6	271 - 280	0.036 - 0.069	1 - 6
Less Reactive	20 - 34	0.8 - 1.4	17 - 19	11 - 16	0.7 - 1.1	281 -300	0.030 - 0.035	0.5 - 0.9
Not Reactive	1 - 9	0.4 - 0.7	1 - 12	5 - 10	1.2 – 1. 7	301 - 310	0.020 - 0.029	0.1 - 0.4
Unreactive	0 - 9	0.0 - 0.3	0 - 12	0 - 4	2>	311 >	0.000 - 0.019	0.0

The guidelines were assumed using the overall analytical and test results. The results do not fully agree with the guidelines on certain coal samples, but do manage to give an idea on the reactivity of the coal sample being tested. An overall liability to self-heat prediction for the 29 coal samples is given in Table 21.

Table 19: Summary of the comparison between the two test methods

	TGA	Smith-Glasser
Accurate correlation on both Petrography and Coal Characterization Analysis (match with two or more analysis components)	9 (31%)	11 (38%)
Accurate correlation with either Petrography and Coal Characterization Analysis (match with one or more analysis components)	25 (86%)	22 (76%)
Accurate correlation between TGA and Smith-Glasser Tests	7 (29%) [ZM1,3,4,8, 15, 19 & 26]	
Correlation, reaction at different times, between TGA and Smith-Glasser Tests (match with two or more TGA components)	17 (59%) [ZM1,3,4,8, 9,10, 12, 13, 15, 19, 20, 22, 24, 25, 26, 27, & 29]	

The summary of the results in Table 19 were obtained from the data in Table 20, where all the analysis results were taken into consideration in order to obtain a conclusion. When one focuses on the correlation of the results between the two self-heating liability determining test and the petrography and coal characterisation analysis; the Smith-Glasser test method has slightly better correspondence with the analytical data as when compared with the TGA method. However, the TGA method's correlation improves when the overall reactivity of the coal samples is studied. When one focuses on the overall definition on whether the coal is liable to self-heat by matching the TGA results with one or two coal characteristics (Table 20), then the TGA results generate better results (86%).

The 59% correspondence between the two test methods was obtained by not looking at the reaction rate of the coal but by checking if the coal will self-heat in general. So, when the TGA method has a 'less reactive' result against the Smith-Glasser method that has a 'high reactive' results (like in ZM9 and ZM19 samples) then these results correspond on the basis that they will both self-heat at different reaction rates, but they will self-heat eventually.

Table 20: Comparison between the two self-heating liability determining test methods against the coal analytical data

	Petrography		Coal Characterisation						TGA						Smith-Glasser	
	Total Reactive Macerals (%)	Reactivity	Total %S	Reactivity	Volatile Matter (%)	Reactivity	CV (MJ/Kg)	Reactivity	Mass Increase (%) at 3°C/min	Reactivity	Peak temperature(°C) at 3°C/min	Reactivity	Tspc Index	Reactivity	Highest Oil Reading (ml)	Reactivity
ZM1	66.0	High Reactive	2.290	High Reactive	31.00	High Reactive	27.0	High Reactive	2.190	High Reactive	265	High Reactive	0.0455	Reactive	8.20	High Reactive
ZM2	22.0	Less Reactive	1.110	Less Reactive	19.11	Less Reactive	16.2	Less Reactive	1.604	Reactive	283	Less Reactive	0.0649	Reactive	0.00	Unreactive
ZM3	40.0	Reactive	1.400	Less Reactive	22.00	Reactive	18.7	Reactive	1.896	Reactive	272	Reactive	0.0548	Reactive	4.90	Reactive
ZM4	44.0	Reactive	1.160	Less Reactive	21.68	Reactive	19.6	Reactive	1.840	Reactive	276	Reactive	0.0594	Reactive	3.20	Reactive
ZM5	59.0	High Reactive	1.470	Less Reactive	27.63	High Reactive	26.2	High Reactive	2.551	High Reactive	267	High Reactive	0.0174	Unreactive	1.10	Reactive
ZM6	40.0	Reactive	1.810	Reactive	22.39	Reactive	22.3	Reactive	2.168	High Reactive	274	Reactive	0.0109	Unreactive	0.20	Not Reactive
ZM7	33.0	Less Reactive	0.290	Unreactive	19.97	Less Reactive	17.0	Reactive	1.844	Reactive	278	Reactive	0.0227	Not Reactive	0.70	Less Reactive
ZM8	47.0	Reactive	0.891	Less Reactive	23.33	Reactive	25.2	High Reactive	2.434	High Reactive	277	Reactive	0.0455	Reactive	2.25	Reactive
ZM9	62.0	High Reactive	1.620	Reactive	27.44	High Reactive	21.6	Reactive	2.033	High Reactive	268	High Reactive	0.0331	Less Reactive	5.90	High Reactive
ZM10	37.0	Reactive	0.915	Less Reactive	20.87	Reactive	17.7	Reactive	1.379	Reactive	278	Reactive	0.04	Reactive	0.50	Less Reactive
ZM11	27.0	Less Reactive	1.250	Less Reactive	21.52	Reactive	16.9	Less Reactive	1.417	Reactive	280	Reactive	0.0623	Reactive	0.40	Not Reactive
ZM12	74.0	High Reactive	2.660	High Reactive	34.15	High Reactive	26.0	High Reactive	1.850	Reactive	265	High Reactive	0.0714	High Reactive	18.00	High Reactive
ZM13	44.0	Reactive	2.400	High Reactive	22.06	Reactive	17.6	Reactive	1.336	Reactive	271	Reactive	0.0491	Reactive	7.60	High Reactive
ZM14	15.0	Not Reactive	0.229	Unreactive	15.02	Not Reactive	6.5	Not Reactive	0.319	Not Reactive	272	Reactive	0.0148	Unreactive	1.85	Reactive
ZM15	31.0	Less Reactive	0.355	Not Reactive	19.08	Less Reactive	18.0	Reactive	1.490	Reactive	281	Less Reactive	0.0423	Reactive	1.00	Reactive
ZM16	24.0	Less Reactive	0.862	Less Reactive	18.46	Less Reactive	12.8	Less Reactive	0.890	Less Reactive	279	Reactive	0.0147	Unreactive	3.70	Reactive
ZM17	57.0	High Reactive	1.730	Reactive	24.82	High Reactive	23.0	High Reactive	1.691	Reactive	275	Reactive	0.0338	Less Reactive	17.00	High Reactive
ZM18	34.0	Reactive	1.450	Less Reactive	20.83	Reactive	16.5	Less Reactive	0.832	Less Reactive	272	Reactive	0.0681	Reactive	0.70	Reactive
ZM19	35.0	Reactive	0.273	Unreactive	17.71	Less Reactive	19.5	Reactive	1.585	Reactive	284	Reactive	0.0849	High Reactive	3.00	Reactive
ZM20	28.0	Less Reactive	0.446	Not Reactive	17.12	Less Reactive	15.0	Less Reactive	1.211	Less Reactive	283	Less Reactive	0.0465	Reactive	0.70	Less Reactive
ZM21	34.0	Less Reactive	0.714	Not Reactive	18.77	Less Reactive	13.4	Less Reactive	0.945	Less Reactive	276	Reactive	0.0652	Reactive	11.50	High Reactive
ZM22	16.0	Not Reactive	0.804	Less Reactive	14.93	Not Reactive	5.9	Not Reactive	0.223	Not Reactive	265	High Reactive	0.0671	Reactive	0.00	Unreactive
ZM23	53.0	Reactive	0.812	Less Reactive	24.07	High Reactive	24.0	High Reactive	1.496	Reactive	275	Reactive	0.0625	Reactive	16.70	High Reactive
ZM24	44.0	Reactive	0.862	Less Reactive	16.99	Less Reactive	17.8	Reactive	1.117	Less Reactive	270	Reactive	0.0666	Reactive	7.80	High Reactive
ZM25	28.6	Less Reactive	0.700	Not Reactive	24.67	High Reactive	26.3	High Reactive	1.934	Reactive	275	Reactive	0.0743	High Reactive	8.85	High Reactive
ZM26	45.4	Reactive	1.620	Reactive	26.48	High Reactive	23.1	High Reactive	1.552	Reactive	271	Reactive	0.0378	Reactive	4.70	Reactive
ZM27	67.8	High Reactive	0.867	Less Reactive	21.48	Reactive	12.7	Less Reactive	0.700	Less Reactive	271	Reactive	0.0614	Reactive	0.00	Unreactive
ZM28	36.4	Reactive	0.600	Not Reactive	21.54	Reactive	16.3	Less Reactive	0.345	Not Reactive	267	High Reactive	0.0757	High Reactive	1.80	Reactive
ZM29	60.0	High Reactive	0.647	Not Reactive	16.08	Less Reactive	15.0	Less Reactive	1.531	Reactive	320	Unreactive	0.0525	Reactive	0.75	Less Reactive

Table 21: Overall Coal Self-Heating Prediction for the 29 coal samples

Coal Samples	Spontaneous Combustion Prediction
ZM1	Highly likely
ZM2	Less likely
ZM3	Likely
ZM4	Likely
ZM5	Highly likely
ZM6	Likely
ZM7	Less likely
ZM8	Likely
ZM9	Highly likely
ZM10	Likely
ZM11	Likely
ZM12	Highly likely
ZM13	Likely
ZM14	Not likely
ZM15	Likely
ZM16	Less likely
ZM17	Highly likely
ZM18	Likely
ZM19	Likely
ZM20	Less likely
ZM21	Less likely
ZM22	Not likely
ZM23	Highly likely
ZM24	Likely
ZM25	Highly likely
ZM26	Likely
ZM27	Likely
ZM28	Likely
ZM29	Less likely

An overall prediction of the coal samples to self-heat was made in Table 21. The predictions were based from Table 16, using all the analytical data and experimental tests performed in the whole project. The prediction were based on the consistency of results for each sample, therefore, meaning that if more 3 or 4 components in Table 20 had the same outcome (High reactive, Reactive, Less Reactive or Not Reactive) then a conclusion was made on the sample's liability to self-heat. The overall predictions agreed with the outcome of the 8 samples that were initially highlighted from the proximate analysis and sulphur results, which also had the same indication regarding the liability of the coal samples to self-heat. The ranking order for all the samples can be viewed in Appendix E.

CHAPTER 5

5 CONCLUSION

As spontaneous combustion is a critical and on-going problem that has been recurring for centuries, it is vital for coal collieries and coal users to establish a spontaneous combustion liability test method that can be swift, and as reliable as possible for routine tests in their processes.

The TGA method O_2 adsorption and ignition test were selected methods to fulfil the research questions asked in the beginning of this report, following the method proposed by Avila (2012). The main aim of this project was to determine if the TGA spontaneous combustion liability method is an accurate method to test the liability of coal to self-heat.

The well-tested Smith-Glasser oxidation test was used to validate the TGA method, and 29 samples were tested in both tests. Unfortunately the results did not correspond as expected. Both test methods were compared to the volatile matter, petrographic, calorific value and sulphur analysis to observe the test that collaborates with all the analyses.

The liability to spontaneous combustion could be predicted by use of a TGA analysis, but with reservations. The method can indicate the propensity of coals to self-heat, but is not always accurate when compared to the other method. The TGA method requires many factors to correlate (such as ignition test TG_{spc} index, O_2 adsorption mass increase and the reactivity of the coal using the peak temperature) before a conclusion can be reached; which is the opposite of the Smith-Glasser oxidation test which requires the oxygen adsorption rate only to make a conclusion, thus being a far simpler test (but takes a longer time).

The chances of human error occurrences in the TGA method depend on the measurements conducted by the analyst. Extra care and accuracy is required when obtaining the results from the graph; this unfortunately is dependent on the skill of the analyst. The TGA method does not fully explain the intensity of the coal reaction with O_2, the way the Smith-Glasser oxidation test does; it can only give an idea when using the initial and peak temperature.

Theoretically, there are many sources of error in the TGA that one would not necessarily be aware of if they occured. The sources of error may come as random fluctuation of the balance mechanism, unstable buoyancy forces, and convection effect arising from the furnace, electrostatic forces, turbulence effect arising from a gas flow, and induction effect coming from the furnace (Czarnecki, 2000). The TGA's has many sources of error, therefore creating more chances of errors occurring. These factors make the TGA a less likely method to be used. The Smith-Glasser test also has a shortfall of incomplete data collection, as the overnight results are missed due to the experiments being run during the day.

The repeatability results were poor mainly due to the low number of samples run and this could not be rectified due to time constrains. A total of 15 tests were run on the TGA for the three samples (ZM9, 27 & 29), in order to have a second set of results to use on the repeatability analysis. This means that in order to have 5 sets (n=5) of results for all 29 coal

samples then 725 tests would have had to be run on the TGA in total, because one set of results for all 29 coal samples equals 145 tests. Time would not have allowed this to be possible for this particular project.

In conclusion, there was a slight correlation between the two self-heating test methods which leads to a conclusion that the TGA method can be used in lab test work but is not accurate enough to be used in the coal industry where accuracy is vital. The TGA spontaneous combustion liability method lacks the ability to identify the intensities in coal reactions and this could be crucial when one coal needs immediate attention due to its high reactivity.

CHAPTER 6

6 RECOMMENDATION

For future projects it is recommended that when the TGA method is used that the petrography, proximate analysis, calorific values and sulphur analysis be performed to help verify the spontaneous combustion liability results.

It is also recommended that the Smith-Glasser test should be used when further clarification is required. The Smith-Glasser oxidation test can be used for samples that did not give a conclusive indication on the coal liability to self-heat in the TGA tests.

Another recommendation is for a reference standard to be made using the Smith-Glasser oxidation test and be used when TGA tests are being conducted to validate the results obtained.

It is recommended that the different types of sulphur analysis (organic, pyritic and sulphate) be performed in order to help give a better indication of coal self-heating.

It is highly recommended that further TGA repeatability test be performed in order to give a more informative outcome. A large number of tests (725) are required for the TGA repeatability test, which leads another recommendation for this section to be set as a project on its own because it is very crucial to the outcome of the TGA reliability project.

BET surface area analyses are also recommended to be performed in order to help give more understanding on the oxidation uptake reaction.

A project plan is also recommended and should be drawn before the test work is started in order to cover everything because both test methods are time consuming and a huge amount of time will be required for the repeatability tests.

CHAPTER 7

7 REFERENCE LIST

Adamski S. The Prevention of spontaneous combustion in back-filled waste materials at Grootgeluk Coal Mine. Safety in Mines Research Advisory Committee: COL713, June, 2003, pp. 1-57.

Avila C. Predicting self-oxidation of coals and coal/biomass blends using thermal and optical methods. Thesis submitted to the University of Nottingham for the degree of Doctor of Philosophy, 2012.

Aziz N. Underground Coal – Outburst. School of Civil, Mining and Environmental Engineering, University of Wollongong, 2012. http://www.undergroundcoal.com.au/outburst/about_outburst.aspx , Date viewed: 06 May 2015.

Barlow D. Differential Thermal Analysis – a complete overview, 2013. http://www.selfgrowth.com/articles/differential-thermal-analysis-a-complete-overview, Date viewed: 06 May 2015.

Beamish B, Arisoy A. Effect of intrinsic coal properties on self-heating rates. 12th U.S./North American Mine Ventilation Symposium - Wallace (ed) ISBN 978-0-615-20009-5, 2008.

Beamish B., Barakat M., St George J. Adiabatic Testing Procedures for Determining the Self-heating Propensity of Coal and Sample Ageing Effects. Thermochimica Acta, Vol 362, Elsevier, 2000, pp.79 - 87.

Beamish B. Proximate analysis of New Zealand and Australian coals by thermogravimetry. New Zealand Journal of Geology and Geophysics, Vol. 37, 1994, pp. 387 - 392.

Bell F., Bullock S., Hälbich T., Lindsay P. Environmental impacts associated with an abandoned mine in the Witbank Coalfields, South Africa. International Journal of Coal Geology 45, 2001, pp. 195 – 216.

Benerjee S., Chakravarty R. Use of DTA in the study of spontaneous combustion of coal. Journal of Mines, Metals and Fuels. 1967, pp. 1-5.

Carras J., Young B. Self-Heating of Coal and Related Materials: Models, Application and Test Methods. Progress in Energy Combustion Science, Vol. 20, 1994, pp.1 – 15.

Coaltech Research Association, Prevention and Control of Spontaneous Combustion. Best Practice Guidelines for Surface Coal Mines in South Africa, 2011.

Coal Marketing International. Advanced Coal Science, 2012. http://www.coalmarketinginfo.com/advanced-coal-science , Viewed 4 February 2016.

Creighton L. Underground Coal Mining - Emergency Response, 2003 http://www.apcoaust.com.au/membership/Presentation_Downloads/2010/2003.ppt

Cumming J., McLaughlin J. The thermogravimetric behaviour of coal. Thermochimica Acta, Vol.57, 1982, pp. 253-272.

Czarnecki J., Šesták J. Practical Thermogravimetry. Journal of Thermal Analysis and Calorimetry, Vol. 60, 2000, pp. 759–778.

de Beer J, (2006). Statistical Method Validation for test laboratories training manual. Technikon Pretoria, Department of Chemistry and Physics

de Korte J. Beneficiation of Weathered Coal. Division of Mining Technology CSIR, Project 4.6.2, 2001.

de Korte J. Test to determine the spontaneous combustion propensity of coal, CSIR, Fossil Fuel Foundation Spontaneous Combustion Conference, 2014. http://www.fossilfuel.co.za/spontaneous-combustion-part-1-causes-and-controls-13-february-2014/, Date viewed: June 01, 2015.

Earnest C. Compositional analysis by thermogravimetry. American society for testing and materials, 1988.

Elder J. Proximate analysis by automated thermogravimetry. Fuel, Vol.62, 1983, pp. 580 – 584.

Energy Information Administration (EIA). Independent Statistics and Analysis, 2013. http://www.eia.gov/energyexplained/index.cfm?page=coal_home#tab1 Date viewed: June 01, 2015.

Eskom. Fact - sheets 13. Environmental Management, 2012 http://financialresults.co.za/2012/eskom_ar2012/fact-sheets/013.php, Date viewed: 29 April 2015.

Falcon R. Spontaneous combustion of the organic matter in discards from the Witbank coalfield. Journal of the South African Institute of Mining and Metallurgy, Vol. 86, No. 7, 1986, pp. 243 – 250.

Feng K., Chakravarty R., Cochrane T. Spontaneous Combustion- a coal mining hazard, CIM Bulletin, 1973, pp. 75 – 84.

Fierro V., Miranda J., Romero C., Andres J., Arriaga A, Schmal D, Visser G. Prevention of spontaneous combustion in coal stockpiles – Experimental results in coal storage yard, Fuel Processing Technology, Vol 59, (1999), pp 23 – 34.

Fraenkel J., Wallen N., 2014, 9th edition. How to Design and Evaluate Research in Education. McGraw-Hill Education

Gouws M., Wade L. The self-heating liability of coal: Predictions based on simple indices. Mining Science and Technology 9, 1989, pp. 75 – 80.

Grapes R., 2010, 2nd Edition. Pyrometamorphism: Thermal Regimes and Effects - The Burning Process, pp. 22.

Hackley P., Kolak J. Petrographic and vitrinite reflectance analyses of a suite of high volatile bituminous coal samples from the United States and Venezuela. U.S. Geological Survey Open-File Report. 2008, pp.36.

Harris M. Practical methods for avoiding spontaneous combustion of coal. The South African Coal Processing Society, Symposium, 1985.

Harvey D. Implementing the Sampling Plan, Modern Analytical Chemistry. DePauw University, 2000. http://chemwiki.ucdavis.edu/Analytical_Chemistry/Analytical_Chemistry_2.0/07%3A_Collecting_and_Preparing_Samples/7C%3A_Implementing_the_Sampling_Plan, Date viewed: 01 June 2015.

Horsfall D. An examination of the spontaneous combustion characteristics of coal. The South African Coal Processing Society, Symposium, 1985.

Humphreys D. A Study of the Propensity of Queensland Coals to Spontaneous Combustion. Brisbane, Australia, the University of Queensland, 1981, pp. 108.

IEA. CO_2 Emissions from Fuel Combustion; OECD, Inter-country Input-Output (ICIO) Data base, 2012.

Jeffrey L. Geotechnical factors associated with previously mined areas of coal and their impact on subsequent extraction. Faculty of Engineering, University of the Witwatersrand, 2002.

Jones H. Spontaneous Combustion is deadly in underground coal mines. O.B.E Services to the mining industry, 1983.

Kizgut S., Yilmaz S. Characterization and non-isothermal decomposition kinetics of some Turkish bituminous coals by thermal analysis. Fuel Processing Technology, Vol.85, 2004, pp.103-111.

Klančnik G., Medved J., Mrvar P. Differential thermal analysis (DTA) and differential scanning calorimetry (DSC) as a method of material investigation. RMZ – Materials and Geoenvironment, Vol. 57, No. 1, 2010, pp. 127–142.

Loane E. Report on an Accident at Kianga No. 1. Underground Mine on Saturday, 20th September, 1975. Warden's Inquiry conducted pursuant to Section 74 of "The Coal Mining Act, 1925-1974, 1975, pp 4.

Luo Y., Wang X. Experimental Studies of Spontaneous Combustion Propensity of Coal. 2011 International Pittsburgh Coal Conference Pittsburgh, PA, 2011.

Luo Y., Wang X. A Mathematical Model of R70 Self-Heating Test for the Propensity of Coal Spontaneous Combustion. 14th USMVS, Salt Lake City, Utah, 2012.

Marinov V. Self-ignition and mechanisms of interaction of coal with oxygen at low temperatures. 2. Changes in weight and thermal effects on gradual heating of coal in air in the range 20–300°C. Fuel, Vol.56, 1977, pp.158-164.

Midwest Geological Sequestration Consortium (MGSC), 2011
http://sequestration.org/science/carbondioxide.html, Date viewed: 24 November 2014.

Mine Accidents and Disasters. Safety in Mines Testing and Research Station (SIMTARS), 2015.
http://www.mineaccidents.com.au/mine-events/disaster/au, Date viewed: 13 July 2015.

Ming T., Richter R., Liu W., Caillol S. Fighting global warming by climate engineering: Is the Earth radiation management and the solar radiation management any option for fighting climate change?. Renewable and Sustainable Energy Reviews 31, 2014, pp. 792–834.

Morgan P., Robertson S., Unsworth J. Combustion studies by thermogravimetric analysis: 1. Coal oxidation. Fuel, Vol.65, 1986, pp. 1546-1551.

Mining Mayhem. Blair Athol, 2009.
http://www.miningmayhem.com/2009/11/blair-athol-spon-com.html Blair Athol Spontaneous Combustion,2009. Date viewed: 13 July 2015.

NIOSH Information Circular No. 9529, Mining Safety and Health, National Institute for Occupational Safety and Health, CDC. Coal Dust Explosibility Meter Evaluation and Recommendations for Application. 2012.
http://permanent.access.gpo.gov/gpo37644/ic9529.pdf

Norton G. A review of the derivative thermogravimetric technique (burning profile) for fuel combustion studies. Thermochimica Acta, Vol.214, 1993, pp. 171-182.

Paris B. The Direct Determination of Organic Sulfur in Raw Coals. Battelle Columbus Laboratories, 1977.

Pask J., Warner M. Differential Thermal Analysis Methods and Techniques. University of Califonia, Institute of Engineering Research. Series No 18, Issue 5, 1953.

Pattanaik D., Behera P., Singh B. Spontaneous Combustibility Characterization of the Chirimiri Coals, Koriya District, Chhatisgarh, India. International Journal of Geosciences, 2011, Vol. 2, pp. 336-347.

Pone D., Hein K., Stracher G., Annegarn H., Finkleman R., Blake D., McCormack J. Schroeder P. The spontaneous combustion of coal and its by-products in the Witbank and Sasolburg coalfields of South Africa. International Journal of Coal Geology 72, 2007, pp. 124–140.

Schalekamp E. The financial viability of coal reserves within previously mined areas of the Witbank Coalfield. Faculty of Natural & Agricultural Science University of Pretoria, 2006.

Schernikau L. Economics of the International Coal Trade: The Renaissance of Steam Coal. Economic of the International Coal Trade Sources of Coal - Review as a Source, 2010, pp. 50.

Serageldin M., Pan W. Coal analysis using thermogravimetry. Thermochimica Acta, Vol.76, 1984, pp.145-160.

Sengupta M. Mine Environmental Engineering, Vol. 11. Chapter 5, Spontaneous Combustion of Coal. CRC Press, 1989, pp. 169.

Sensogut C., Cinar I. A research on the Spontaneous Combustion Tendency of Turkish Coal-Ilgin Lignite's Case. Trends in Applied Science Research 1(1), 2006, pp. 9 – 14.

Sevenster P. Studies on the interaction of oxygen with coal in the temperature range 0°C to 90°C. Fuel 40, 1961, pp. 7-17.

SGS Mining. Coal Calculations, 2013. http://www.sgs.com/en/Mining/Analytical-Services/Coal-and-Coke/Coal-Calculations.aspx, Date viewed: 04 August 2015.

SGS Mining. Coal petrography, 2013. http://www.sgs.com/Mining/Metallurgy-and-Process-Design/High-Definition-Mineralogy/Coal-Petrography.aspx, Date viewed: 06 May 2015.

Shimp L., Kuhn J., Helfinstine J. Determination of Forms of Sulfur in Coal. Illinois State Geological Survey, 1997, pp. 99.

Shubert D., Lebya J. Chemistry and Physics for nurse Anesthesia, Springer Publishing Company, 2nd Edition, Accuracy and Precision, 2013, pp. 15.

Sima-Ella E., Yuan G., Mays T. A simple kinetic analysis to determine the intrinsic reactivity of coal chars. Fuel, Vol.84, 2005, pp. 1920-1925.

Sipilä J., Auerkari P., Holmstrom S., Itkonen J. and Aaltonen K. Observations on the Smith - Glasser index for self-heating of bituminous coal. Journal of Fire Sciences 30 (4), 2012, pp. 331 - 338.

Smith M, Glasser D. Spontaneous combustion of carbonaceous stockpiles. Part II. Factors affecting the rate of the low-temperature oxidation reaction. Fuel 84, 2005, pp. 1161 – 1170.

Snedecor G., Cochran W., 1989, 8th Edition. Statistical Methods, Iowa State University Press, pp. 121-124.

Stephenson H. Fire at Michael Colliery Fife. Ministry of Power, 1968.

Stenzel J. The Effects of Spontaneous Combustion on Safety, Health and the Environment at New Vaal Colliery. (SACMA), 2002. http://www. sacollierymanagers.org.za/Publications/publications/Papers/sacma9.pdf viewed 2 February 2016.

Thomas L. (2002). Coal Geology. (Chichester, John Wiley & Sons, Ltd, 2002).pp. 106 Retrieved from https://books.google.co.za/books?isbn=0471485314, viewed 2 February 2016.

Transnet. Increment of volumes as road-to-rail drive gains momentum, capex breaks record, 2014. http://www.transnet.net/PressOffice/Press%20Office%20Release/Transnet%20ups%20volumes%20as%20road-to- rail%20drive%20gains%20momentum%20and%20capex%20breaks %20record.pdf, Date viewed: 13 May 2015

Truś T. IEA Coal Data System. Energy Statistics Division Coal, Renewables, Electricity and Heat Section. 2010.

Uludag S. A visit to the research on Wits-Ehac index and its relationship to inherent coal properties for Witbank Coalfield. The Journal of the Southern African Institute of Mining and Metallurgy, Vol 107, 2007, pp. 671 – 679.

Uludag S. Spontaneous combustion index at University of Witwatersrand and its application: the past, present and future. Reviews in Engineering Geology 18, 2007, pp. 15 – 22.

Wang H., Dlugogorski B., Kennedy E. Coal oxidation at low temperatures: oxygen consumption, oxygen products, reaction mechanism and kinetic modelling. Progress in Energy and Combustion Science 29, 2003, pp. 487 – 513.

Wang H., Dlugogorski B., Kennedy E. Examination of CO_2, CO and H_2O formation during low-temperature oxidation of a bituminous coal. Energy & Fuels, Vol.16, 2002, pp. 586-592.

Wikipedia, Mount Mulligan mine disaster, 1921. https://en.wikipedia.org/wiki/Mount_Mulligan_mine_disaster. Date viewed: 29 January 2016.

World Coal Association. What is Coal?, The Coal Resource: A Comprehensive Overview of Coal Publication, 2005. http://www.worldcoal.org/bin/pdf/original_pdf_file/coal_resource_overview_of_coal_report(03_06_2009).pdf, Date viewed: April 29 2015.

Yuan L., Smith A. The effect of ventilation on spontaneous heating of coal. Office of Mine Safety and Health Research, National Institute for Occupational Safety and Health, 1991.

CHAPTER 8

8 APPENDICES

8.1 Appendix A

8.1.1 Proximate Analysis

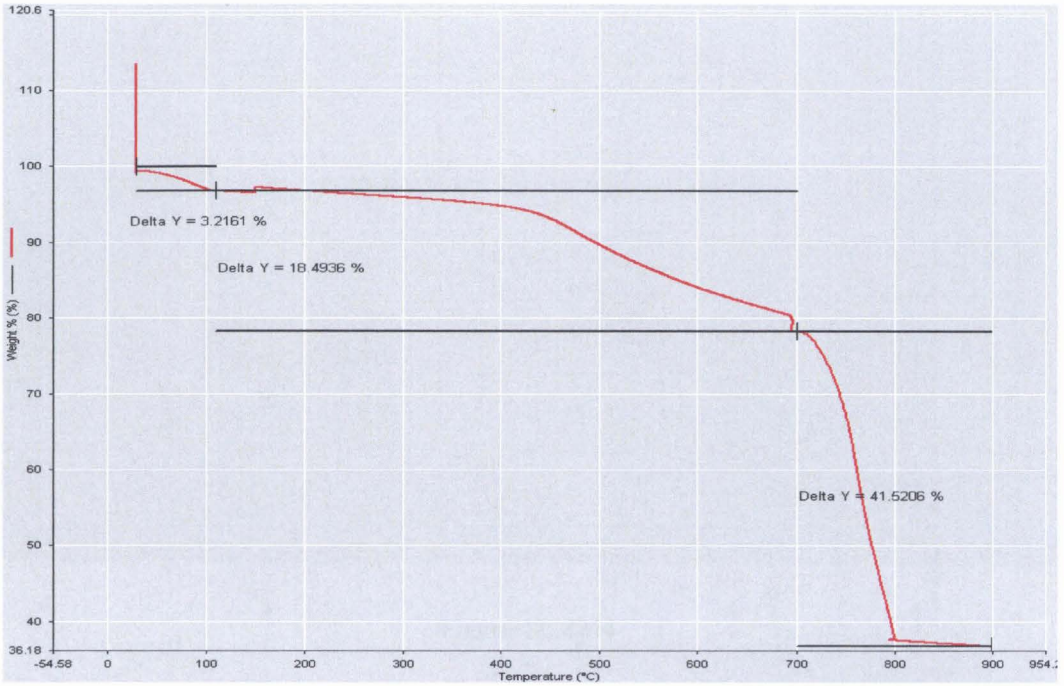


Figure 38: ZM2

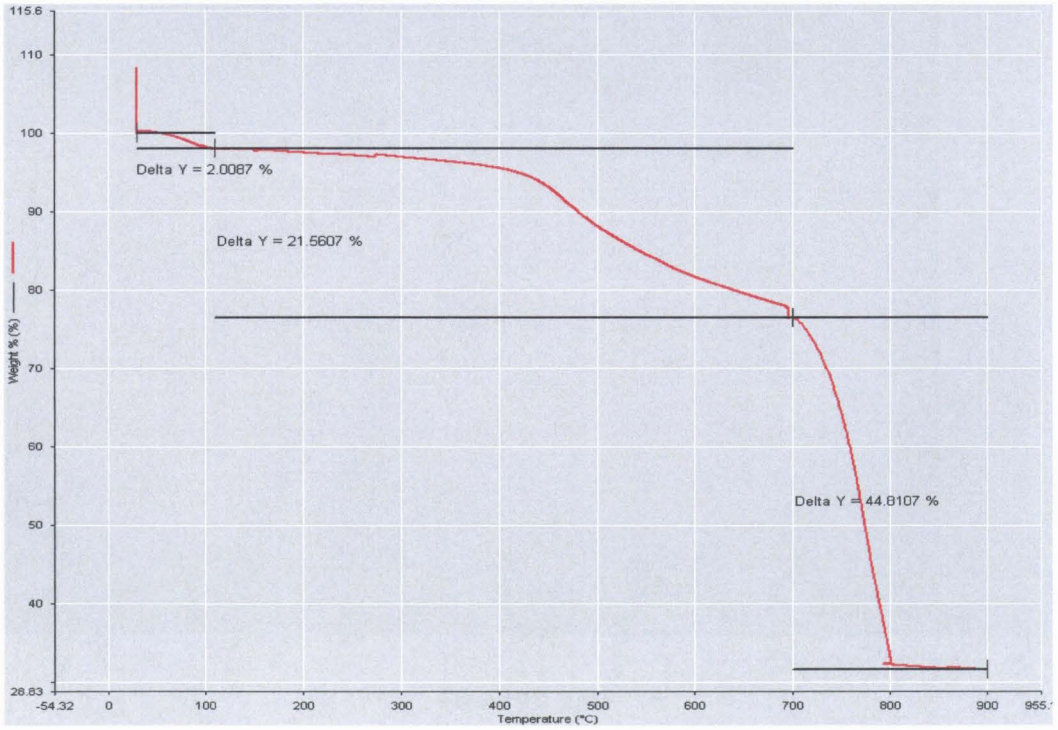


Figure 39: ZM3

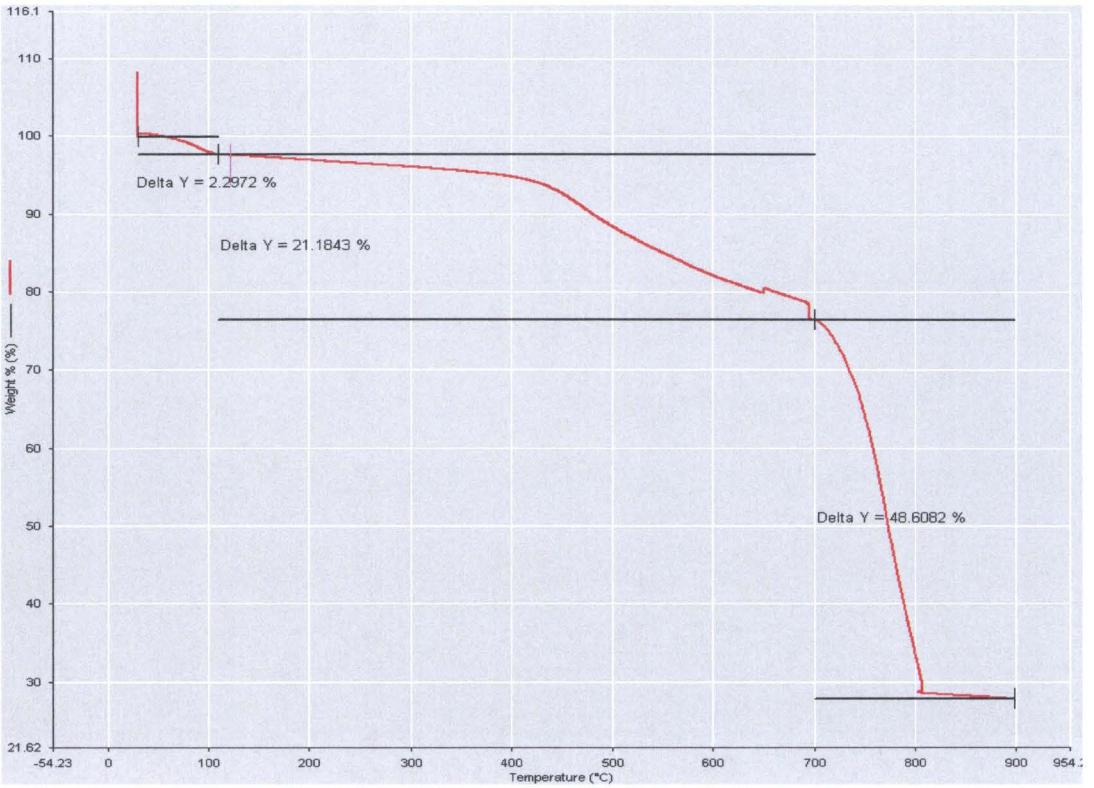


Figure 40: ZM4

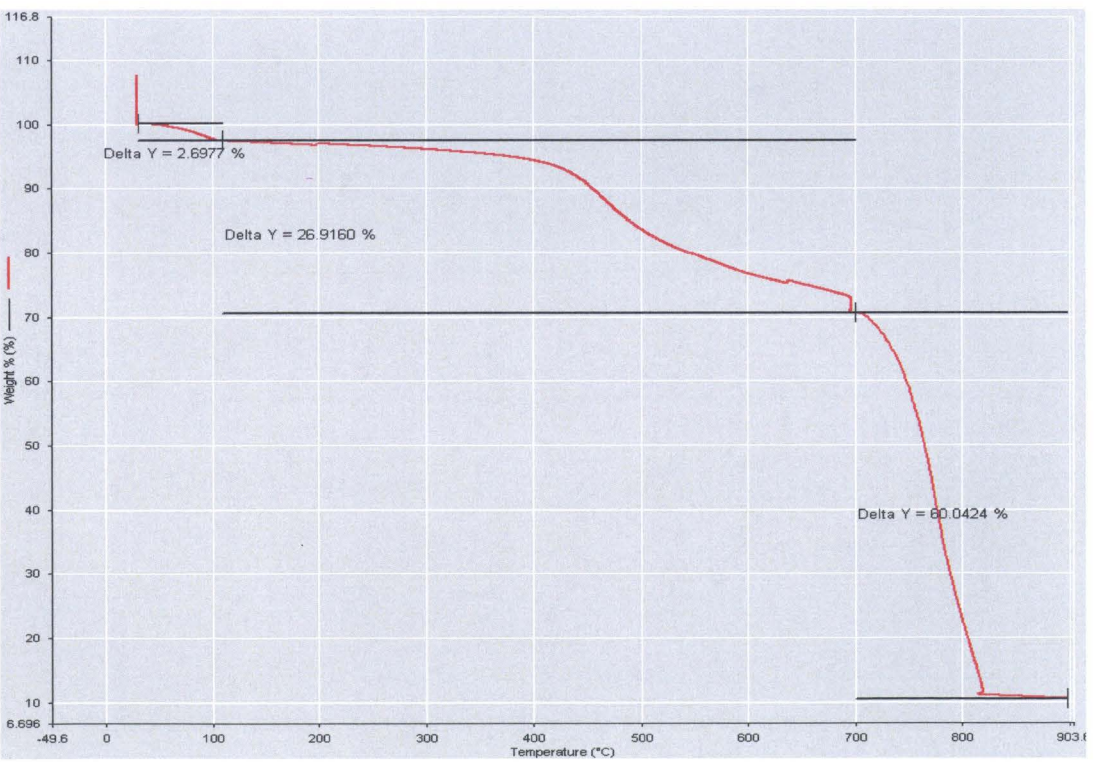


Figure 41: ZM5

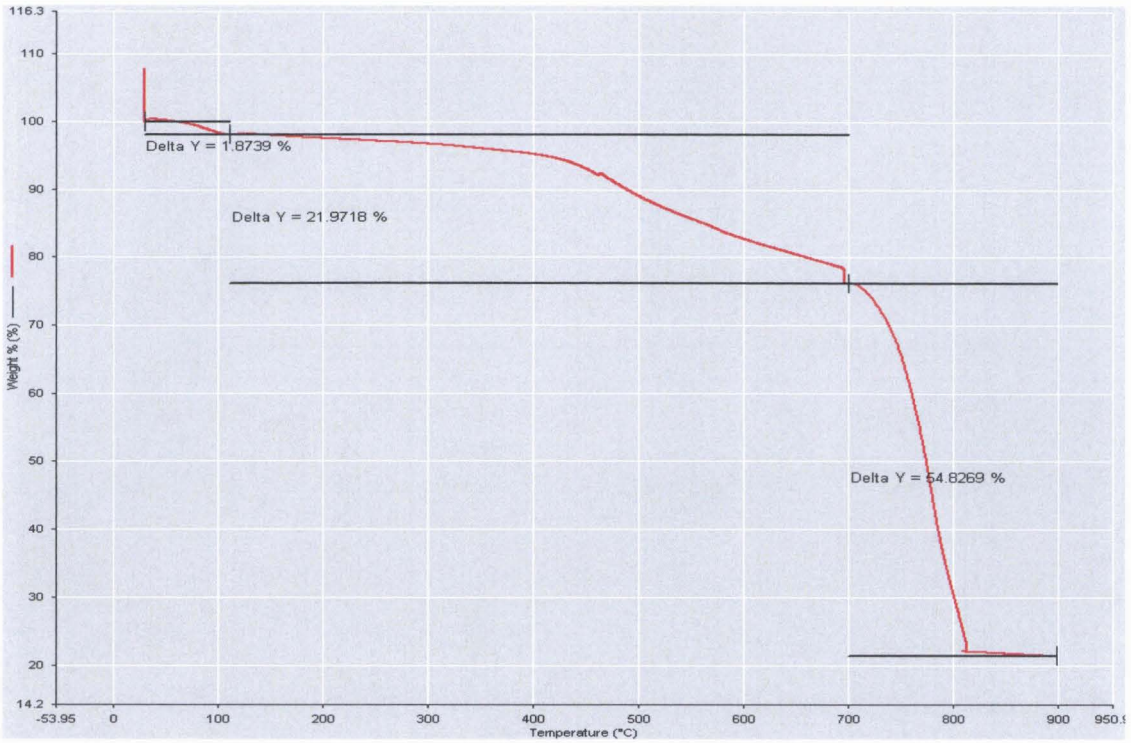


Figure 42: ZM6

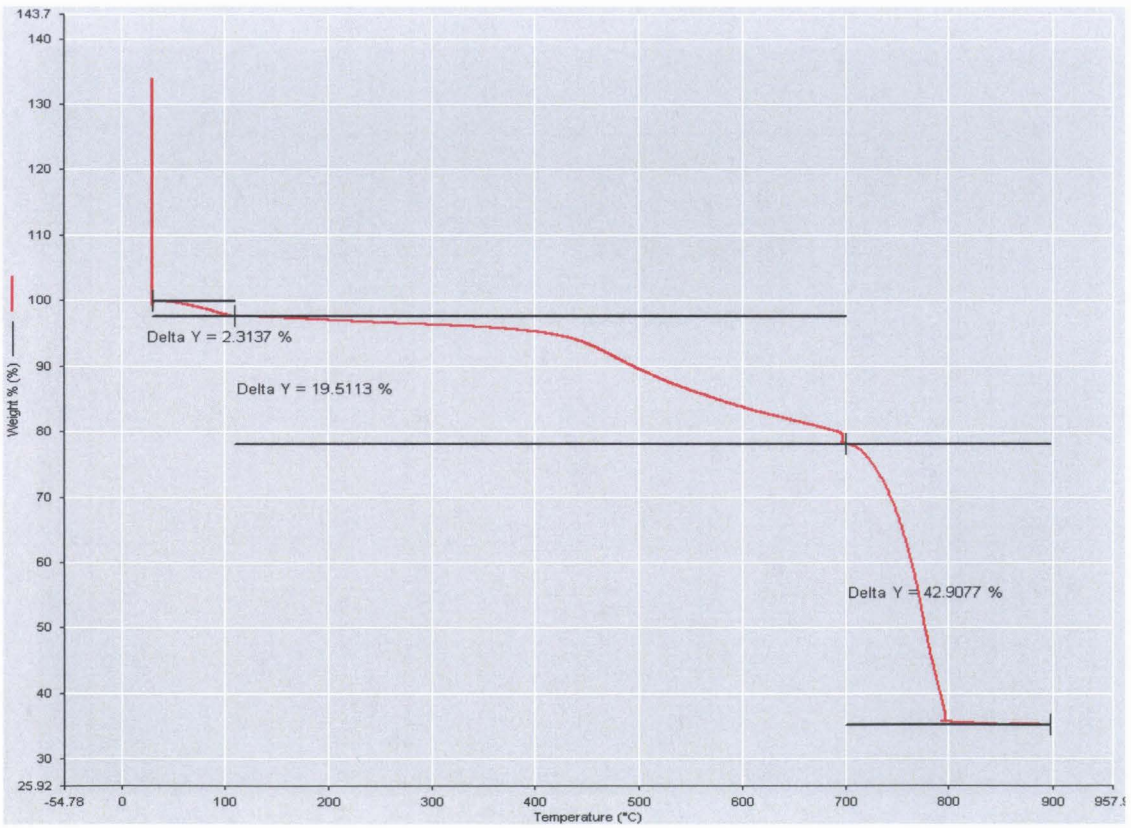


Figure 43: ZM7

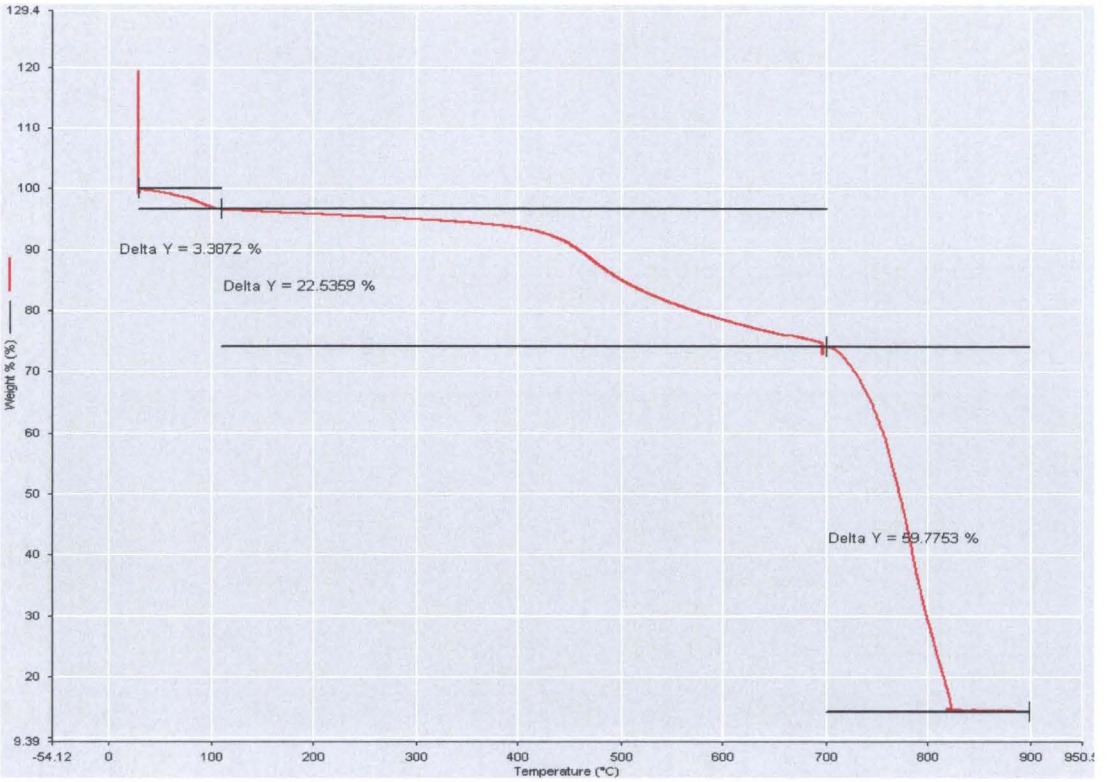


Figure 44: ZM8

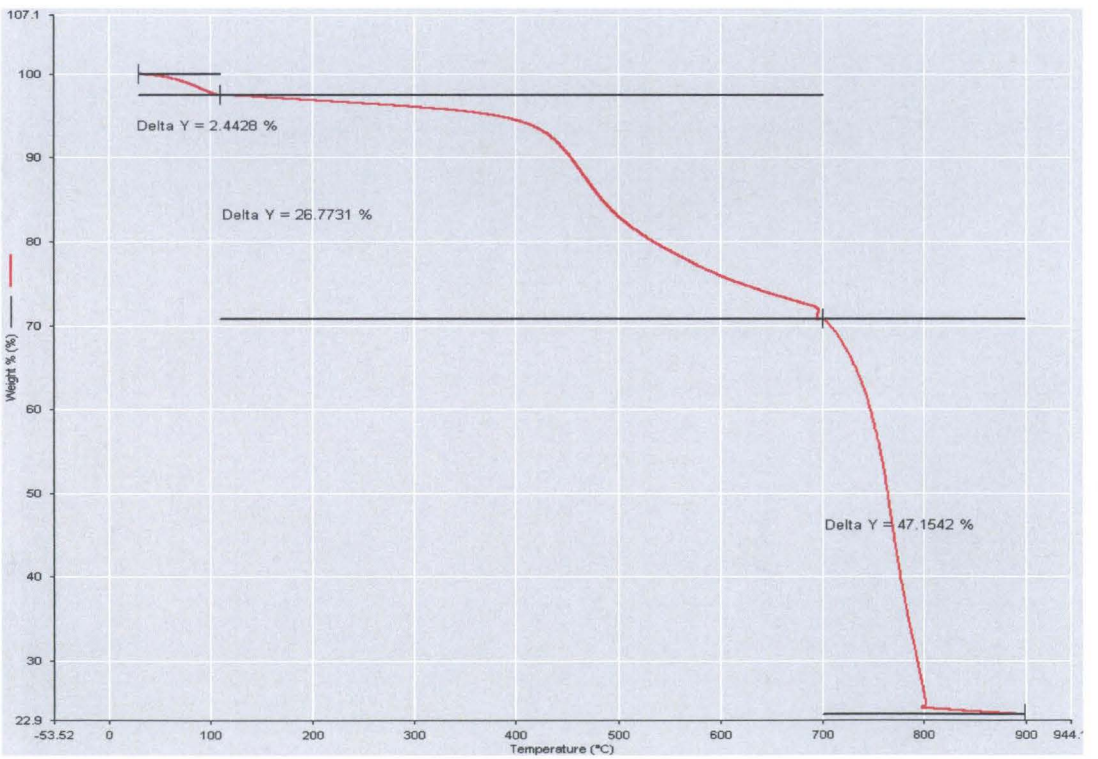


Figure 45: ZM9

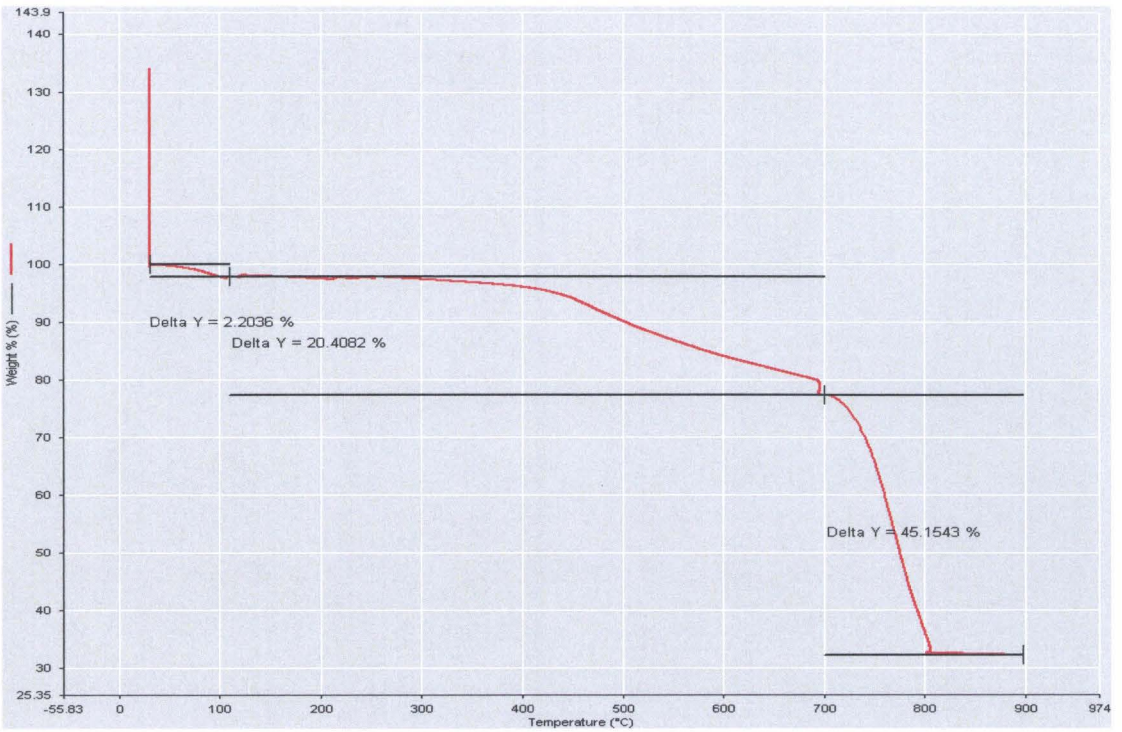


Figure 46: ZM10

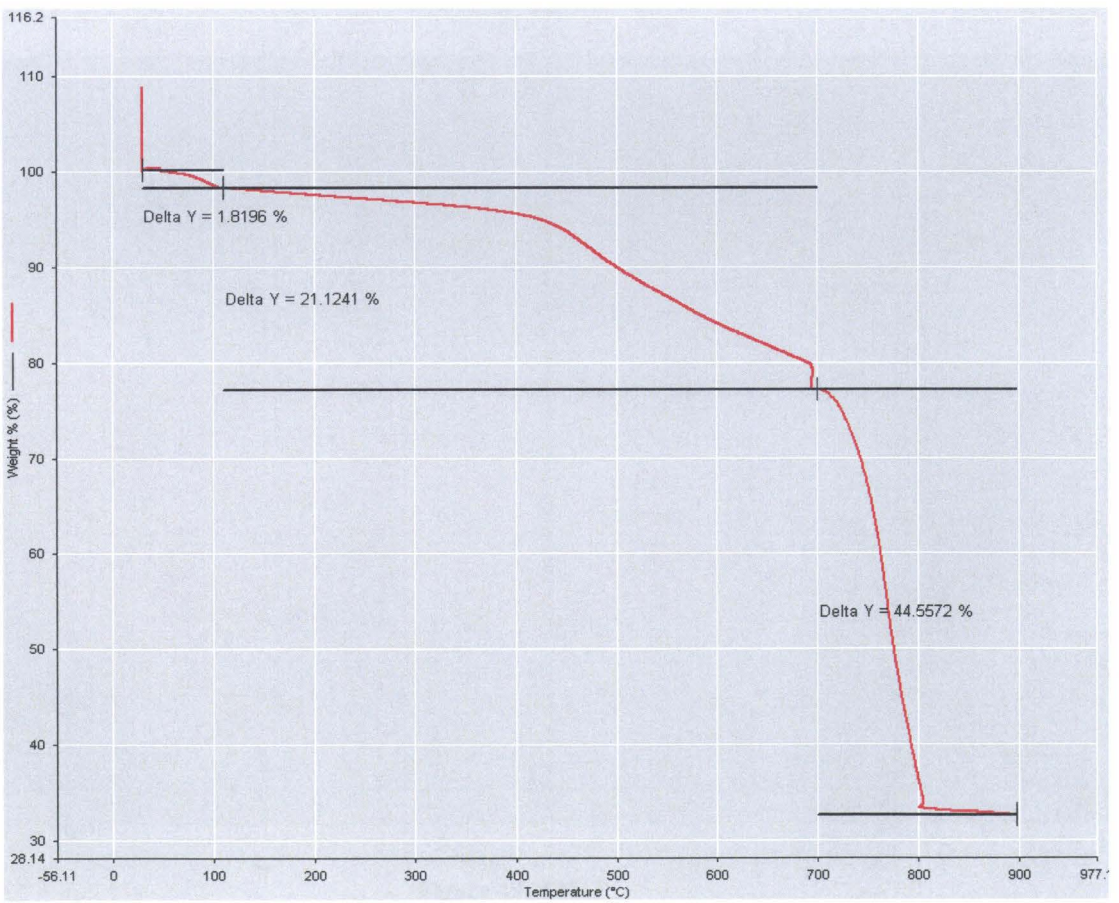


Figure 47: ZM11

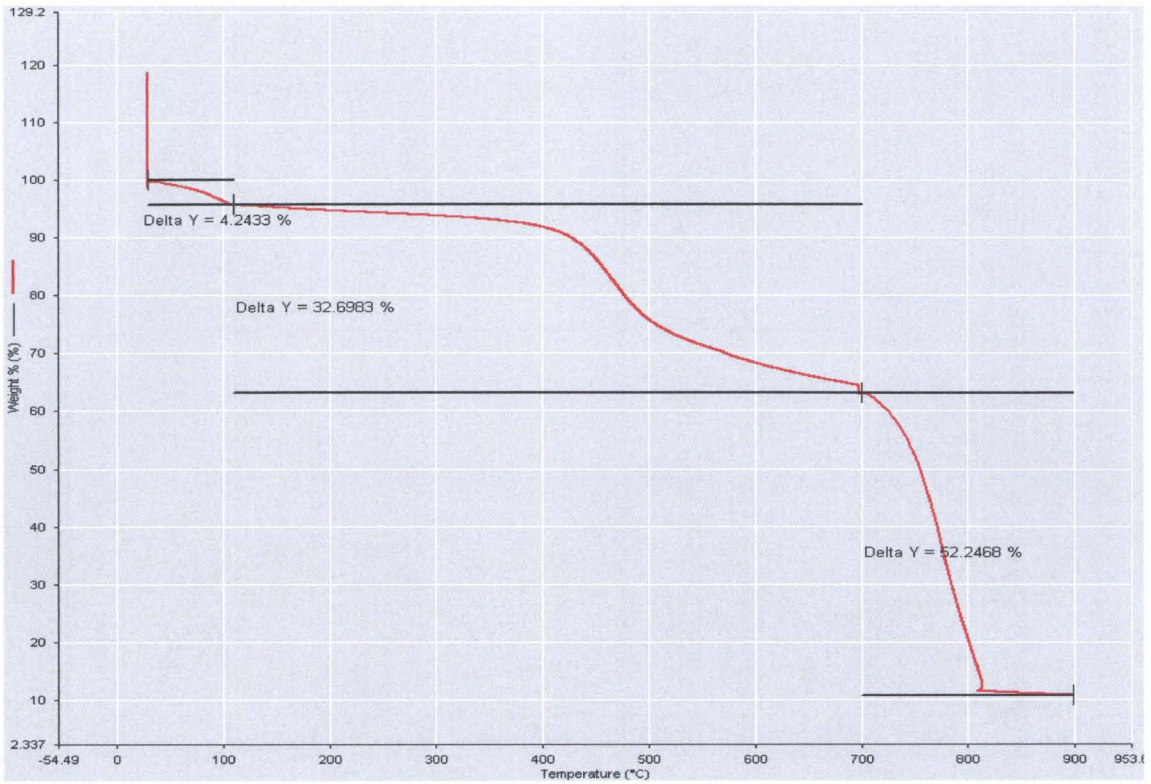


Figure 48: ZM12

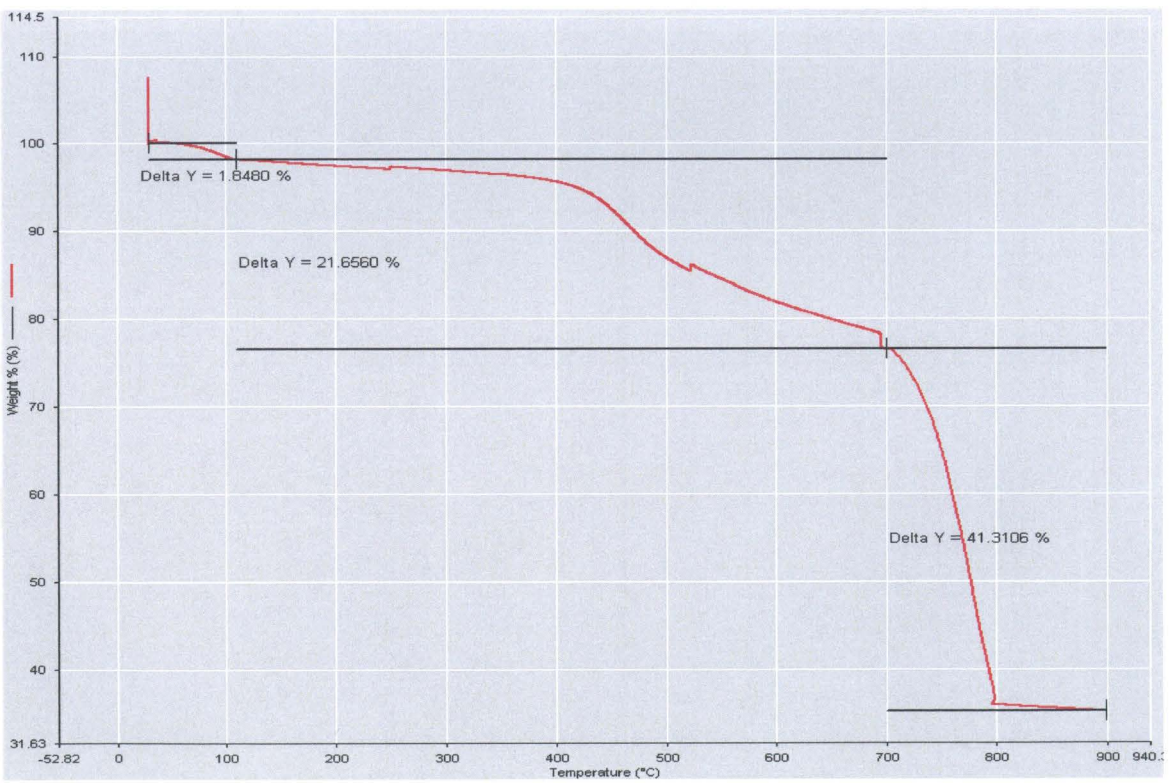


Figure 49: ZM13

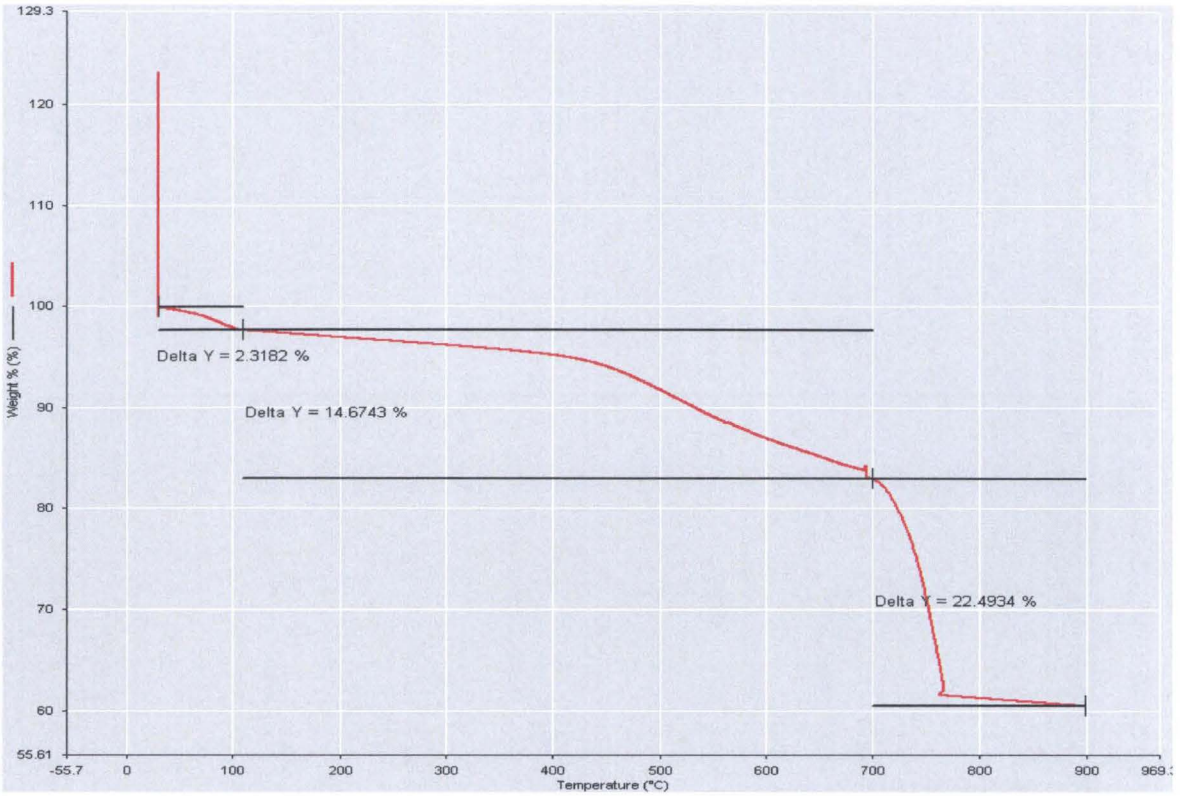


Figure 50: ZM14

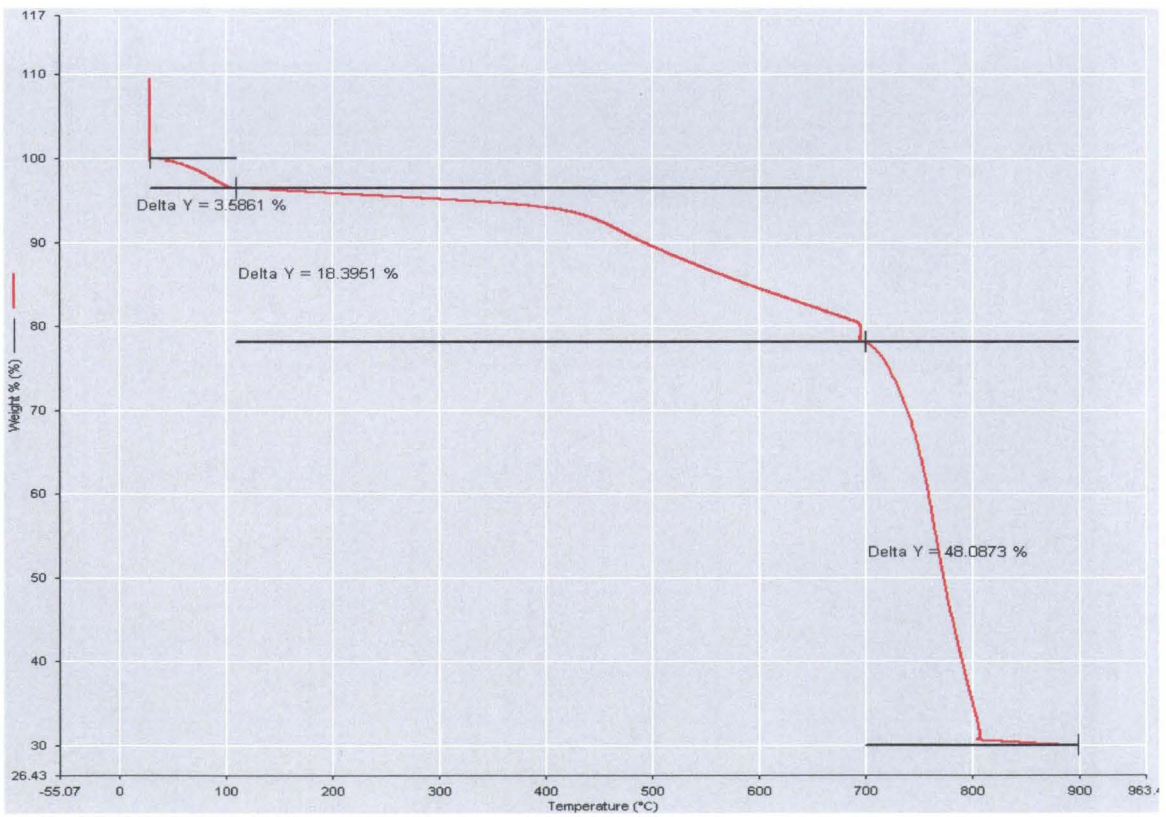


Figure 51: ZM15

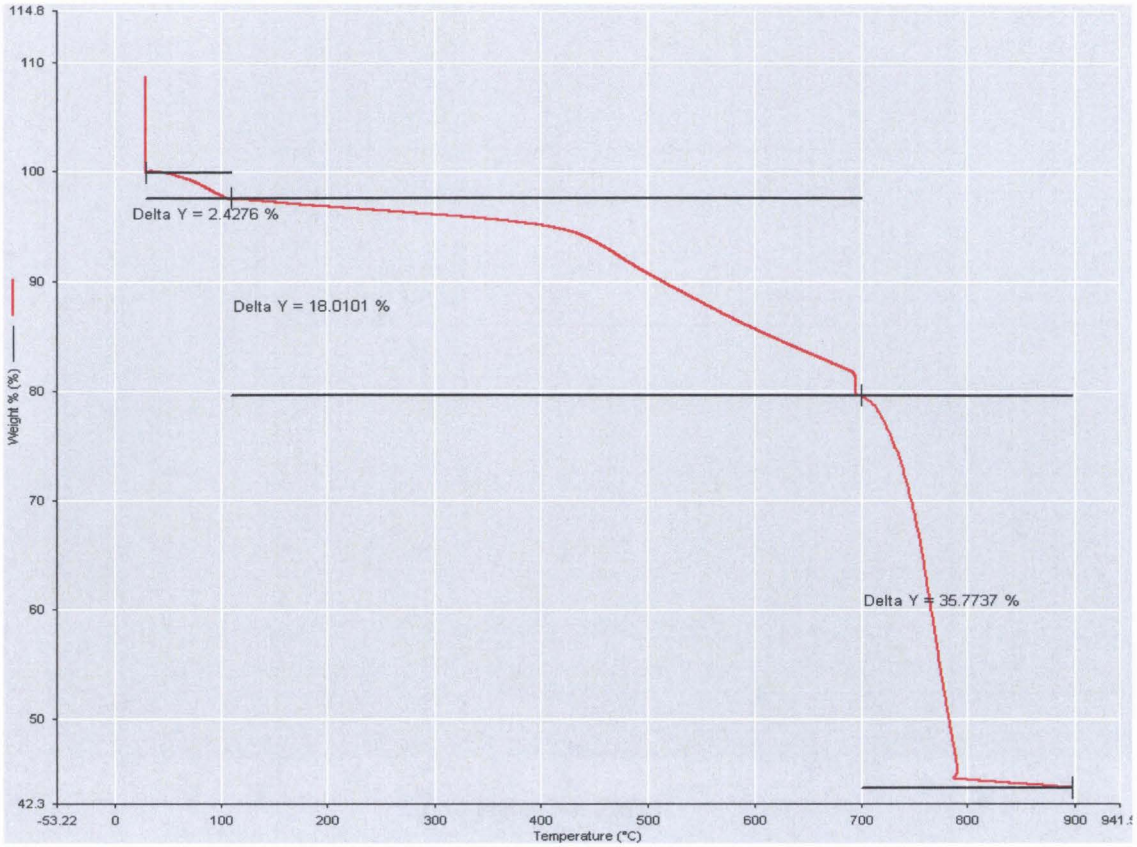


Figure 52: ZM16

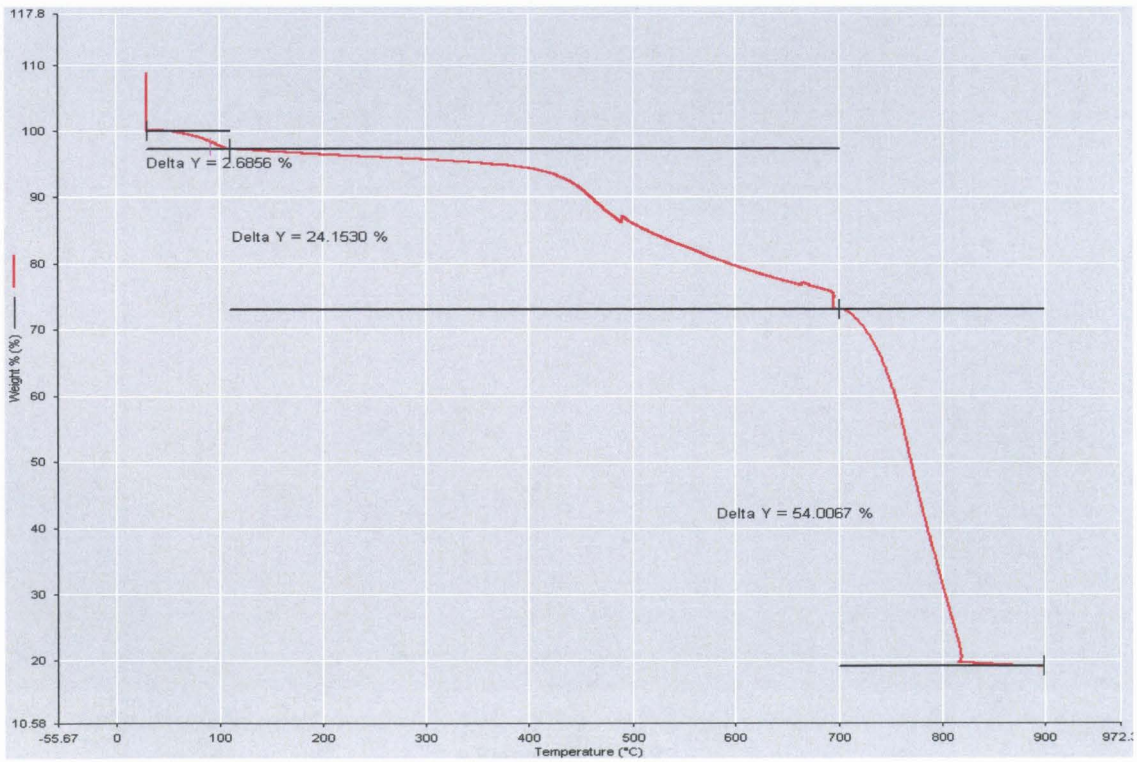


Figure 53: ZM17

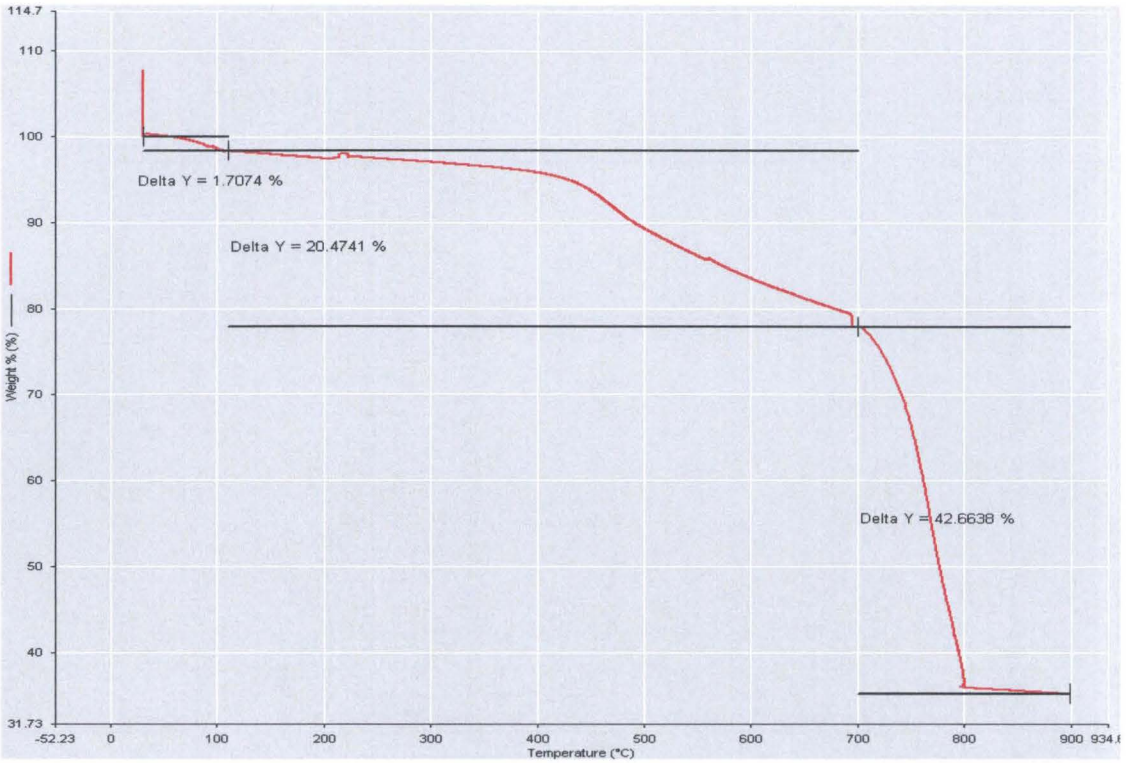


Figure 54: ZM18

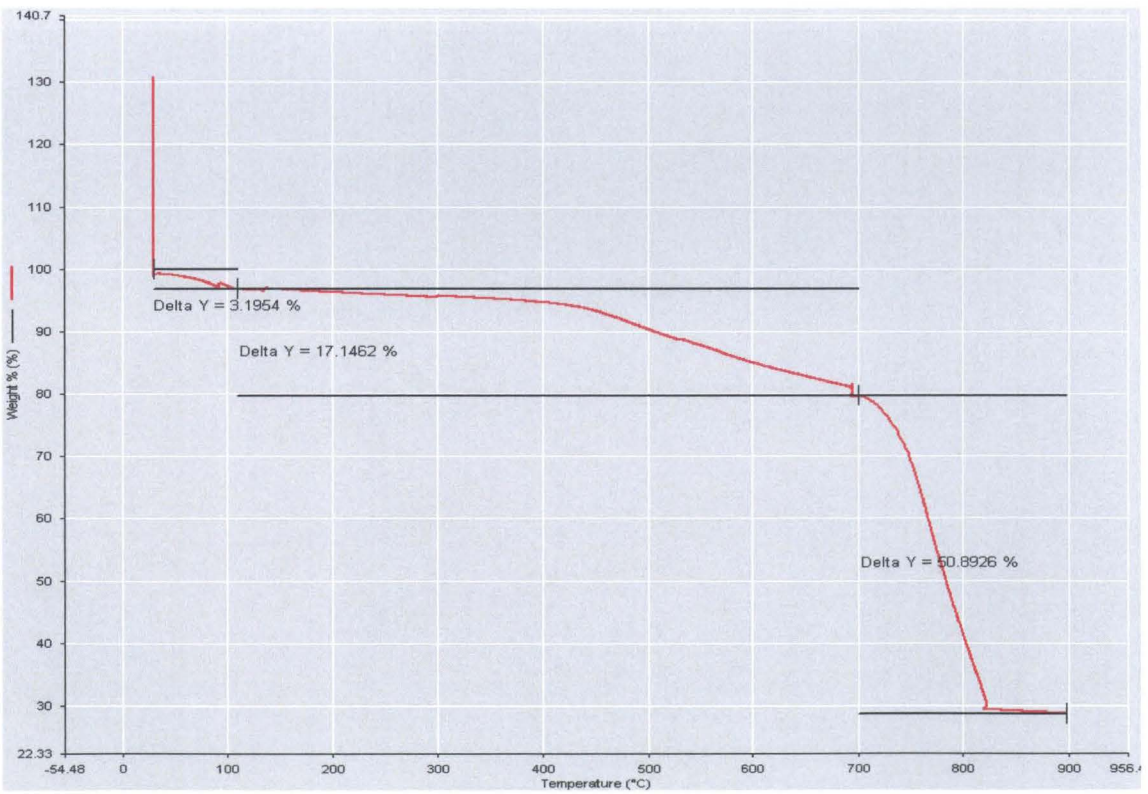


Figure 55: ZM19

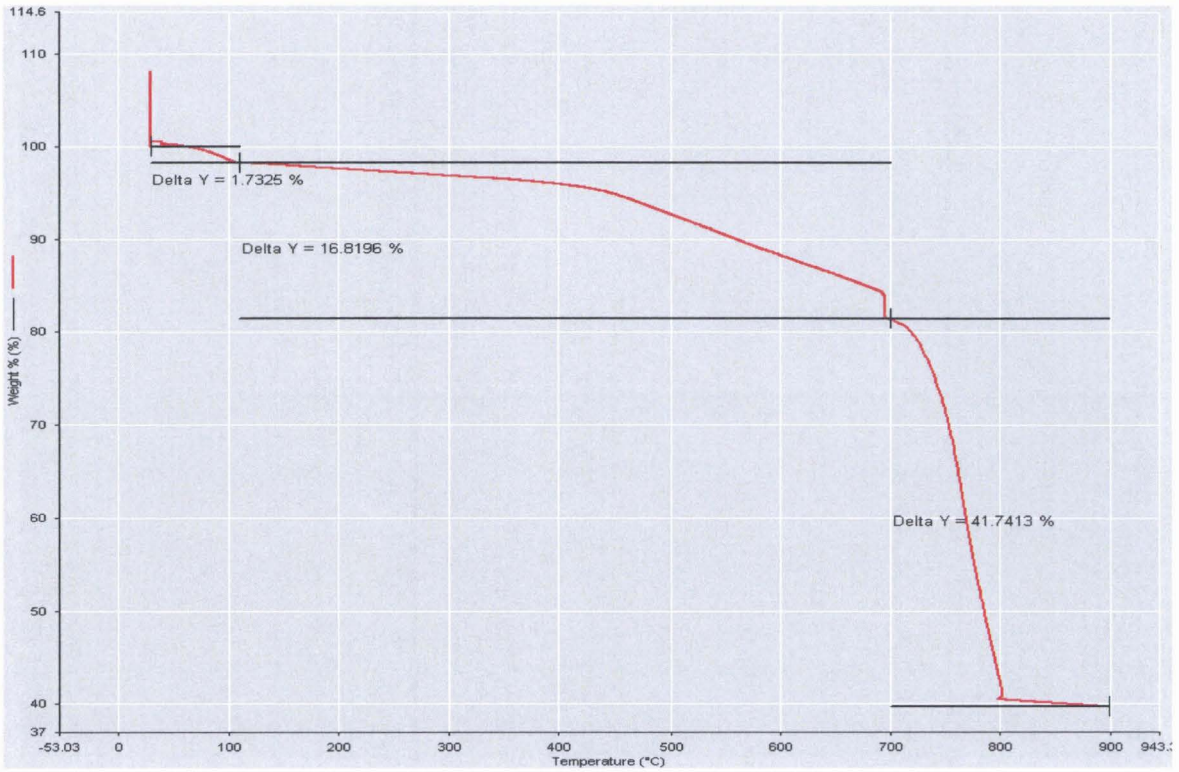


Figure 56: ZM20

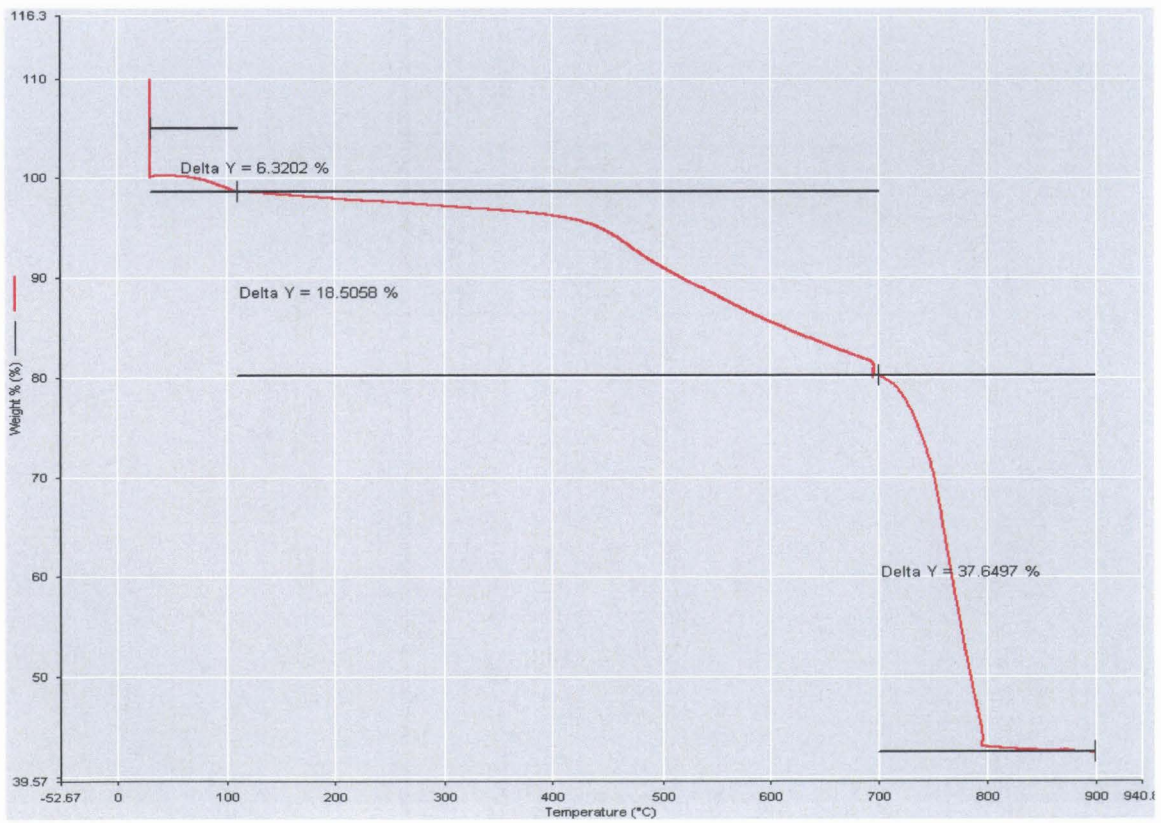


Figure 57: ZM21

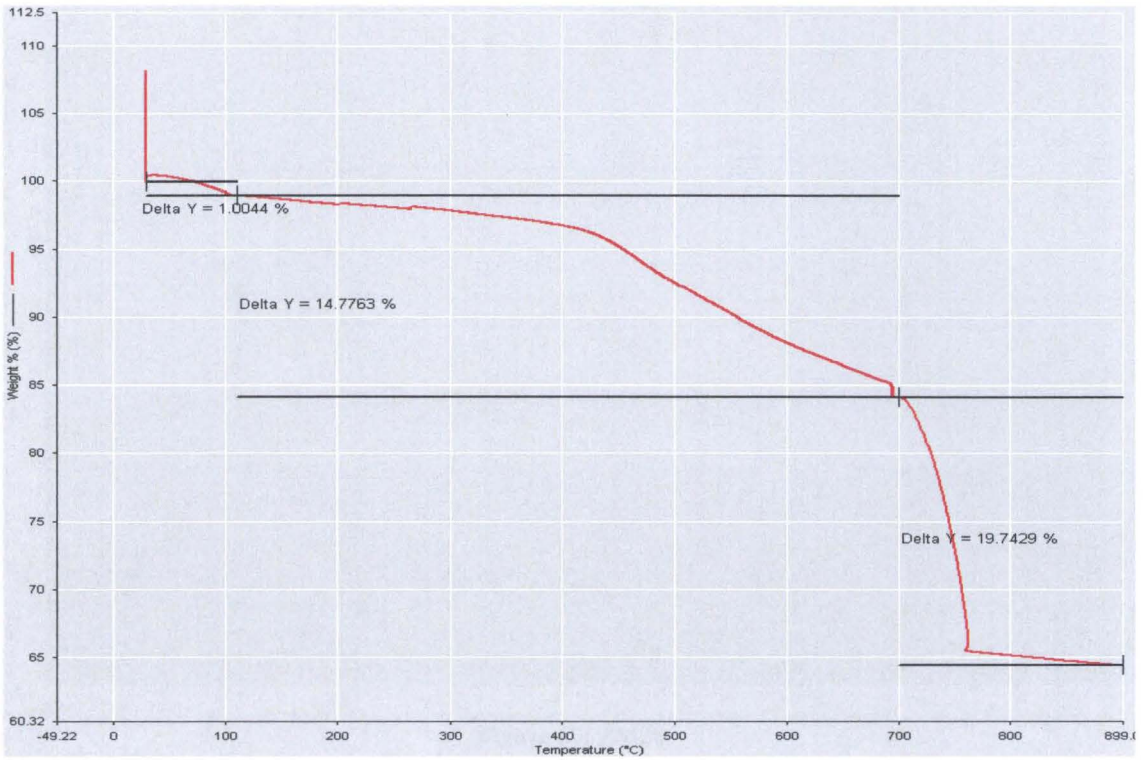


Figure 58: ZM22

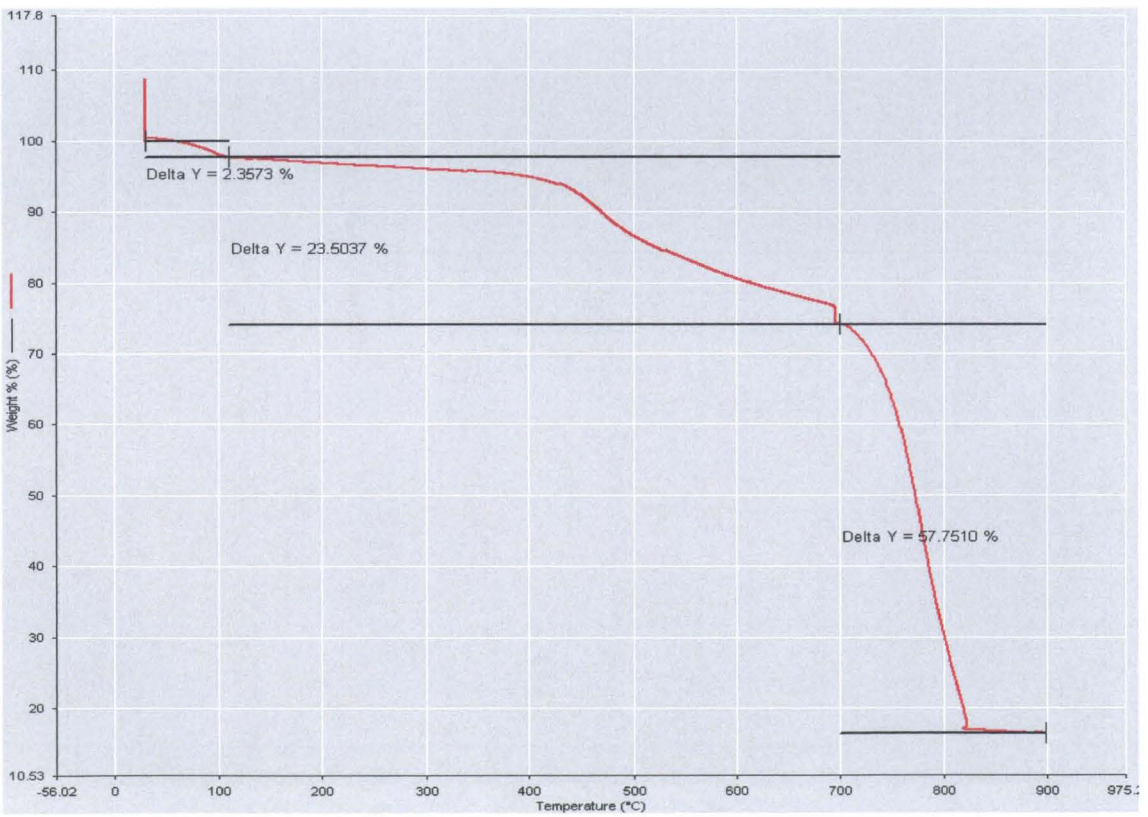


Figure 59: ZM23

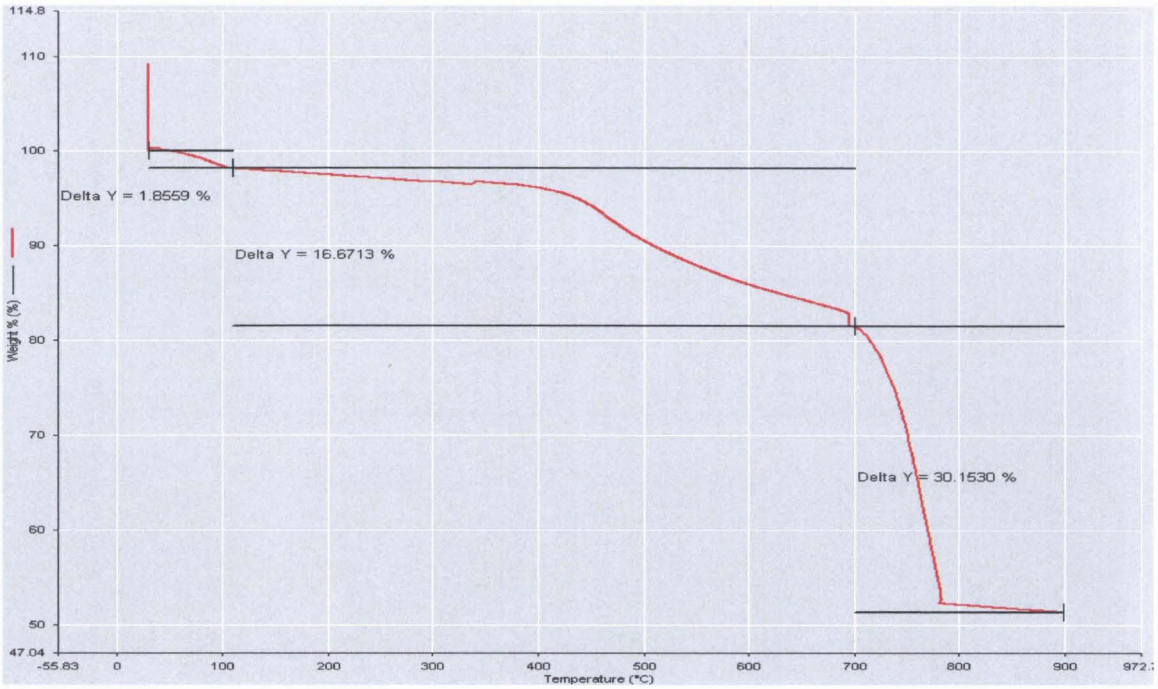


Figure 60: ZM24

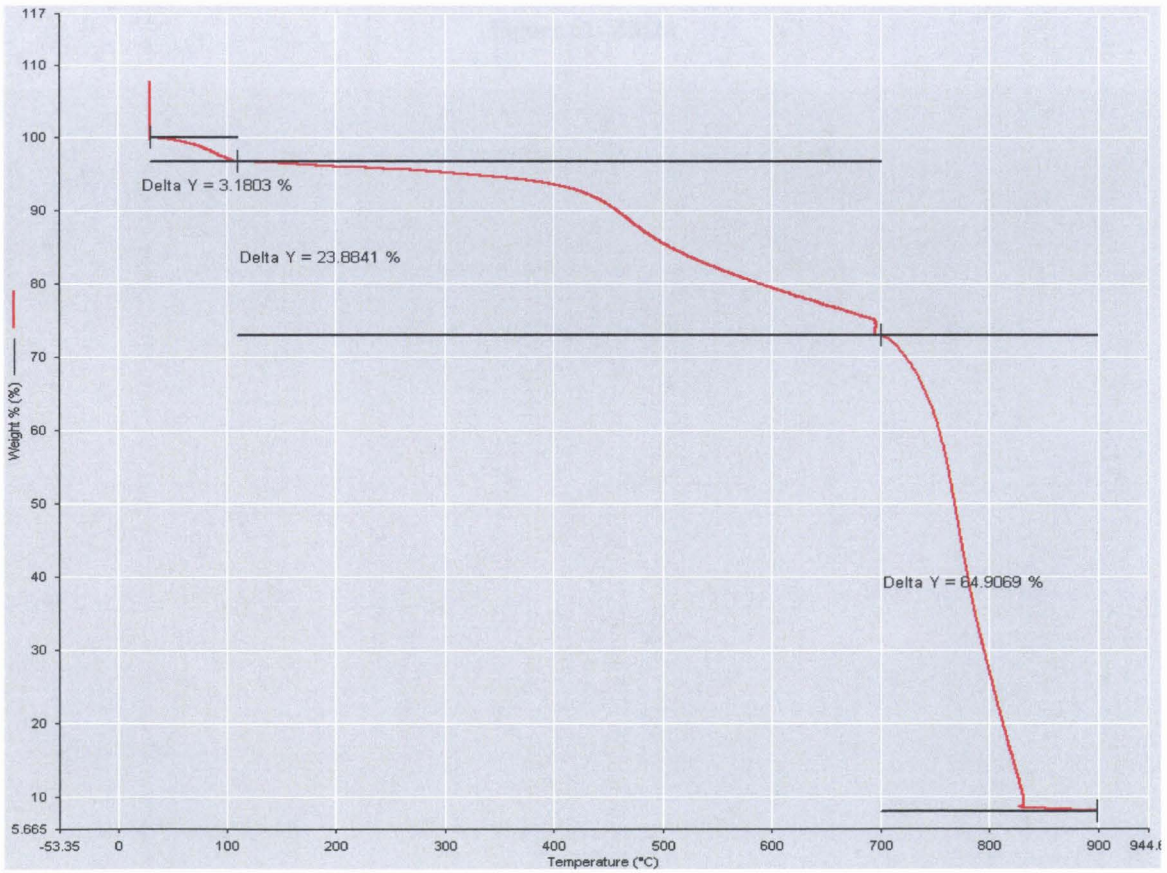


Figure 61: ZM25

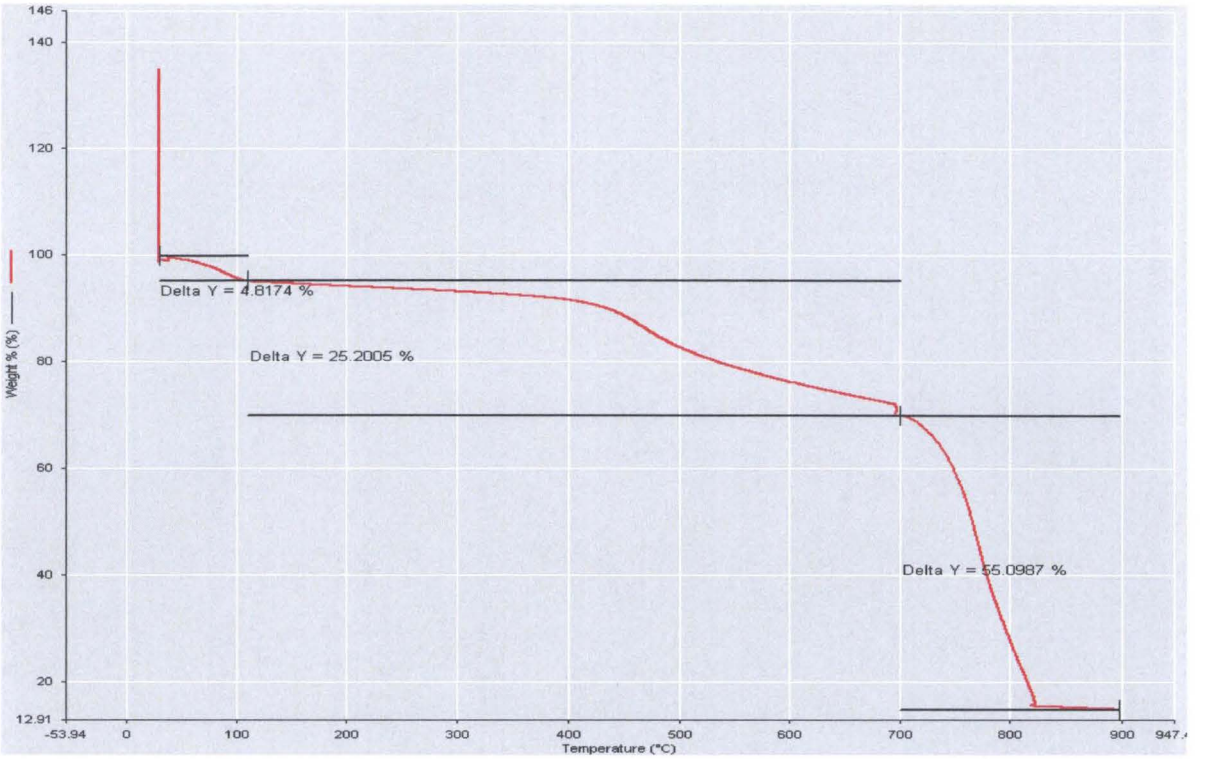


Figure 62: ZM26

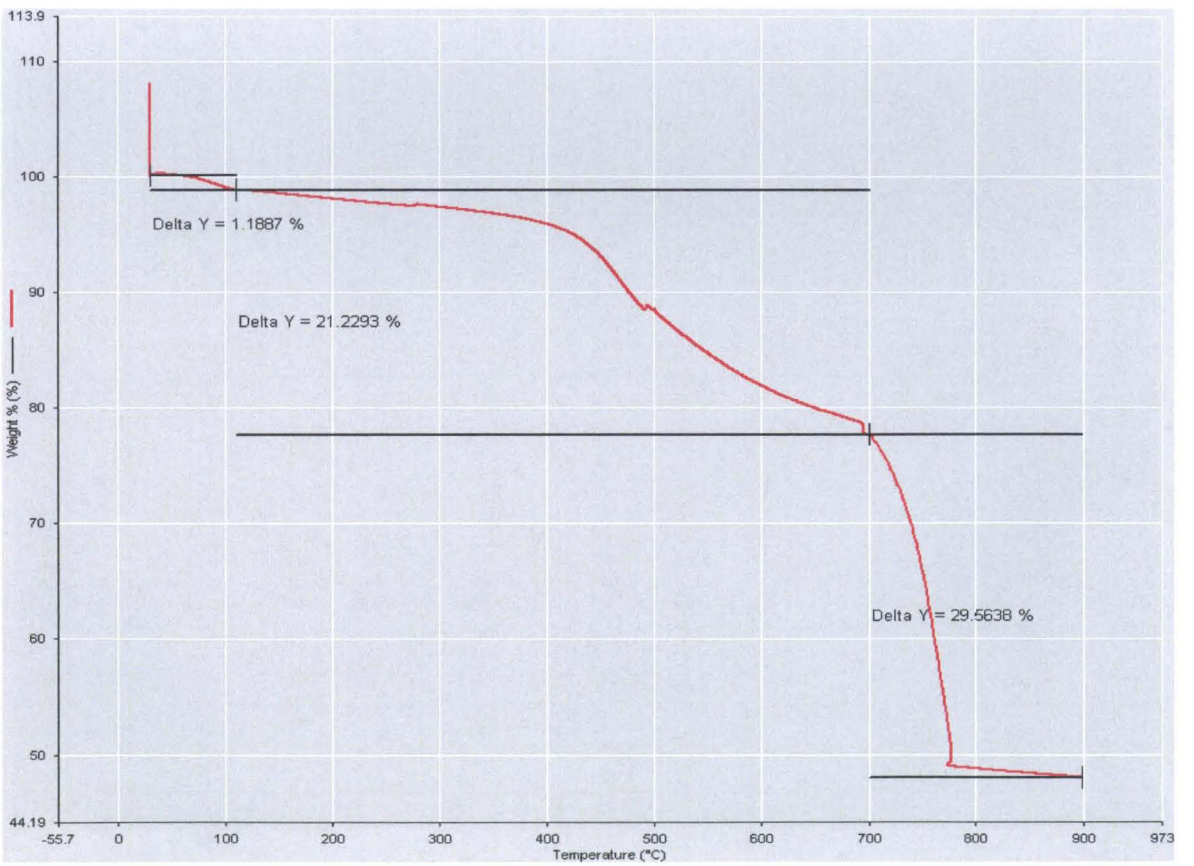


Figure 63: ZM27

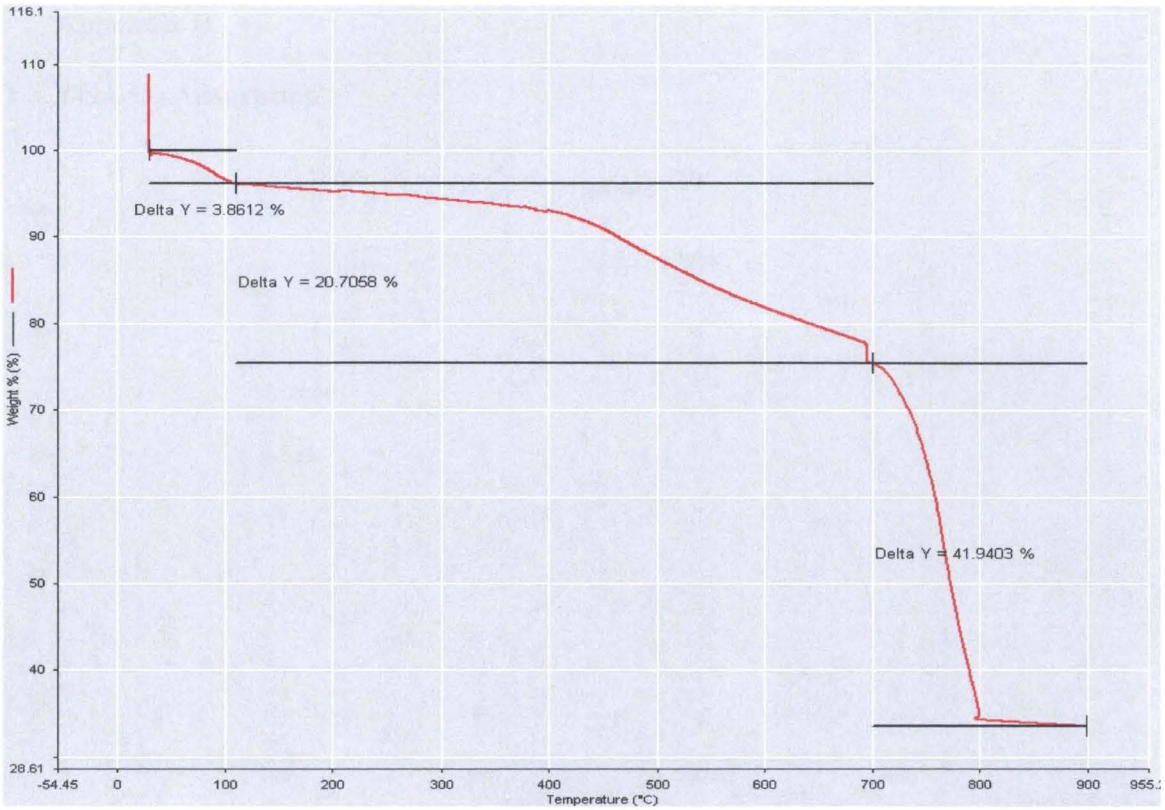


Figure 64: ZM28

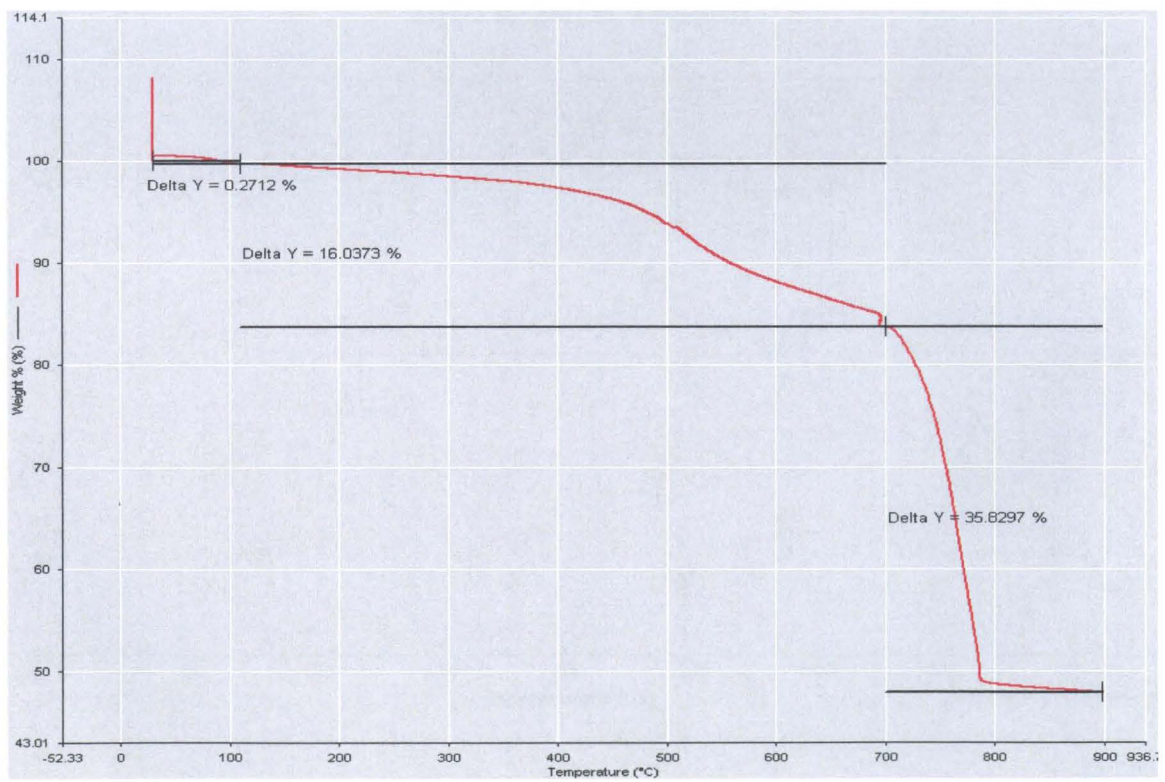


Figure 65: ZM29

8.2 Appendix B

8.2.1 TGA O_2 Adsorption

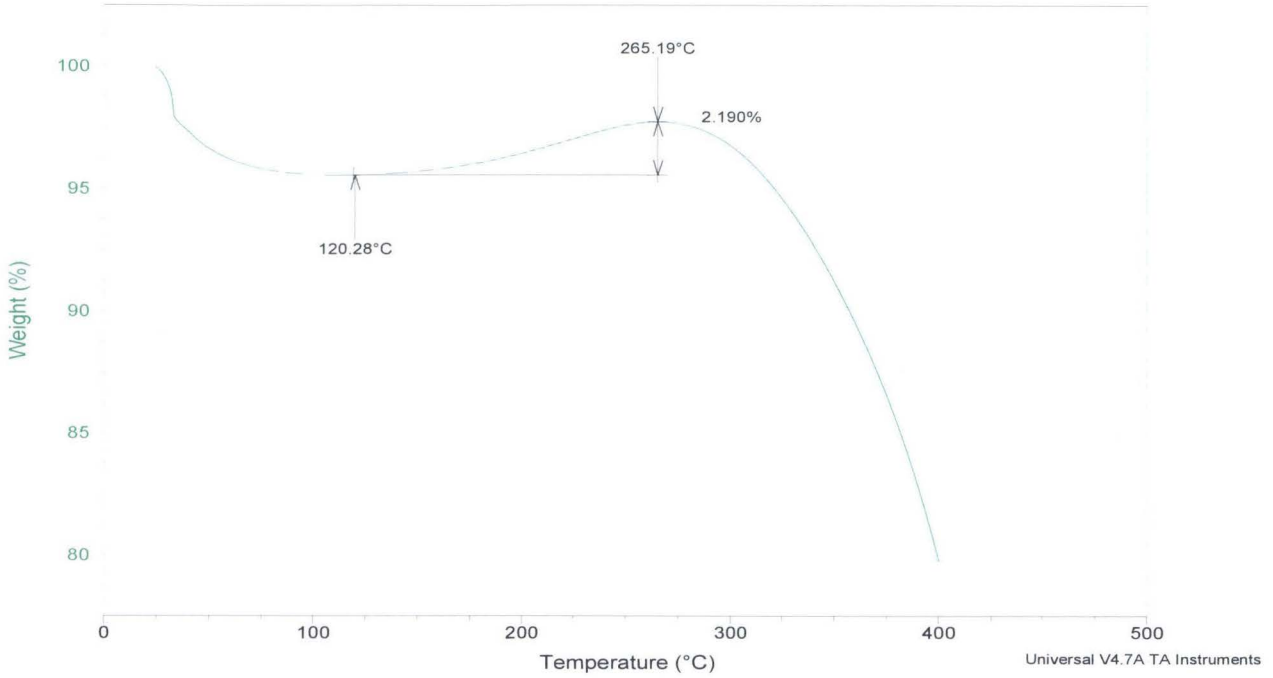


Figure 66: ZM1 O_2 Adsorption

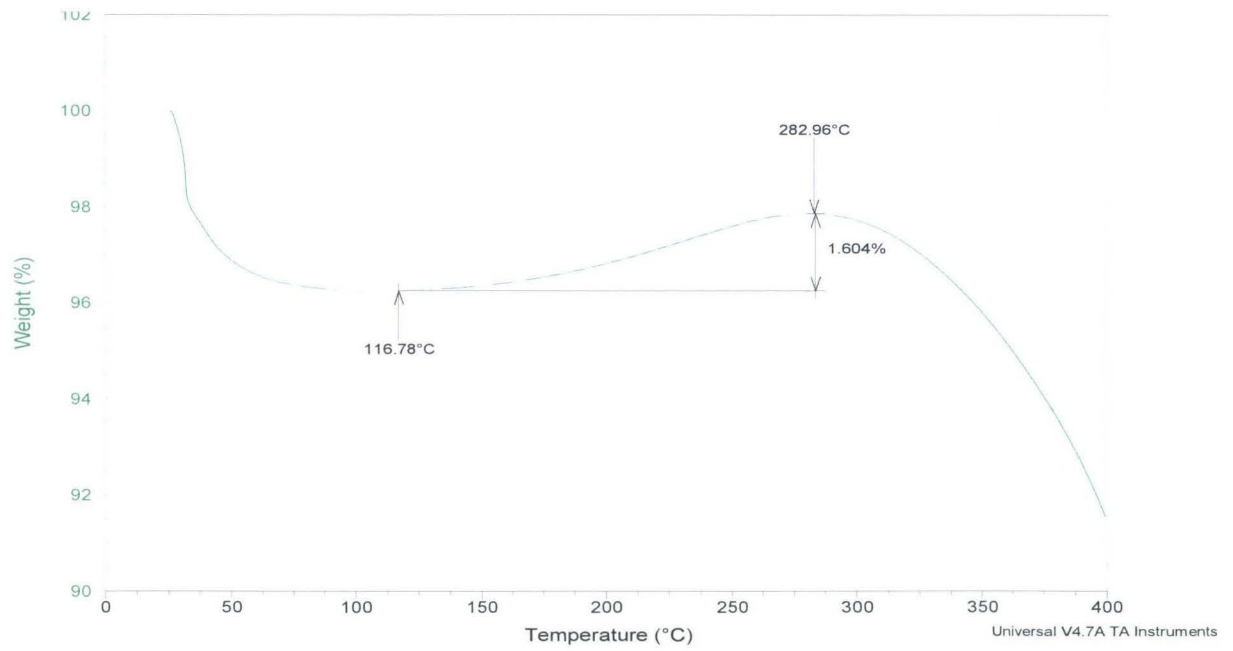


Figure 67: ZM2 O_2 Adsorption

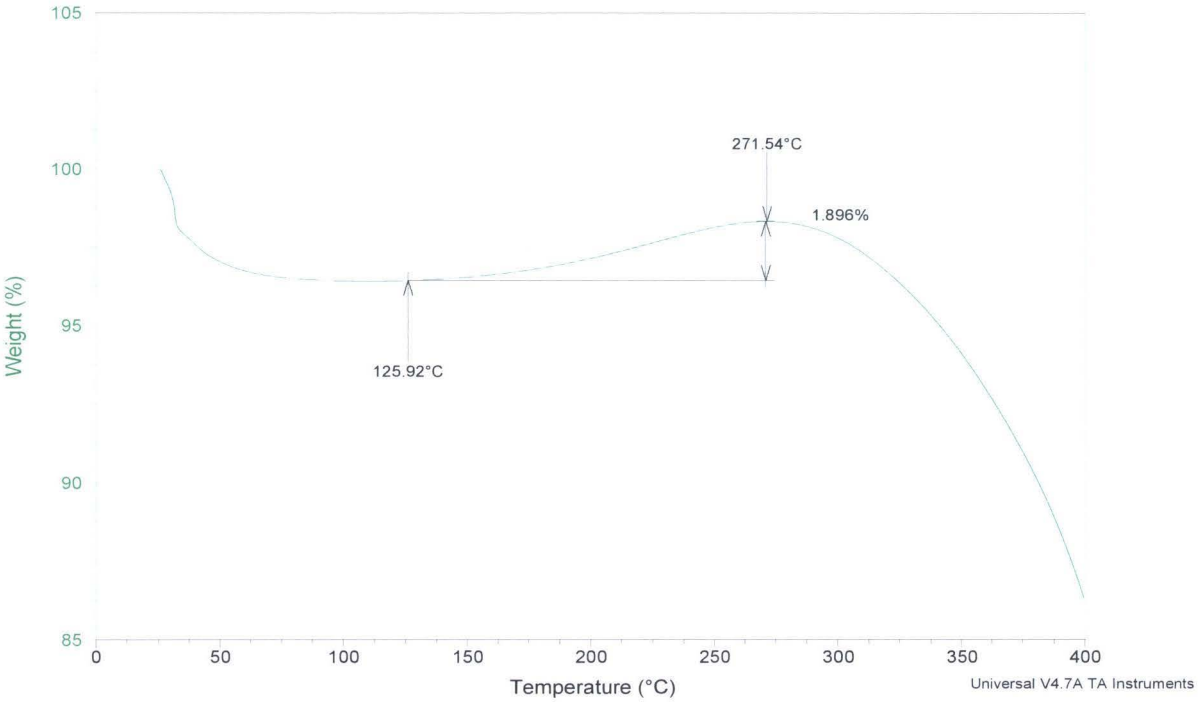


Figure 68: ZM3 O_2 Adsorption

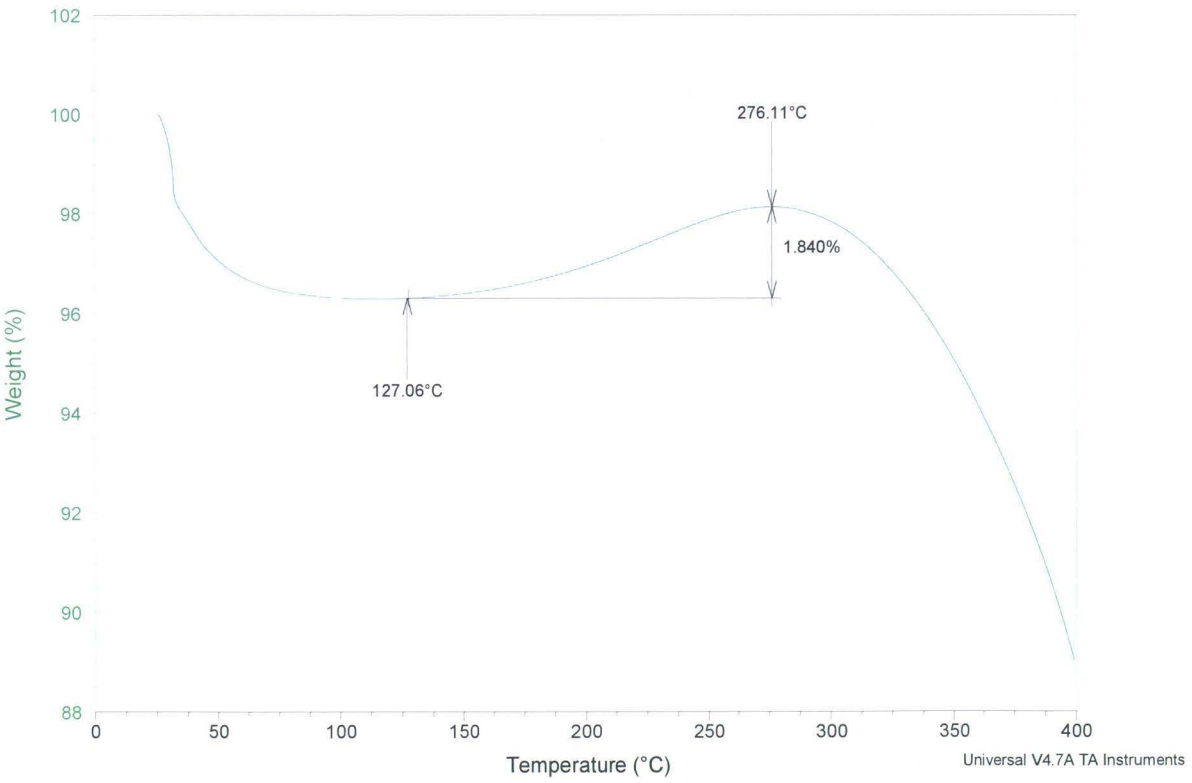


Figure 69: ZM4 O_2 Adsorption

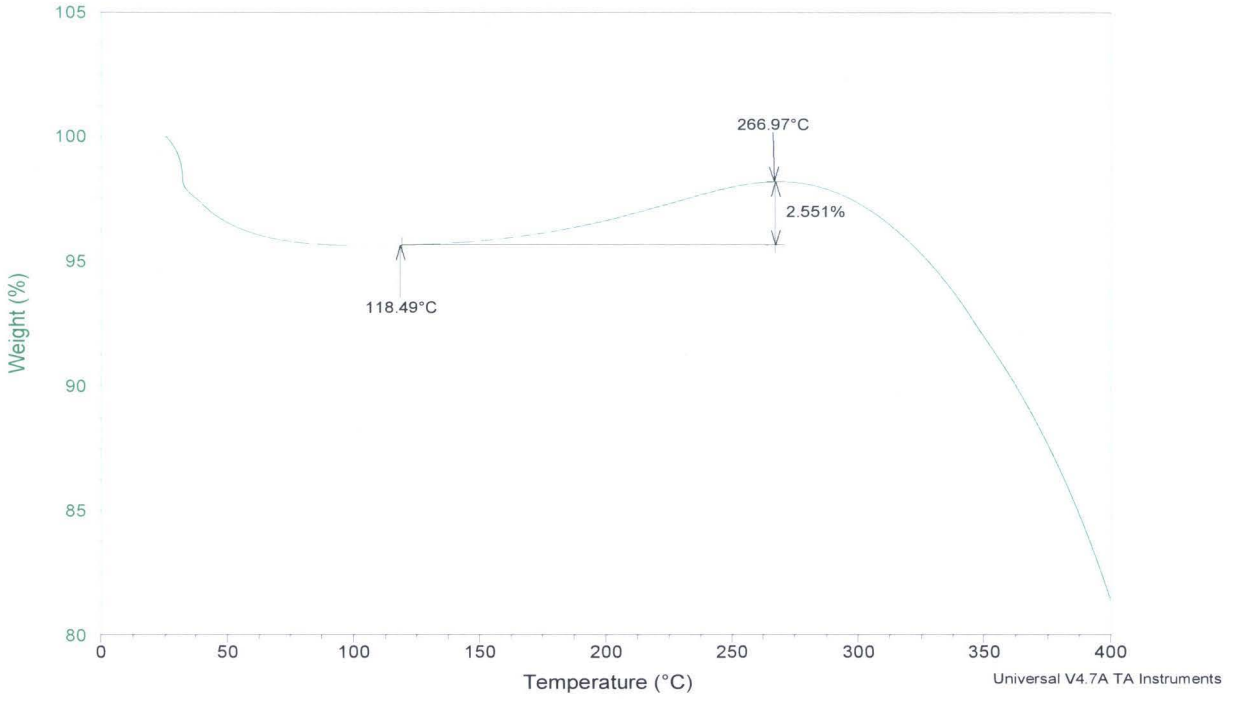


Figure 70: ZM5 O_2Adsorption

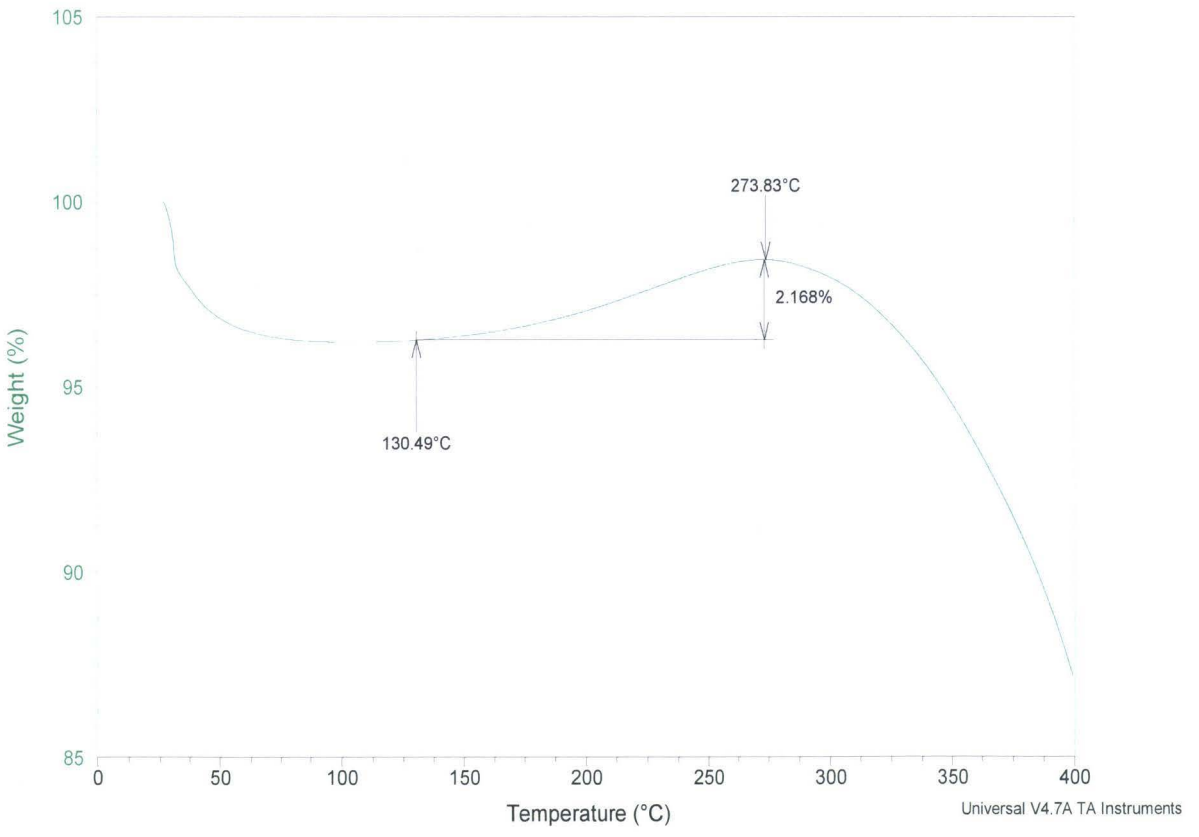


Figure 71: ZM6 O_2 Adsorption

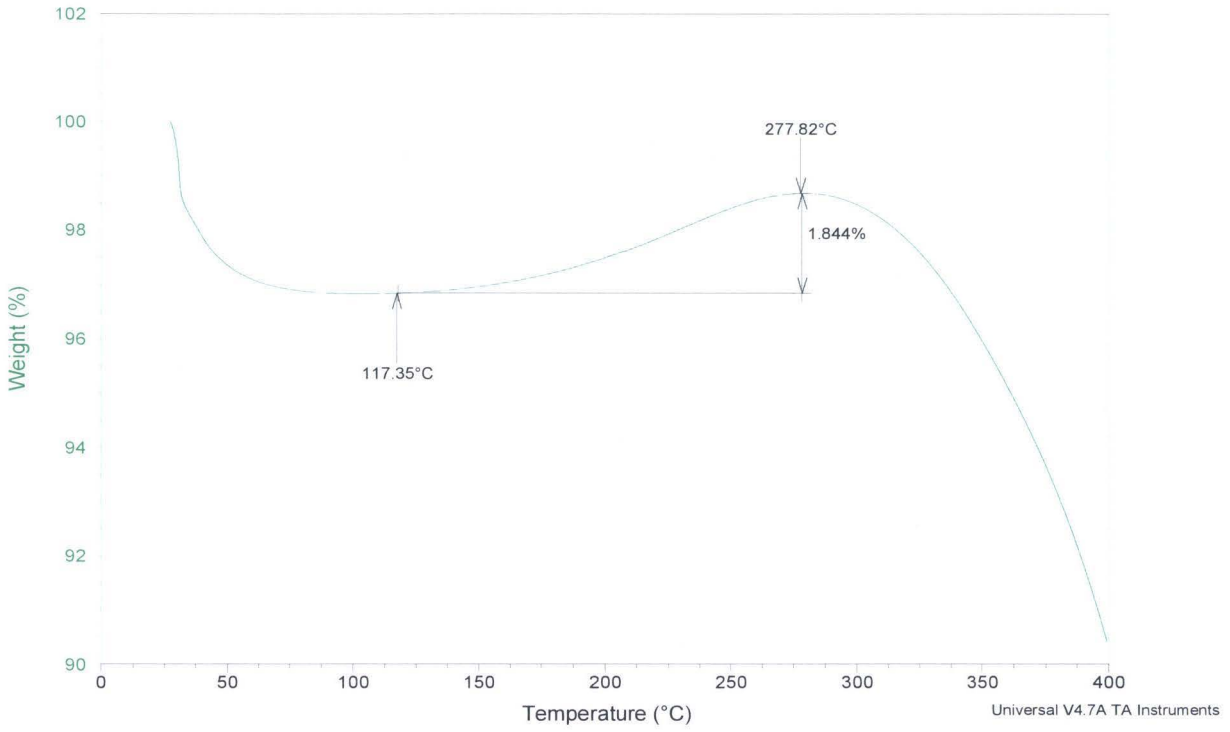


Figure 72: ZM7 O_2 Adsorption

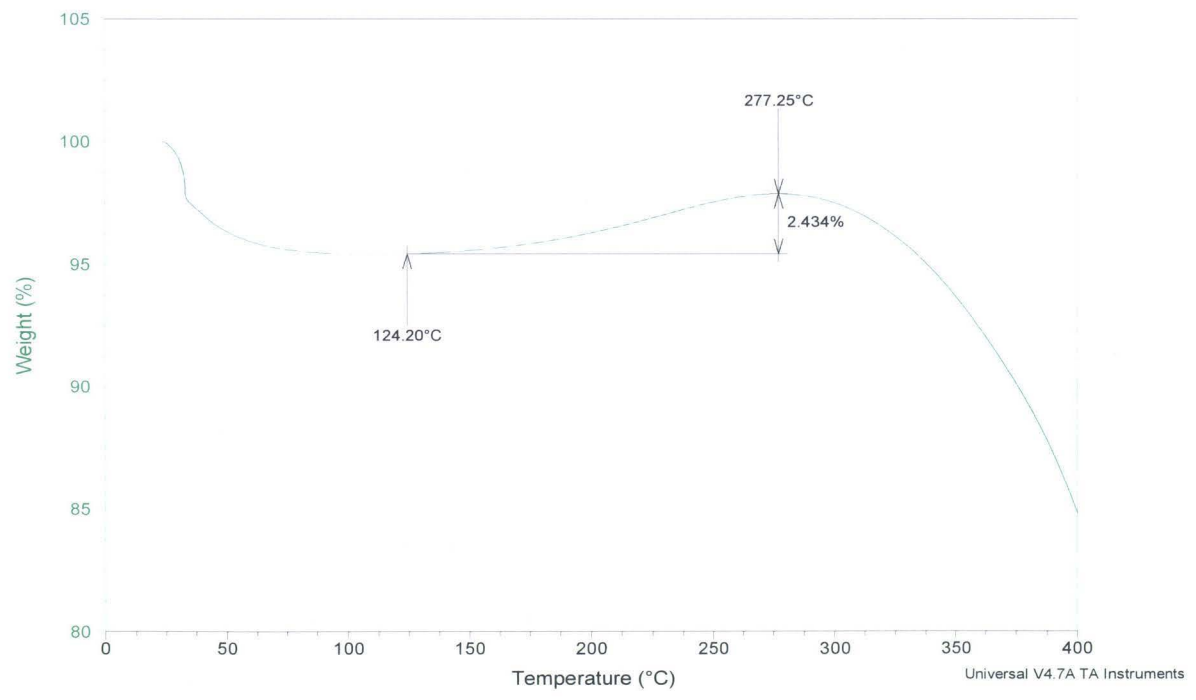


Figure 73: ZM8 O_2 Adsorption

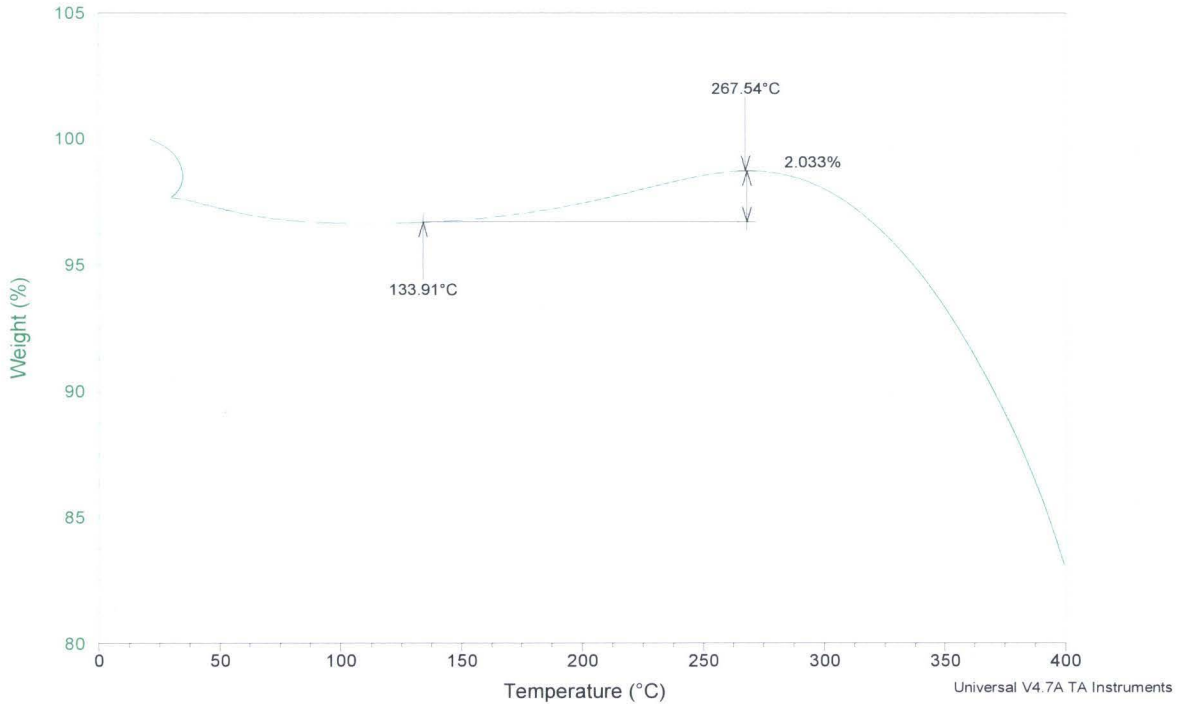


Figure 74: ZM9 O_2 Adsorption

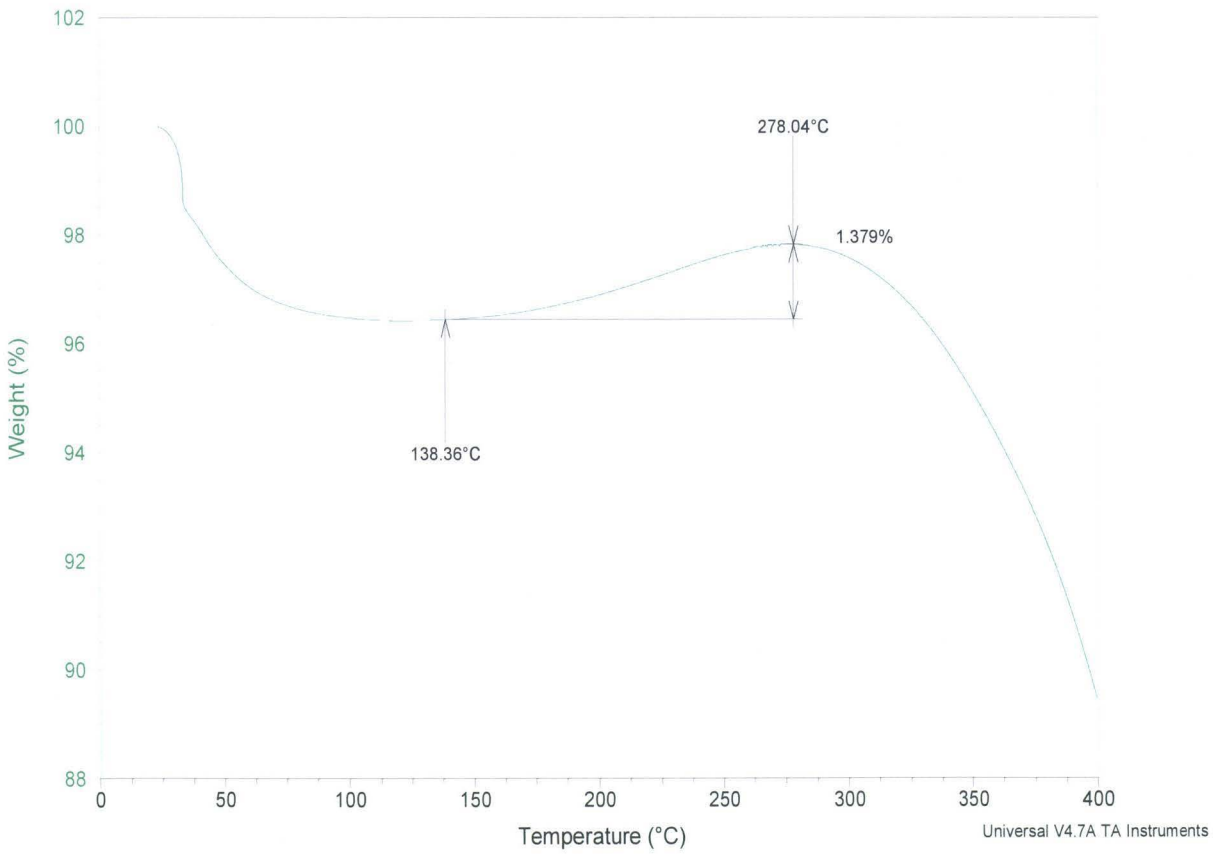


Figure 75: ZM10 O_2 Adsorption

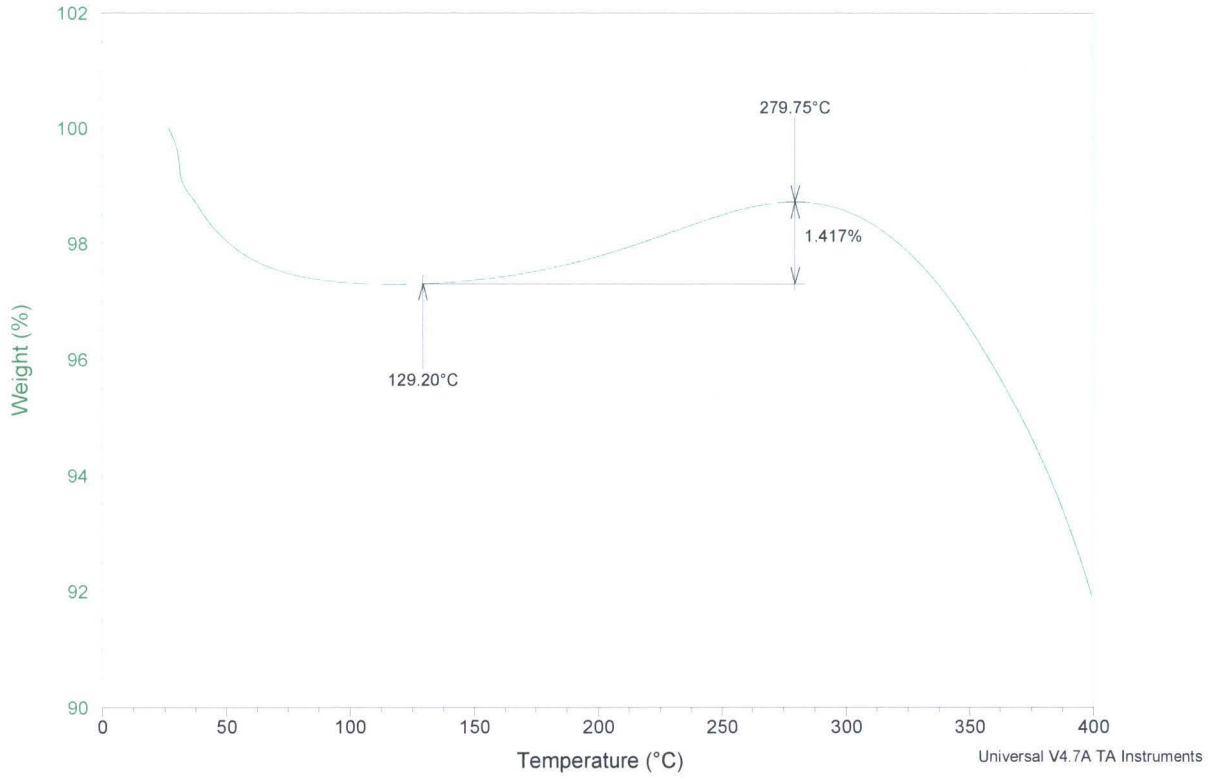


Figure 76: ZM11 O_2 Adsorption

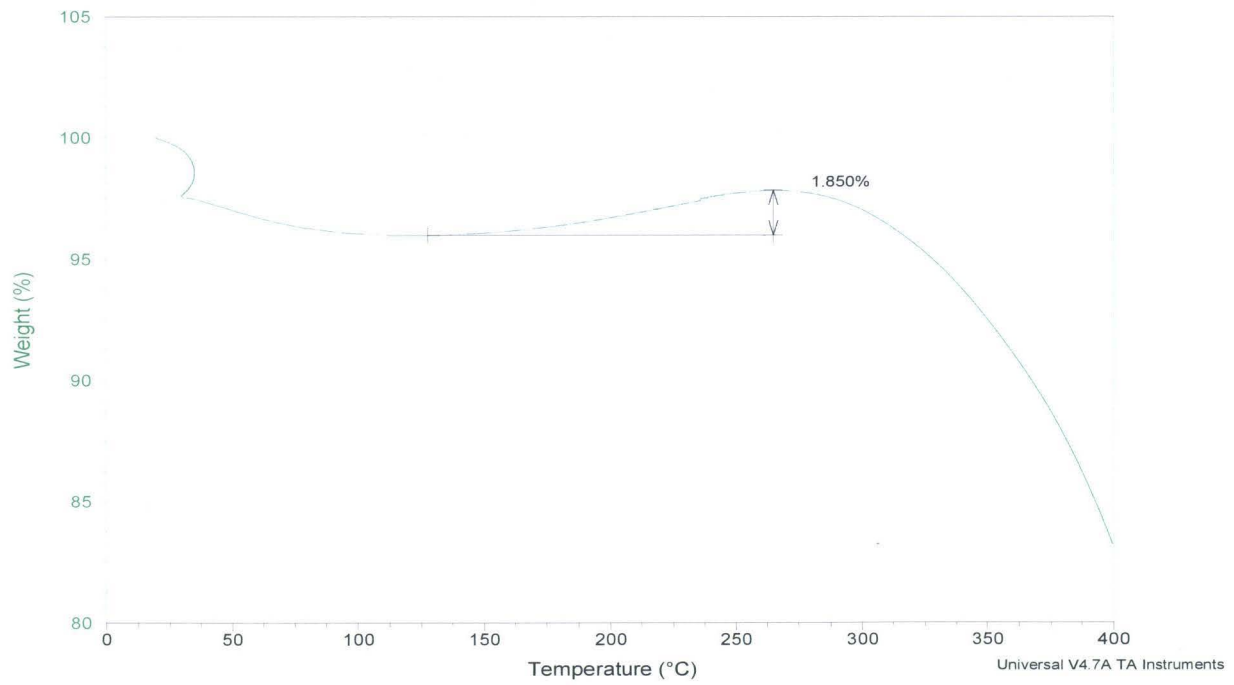


Figure 77: ZM12 O_2 Adsorption

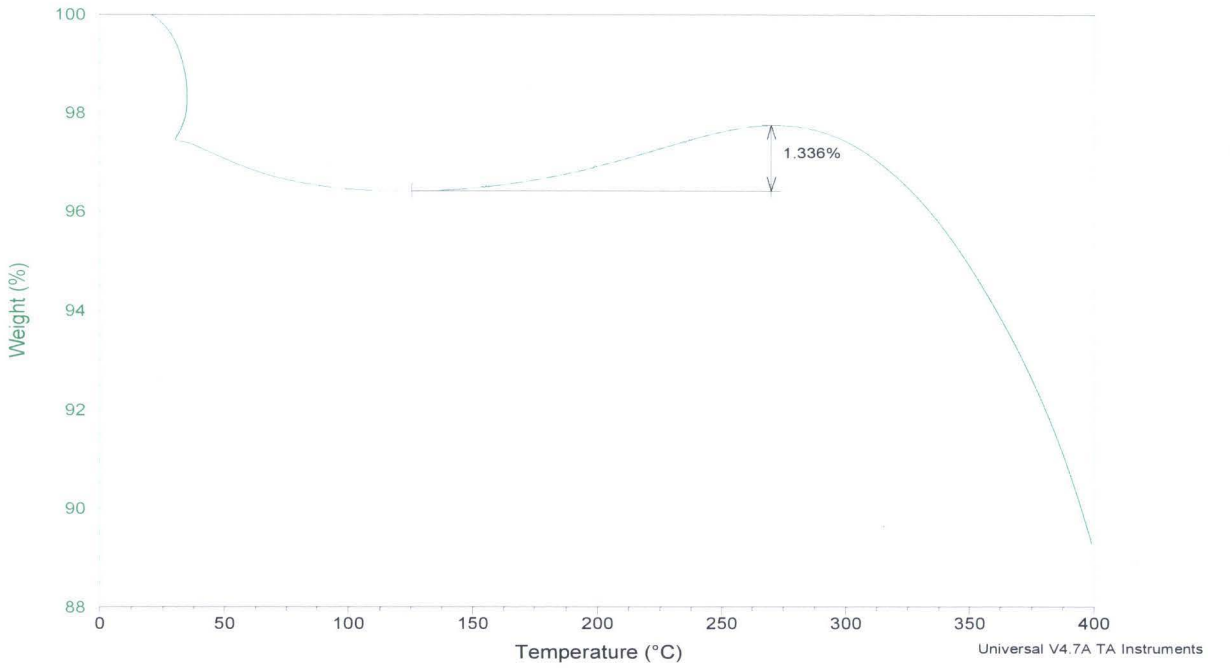


Figure 78: 13 O_2 Adsorption

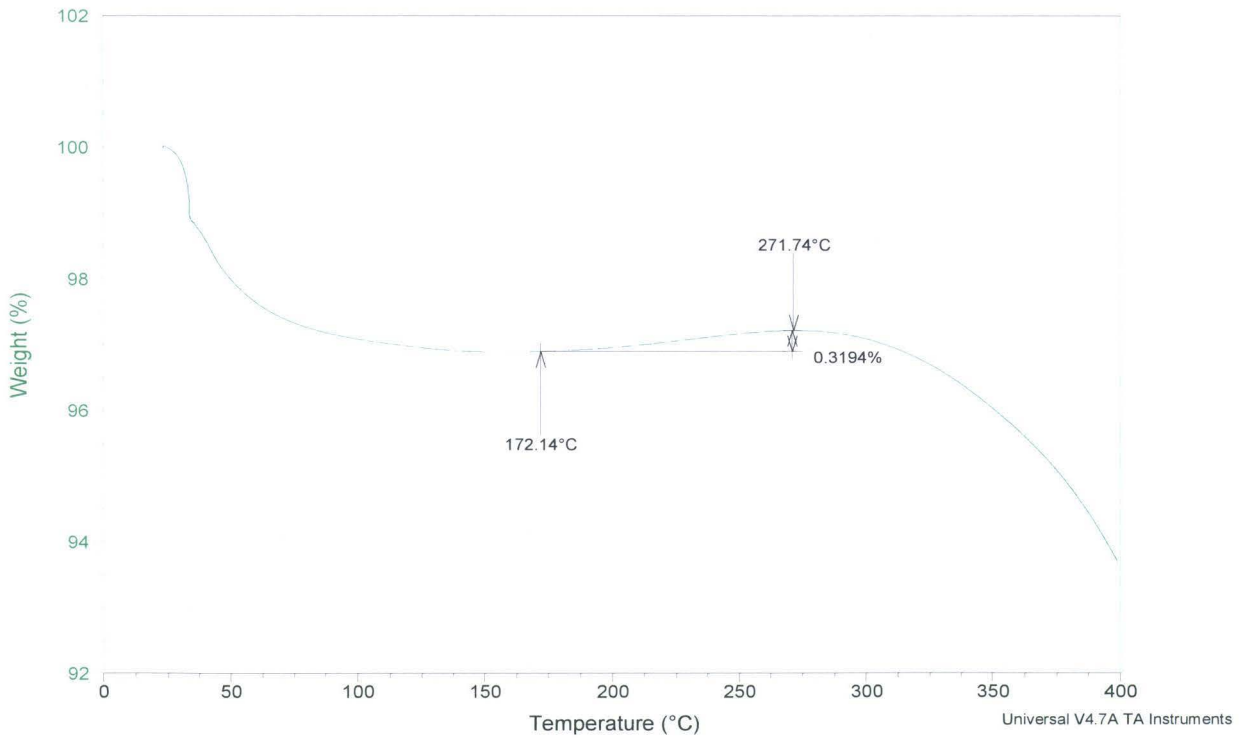


Figure 79: ZM14 O_2Adsorption

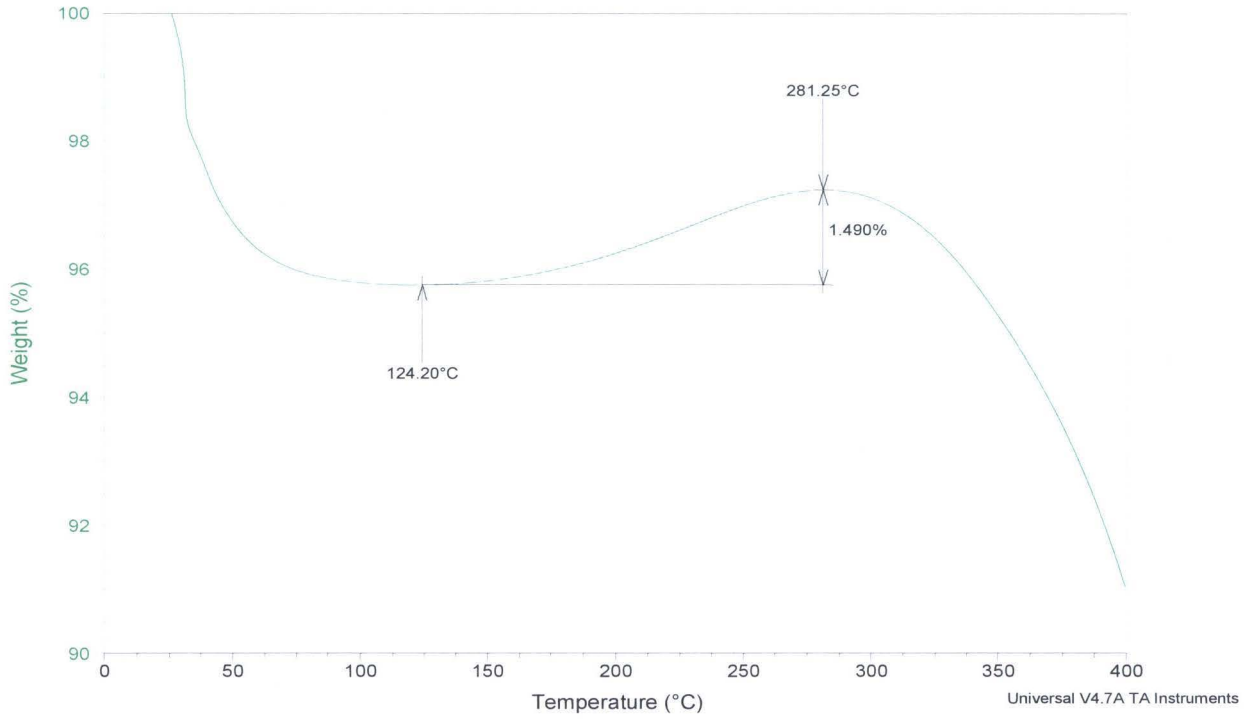


Figure 80: ZM15 O_2 Adsorption

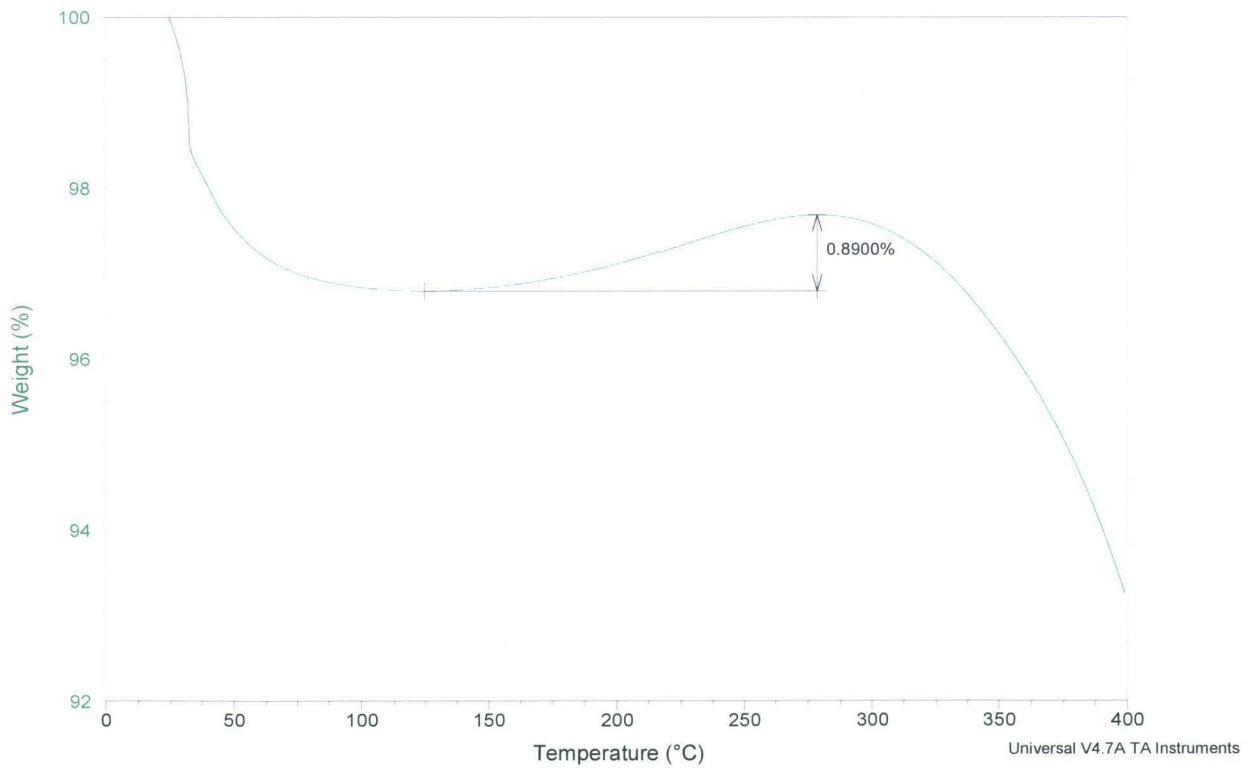


Figure 81: ZM16 O_2 Adsorption

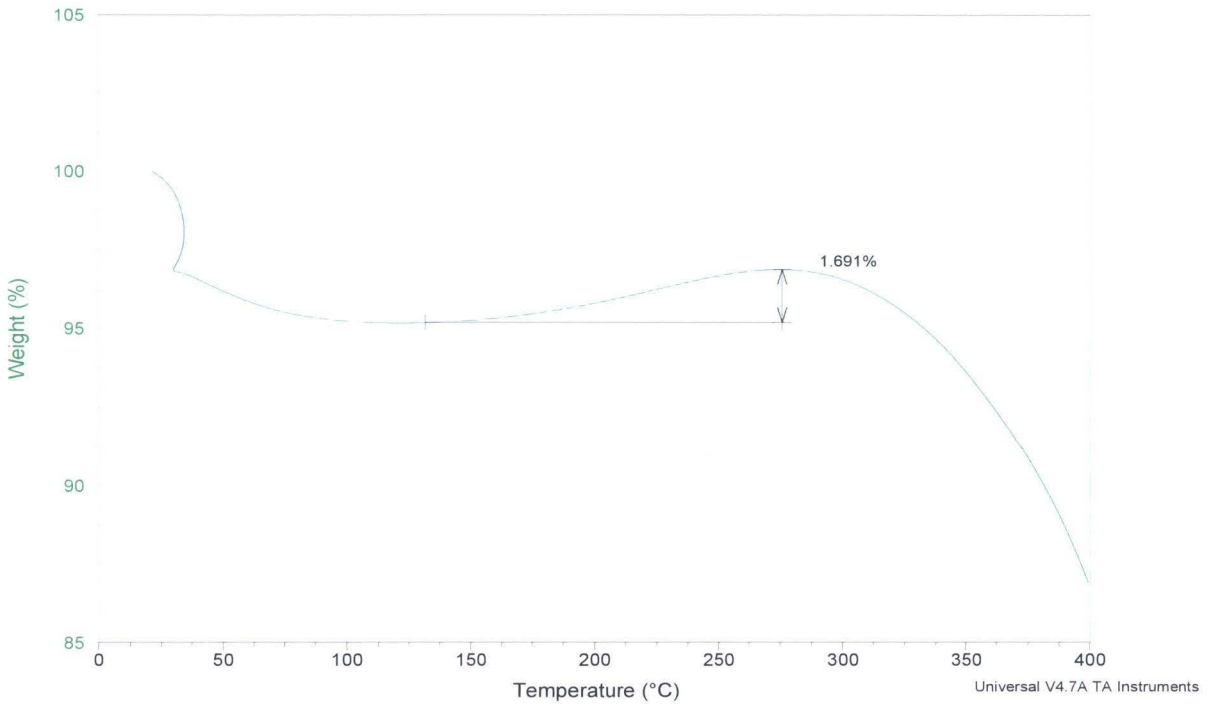


Figure 82: ZM17 O_2 Adsorption

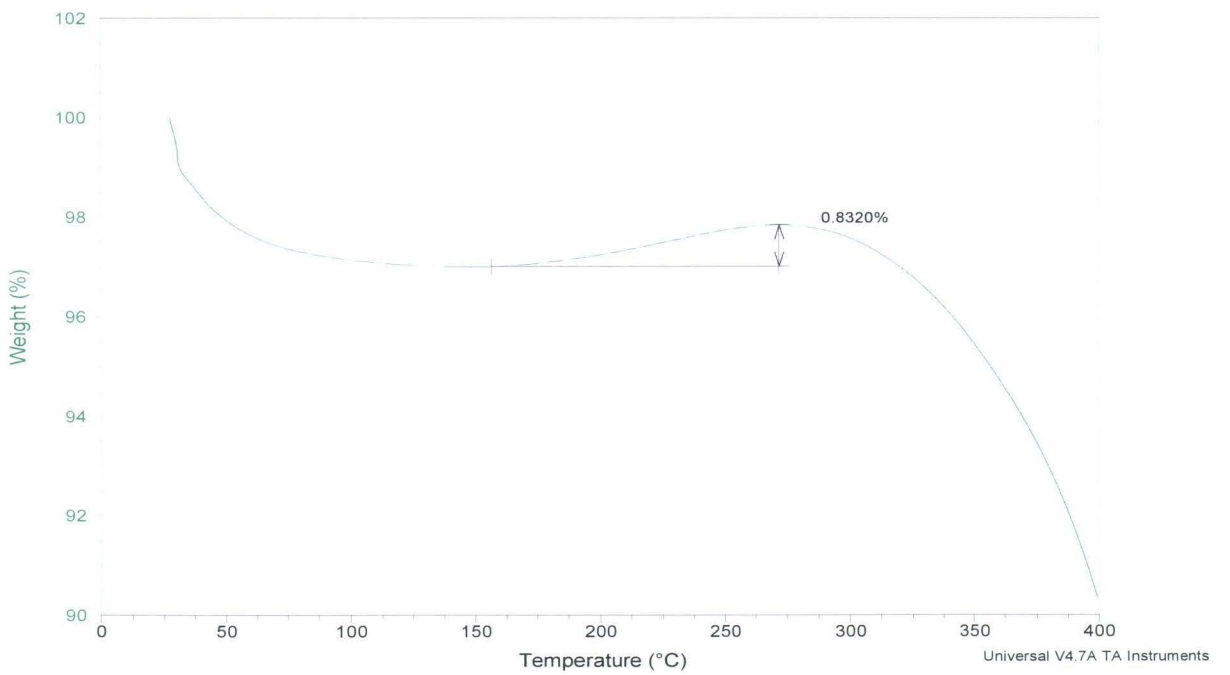


Figure 83: ZM18 O_2 Adsorption

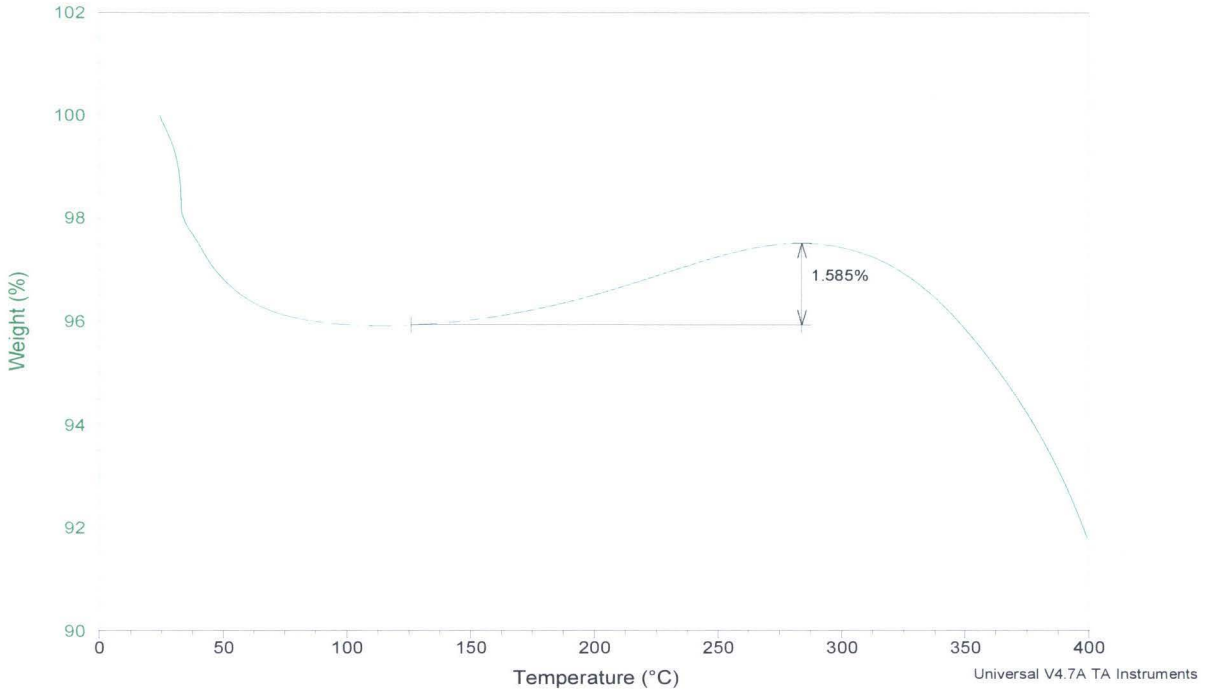


Figure 84: ZM19 O_2 Adsorption

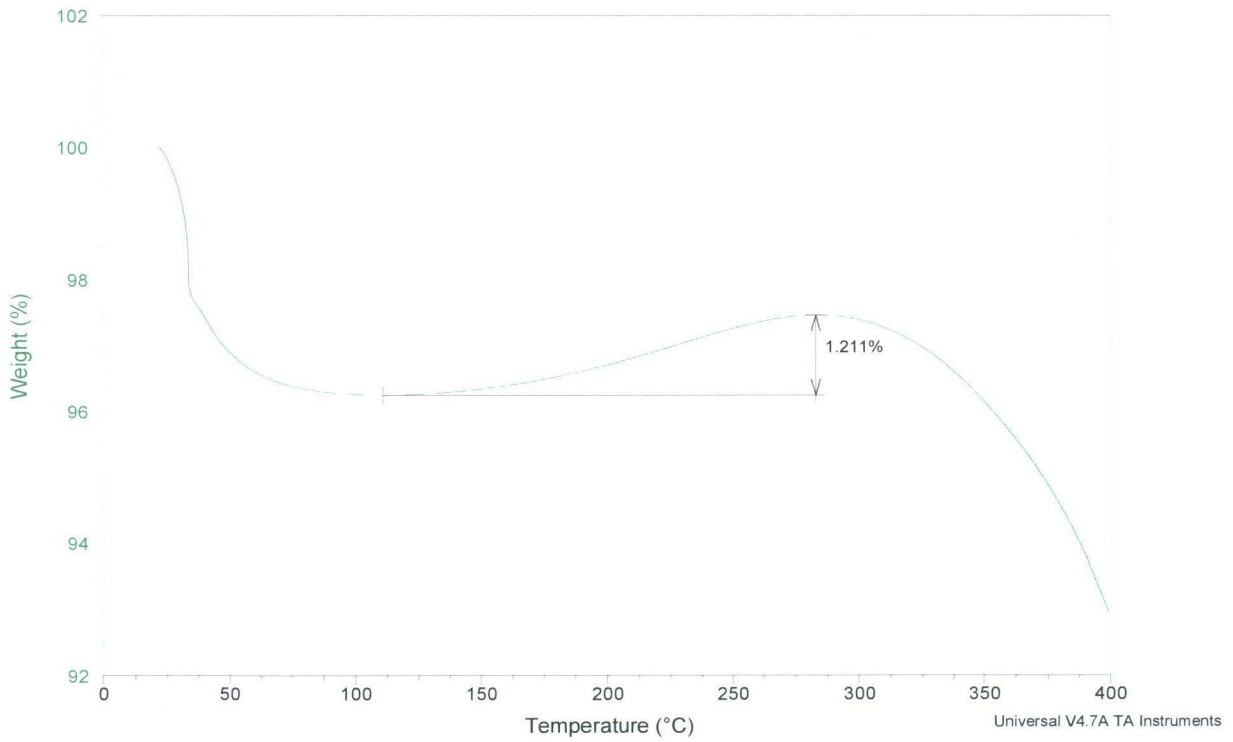


Figure 85: ZM20 O_2 Adsorption

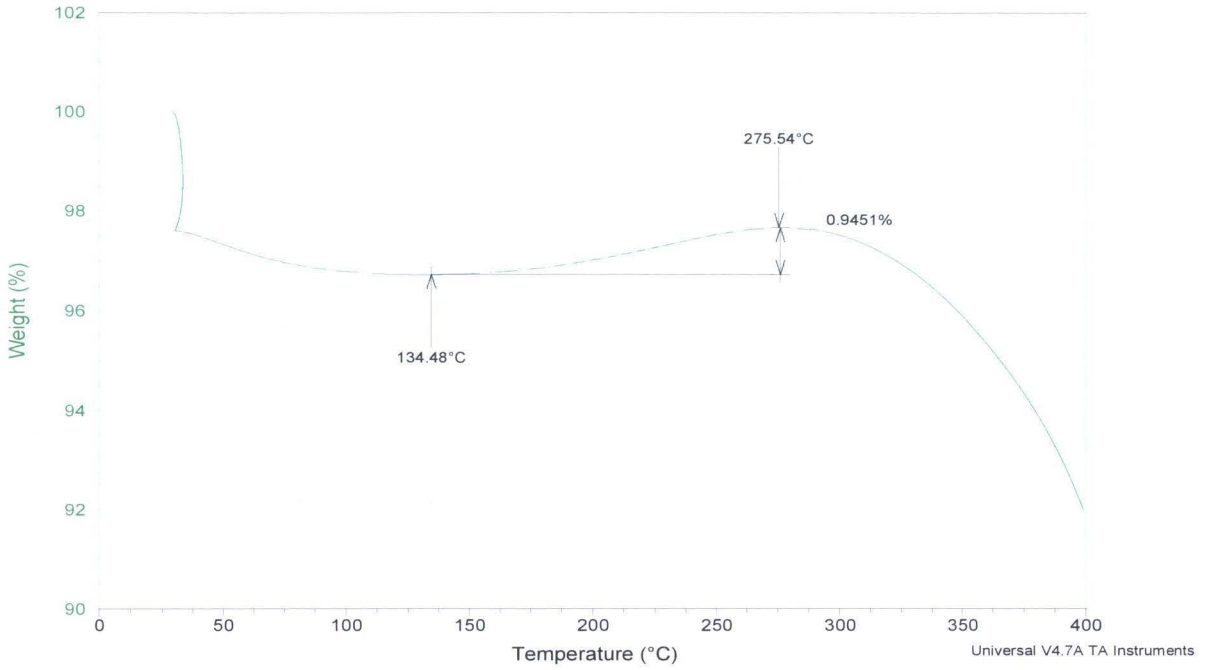


Figure 86: ZM21 O_2 Adsorption

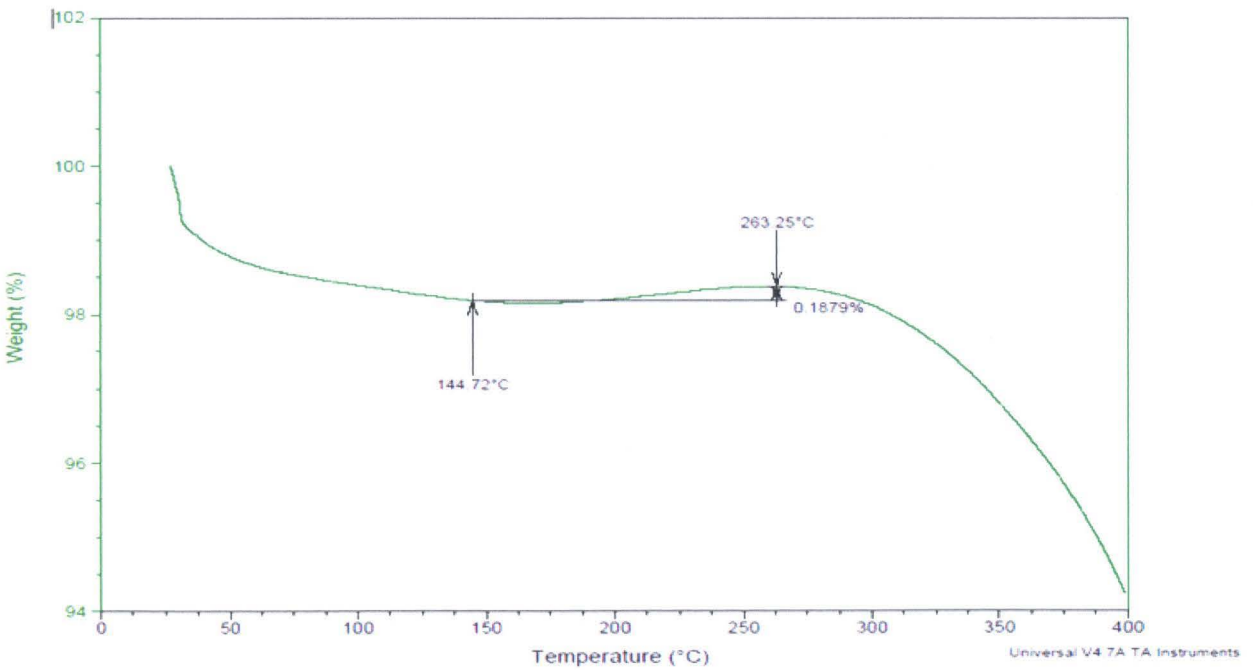


Figure 87: ZM22 O_2 Adsorption

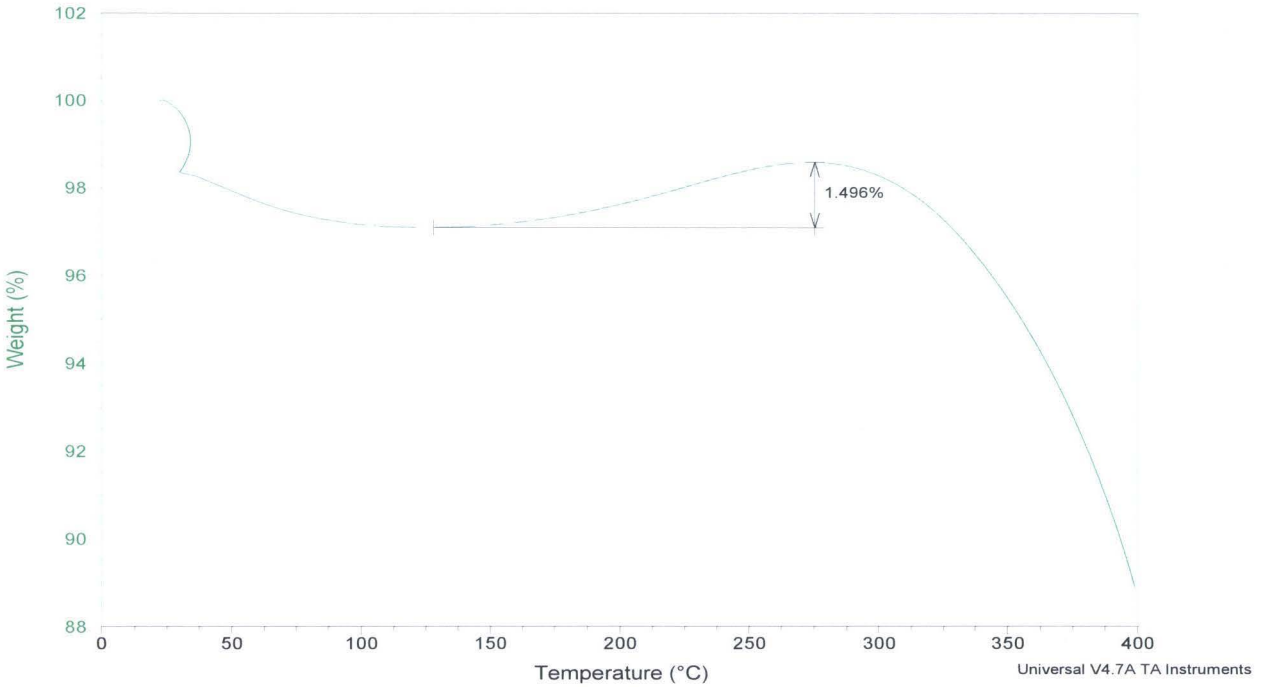


Figure 88: ZM23 O_2 Adsorption

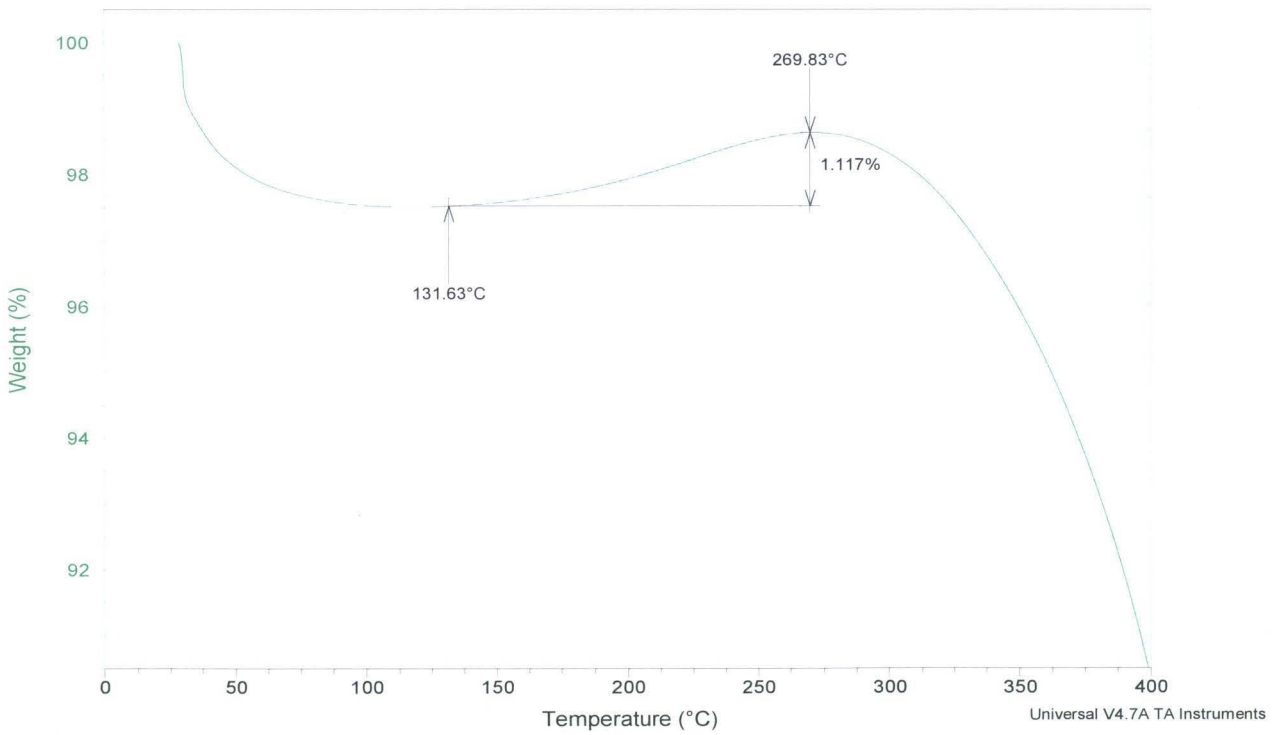


Figure 89: ZM24 O_2 Adsorption

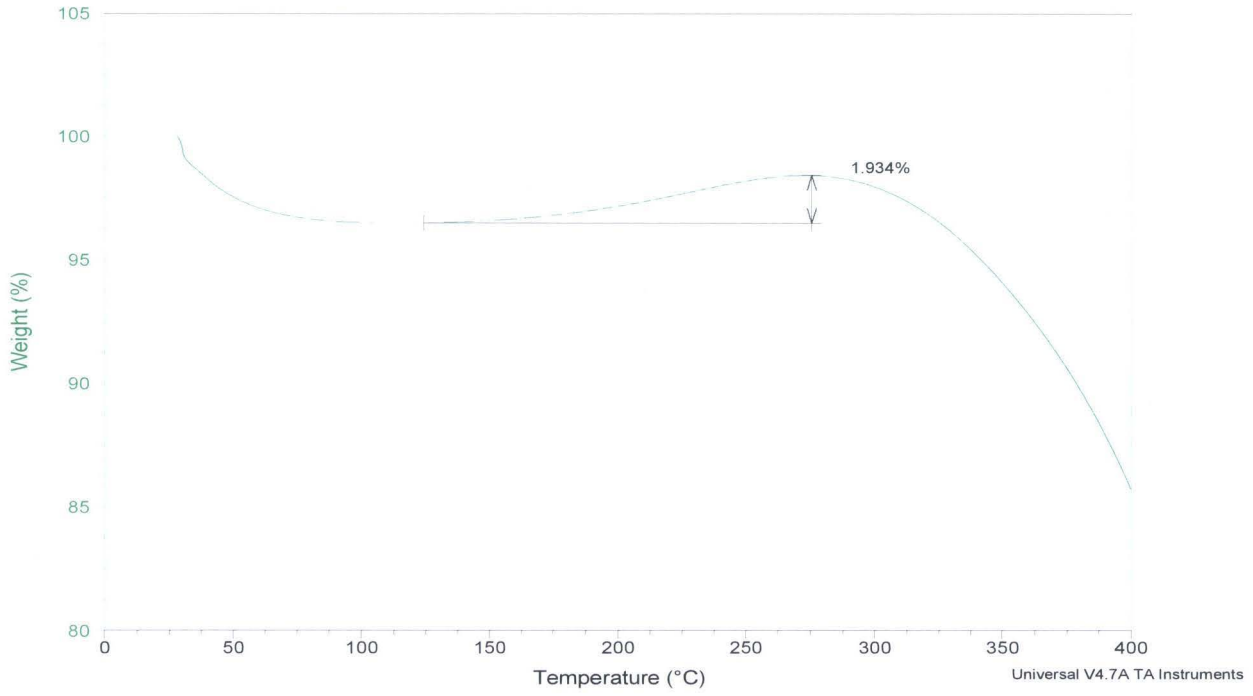


Figure 90: ZM25 O_2 Adsorption

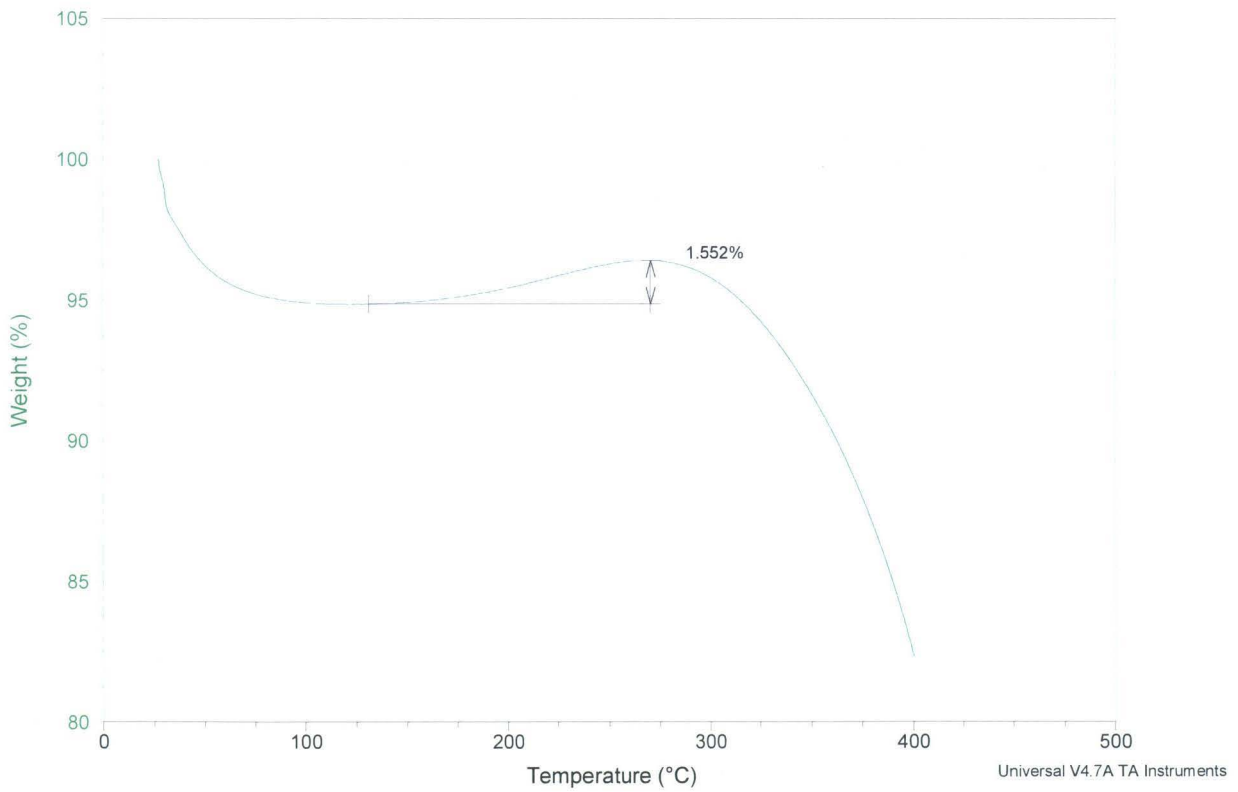


Figure 91: ZM26 O_2 Adsorption

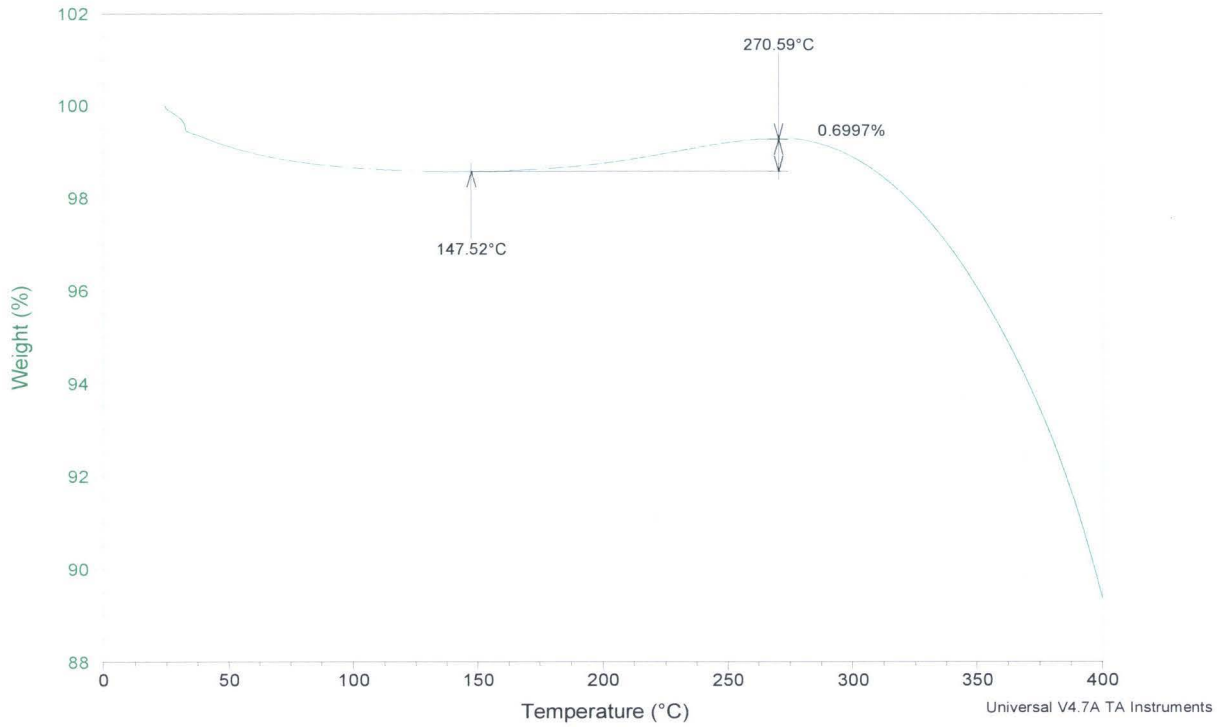


Figure 92: ZM27 O_2 Adsorption

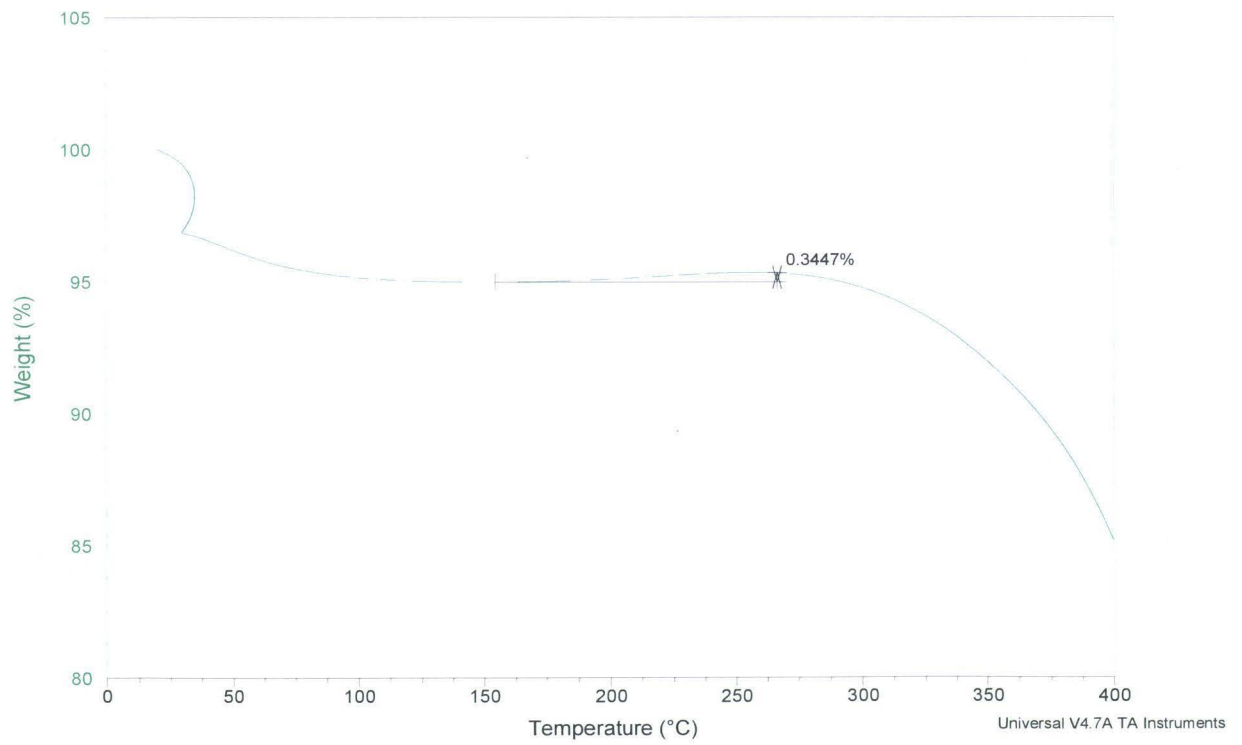


Figure 93: ZM28 O_2 Adsorption

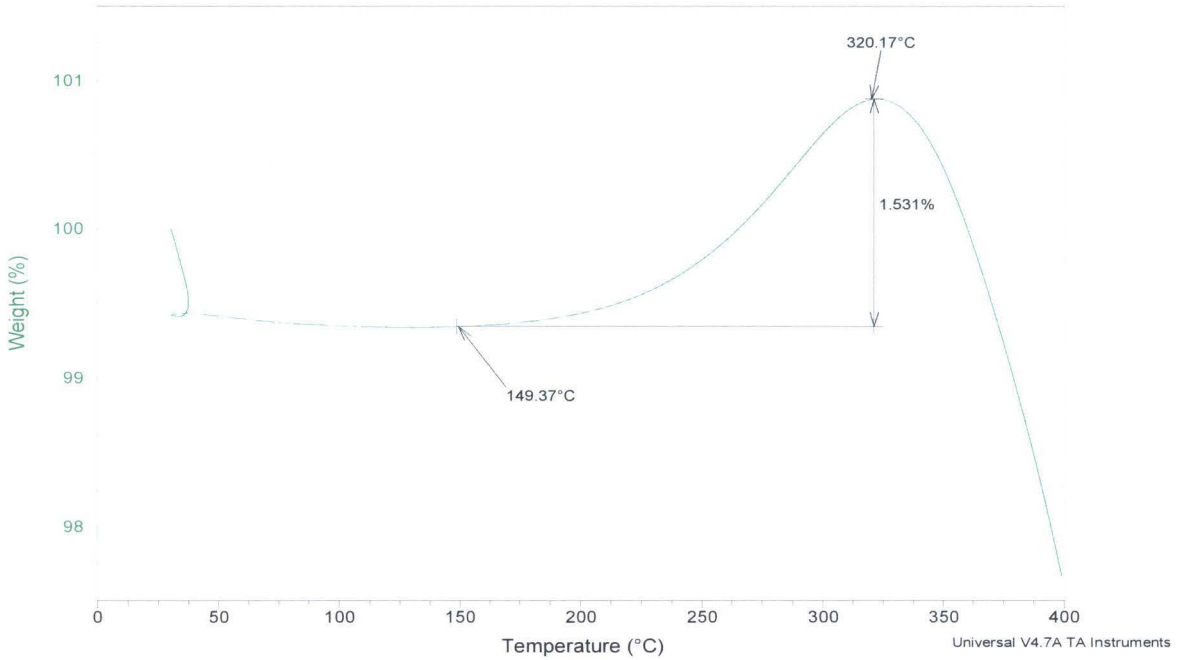


Figure 94: ZM29 O_2 Adsorption

8.2.2 TGA Ignition Test

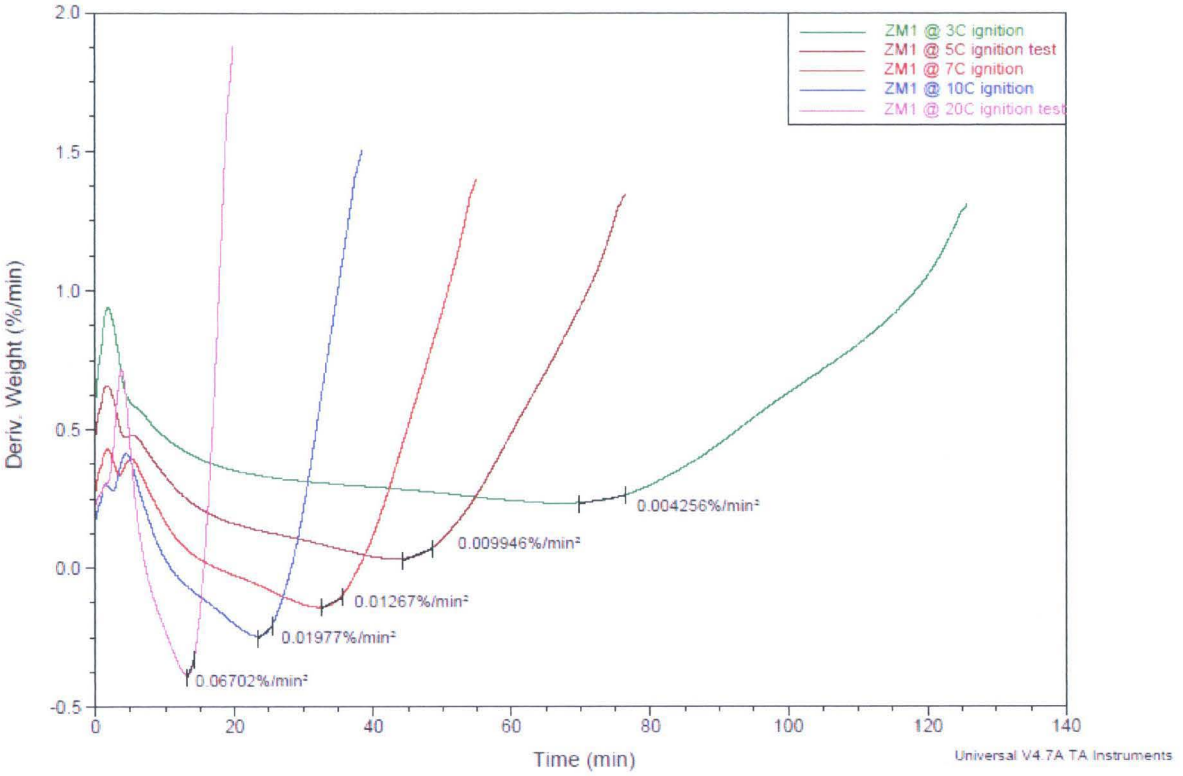


Figure 95: ZM1 Derivative curves and their slopes

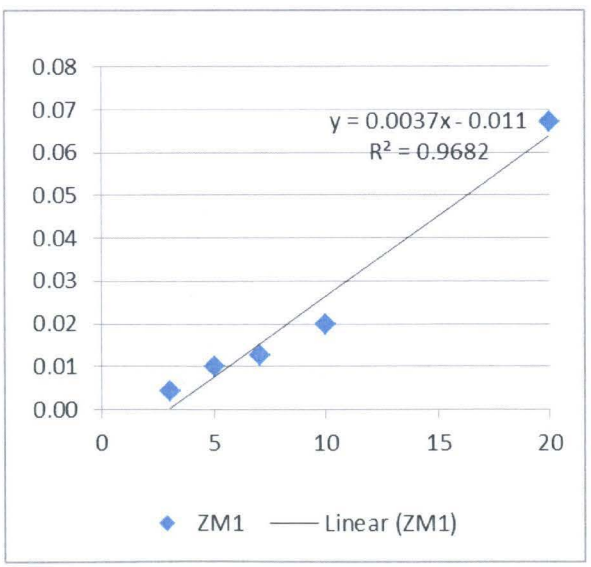


Figure 96: ZM1 R^2_{graph}

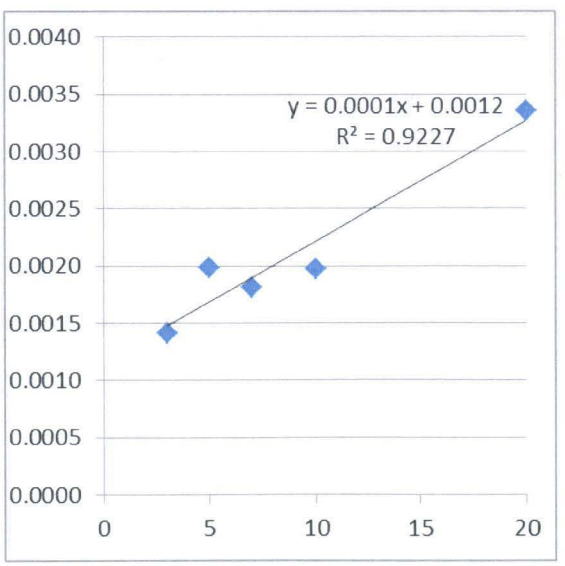


Figure 97: ZM1 $R^2_{calculated}$

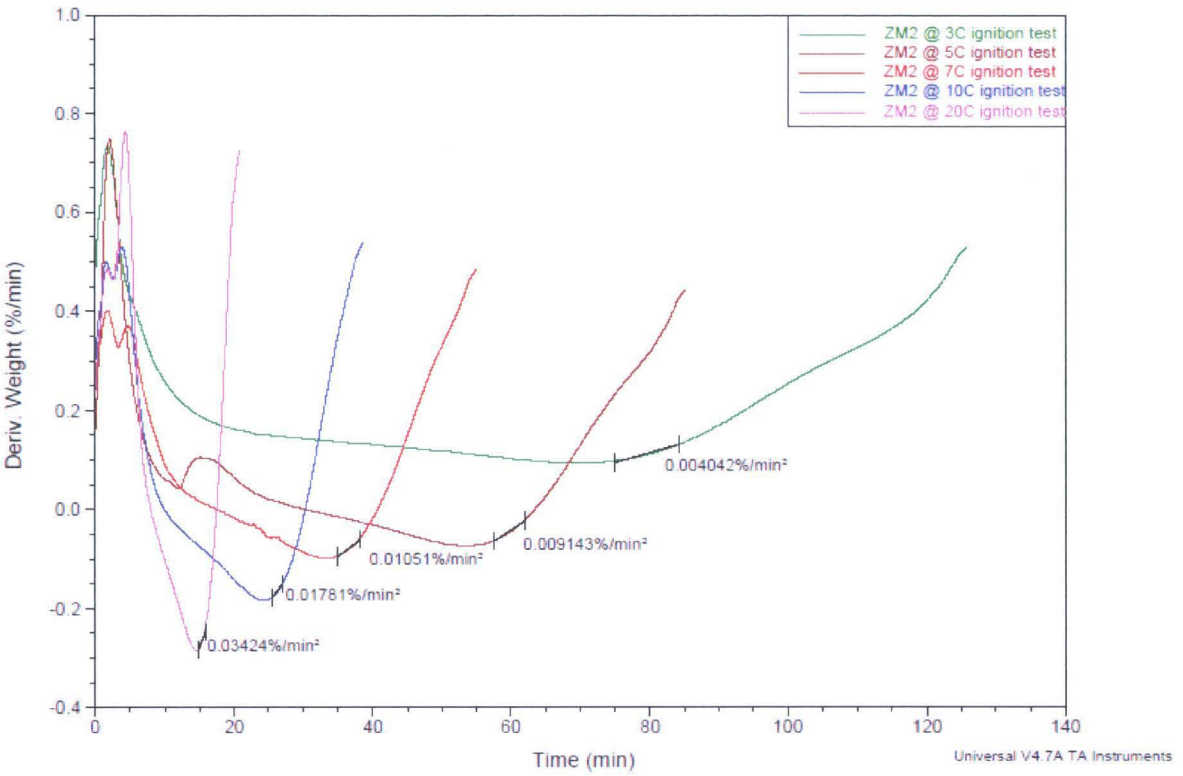


Figure 98: ZM2 Derivative curves and their slopes

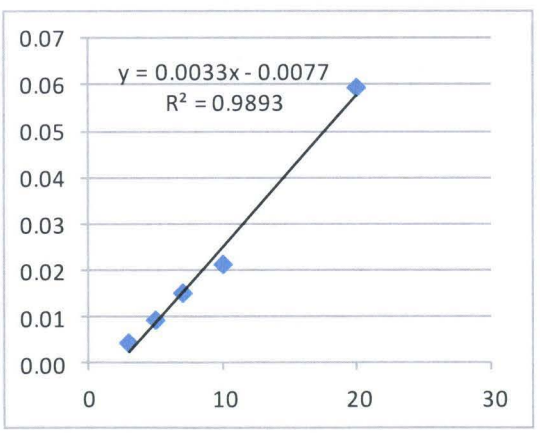


Figure 99: ZM2 R^2_{graph}

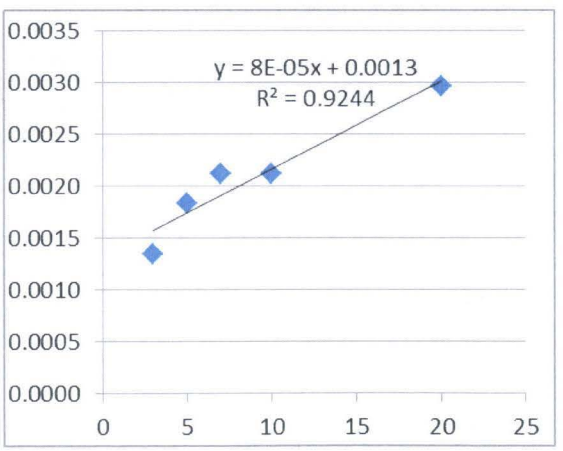


Figure 100: ZM2 $R^2_{calculated}$

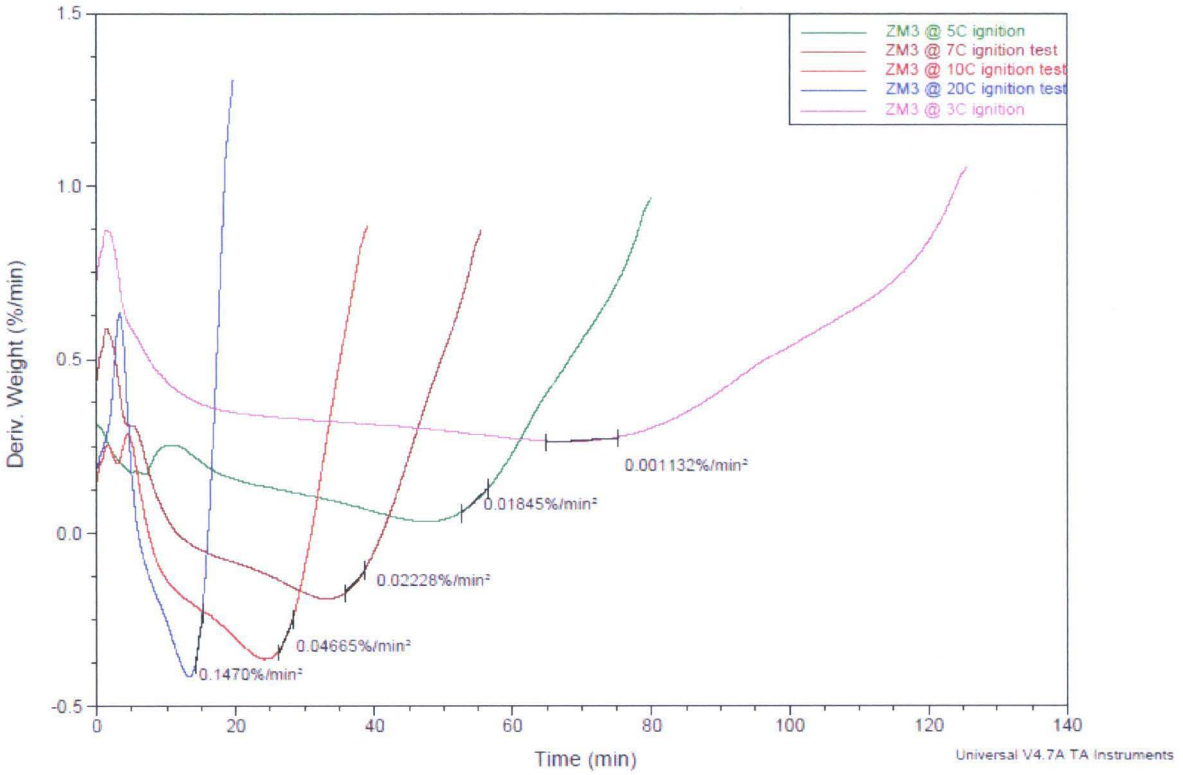


Figure 101: ZM3 Derivative curves and their slopes

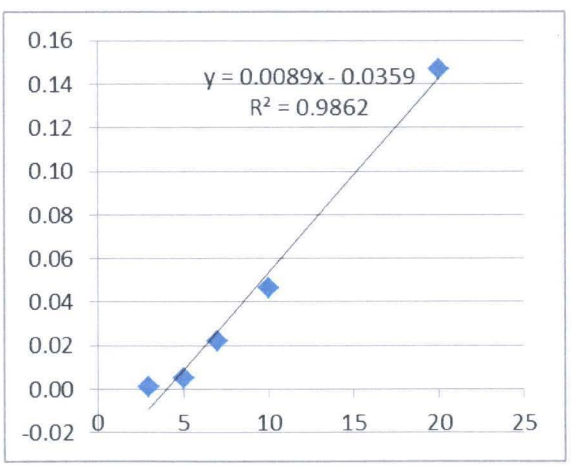


Figure 102: ZM3 R^2_{graph}

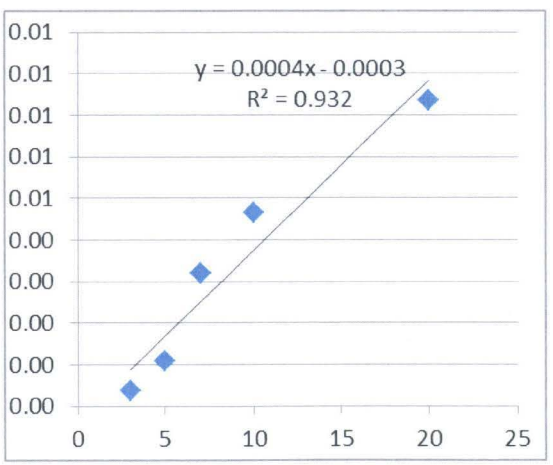


Figure 103: ZM3 $R^2_{calculated}$

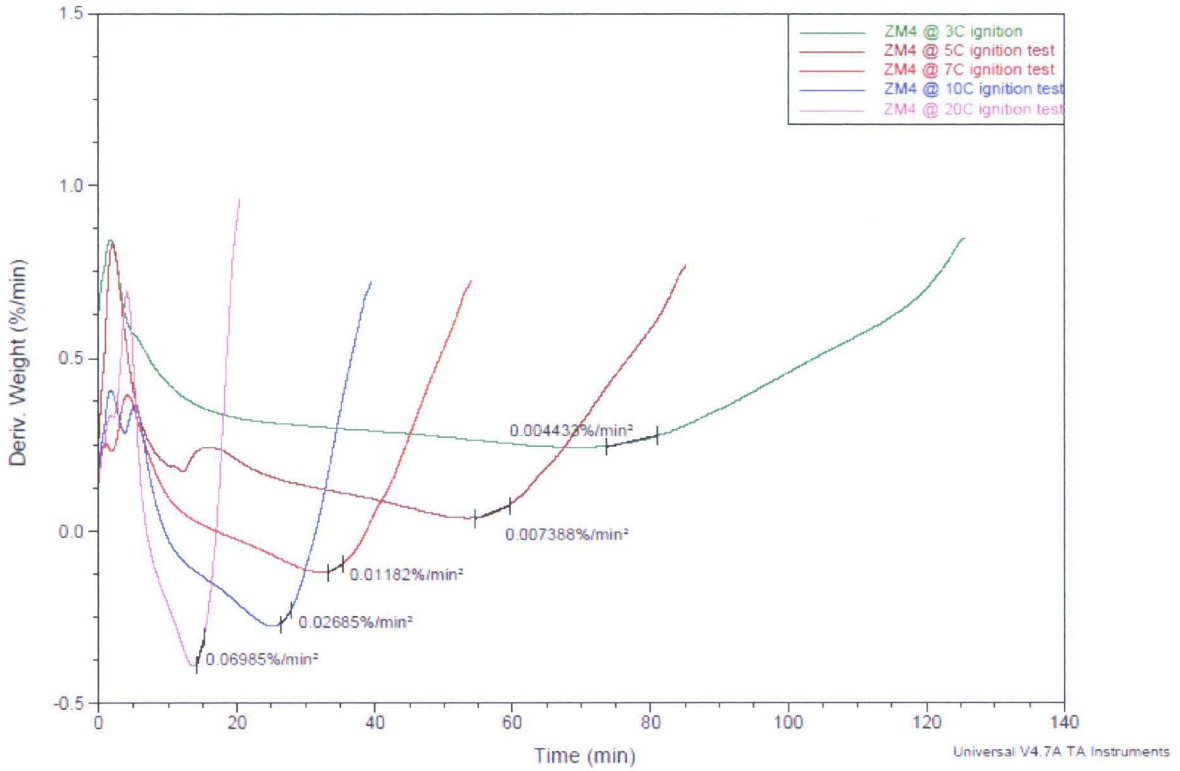


Figure 104: ZM4 Derivative curves and their slopes

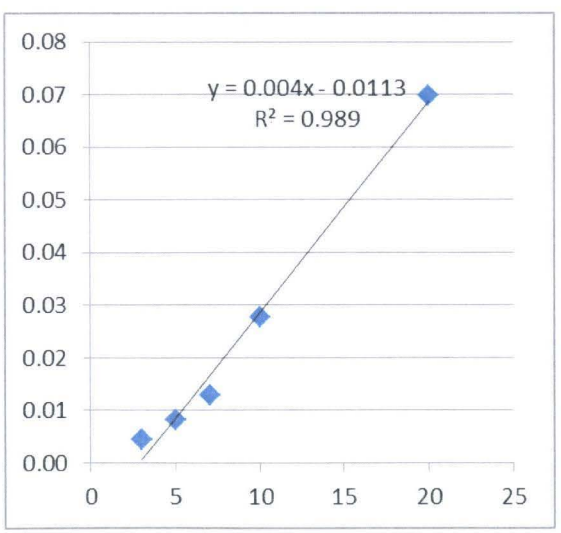


Figure 105: ZM4 R^2_{graph}

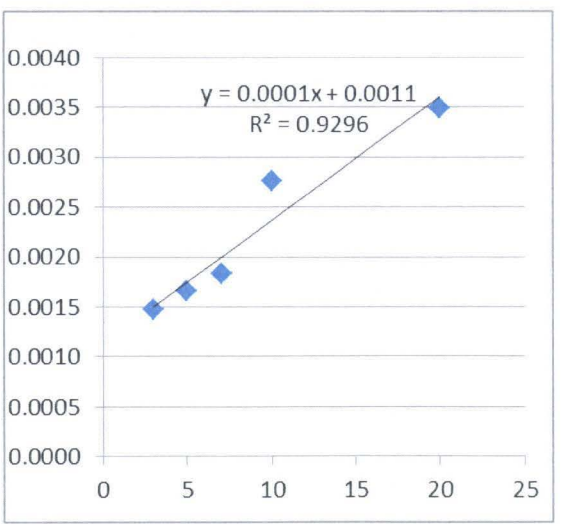


Figure 106: ZM4 $R^2_{calculated}$

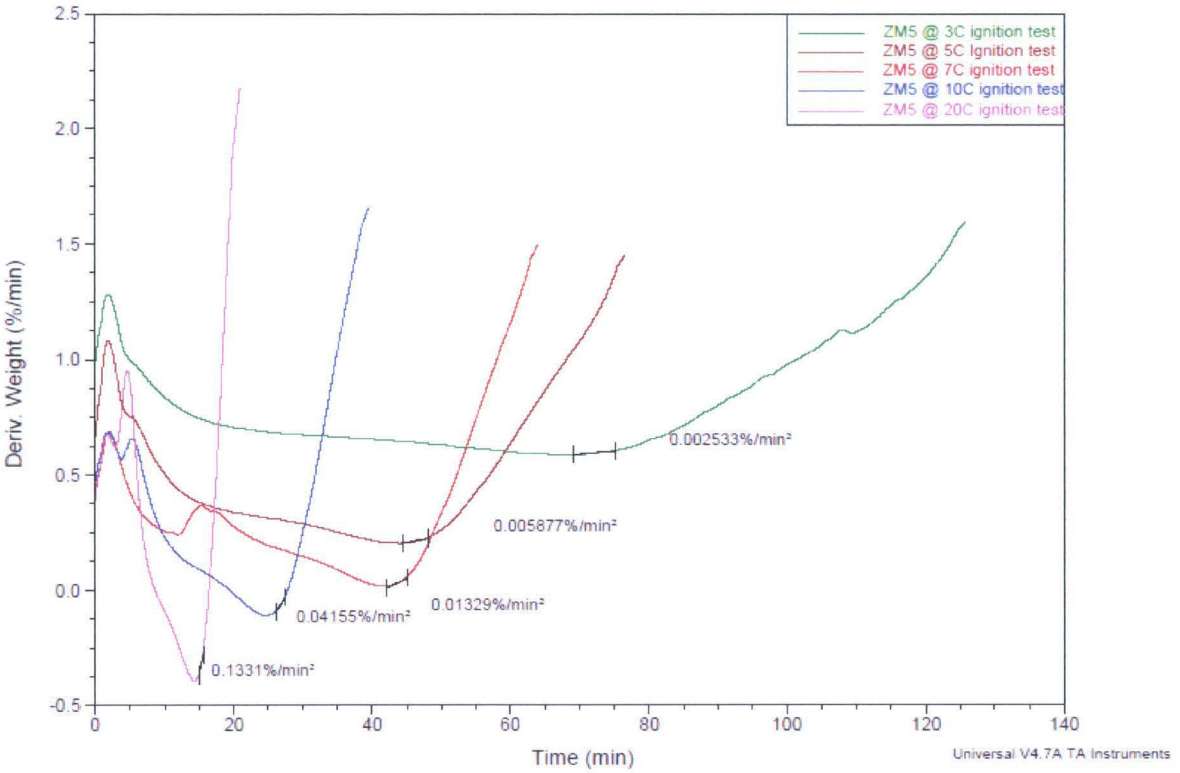


Figure 107: ZM5 Derivative curves and their slopes

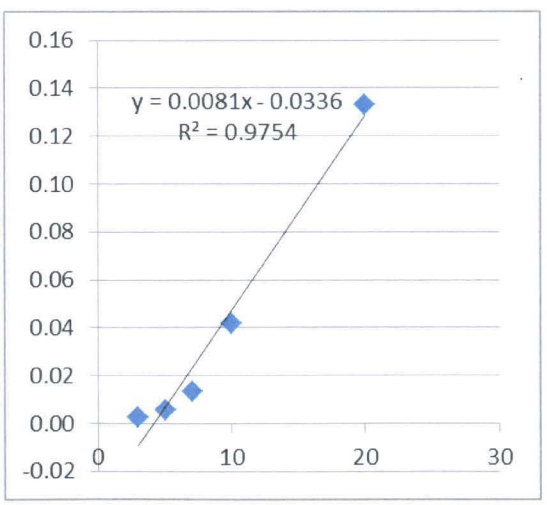


Figure 108: ZM5 R^2_{graph}

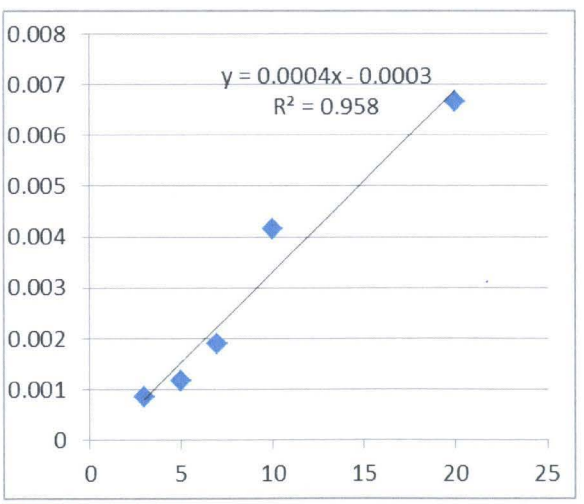


Figure 109: ZM5 $R^2_{calculated}$

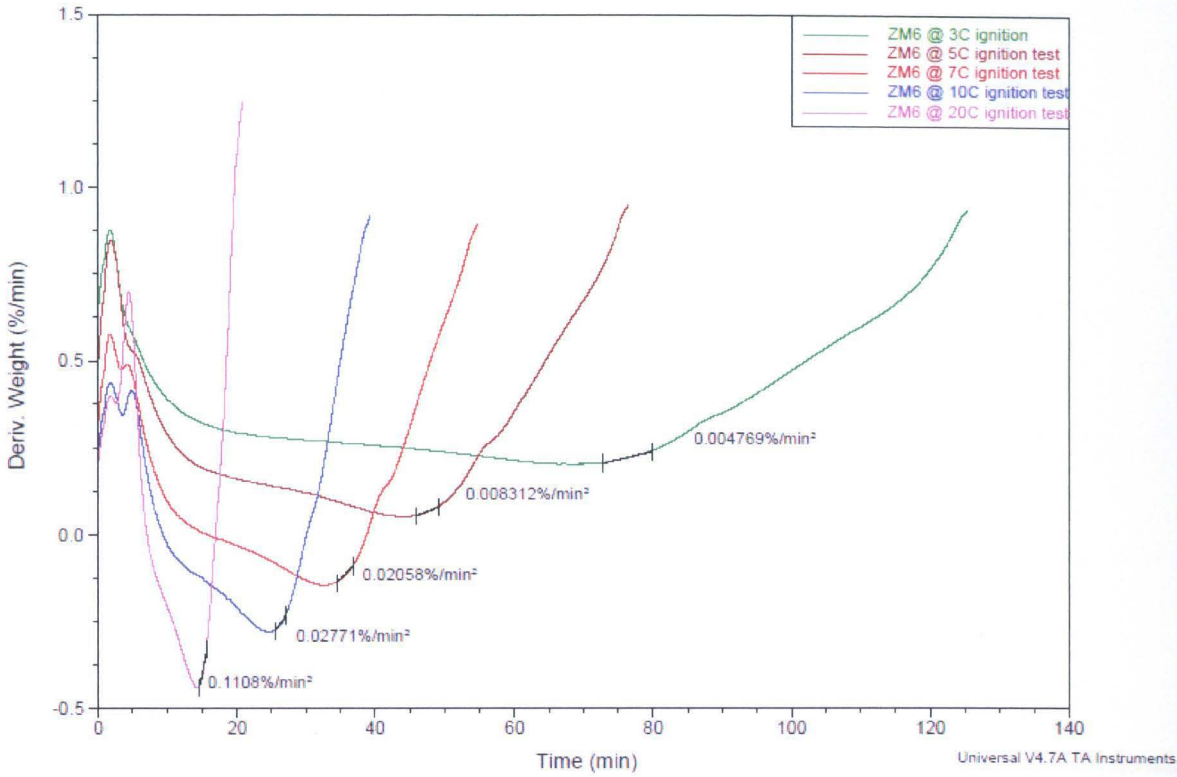


Figure 110: ZM6 Derivative curves and their slopes

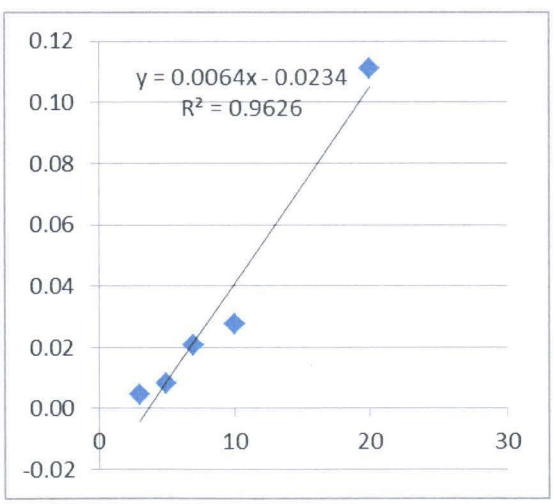


Figure 111: ZM6 R^2_{graph}

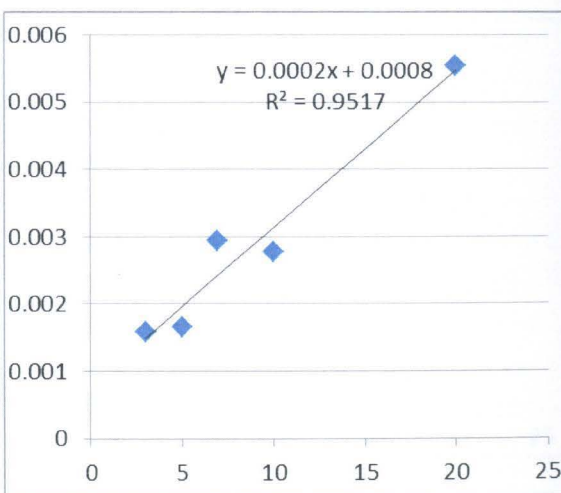


Figure 112: ZM6 $R^2_{calculated}$

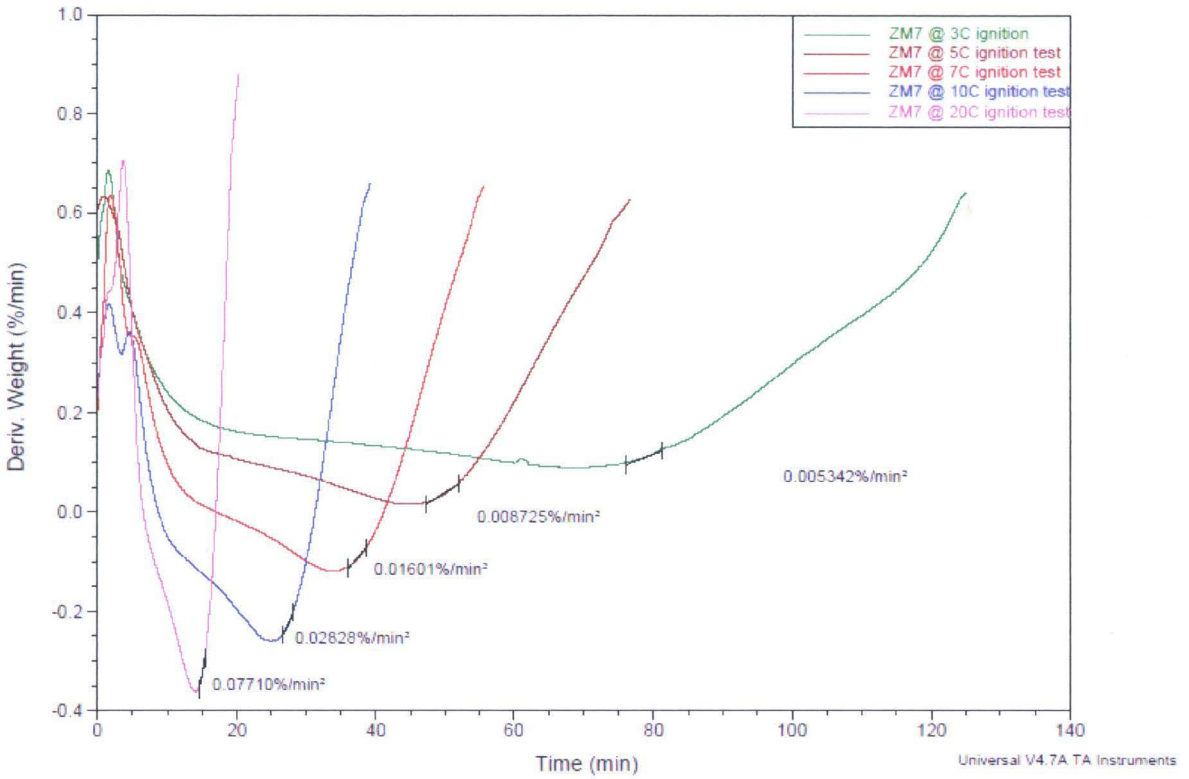


Figure 113: ZM7 Derivative curves and their slopes

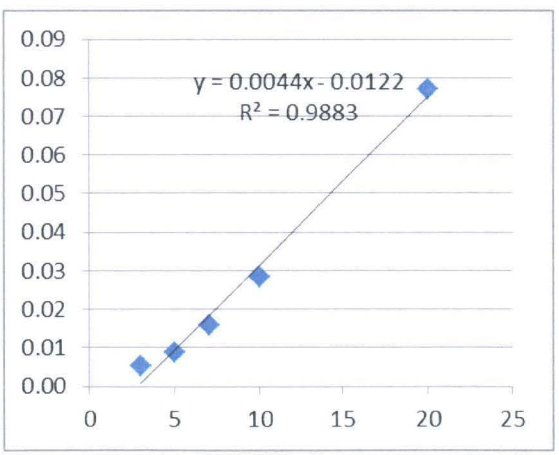


Figure 114: ZM7 R^2_{graph}

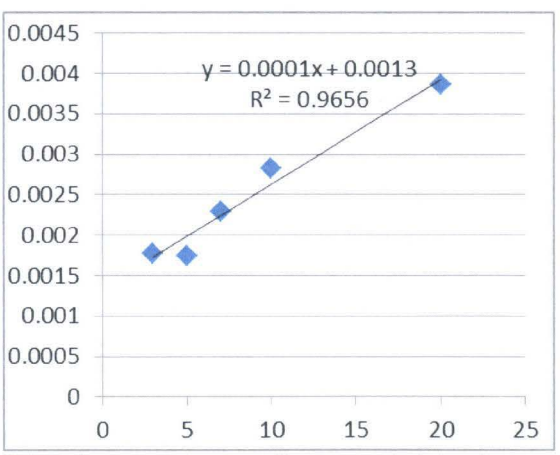


Figure 115: ZM7 $R^2_{calculated}$

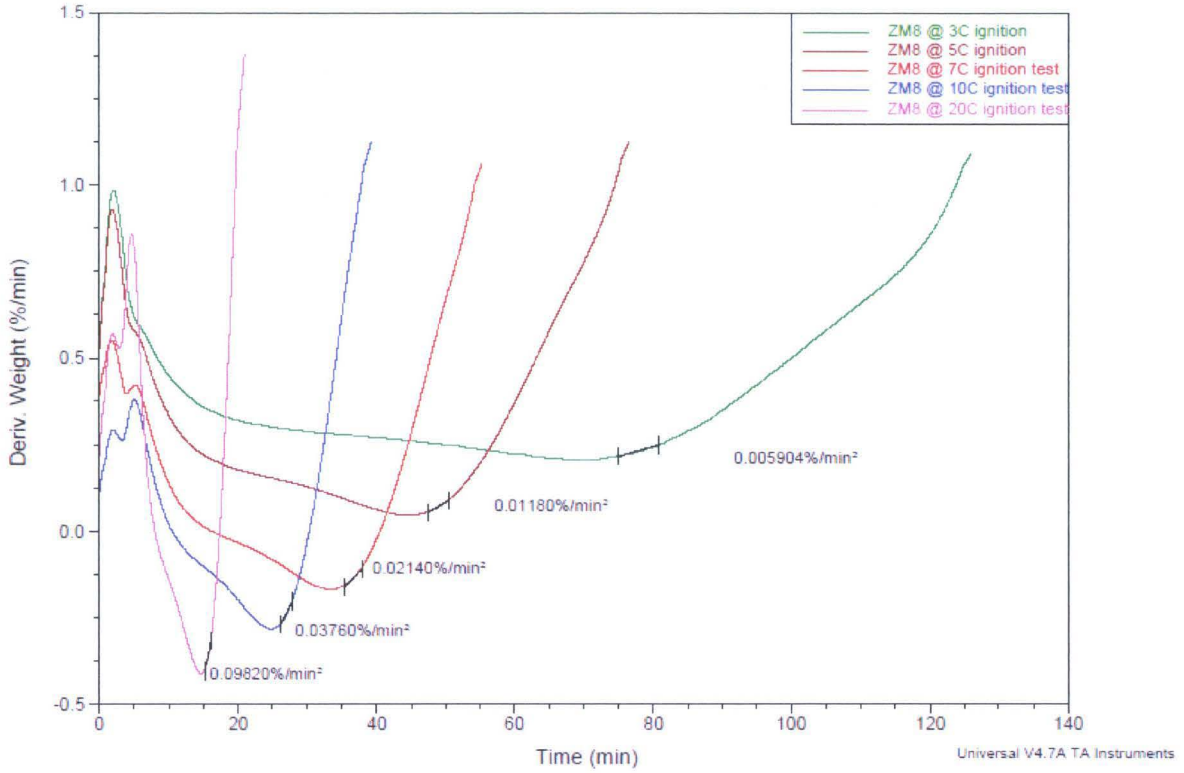


Figure 116: ZM8 Derivative curves and their slopes

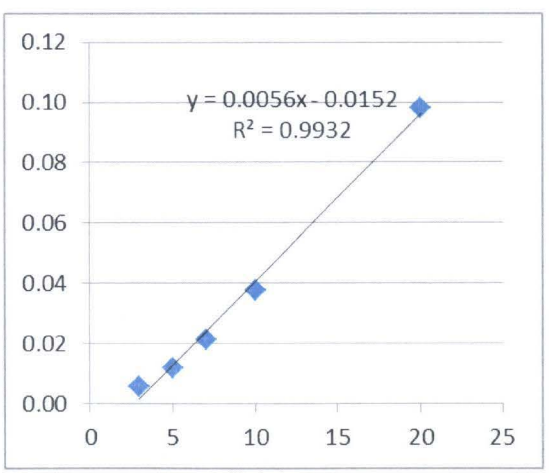


Figure 117: ZM8 R^2_{graph}

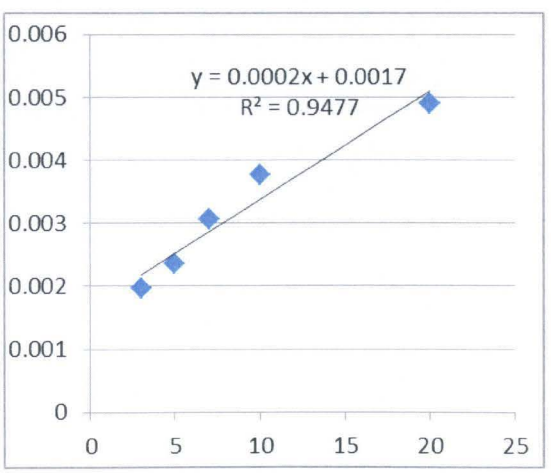


Figure 118:ZM8 $R^2_{calculated}$

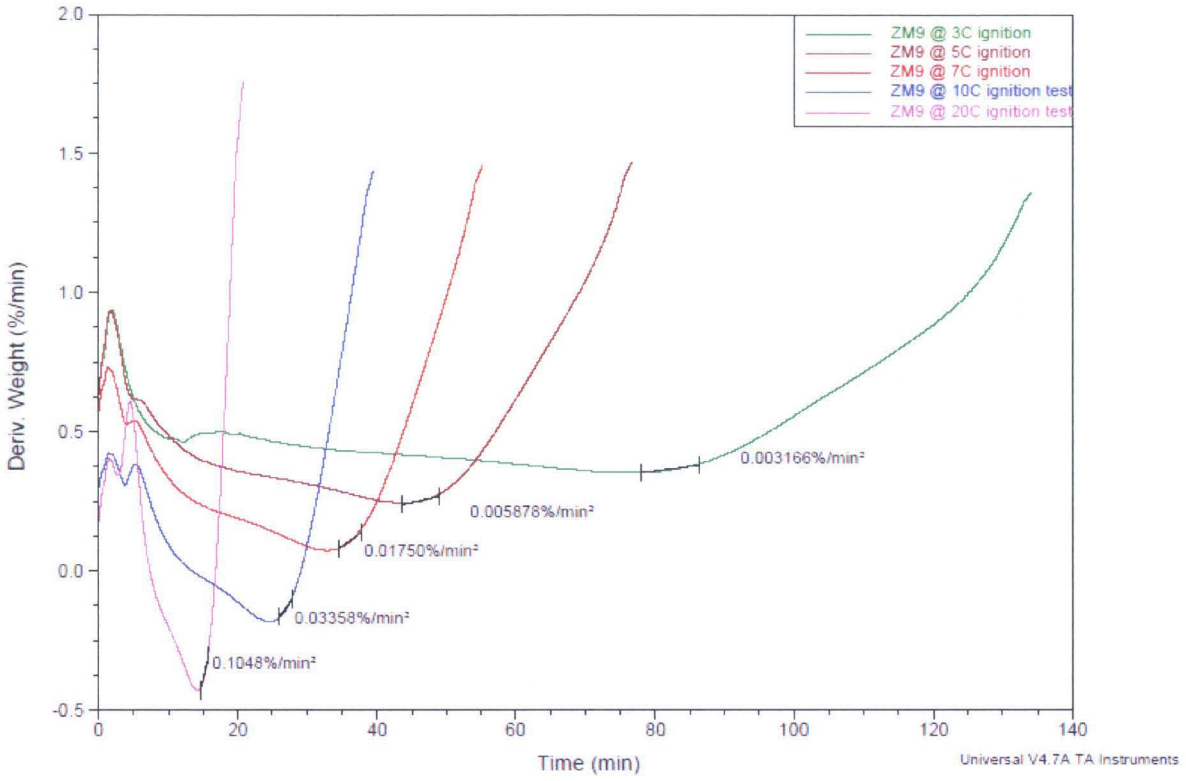


Figure 119: ZM9 Derivative curves and their slopes

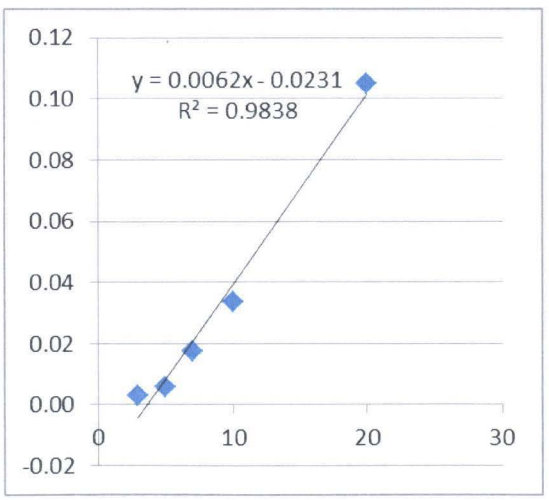


Figure 120: ZM9 R^2_{graph}

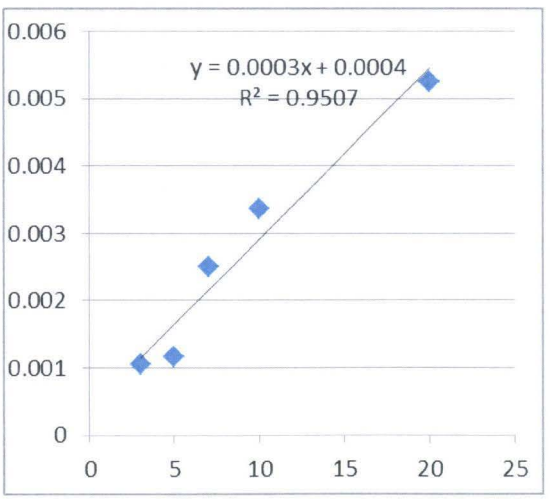


Figure 121: ZM9 $R^2_{calculated}$

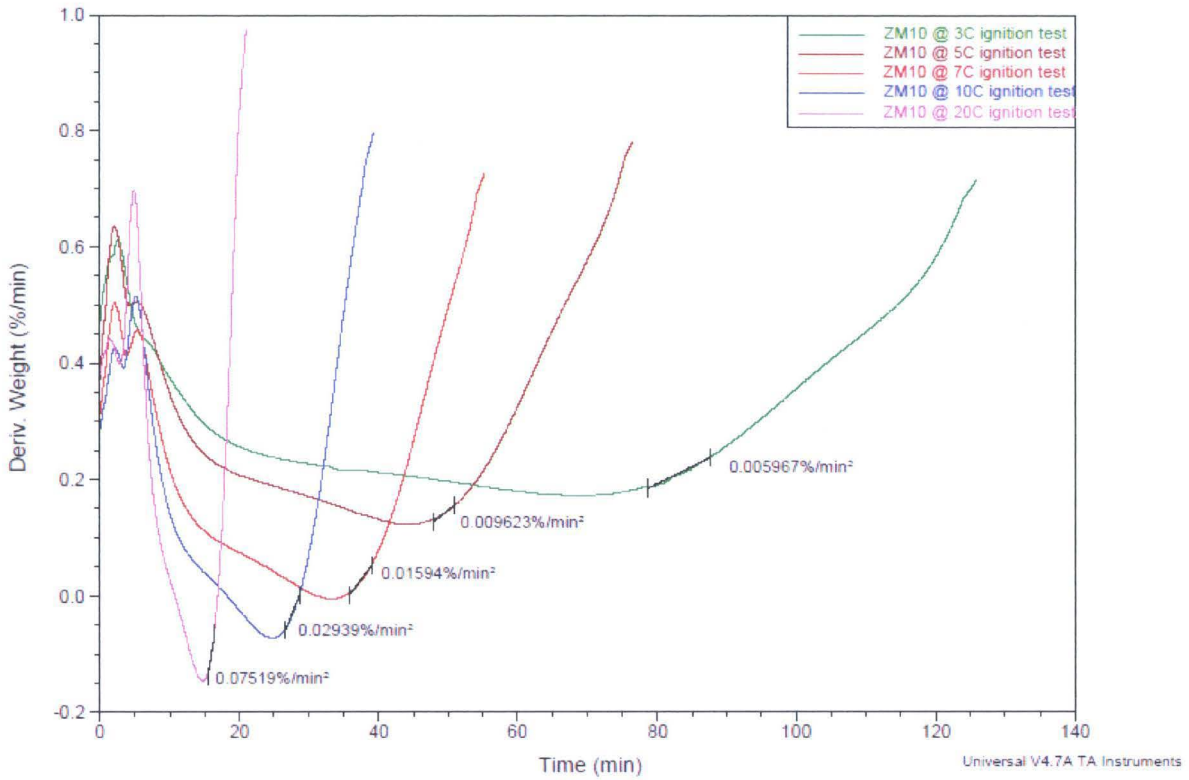


Figure 122: ZM10 Derivative curves and their slopes

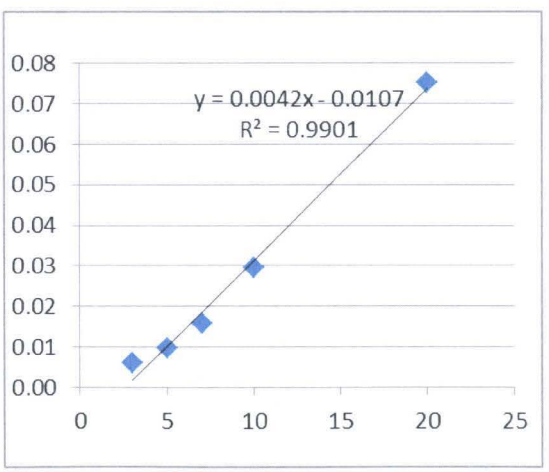


Figure 123: ZM10 R^2_{graph}

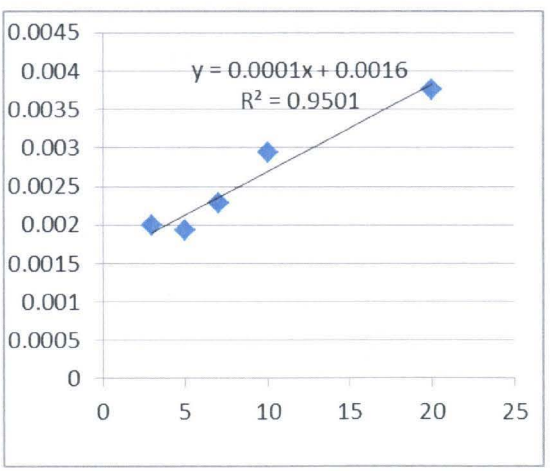


Figure 124: ZM10 $R^2_{calculated}$

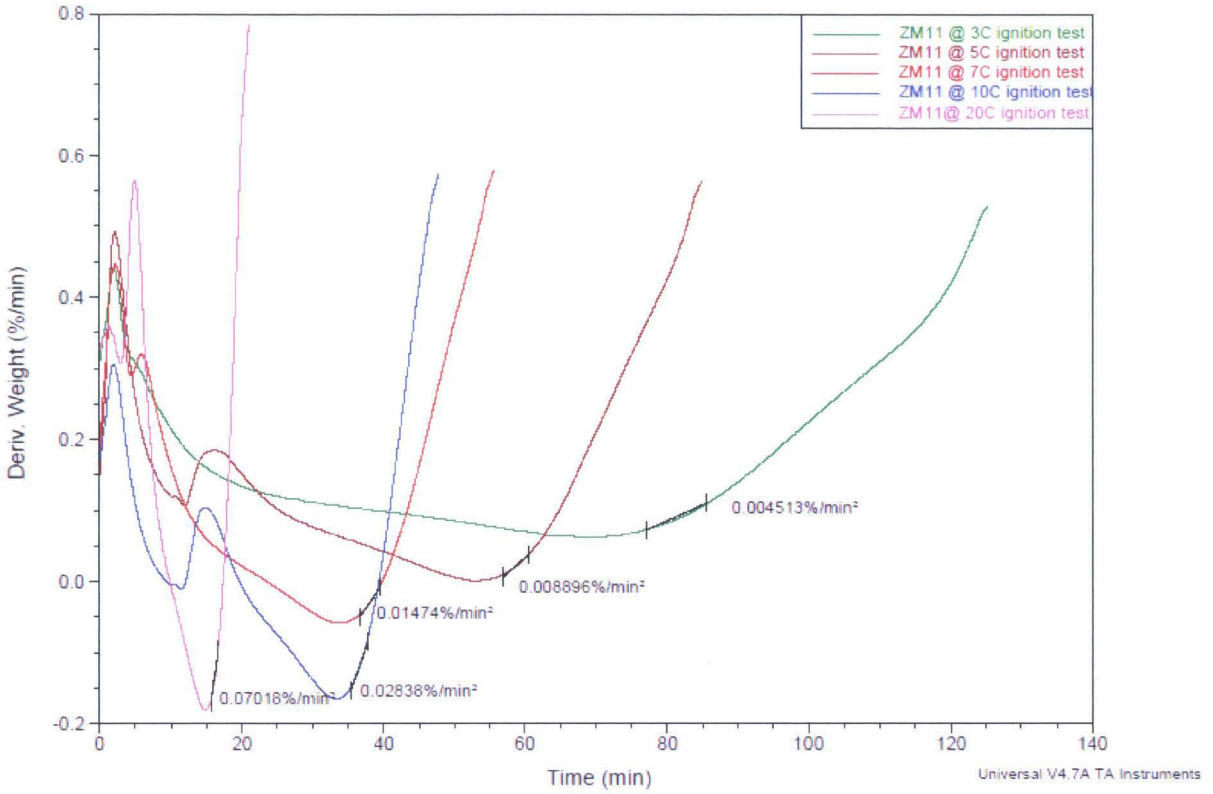


Figure 125: ZM11 Derivative curves and their slopes

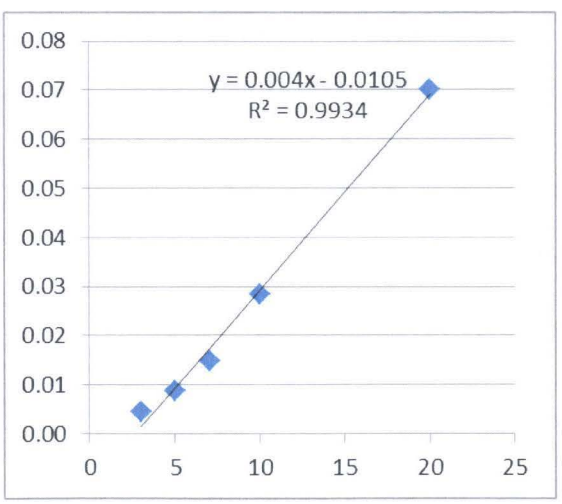


Figure 126: ZM11 R^2_{graph}

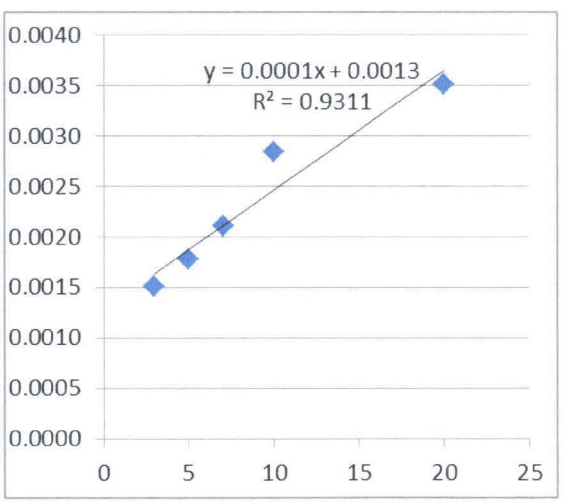


Figure 127: ZM11 $R^2_{calculated}$

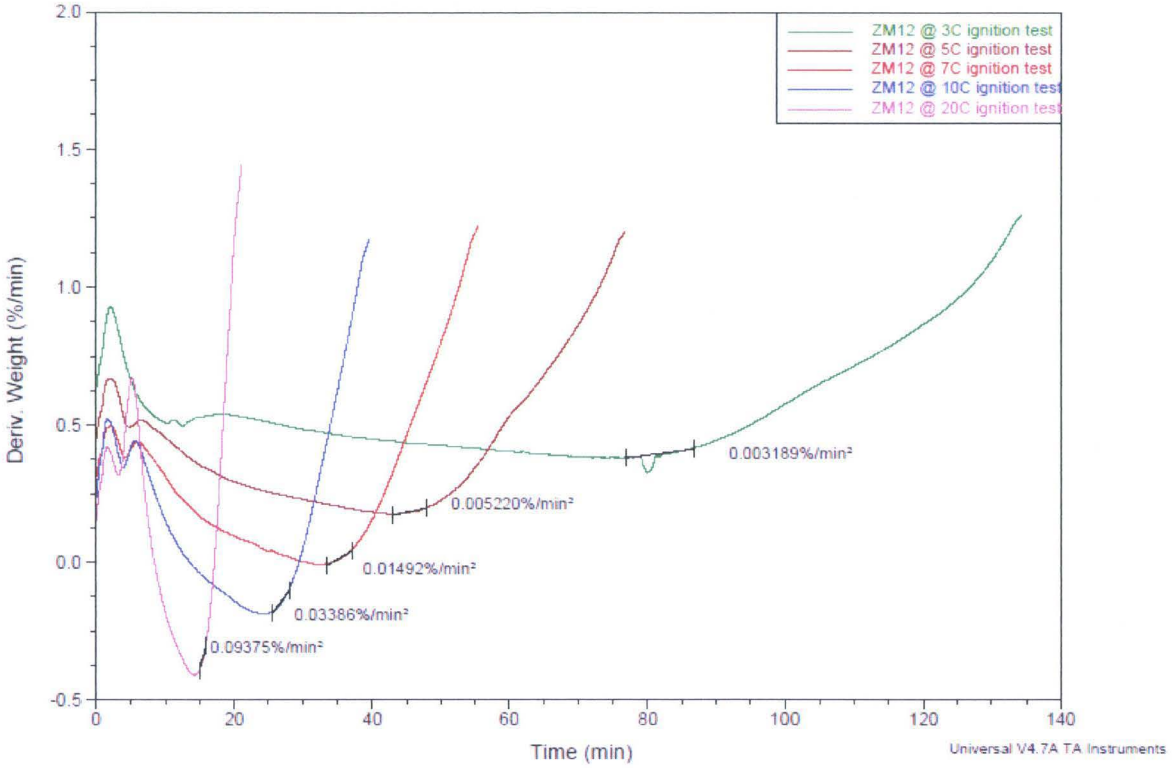


Figure 128: ZM12 Derivative curves and their slopes

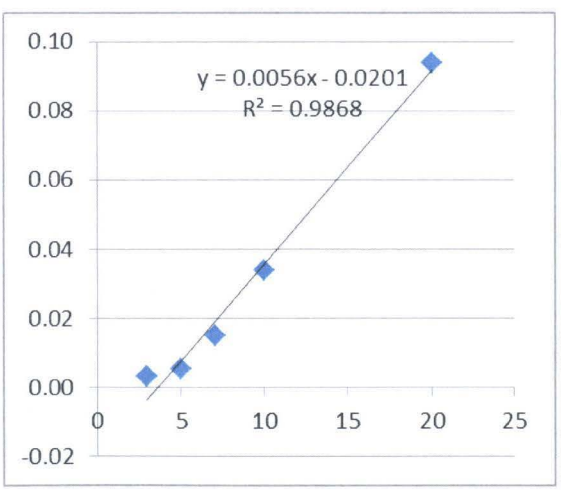


Figure 129: ZM12 R^2_{graph}

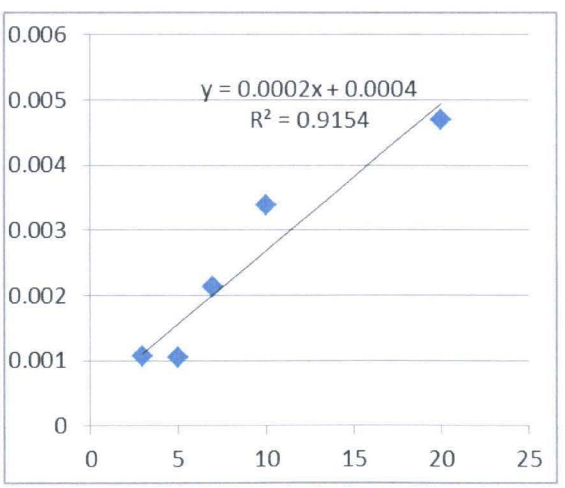


Figure 130: ZM12 $R^2_{calculated}$

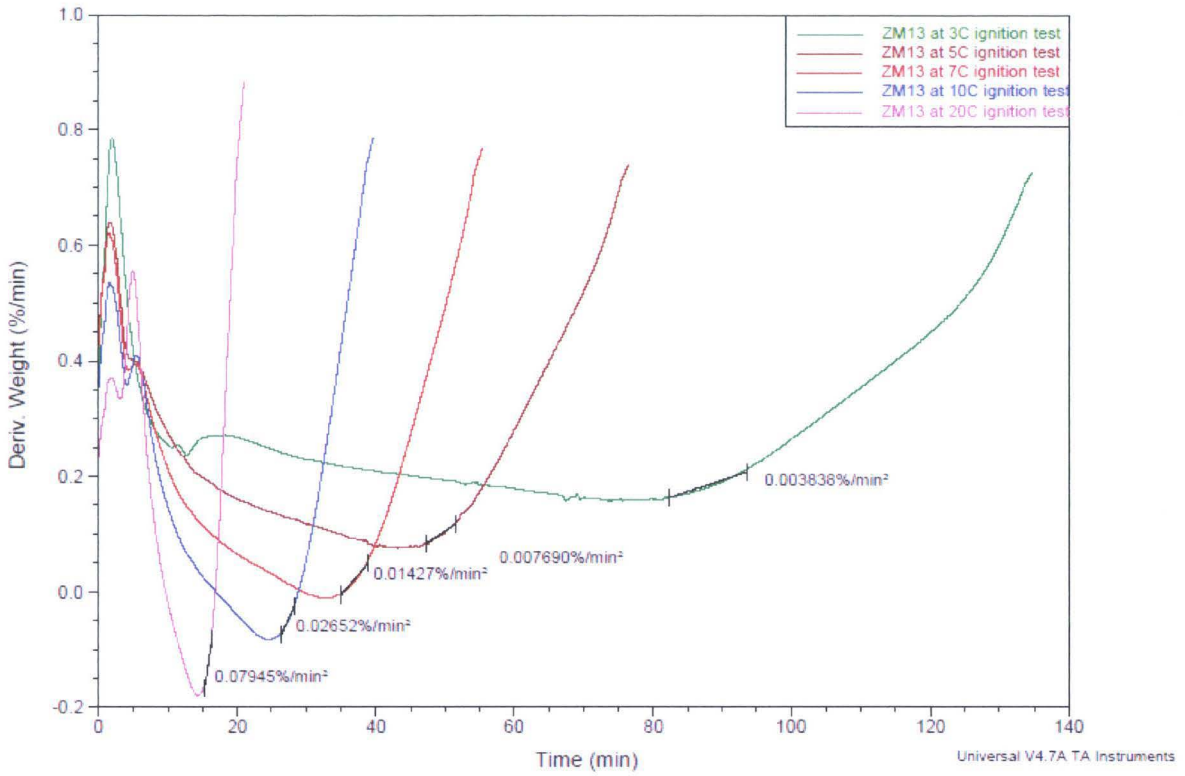


Figure 131: ZM13 Derivative curves and their slopes

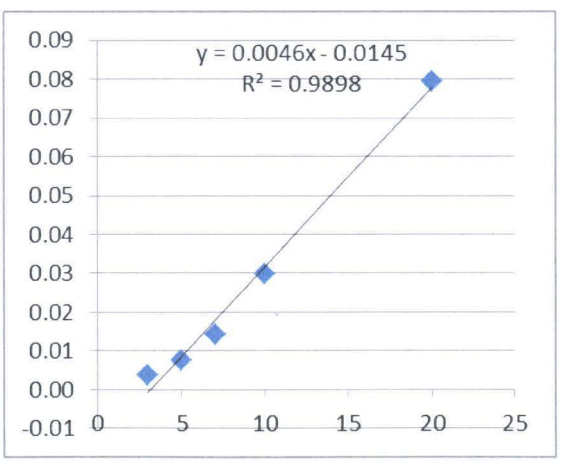


Figure 132: ZM13 R^2_{graph}

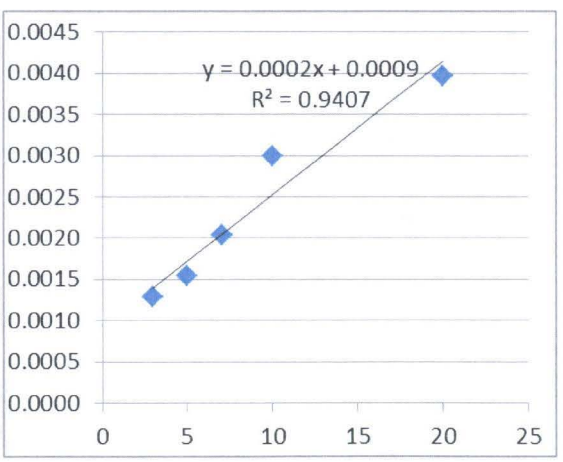


Figure 133: ZM13 $R^2_{calculated}$

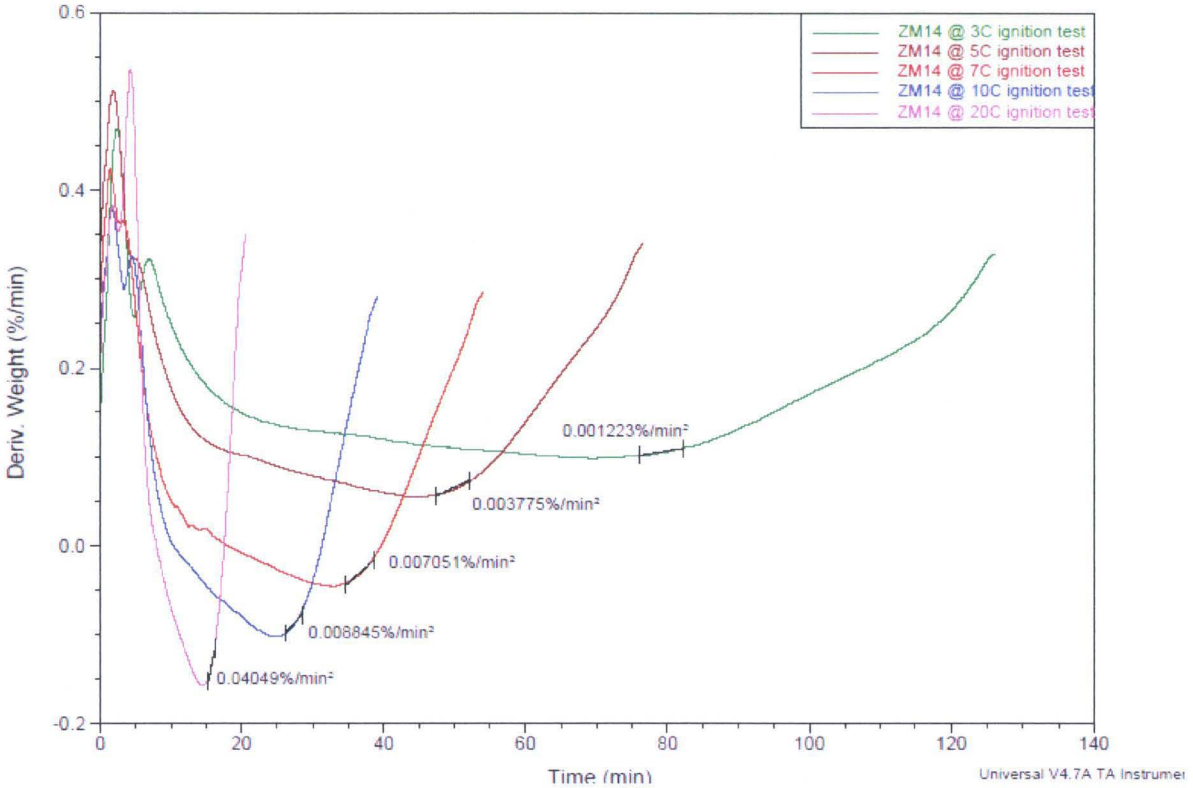


Figure 134: ZM14 Derivative curves and their slopes

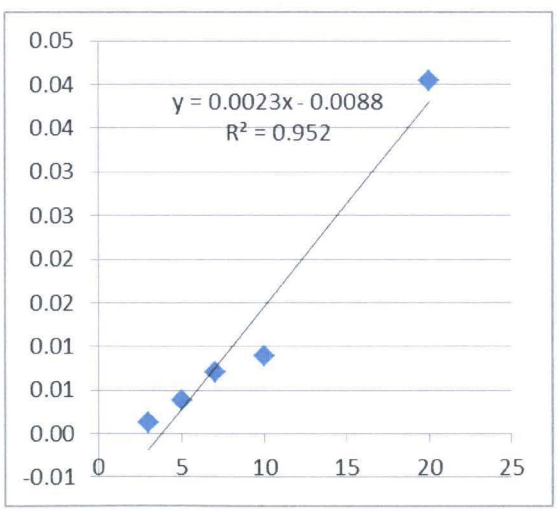


Figure 135: ZM14 R^2_{graph}

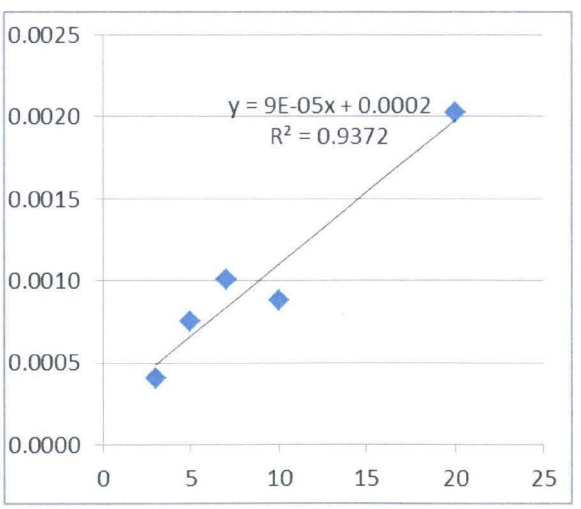


Figure 136: ZM14 $R^2_{calculated}$

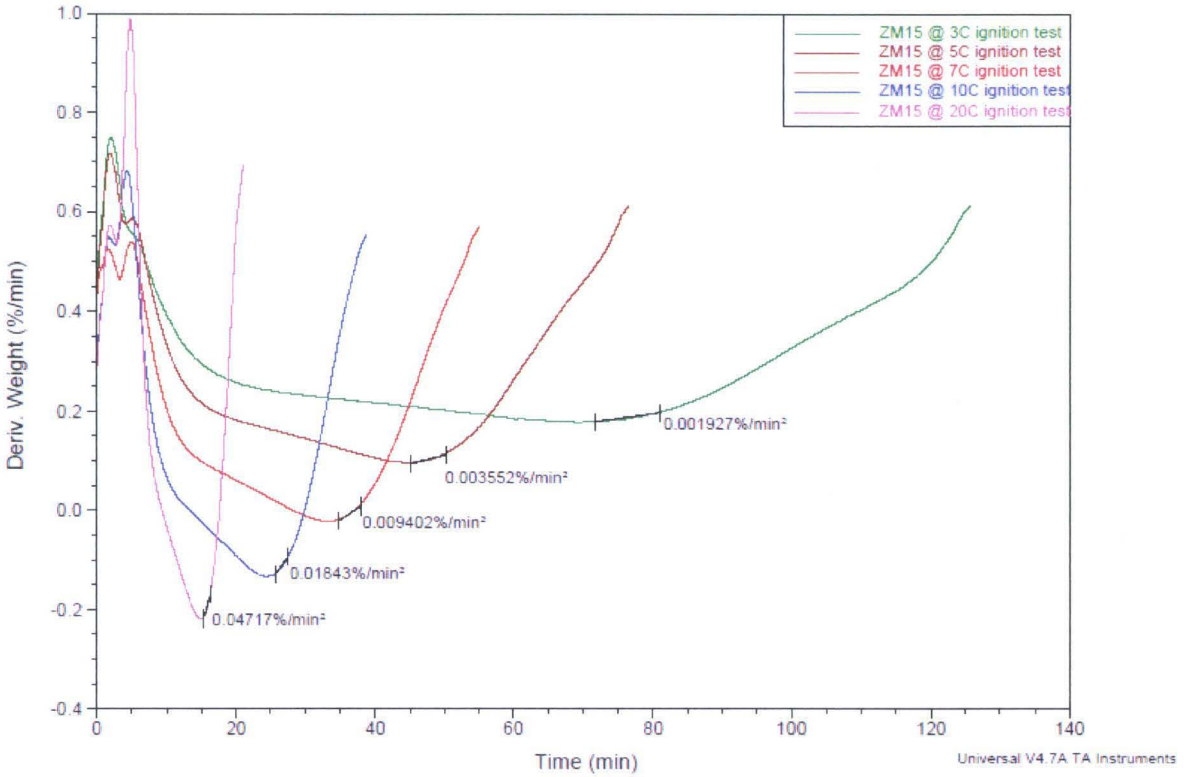


Figure 137: ZM15 Derivative curves and their slopes

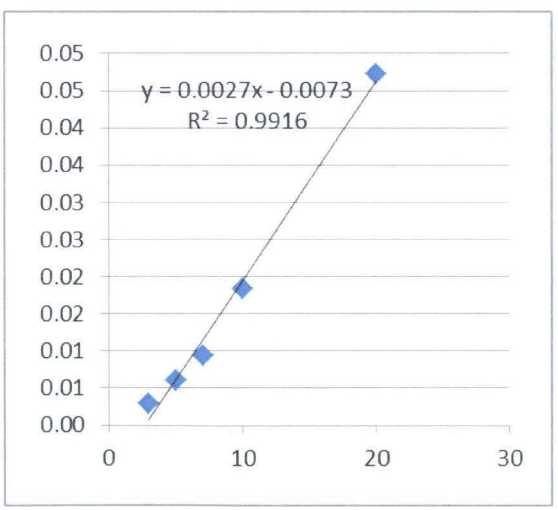


Figure 138: ZM15 R^2_{graph}

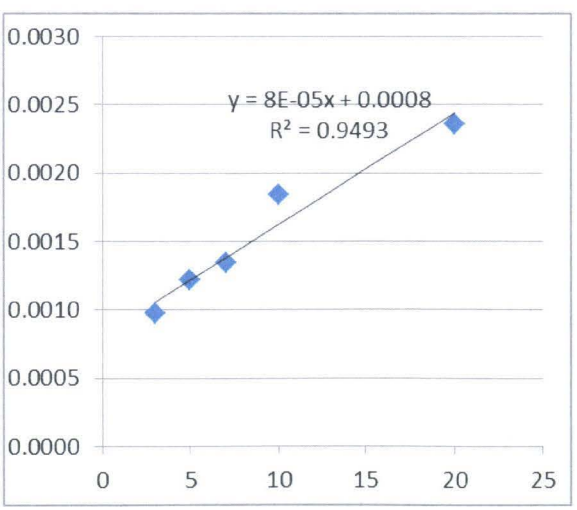


Figure 139: ZM15 $R^2_{calculated}$

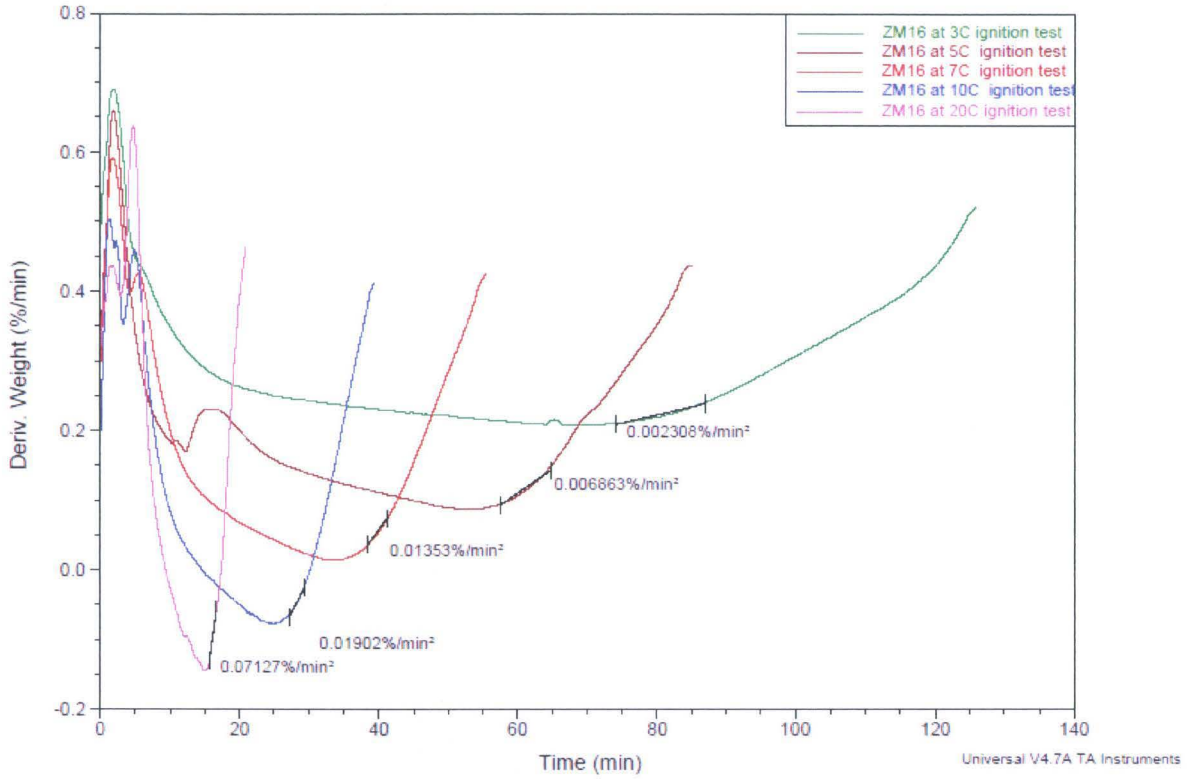


Figure 140: ZM16 Derivative curves and their slopes

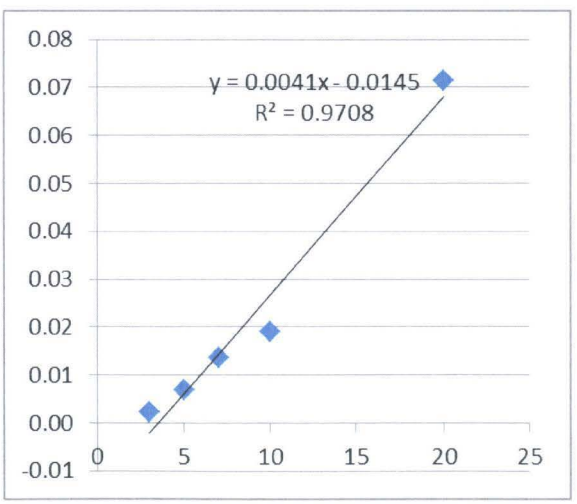


Figure 141: ZM16 R^2_{graph}

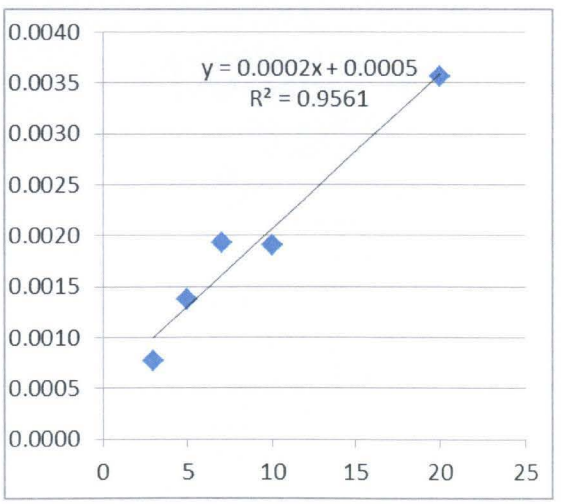


Figure 142: ZM16 $R^2_{calculated}$

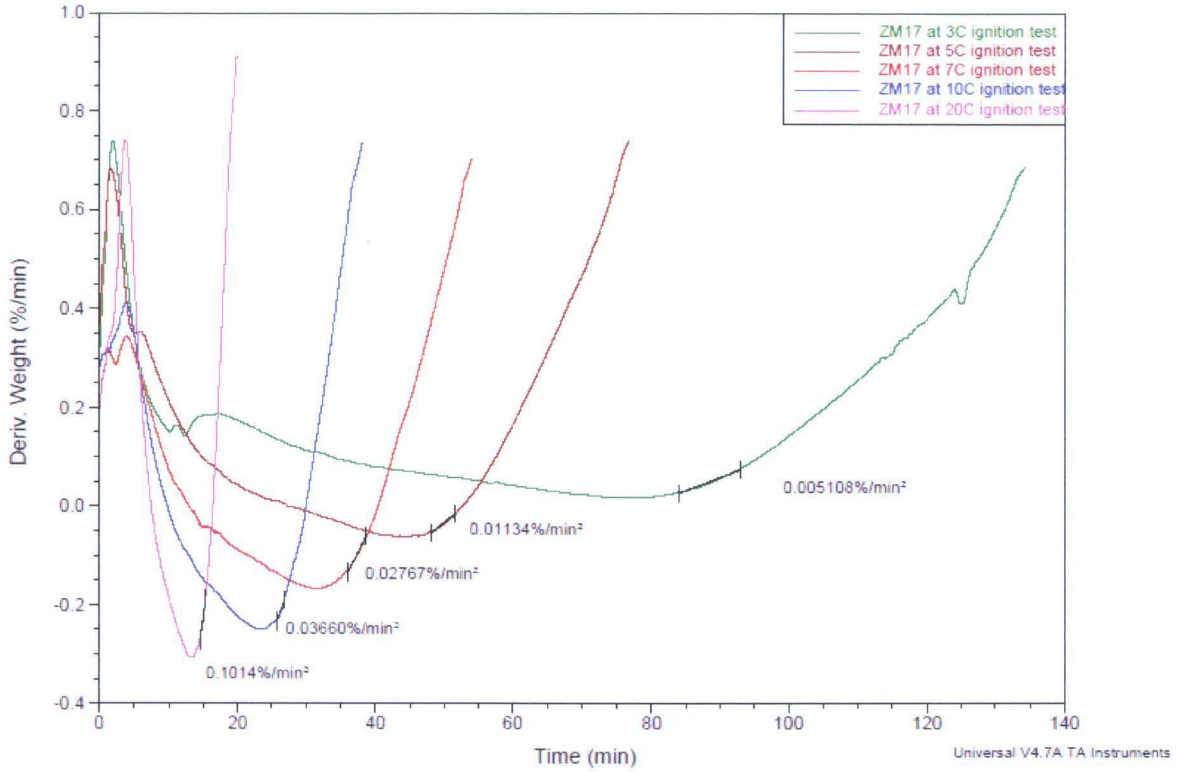


Figure 143: ZM17 Derivative curves and their slopes

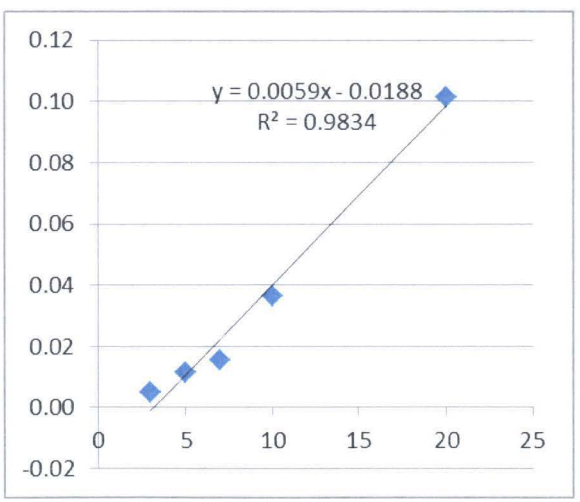


Figure 144: ZM17 R^2_{graph}

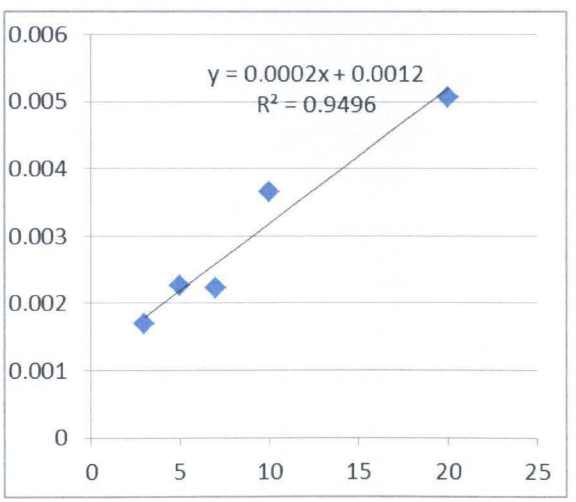


Figure 145: ZM17 $R^2_{calculated}$

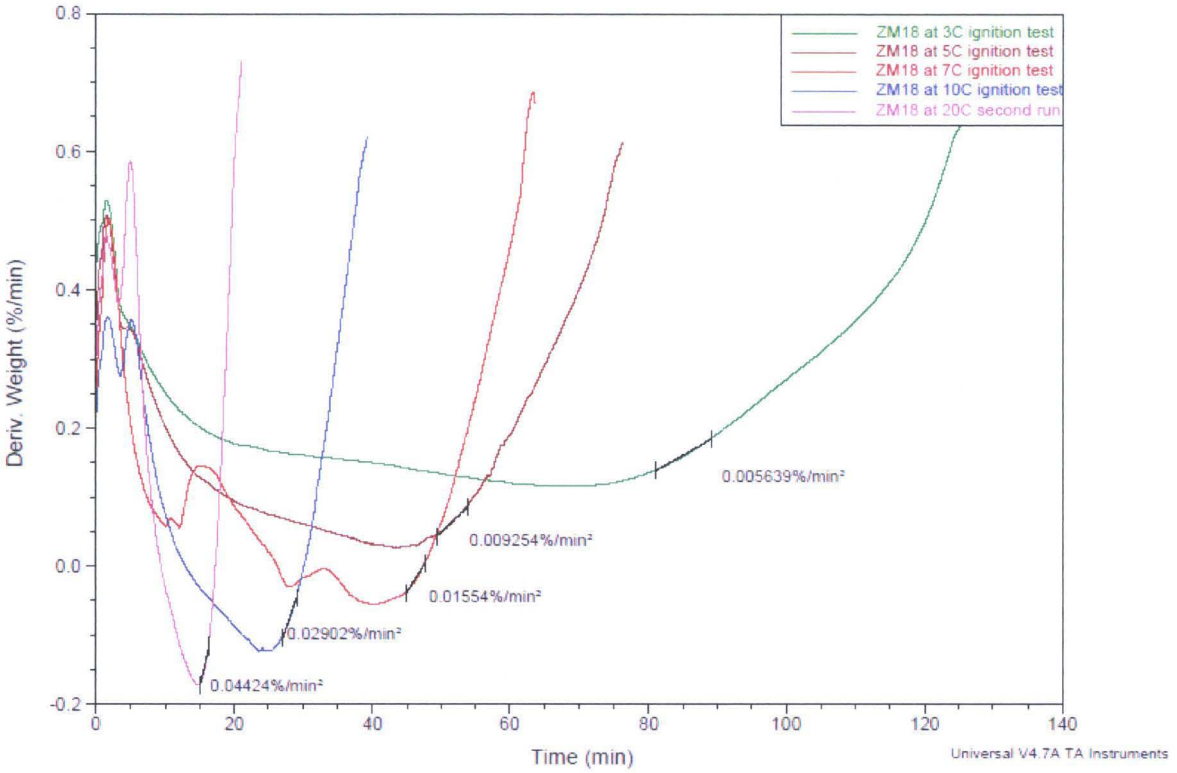


Figure 146: ZM18 Derivative curves and their slopes

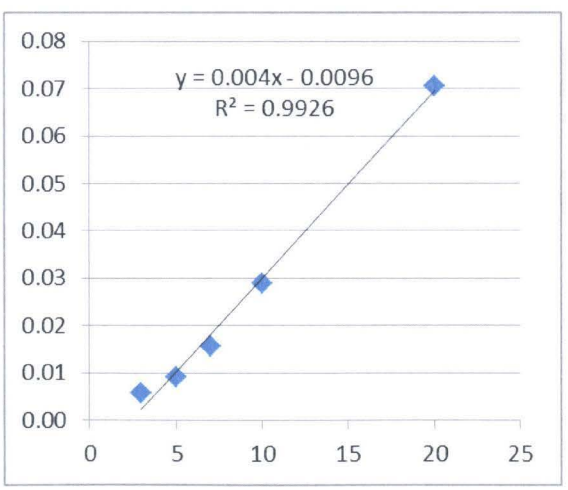


Figure 147: ZM18 R^2_{graph}

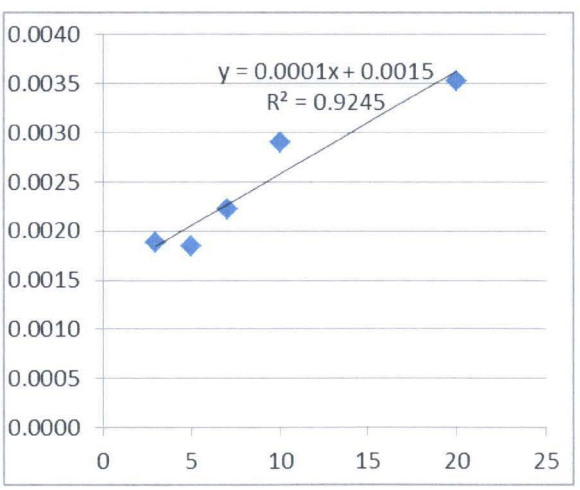


Figure 148: ZM18 $R^2_{calculated}$

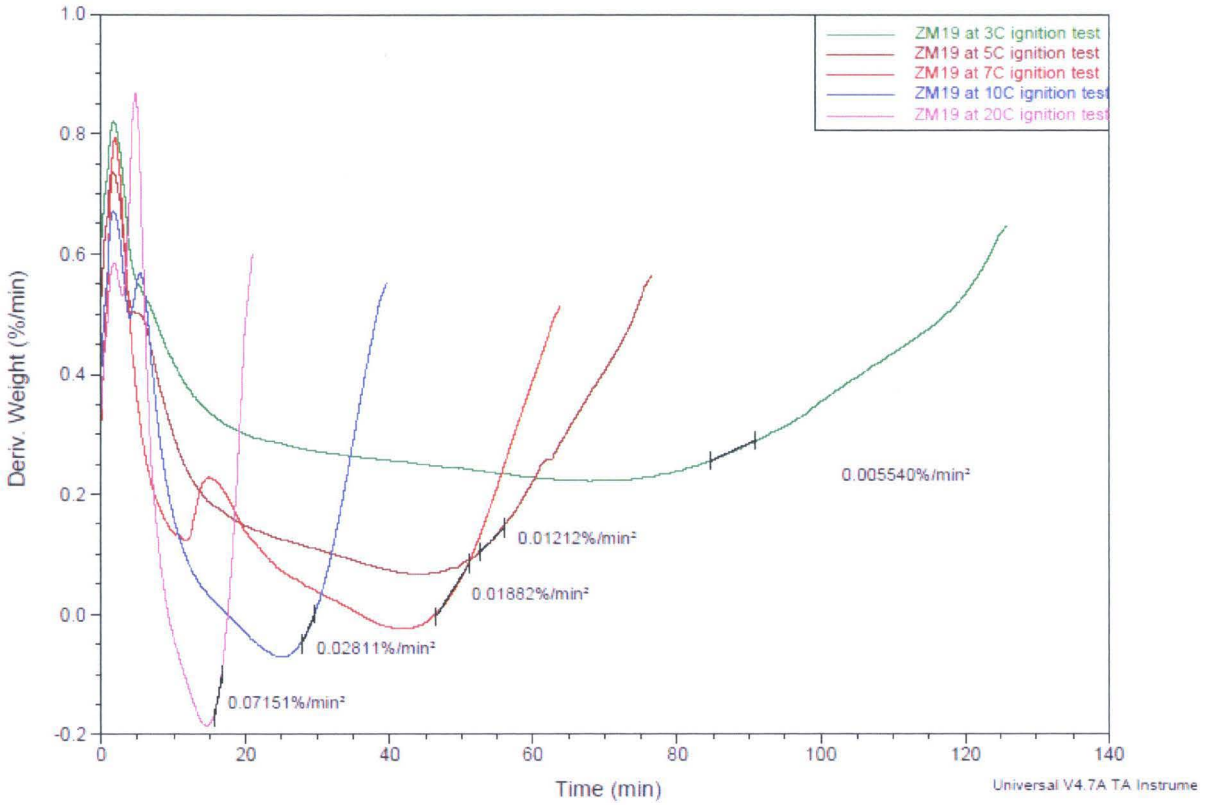


Figure 149: ZM19 Derivative curves and their slopes

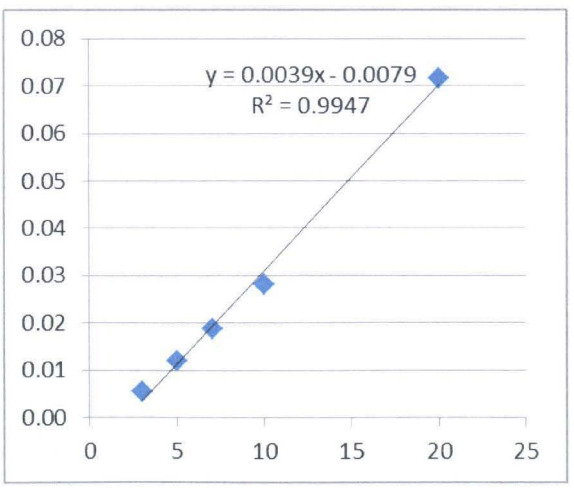


Figure 150: ZM19 R^2_{graph}

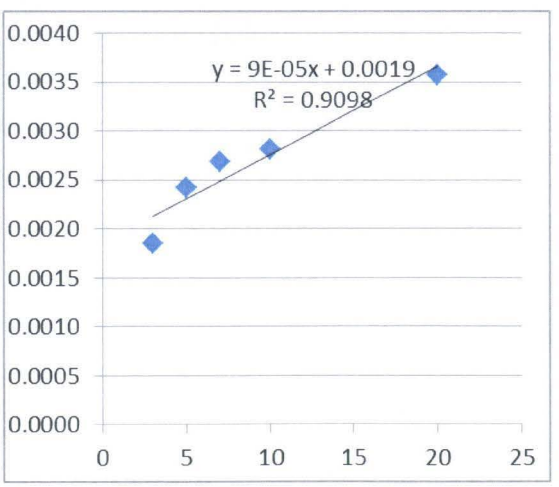


Figure 151: ZM19 $R^2_{calculate}$

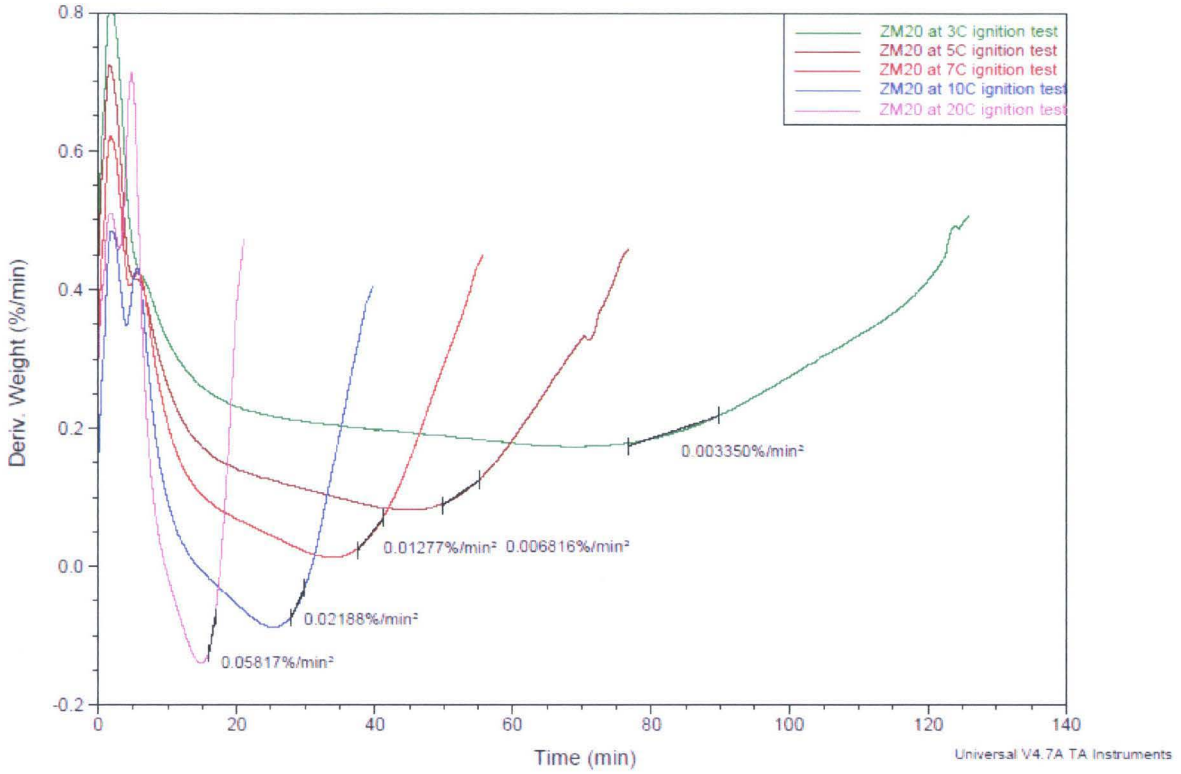


Figure 152: ZM20 Derivative curves and their slopes

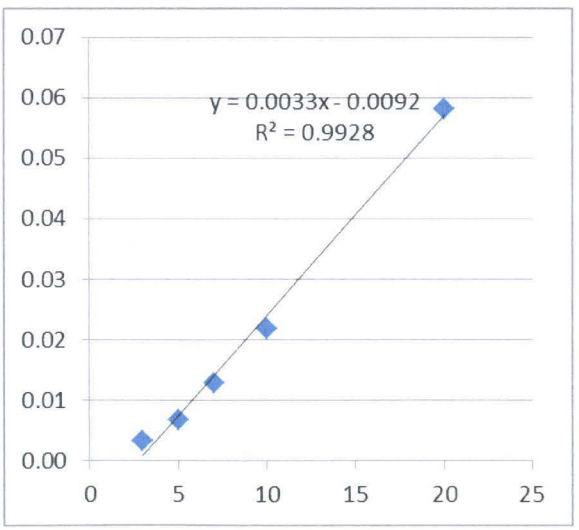


Figure 153: ZM20 R^2_{graph}

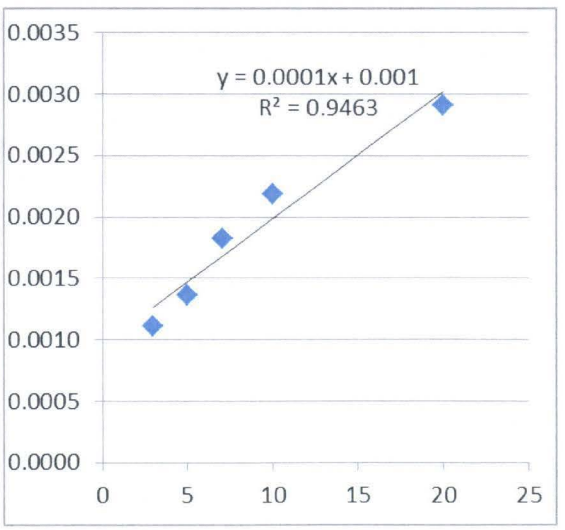


Figure 154: ZM20 $R^2_{calculate}$

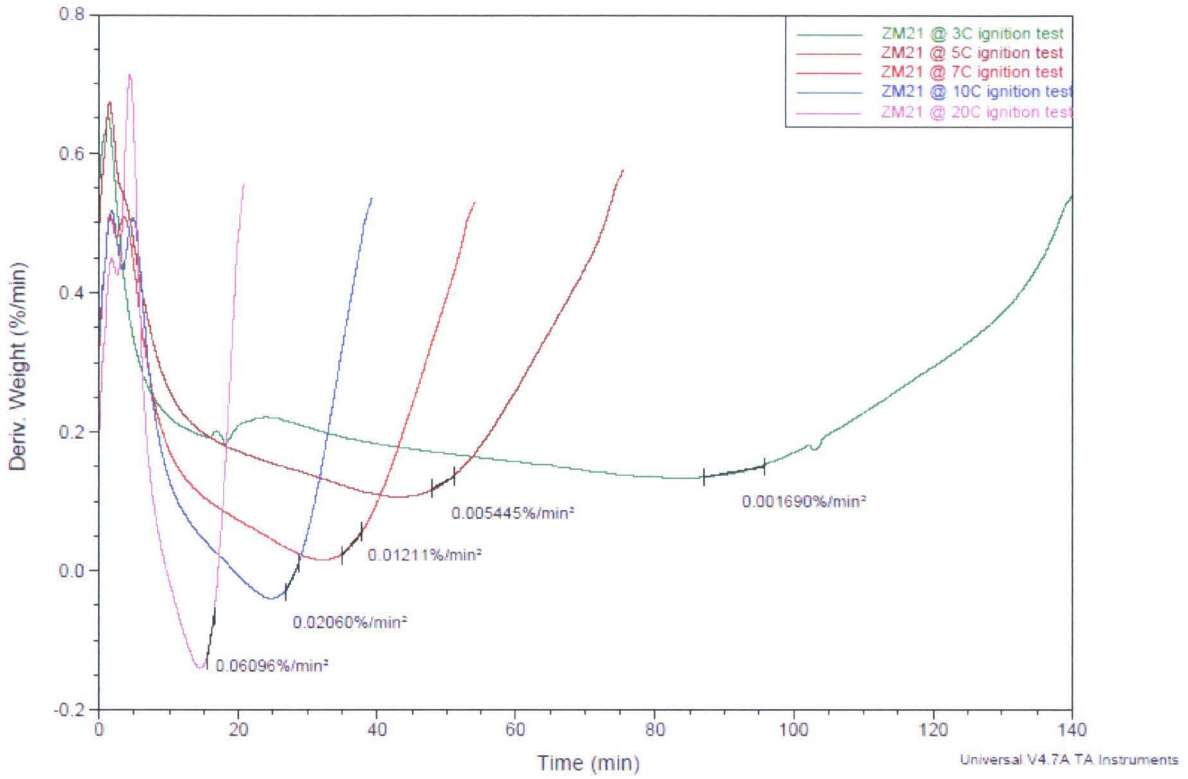


Figure 155: ZM21 Derivative curves and their slopes

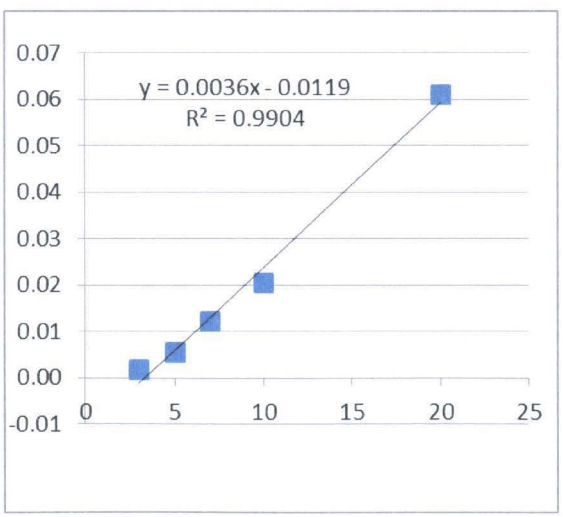


Figure 156: ZM21 R^2_{graph}

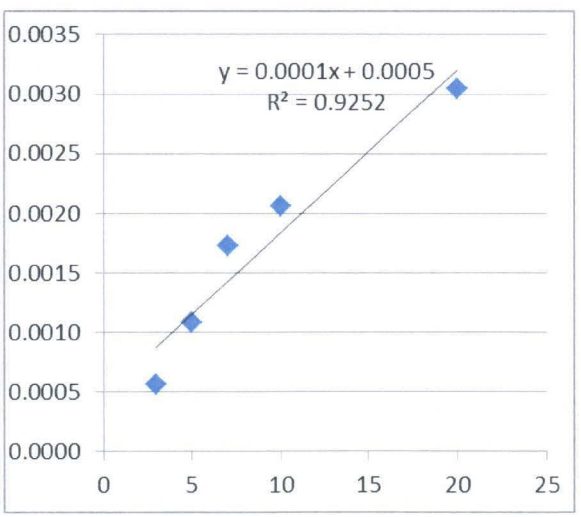


Figure 157: ZM21 $R^2_{calculate}$

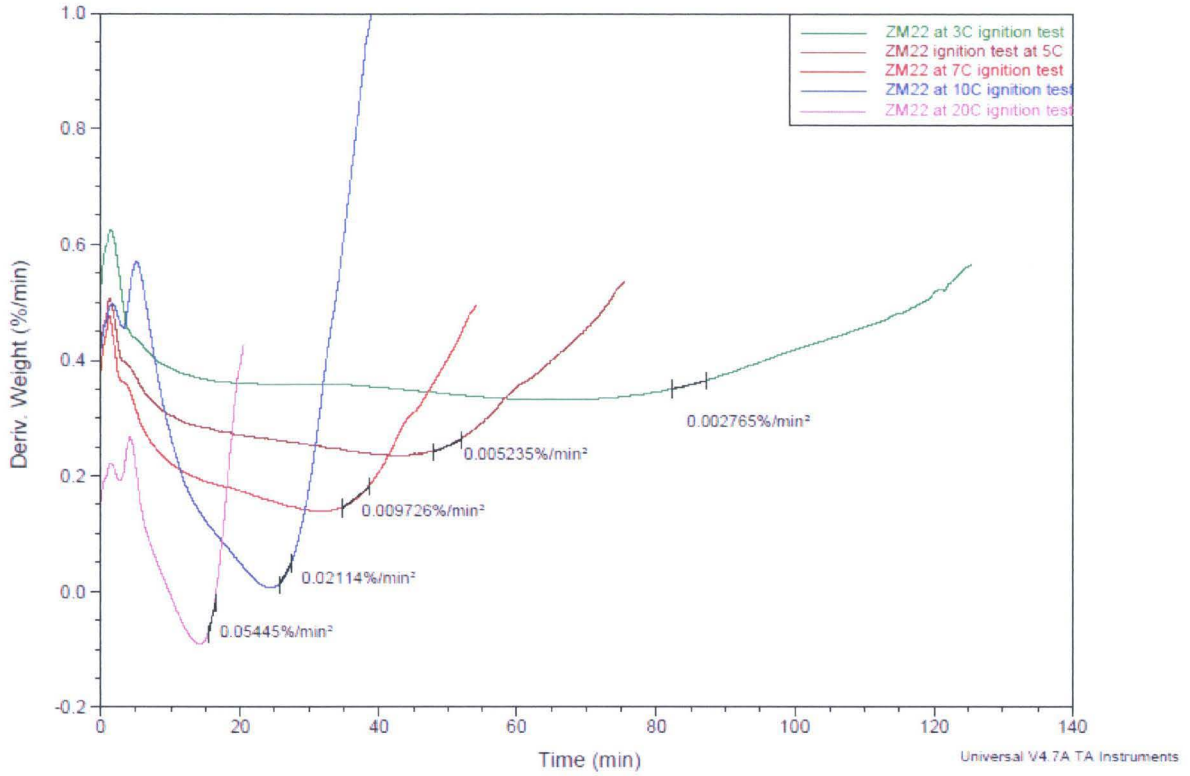


Figure 158: ZM22 Derivative curves and their slopes

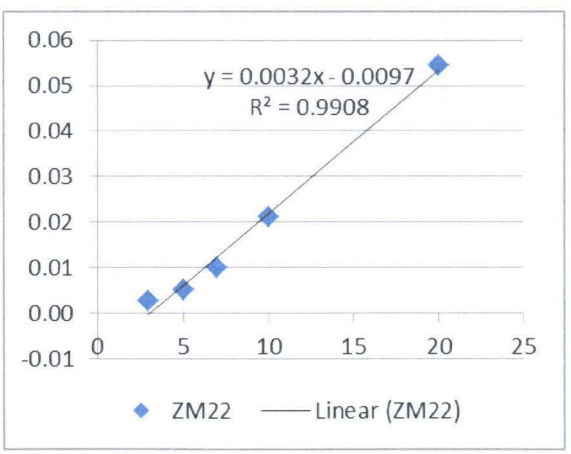


Figure 159: ZM22 R^2_{graph}

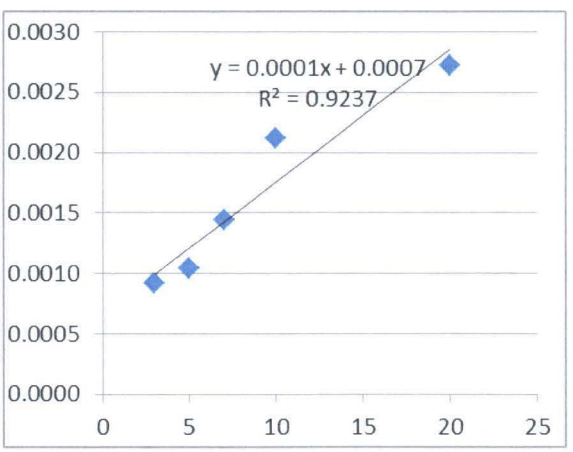


Figure 160: ZM22 $R^2_{calculate}$

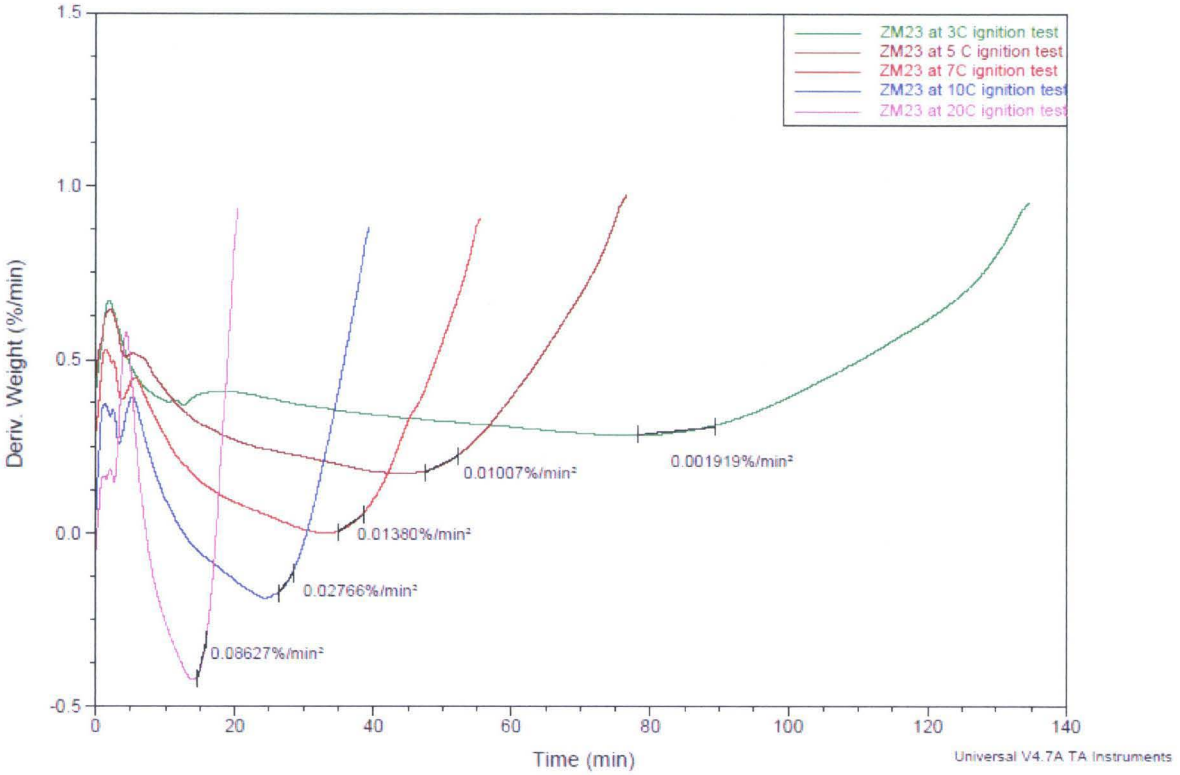


Figure 161: ZM23 Derivative curves and their slopes

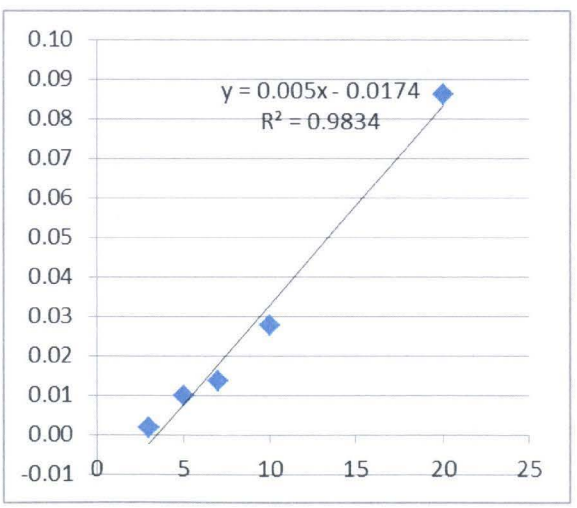


Figure 162: ZM23 R^2_{graph}

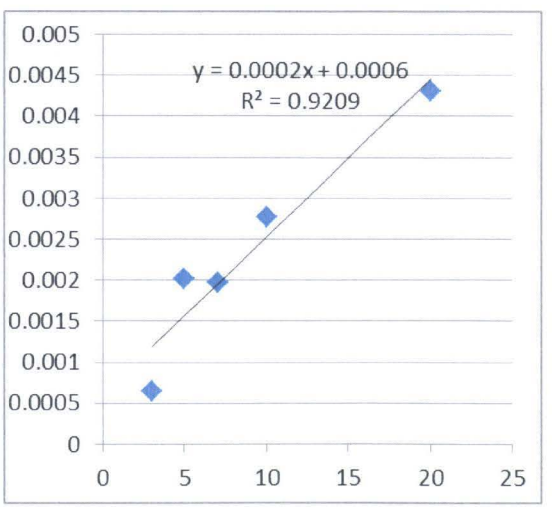


Figure 163: ZM23 $R^2_{calculate}$

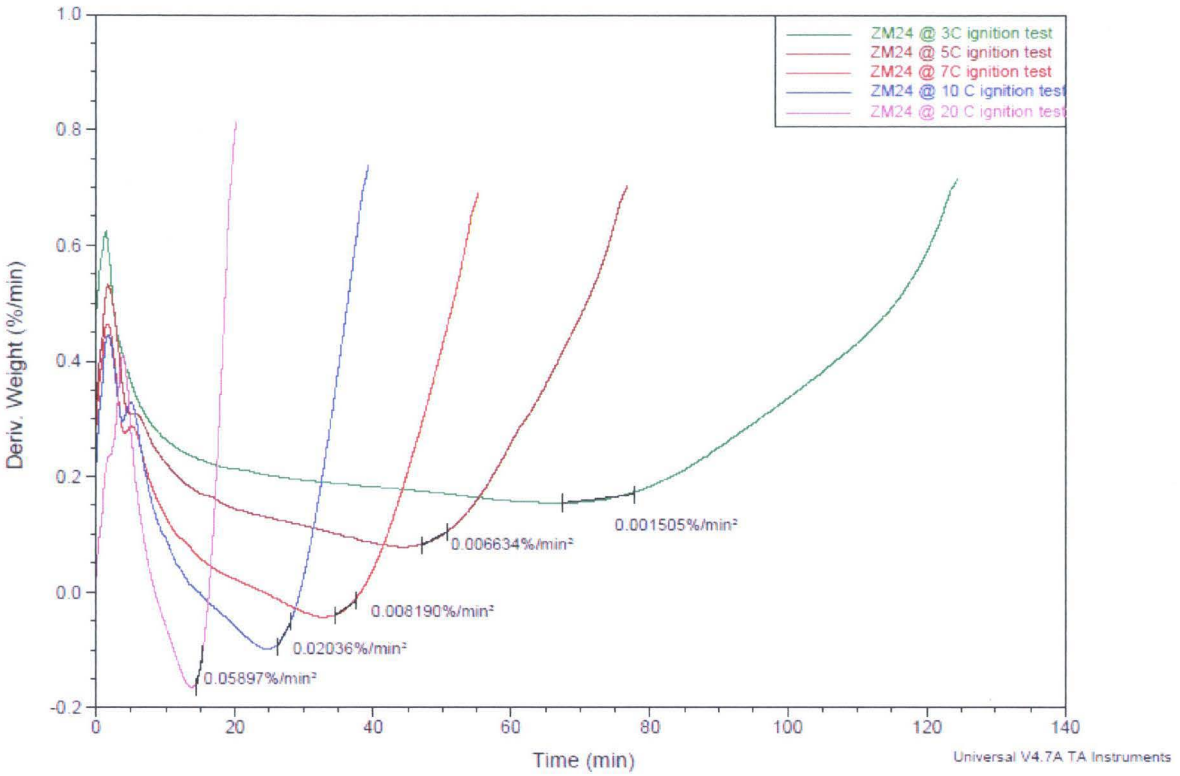


Figure 164: ZM24 Derivative curves and their slopes

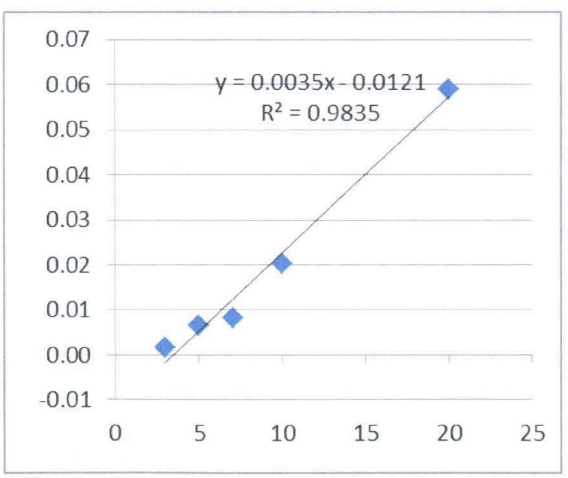


Figure 165: ZM24 R^2_{graph}

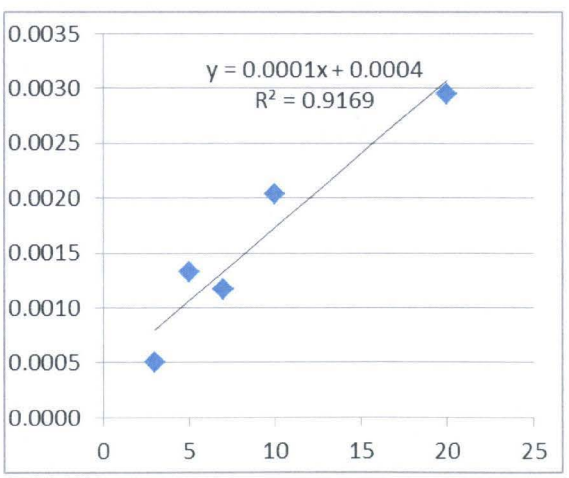


Figure 166: ZM24 $R^2_{calculate}$

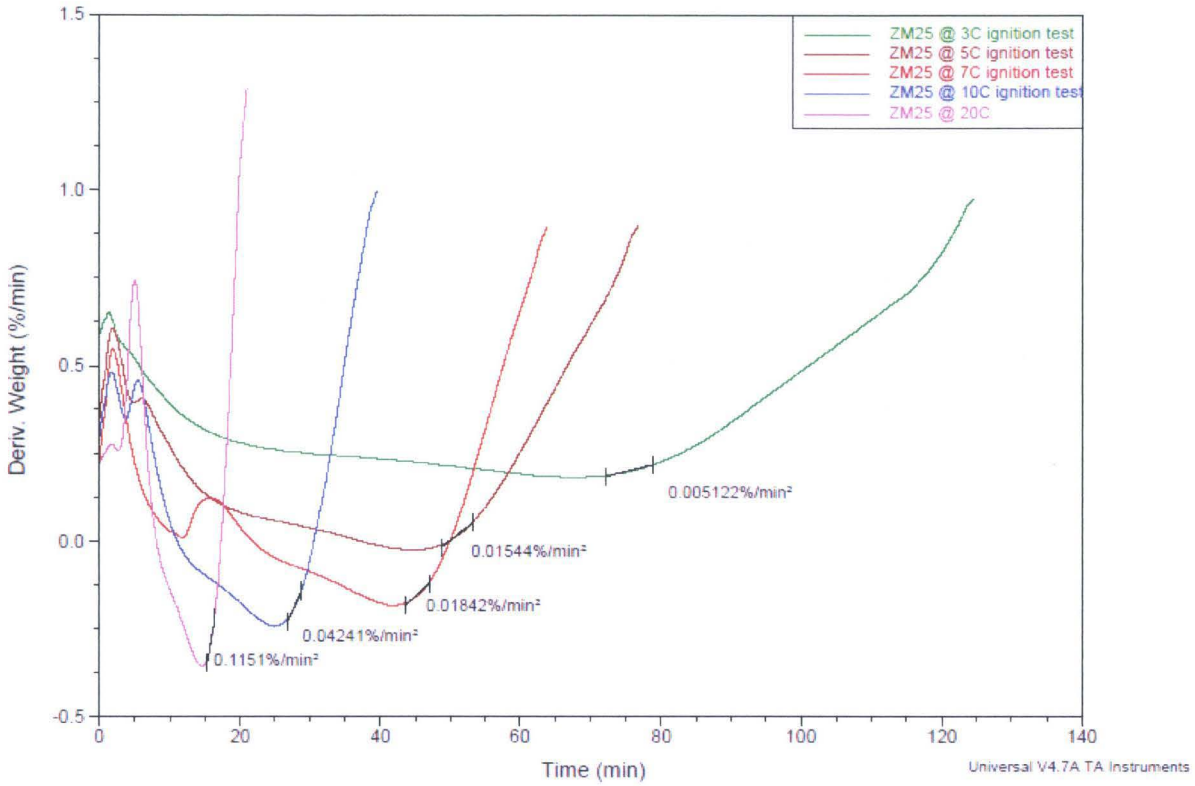


Figure 167: ZM25 Derivative curves and their slopes

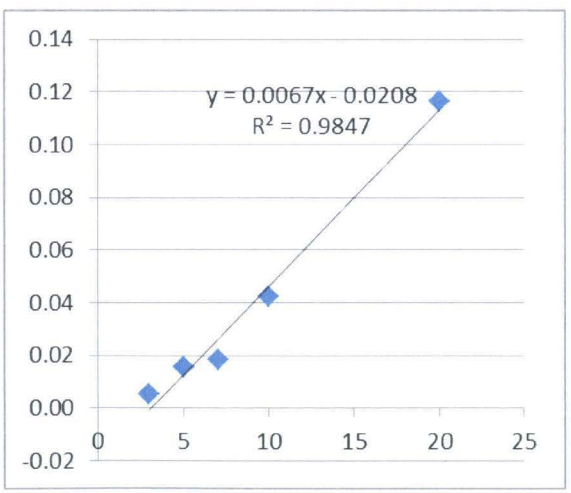


Figure 168: ZM25 R^2_{graph}

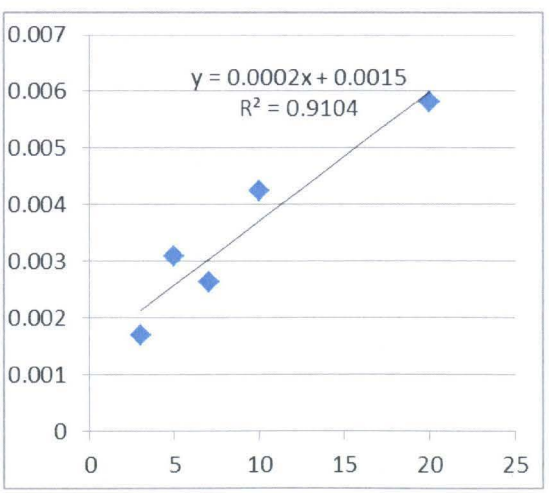


Figure 169: ZM25 $R^2_{calculate}$

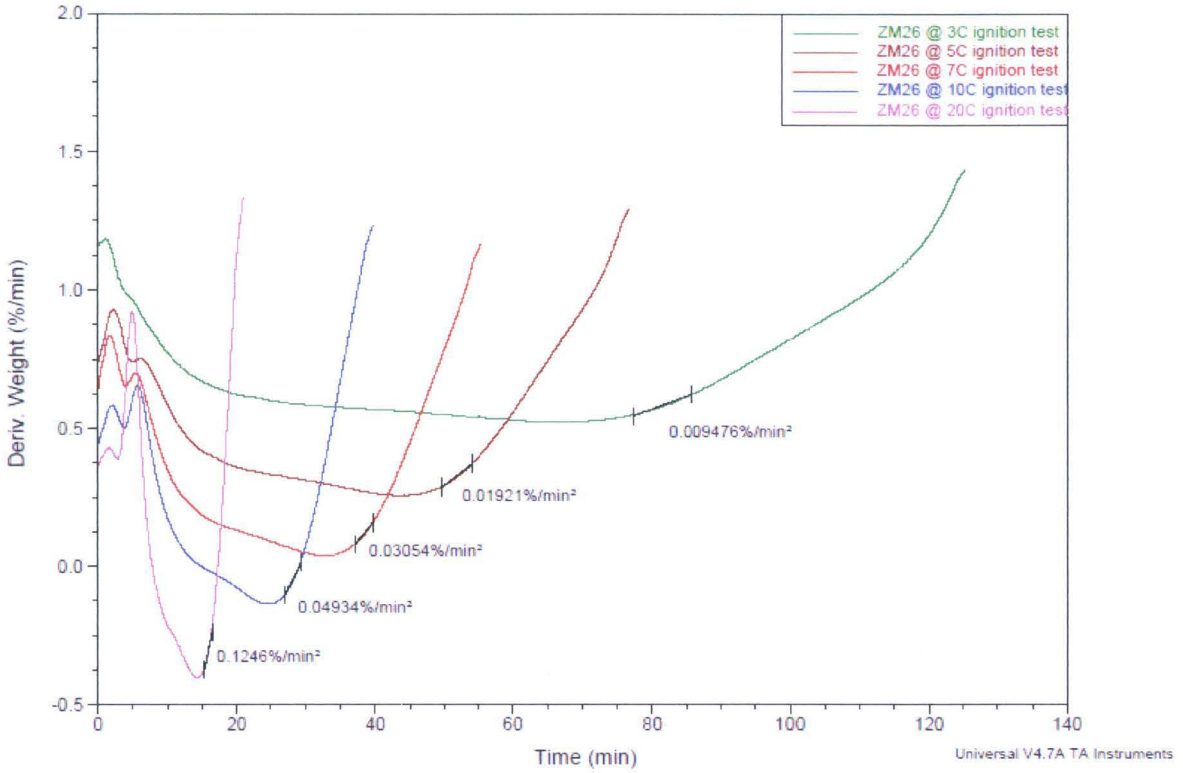


Figure 170: ZM26 Derivative curves and their slopes

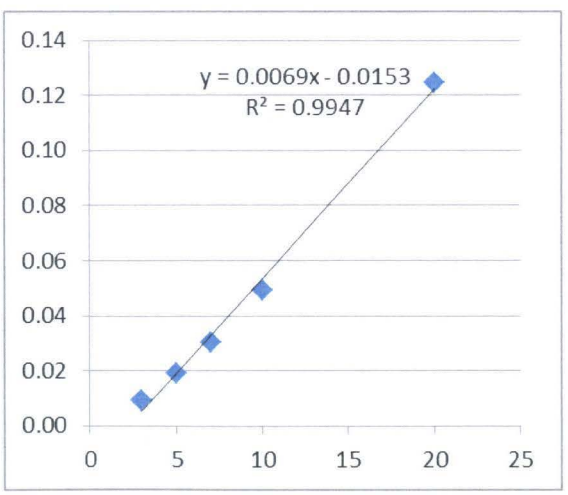


Figure 171: ZM26 R^2_{graph}

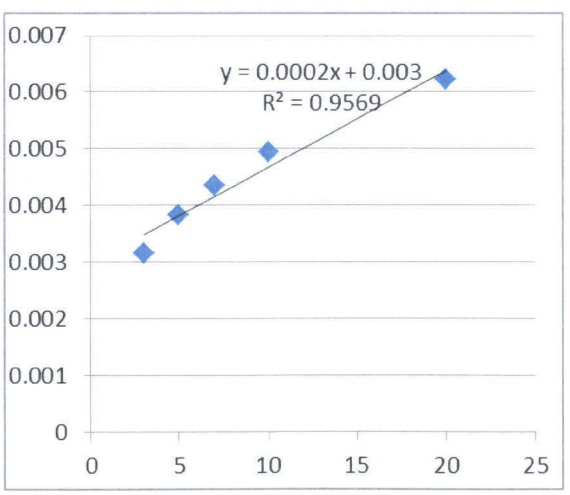


Figure 172:ZM26 $R^2_{calculate}$

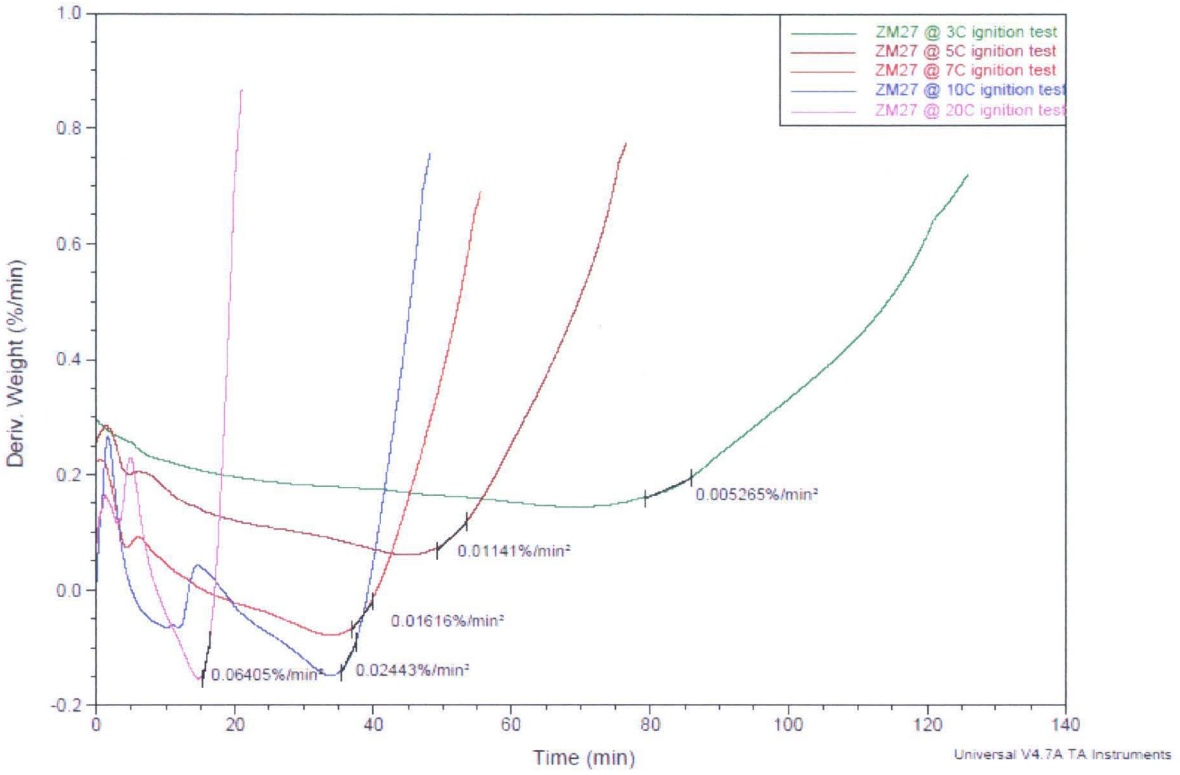


Figure 173: ZM27 Derivative curves and their slopes

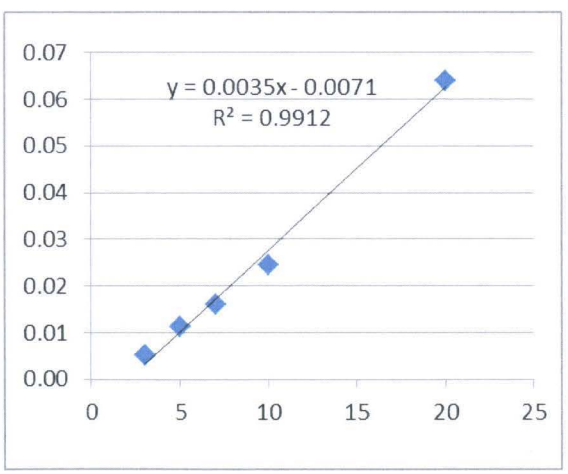


Figure 174: ZM27 R^2_{graph}

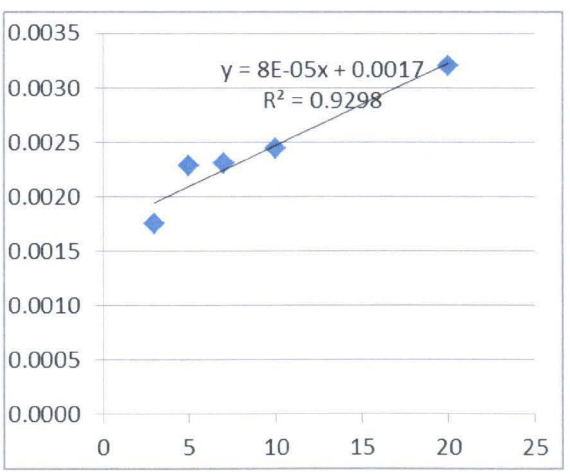


Figure 175: ZM27 $R^2_{calculate}$

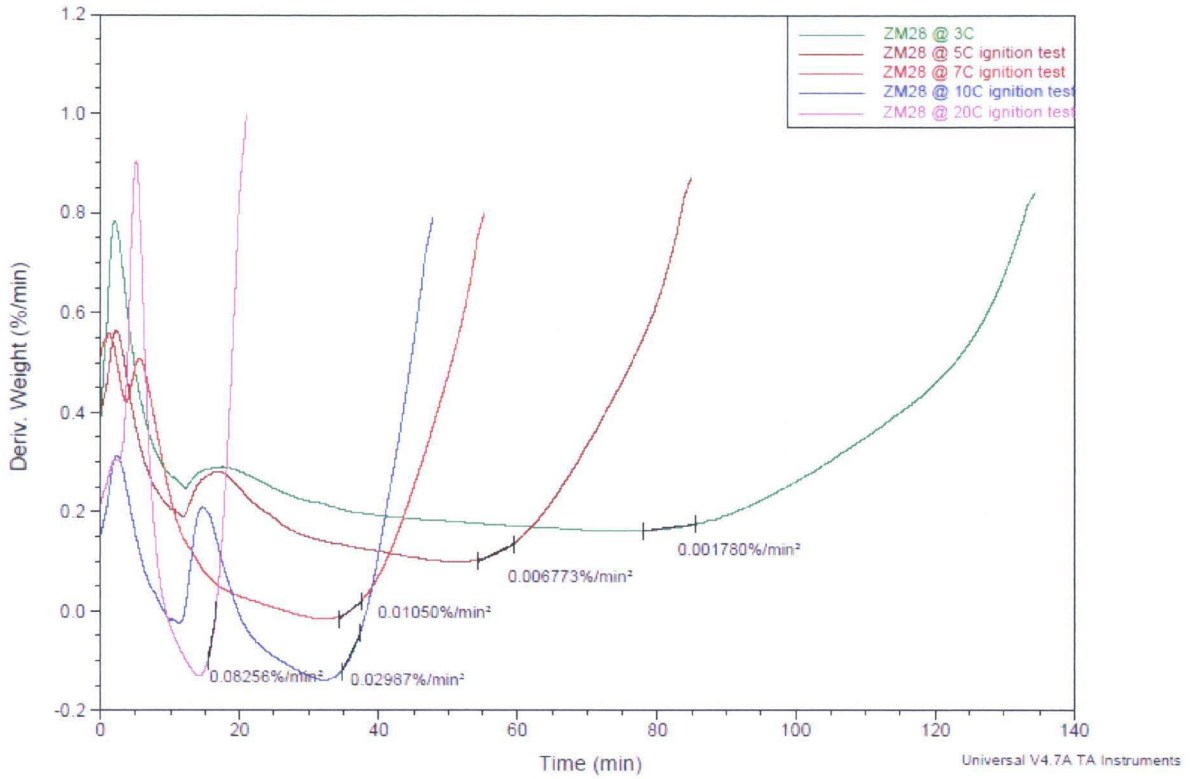


Figure 176: ZM28 Derivative curves and their slopes

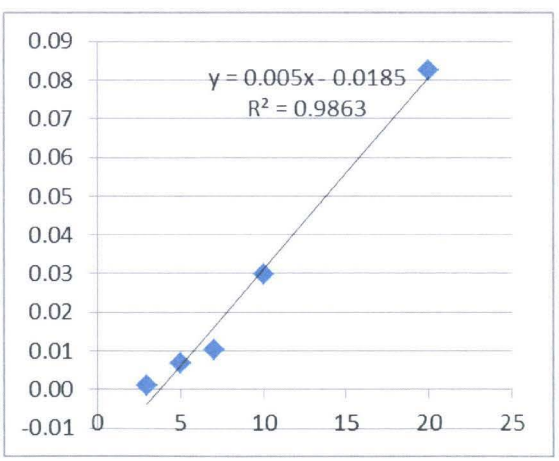


Figure 177: ZM28 R^2_{graph}

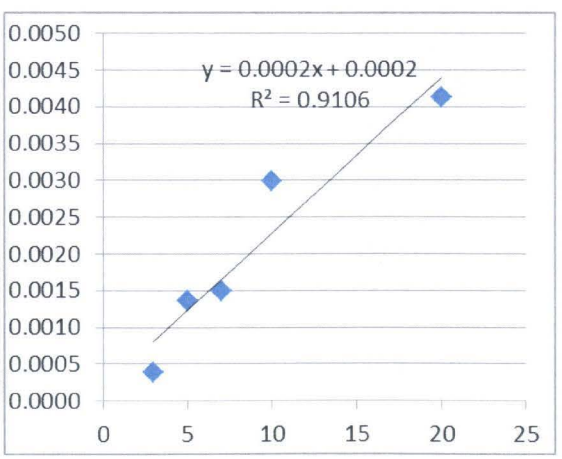


Figure 178: ZM28 $R^2_{calculate}$

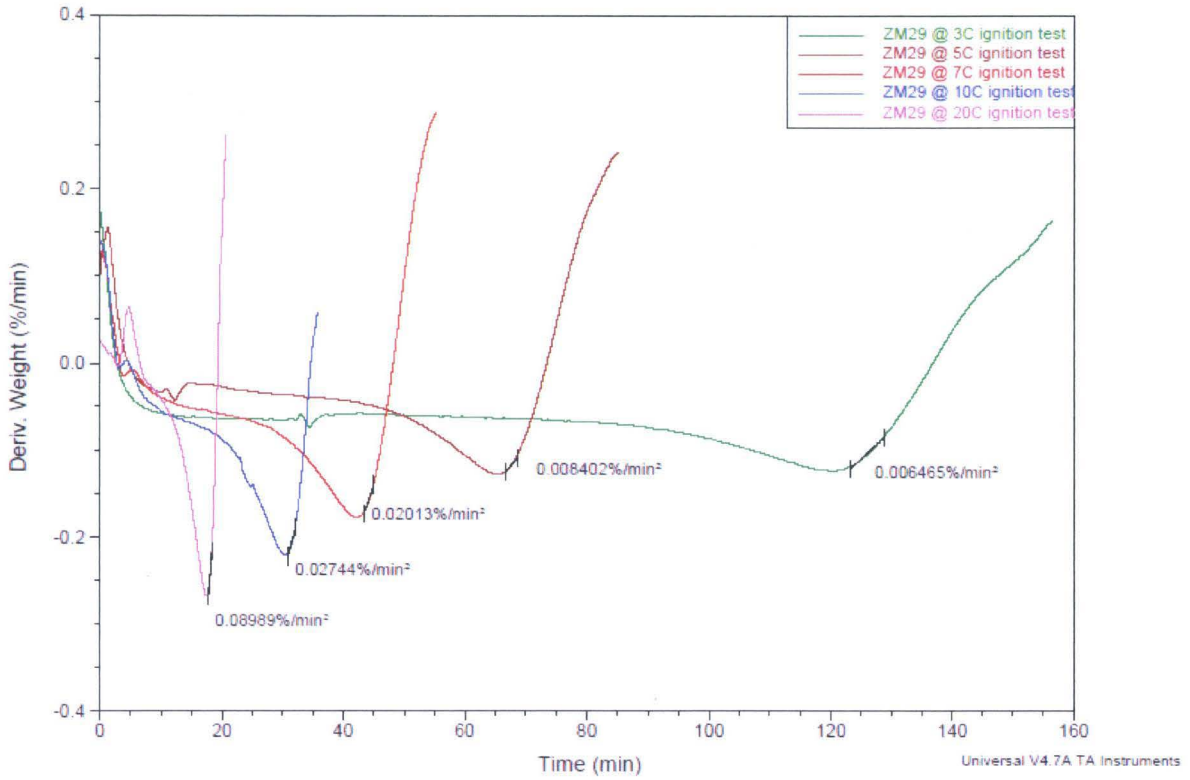


Figure 179: ZM29 Derivative curves and their slopes

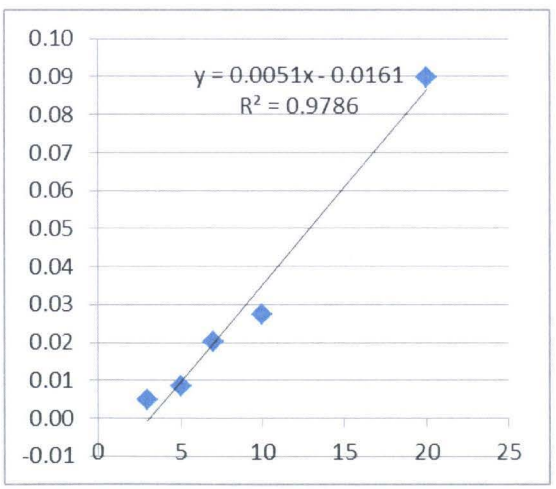


Figure 180: ZM29 R^2_{graph}

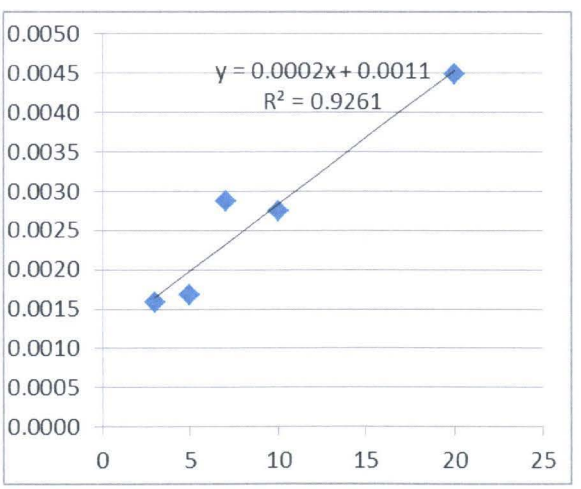


Figure 181: ZM29 $R^2_{calculate}$

8.3 Appendix C

8.3.1 Smith-Glasser Oxidation Test

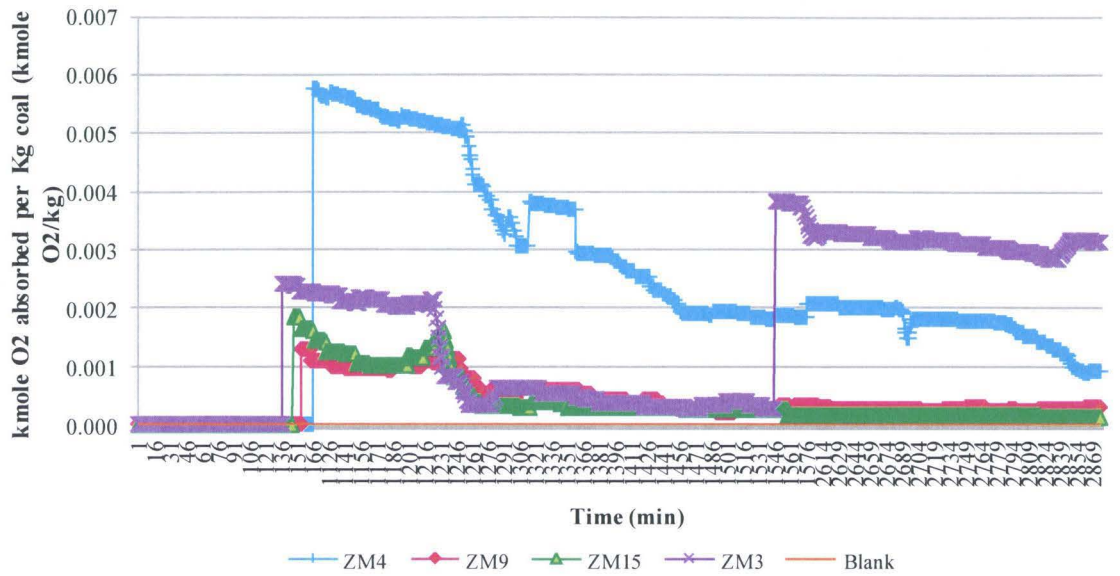


Figure 182: Smith-Glasser Oxygen absorption (ZM4, ZM9, ZM15 & ZM3)

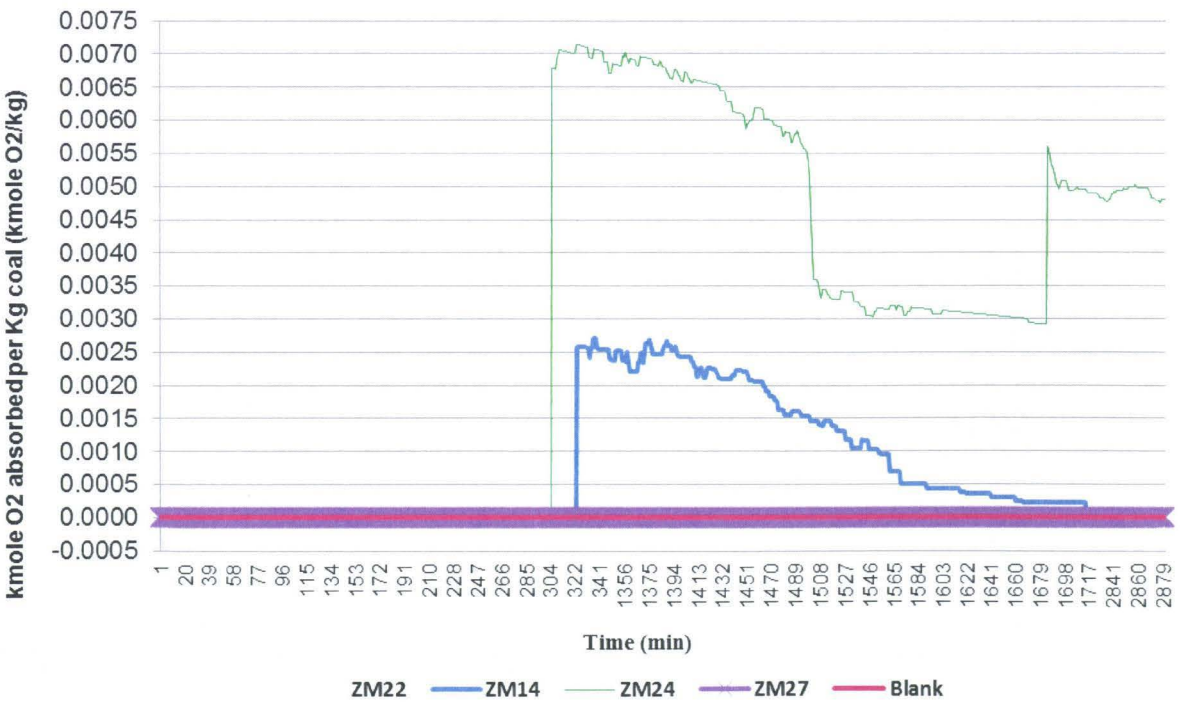


Figure 183: Smith-Glasser Oxygen absorption (ZM22, ZM14, ZM24, ZM27)

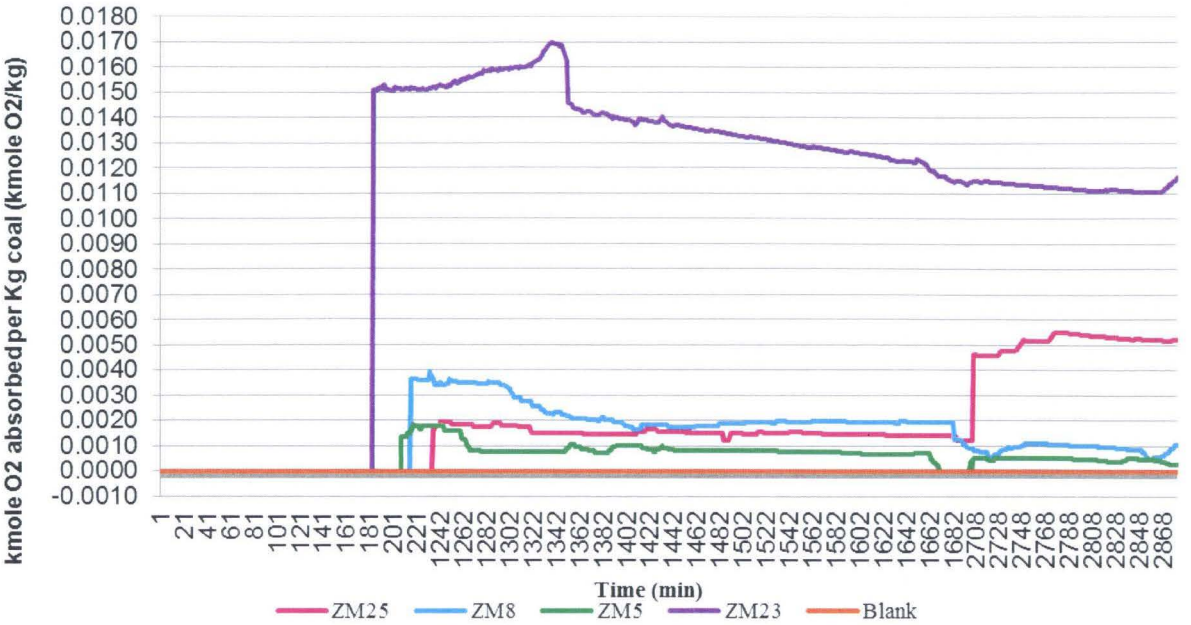


Figure 184: Smith-Glasser Oxygen absorption (ZM25, ZM8, ZM5, ZM23)

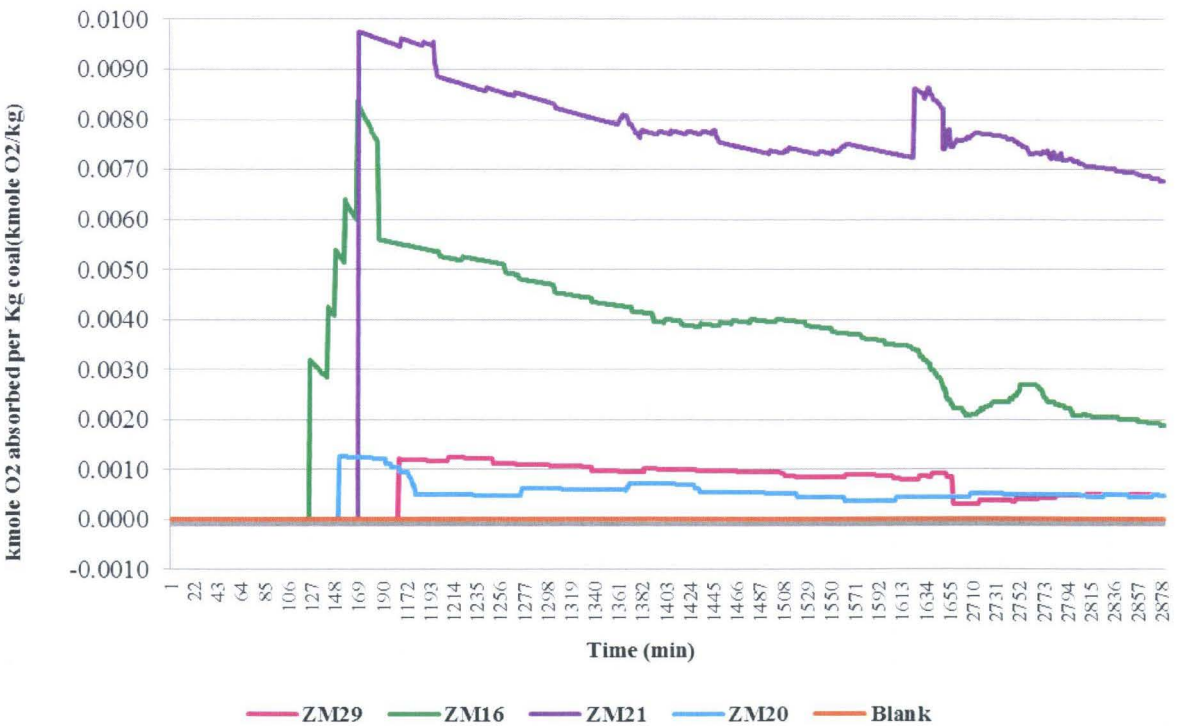


Figure 185: Smith-Glasser Oxygen absorption (ZM29, ZM16, ZM21, ZM20)

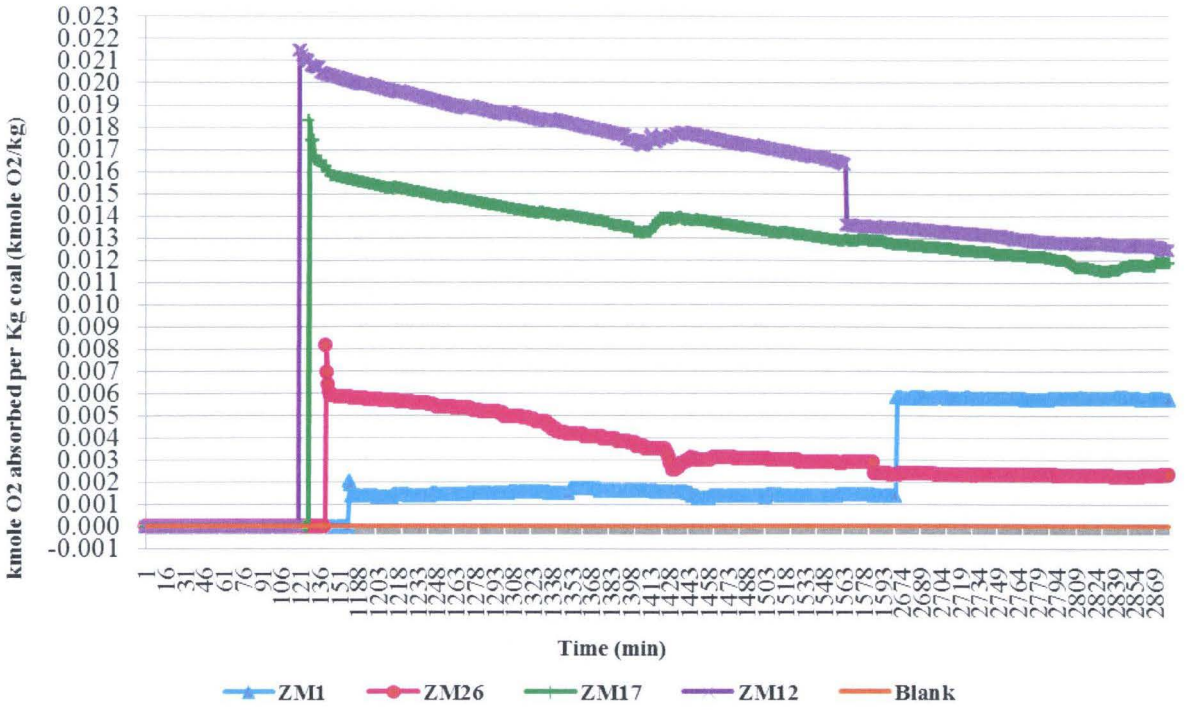


Figure 186: Smith-Glasser Oxygen absorption (ZM1, ZM26, ZM17, ZM12)

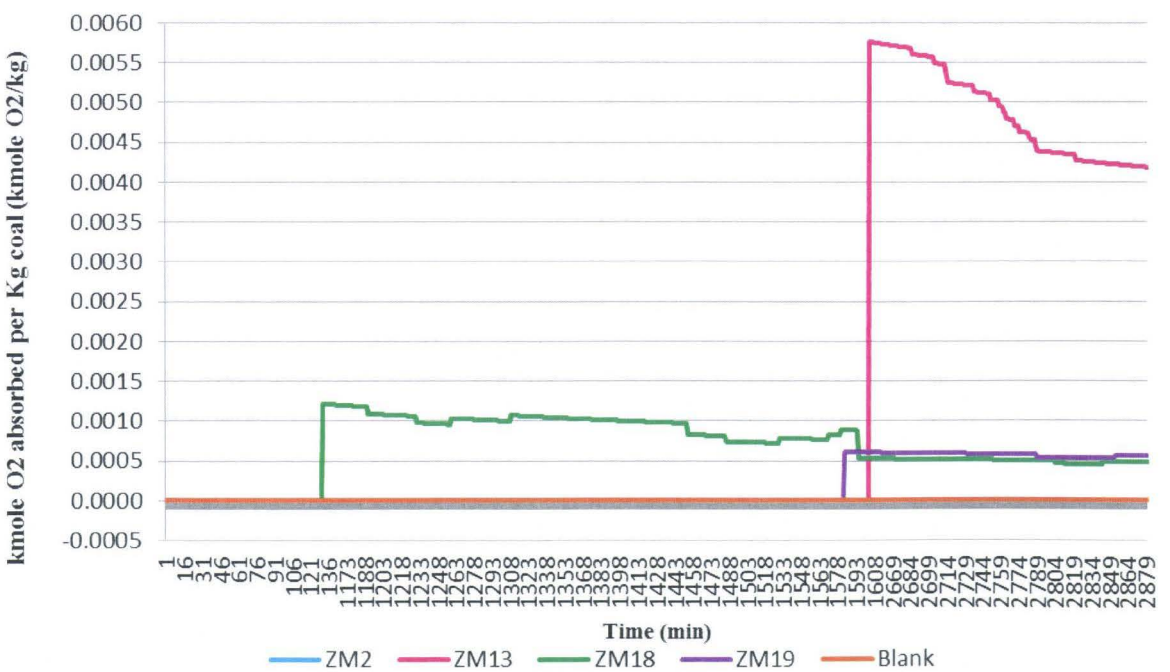


Figure 187: Smith-Glasser Oxygen absorption (ZM12, ZM13, ZM18, ZM19)

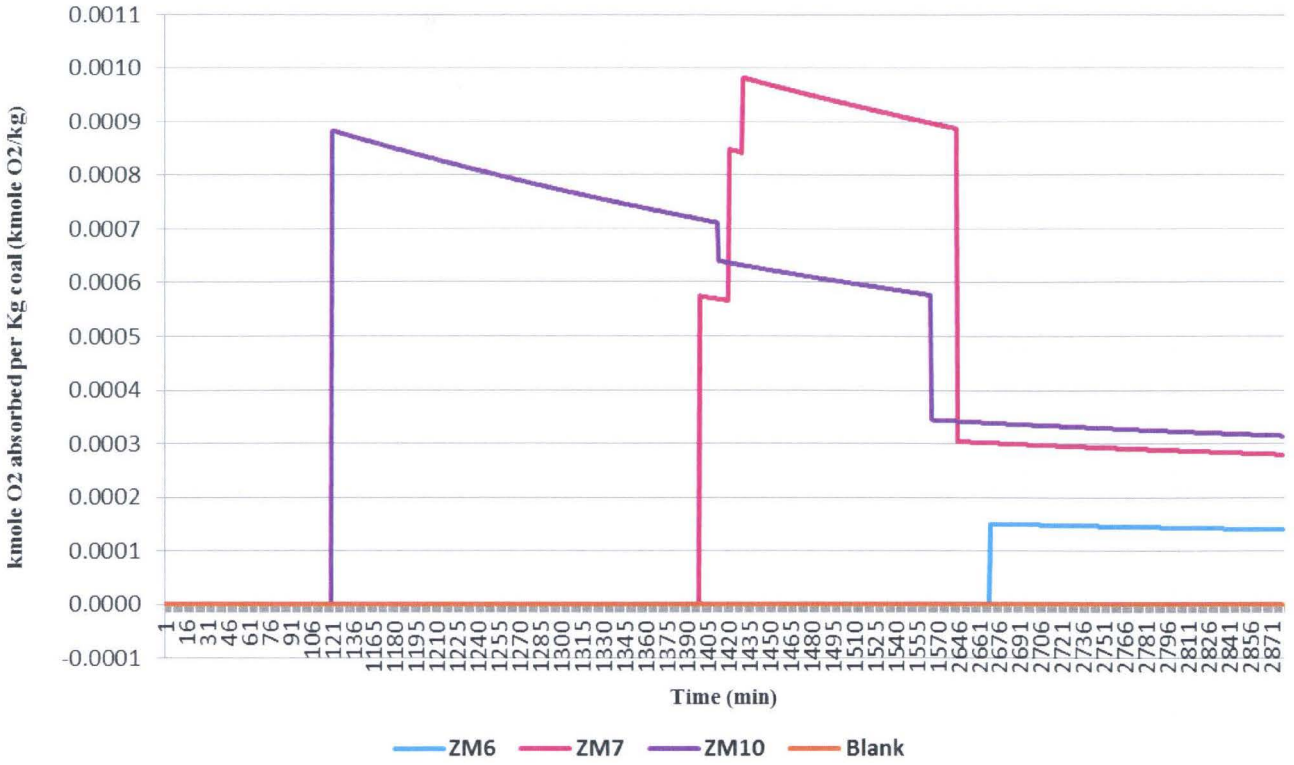


Figure 188: Smith-Glasser Oxygen absorption (ZM6, ZM7, ZM8, ZM10)

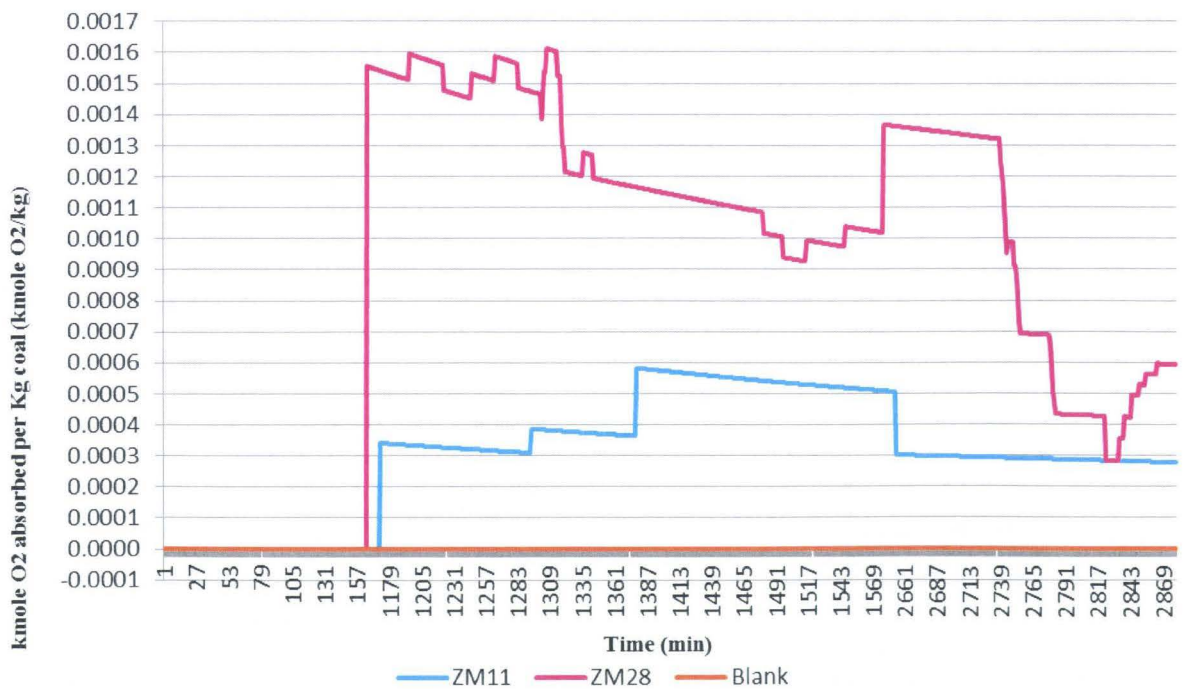


Figure 189: Smith-Glasser Oxygen absorption (ZM11, ZM28)

8.4 Appendix D

8.4.1 Repeatability Tests

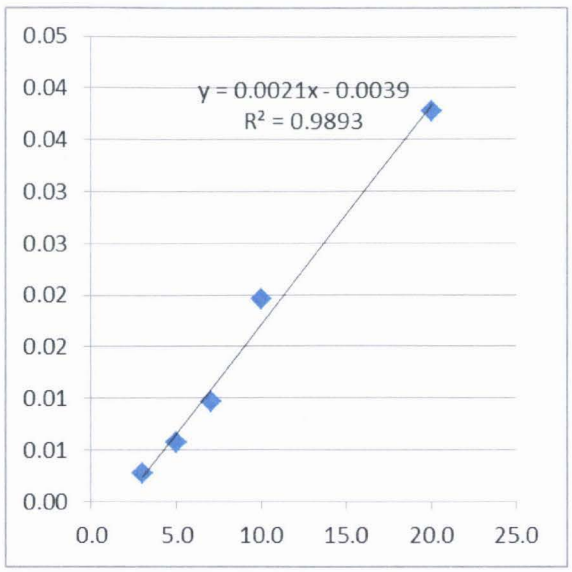


Figure 190: ZM28 R^2_{graph} Repeat

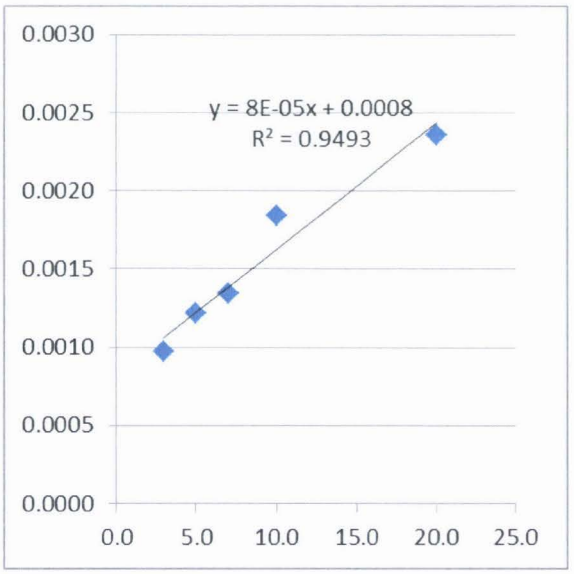


Figure 191: ZM28 $R^2_{calculate}$ Repeat

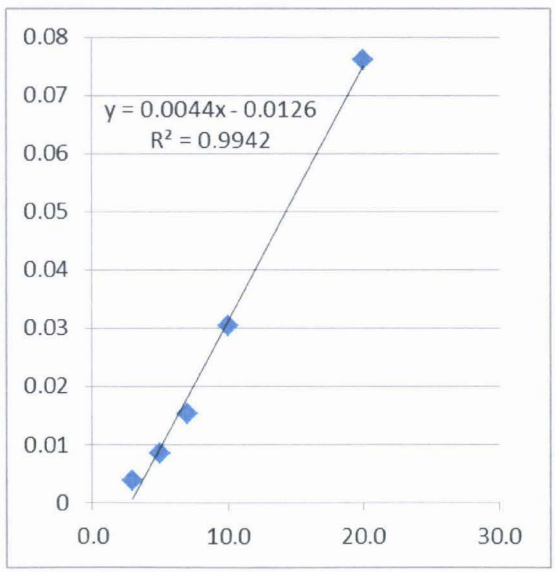


Figure 192: ZM27 R^2_{graph} Repeat

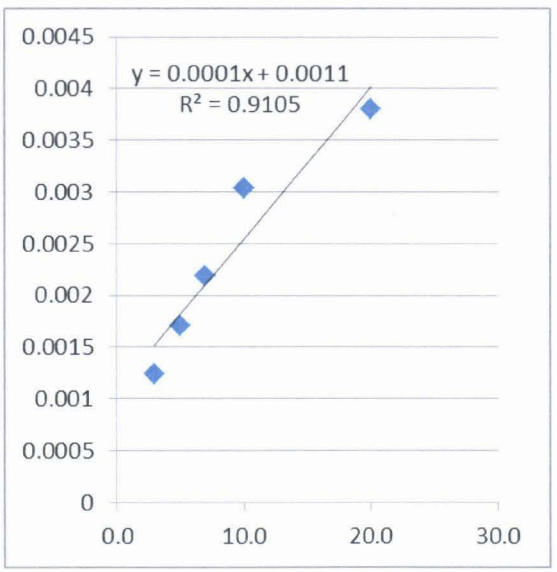


Figure 193: ZM27 $R^2_{calculate}$ Repeat

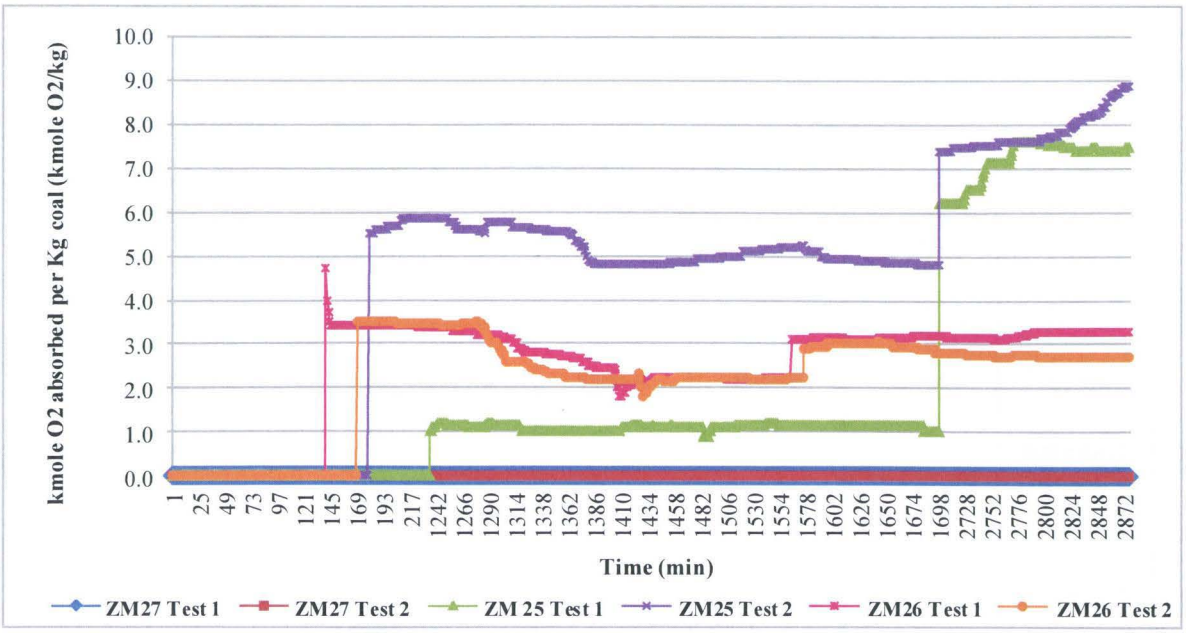


Figure 194: Smith-Glasser Repeatability Test (ZM 27, ZM25, ZM26)

8.5 Appendix E

8.5.1 Petrography Analysis

	1 ZM1	2 ZM2	3 ZM3	4 ZM4	5 ZM5	6 ZM6
RANK (degree of maturity) ISO 11760-2005 Classification of Coals	Bituminous Medium Rank C	Bituminous Medium Rank C	Bituminous Medium Rank C	Bituminous Medium Rank C	Bituminous Medium Rank C	Bituminous Medium Rank C
Mean random reflectance of vitrinite % (determined)	0.74	0.78	0.69	0.67	0.66	0.70
Vitrinite-class distribution Standard deviation σ	V 5 to V 8 0.080	V 5 to V 9 0.098	V 5 to V 8 0.073	V 5 to V 8 0.609	V 5 to V 8 0.060	V 5 to V 8 0.078
Mean maximum reflectance of vitrinite % (calculated)	0.79	0.83	0.74	0.72	0.71	0.75
Abnormalities	None observed	None observed	None observed	None observed	None observed	None observed
PETROGRAPHIC COMPOSITION (% by volume) Maceral analysis (mineral matter basis)						
Total reactive macerals %	66	22	40	44	59	40
Vitrinite content %	54	8	29	25	40	19
Total inertinite %	35	48	39	48	47	60
Heat altered (coke, char etc.) %	0	0	0	0	0	0
Visible minerals %	6	38	26	21	7	17
Maceral analysis - Total %	100	100	100	100	100	100
Condition analysis - Total %	0	0	0	0	0	0

Figure 195: Summary of major coal characteristics (ZM1 – ZM6)

	7 ZM7	8 ZM8	9 ZM9	10 ZM10	11 ZM11
RANK (degree of maturity) ISO 11760-2005 Classification of Coals	Bituminous Medium Rank C	Bituminous Medium Rank C	Bituminous Medium Rank C	Bituminous Medium Rank C	Bituminous Medium Rank C
Mean random reflectance of vitrinite % (determined)	0.72	0.74	0.69	0.73	0.69
Vitrinite-class distribution Standard deviation σ	V 5 to V 8 0.063	V 5 to V 8 0.064	V 5 to V 8 0.063	V 5 to V 9 0.074	V 5 to V 9 0.078
Mean maximum reflectance of vitrinite % (calculated)	0.77	0.79	0.74	0.78	0.74
Abnormalities	None observed	None observed	None observed	None observed	None observed
PETROGRAPHIC COMPOSITION (% by volume) Maceral analysis (mineral matter basis)					
Total reactive macerals %	33	47	62	37	27
Vitrinite content % Liptinite content % Visible minerals %	16 3 30	27 4 9	48 8 20	23 4 28	12 3 32
Maceral analysis - Total %	100	100	100	100	100
Condition analysis - Total %	0	0	0	0	0

Figure 196: Summary of major coal characteristics (ZM7 – ZM11)

	1 ZM12	2 ZM13	3 ZM14	4 ZM15	5 ZM16	6 ZM17
RANK (degree of maturity)	Bituminous	Bituminous	Bituminous	Bituminous	Bituminous	Bituminous
ISO 11760-2005 Classification of Coals	Medium Rank C	Medium Rank C	Medium Rank C	Medium Rank C	Medium Rank C	Medium Rank C
Mean random reflectance of vitrinite % (determined)	0.68	0.70	0.78	0.85	0.75	0.67
Vitrinite-class distribution	V 5 to V 8	V 5 to V 8	V 5 to V 9	V 5 to V 11	V 5 to V 9	V 5 to V 8
Standard deviation σ	0.062	0.056	0.088	0.095	0.075	0.063
Mean maximum reflectance of vitrinite % (calculated)	0.73	0.75	0.83	0.89	0.80	0.72
Abnormalities	None observed	None observed	None observed	None observed	None observed	None observed
PETROGRAPHIC COMPOSITION (% by volume) Maceral analysis (mineral matter basis)						
Total reactive macerals %	74	44	15	31	24	57
Vitrinite content %	60	33	9	14	13	41
Liptinite content %	7	4	2	4	3	7
Total inertinite %	27	35	25	52	42	40
Heat altered (coke, char etc.) %	0	0	0	0	0	0
Visible minerals %	6	28	64	30	42	12
Maceral analysis - Total %	100	100	100	100	100	100
Condition analysis - Total %	0	0	0	0	0	0

Figure 197: Summary of major coal characteristics (ZM12 – ZM17)

	7 ZM18	8 ZM19	9 ZM20	10 ZM21	11 ZM22	12 ZM23	13 ZM24
RANK (degree of maturity) ISO 11760-2005 Classification of Coals	Bituminous Medium Rank C	Bituminous Medium Rank C	Bituminous Medium Rank C	Bituminous Medium Rank C	Bituminous Medium Rank C	Bituminous Medium Rank C	Bituminous Medium Rank C
Mean random reflectance of vitrinite % (determined)	0.72	0.76	0.79	0.75	0.63	0.68	0.67
Vitrinite-class distribution Standard deviation σ	V 5 to V 8 0.071	V 5 to V 9 0.072	V 6 to V 9 0.061	V 6 to V 8 0.061	V 5 to V 8 0.060	V 5 to V 7 0.055	V 5 to V 8 0.054
Mean maximum reflectance of vitrinite % (calculated)	0.77	0.81	0.84	0.80	0.69	0.73	0.72
Abnormalities	None observed	None observed	None observed	None observed	None observed	None observed	None observed
PETROGRAPHIC COMPOSITION (% by volume) Maceral analysis (mineral matter basis)							
Total reactive macerals %	34	35	28	34	16	53	44
Vitrinite content %	21	13	14	20	11	40	36
Total inertinite %	34	63	46	37	11	45	30
Heat altered (coke, char etc.) %	0	0	0	0	0	0	0
Visible minerals %	43	22	38	39	76	11	31
Maceral analysis - Total %	100	100	100	100	100	100	100
Condition analysis - Total %	0	0	0	0	0	0	0

Figure 198: Summary of major coal characteristics (ZM18 – ZM24)

8.6 Appendix F

8.6.1 Mine Disasters

Sixty-three Mining Disasters, 1882-2000 (Three or More Fatalities)

No.	Year	Mine	Disaster	Metal Miners	Coal Miners	Total
1	1882	New Australasian goldmine, Vic	Flooding	22		22
2	1886	Lithgow Valley colliery, NSW	Explosion		5	5
3	1886	Vale of Clwydd colliery, NSW	Fire		3	3
4	1887	Bulli colliery, NSW	Explosion		81	81
5	1889	Hamilton colliery, NSW	Rock fall		11	11
6	1893	Eclipse colliery, Ipswich, Qld	Flooding		7	7
7	1893	Fortuna Hustler goldmine, Vic	Explosion	3		3
8	1895	South Broken Hill silver mine, NSW	Rock fall	9		9
9	1895	McEwoy goldmine, Eldorado, Vic	Flooding	6		6
10	1896	Stockton colliery, NSW	Poison gas		11	11
11	1896	Metropolitan colliery, NSW	Outburst		3	3
12	1898	Dudley colliery, NSW	Explosion		15	15
13	1898	East Greta colliery, NSW	Rock fall		3	
14	1900	Sydney Harbour colliery, NSW	Machinery		5	5
15	1900	Torbanlea colliery, Qld	Explosion		5	5
16	1900	Greta colliery, NSW	Fire		5	5
17	1901	Burwood colliery, NSW	Explosion		3	3
18	1902	Cardigan goldmine, Ballarat, Vic	Flooding	4		4
19	1902	Mt Kembla colliery, NSW	Explosion		96	96
20	1904	Great Boulder goldmine, WA	Machinery	5		5
21	1904	Brilliant PC goldmine, Qld	Fire	7		7
22	1905	Stanford colliery, NSW	Explosion		6	6
23	1907	South Clifton coalmine, NSW	Rock fall		4	4
24	1908	Mt Morgan copper & goldmine, Qld	Rock fall	7		7
25	1908	Mt Morgan copper & goldmine, Qld	Rock fall	5		5
26	1912	North Mt Lyell copper mine, Tas	Fire	42		42
27	1914	Great Extended Hustler goldmine, Vic	Explosion	7		7
28	1919	Cardiff colliery, Ipswich, Qld	Explosion		3	3
29	1921	Mt Mulligan colliery, Qld	Explosion		75	75
30	1922	Golden Horseshoe goldmine, WA	Machinery	6		6
31	1923	Bellbird colliery, NSW	Explosion		21	21
32	1926	Ivanhoe goldmine, Coolgardie, WA	Rock fall	4		*4
33	1926	Redhead colliery, Newcastle, NSW	Explosion		5	5
34	1928	Redbank colliery, Ipswich, Qld	Explosion		3	3
35	1929	Briseis tin mine, Derby, Tas	Flooding	3		**3
36	1929	Jumbunna colliery, Vic	Poison gas		3	3
37	1931	[Colliery], Launceston, Tas	Explosion		4	4
38	1931	Wonthaggi colliery, Vic	Explosion		4	5
39	1932	[Metal mine], WA	Explosion	3		3
40	1934	Blackwater colliery, Qld	Explosion		4	4
41	1936	Hart's Aberdare colliery, Ipswich, Qld	Explosion		4	4
42	1937	Wonthaggi colliery, Vic	Explosion		13	13
43	1945	New Ebbw Vale colliery, Qld	Explosion		4	4
44	1945	Balmain colliery, NSW	Explosion		3	3
45	1954	Collinsville colliery, Qld	Poison gas		7	7
46	1965	Bulli colliery, NSW	Explosion		4	4
47	1966	Wyee colliery, NSW	Rock fall		5	5
48	1971	Hilton copper & lead mine, Qld	Rock fall	3		3
49	1972	Box Flat colliery, Ipswich, Qld	Explosion		17	17
50	1972	Blackman's Flat coalmine, NSW	Rock fall		3	3
51	1975	Kianga No. 1, Moura colliery, Qld	Explosion		13	13
52	1977	Agnew nickel mine, WA	Machinery	5		5
53	1978	Duncan colliery, Tas	Explosion		3	3
54	1979	Appin colliery, NSW	Explosion		14	14
55	1982	Lalcham colliery, Blackwater, Qld	Rock fall		3	3
56	1986	Moura colliery, Qld	Explosion		12	12
57	1989	Emu goldmine, Agnew, WA	Flooding	6		6
58	1991	Western Main coal mine, NSW	Rock fall		3	3
59	1991	South Bulli, NSW	Poison gas		3	3
60	1994	Moura colliery, Qld	Explosion		11	11
61	1996	Gretley colliery, NSW	Flooding		4	4
62	1999	Northparkes copper & goldmine NSW	Rock fall	4		4
63	2000	Bronzewing goldmine, Leinster, WA	Flooding	3		3
		Subtotal metal miners killed in 20 events		**154**		
		Subtotal coal miners killed in 43 events			**511**	
		Total killed in 63 events				**665**

Figure 199: Sixty-three Mining Disaster, 1882 - 2000 (Three or More Fatalities), Mine Accidents database (2015)

8.6.2 Spontaneous Combustion Mine Disasters

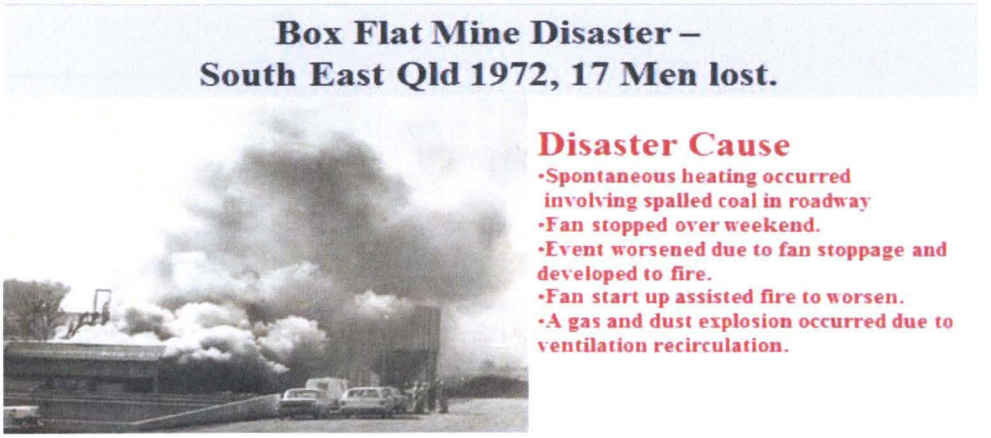


Figure 200: Box Flat Mine Disaster, Creighton (2003)

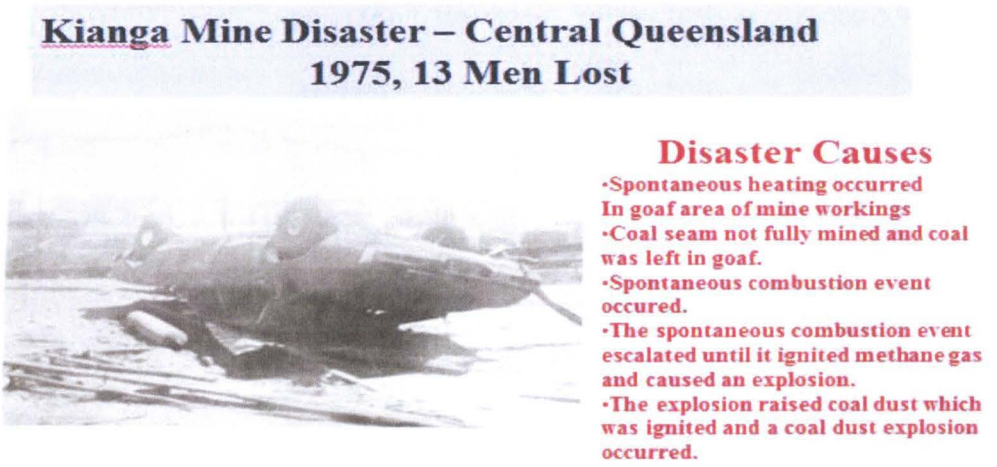


Figure 201: Kianga Mine Disaster, Creighton (2003)

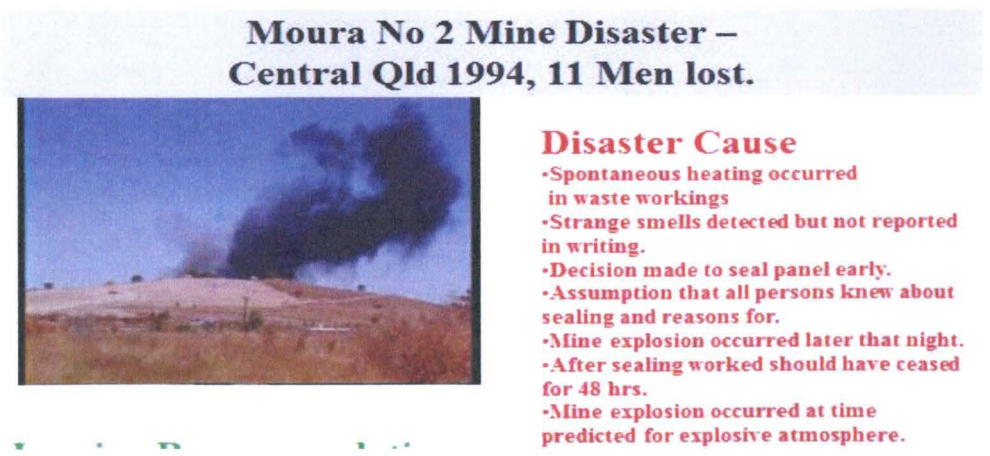


Figure 202: Moura No 2 Mine Disaster, Creighton (2003)

8.7 Appendix G

8.7.1 Changes in Coal Properties

	Moisture	Volatile Matter	Carbon Content	Calorific Value	Oxygen Content
Coalification Stage	As Recieved	Dry Ash Free	Dry Ash Free	Asrecieved	Dry Ash Free
Peat	~75%	69 - 63%	<60%	3,500 kcal/kg	>23%
Lignite	35 - 55%	63 - 53%	65 - 70%	4,000 - 4,200 kcal/kg	23%
Sub-bituminous C	30 - 38%	53 - 50%	70 - 72%	4,200 - 4,600 kcal/kg	20%
Sub-bituminous B	25 - 30%	50 - 46%	72 - 74%	4,600 - 5,000 kcal/kg	18%
Sub-bituminous A	18 - 25%	46 - 42%	74 - 76%	5,000 - 5,500 kcal/kg	16%
High Volatile Bituminous C	12 - 18%	46 - 42%	76 - 78%	5,500 5,900 kcal/kg	12%
High Volatile Bituminous B	10 -12%	42 - 38%	78 - 80%	5,900 - 6,300 kcal/kg	10%
High Volatile Bituminous A	8 - 10%	38 - 31%	80 - 82%	6,300 - 7,000 kcal/kg	8%
Medium Volatile Bituminous	8 - 10%	31 - 22%	82 - 86%	7,000 - 8,000 kcal/kg	4%
Low Volatile	8 - 10%	22 - 14%	86 - 90%	8,000 - 8,600 kcal/kg	3%
Semi-Anthracite	8 - 10%	14 - 8%	90%	7,800 8,000 kcal/kg	3.5%
Anthracite	7 - 9%	8 -3%	92%	7,600 - 7,800 kcal/kg	4.5%
Meta-Anthracite	7 - 9%	8 - 3%	>92%	7,600 kcal/kg	5%

Figure 203: Changes in Coal Properties as Rank increases, Coal Marketing International (2012)